Enhancing the Engineering Properties of Expansive Soil Using Bagasse Ash, Bagasse Fibre and Hydrated Lime

A thesis in fulfilment of the requirement
for the award of the degree

Doctor of Philosophy

from

University of Technology Sydney (UTS)

by

Liet Chi Dang, BEng., MEng.

School of Civil and Environmental Engineering
Faculty of Engineering of Information Technology

January 2019

CERTIFICATE OF ORIGINAL AUTHORSHIP

I certify that the work in this thesis has not previously been submitted for a degree nor has it been submitted as part of requirements for a degree except as fully acknowledged within the text.

I also certify that the thesis has been written by me. Any help that I have received in my research work and the preparation of the thesis itself has been acknowledged. In addition, I certify that all information sources and literature used are indicated in the thesis.

Production Note:
Signature removed prior to publication.

Signature of candidate

Liet Chi Dang

Date: January 2019

DEDICATION

I would like to deeply dedicate this thesis to my family, especially my respective parents, Chien Minh Dang and Oanh Thi Truong, for their sacrifices, endless love, inspiration and hard working, my brother Cong Chi Dang and my sister Hanh Nhu Thi Dang for imparting to me the wisdom, the strength and the determination necessary to fully finish my PhD research study.

ABSTRACT

Expansive soils exhibit massive volume change against fluctuations of moisture content. Shrinkage and expansion of soil can commonly take place near the ground surface, where it is directly subjected to seasonal and environmental variations. Construction of civil engineering structures on expansive soils is highly risky, as this type of soil is susceptible to seasonal drying and wetting cycles, causing significant deformations. Frequent soil movements can generate cracks and damage residential buildings, roads, and other civil structures directly placed on this type of problematic soil. Many efforts have been applied in practice to overcome the adverse effects of expansive soil including replacement of existing expansive soil with non-expansive soil, maintaining a constant moisture content, and ground improvement techniques such as the application of granular pile-anchors, sand cushion technique, and belled piers, and soil stabilisation with chemical agents (e.g. lime or cement) and so on. On top of that, lime stabilisation is the most commonly used method for controlling the shrink-swell behaviour of expansive soil due to seasonal variations. Lime reacts with expansive clay in the presence of water and changes the physicochemical properties of expansive soil, which in turn alters the engineering properties of treated soil. Moreover, soil stabilisation and reinforcement using lime combined with agricultural and industrial waste by-products (e.g. fly ash, rice husk ash, recycled fibres) can extend the effectiveness of lime stabilised expansive soil.

This study presents an experimental investigation on the improvement of the geotechnical properties of expansive soil stabilised with bagasse fibre, bagasse ash combined without or with lime stabilisation. The agricultural waste by-products of bagasse ash and fibre, remained after crushing of sugar-cane for juice extraction, and the expansive soils, used in this investigation, were collected from Queensland, Australia. The stabilised soil specimens were prepared by changing the contents of bagasse ash from 0% to 25%, bagasse fibre from 0% to 2%, hydrated lime from 0% to 6.25%, and combined bagasse ash-hydrated lime from 0% to 25% by the dry mass of expansive soil. Several series of laboratory experiments have been performed on untreated and treated expansive soil samples with different additive contents and various curing times of 3, 7, 28, and 56 days. Another extensive microstructural analysis using scanning electron microscopy

(SEM), pH measurements, and Fourier transform infrared (FTIR) techniques has been carried out to evaluate the microstructure development of untreated and treated expansive soils. The outcomes of these experimental investigations showed that when the addition of bagasse ash into the expansive soils increased from 0% to 25%, the linear shrinkage reduced by 47%, the free swell potential decreased from approximately 10% to less than 0.5%, the swelling pressure reduction was from 80 kPa to 35 kPa (about 60%), the compressive strength at failure and the corresponding strain increased significantly by 48% and 40%. Meanwhile, the combination of bagasse ash and lime to stabilise soils when combined additive content increased up to 25% caused a significant increase in the compressive strength of 815% and the secant modulus of elasticity from 7.2 MPa to 107.2 MPa; reduced the linear shrinkage of 84% and the free swell potential down to less 0.5%; significantly decreased the swelling pressure from 80 kPa to around 10 kPa (88% reduction) and the compression indices from 0.484 to 0.083, just to name a few. It was noted that the improved geotechnical characteristics were more pronounced for lime treated soils with the combination of bagasse ash or fibre. The utilisation of bagasse ash or fibre for expansive soil stabilisation without or with lime combination not only effectively improved the geotechnical properties of expansive soil as curing time and additive content increased, but also assisted in minimising the adverse effects of agricultural waste by-products on the environment.

Numerical investigations based on the finite element method (FEM) incorporated in PLAXIS were carried out to evaluate a possible practical application of recycled fibre-lime reinforced soil as a replacement of geosynthetic reinforced traditional angular load transfer platform layer combined with columns or piles supported embankments founded on soft soils. An equivalent two-dimensional FEM model with proper modified parameters of structure and soil models has been adopted to investigate the performance of floating columns supported embankment reinforced without or with an FRLTP (fibre reinforced load transfer platform). Firstly, a series of numerical analysis was performed on the full geometry of columns supported embankment reinforced without or with an FRLTP of 0.5 m to examine the effectiveness of the FRLTP inclusion into the columns supported embankment system. The numerical results revealed that the embankment with FRLTP could effectively reduce the total and differential settlements, and the lateral

displacement of the embankment by 20%, 74% and 46%, respectively, when compared with the embankment without FRLTP. Subsequently, several series of extensive parametric studies on the influence of FRLTP properties, and the improvement depth ratios of soft soils, have been carried out to assess the behaviour of the columns supported embankment with FRLTP. The findings of the extensive parametric study indicated that the platform thickness has a significant influence on the embankment behaviour, especially in improving the total and differential settlements, the rigidity and stability of the embankment, and the more load transfer from the embankment to DCM columns. Meanwhile, Young's modulus of the FRLTP shows considerable effects on the differential settlement, the stress concentration ratio, but has a negligible effect on the lateral deformation of the investigated embankment. The improvement depth ratio reveals substantial impacts on the final settlement and the lateral deformation, but shows insignificant influence on the stress concentration ratio and the differential settlement during the embankment construction and post-construction time. The FRLTP shear strength parameters show significant influences on the stress concentration ratio and the differential settlement of the embankment. However, the enhancement in the embankment performance was more noticeable for the cohesion than the internal friction angle of the FRLTP.

ACKNOWLEDGEMENT

My PhD journey could not have been possible without the support provided by numerous people. Particularly, I would like to express my sincere appreciation and gratitude to my supervisors, family members and research colleagues.

Firstly, I would like to take this opportunity to express my deepest gratitude to my principal supervisor, A/Prof Hadi Khabbaz, and my co-supervisor, A/Prof Behzad Fatahi, for their continuous support associated with my research project, other aspects of my life, their guidance, time, patience, and leadership. Since the begin of my study, I have learnt many important things from them such as interpersonal and technical skills, critical thinking, presentation skills, and their knowledge and motivation encourage me to overcome many challenges and difficulties to achieve this milestone.

Secondly, I also gratefully thank all geotechnical research fellows who have been involved in my PhD study directly or indirectly. In particular, I would like to say thank you to supporting staff at UTS laboratories including Dr Lam Nguyen, Katie McBean, Md Johir, and my research colleagues Mr Harry Nguyen, Hayder Hassan and Thang Pham for either helping me complete the experimental program or giving me their valued advice.

In addition, I would like to sincerely acknowledge UTS Faculty of Engineering and Information Technology, and Centre of Built Infrastructure Research (CBIR) for their support and scholarships, which enable me to complete this PhD research. I also appreciate Ms Van Le for her kind support.

Finally yet importantly, I owe my immeasurable gratitude to my parents for their support always, their endless and unconditional love. I am also grateful to my brother and sister who always bring joys and happiness, motivate and encourage me to work hard and successfully achieve my goals.

LIST OF PUBLICATIONS

Conference Papers

1. Dang, L.C., Dang, C., Fatahi, B. & Khabbaz, H. 2016, 'Numerical Assessment of Fibre Inclusion in a Load Transfer Platform for Pile-Supported Embankments over Soft Soil', *Geo-China 2016*, eds D. Chen, J. Lee & W.J. Steyn, vol. GSP 266, ASCE, pp. 148-55.
2. Dang, L.C., Hasan, H., Fatahi, B., Jones, R. & Khabbaz, H. 2015, 'Effects of Bagasse Ash and Hydrated Lime Addition on Engineering Properties of Expansive Soil', *Fifth International Conference on Geotechnique, Construction Materials and Environment (GEOMATE 2015)*, Osaka, Japan, pp. 90-5.
3. Dang, L., Hasan, H., Fatahi, B. & Khabbaz, H. 2015b, 'Influence of Bagasse Ash and Hydrated Lime on Strength and Mechanical Behaviour of Stabilised Expansive Soil', *the 68th Canadian Geotechnical Conference and the 7th Canadian Permafrost Conference (GEOQuébec 2015)*, eds J. Côté & M. Allard, the Canadian Geotechnical Society (CGS), Québec City, Canada, pp. 1-8.
4. Dang, L.C., Dang, C.C. & Khabbaz, H. 2017a, 'Behaviour of Columns and Fibre Reinforced Load Transfer Platform Supported Embankments Built on Soft Soil', *the 15th International Conference of the International Association for Computer Methods and Advances in Geomechanics*, Wuhan, China.
5. Dang, L.C. & Khabbaz, H. 2018a, 'Assessment of the Geotechnical and Microstructural Characteristics of Lime Stabilised Expansive Soil with Bagasse Ash', *the 71st Canadian Geotechnical Conference and the 13th Joint CGS/IAH-CNC Groundwater Conference (GeoEdmonton 2018)*, the Canadian Geotechnical Society (CGS), Alberta, Canada.
6. Dang, L.C. & Khabbaz, H. 2018b, 'Enhancing the Strength Characteristics of Expansive Soil Using Bagasse Fibre', in W. Wu & H.-S. Yu (eds), *Proceedings of China-Europe Conference on Geotechnical Engineering. Springer Series in Geomechanics and Geoengineering*, Springer, Cham, pp. 792-6.

7. Dang, L.C. & Khabbaz, H. 2018c, 'Shear Strength Behaviour of Bagasse Fibre Reinforced Expansive Soil', *IACGE2018*, vol. Geotechnical Special Publications, ASCE, Chongqing, China.

8. Dang, L.C., Khabbaz, H. & Fatahi, B. 2017b, 'Evaluation of Swelling Behaviour and Soil Water Characteristic Curve of Bagasse Fibre and Lime Stabilised Expansive Soil', *PanAm-UNSAT 2017*, vol. GSP 303, ASCE, Texas, USA, pp. 58-70.

9. Dang, L.C., Khabbaz, H. & Fatahi, B. 2017c, 'An Experimental Study on Engineering Behaviour of Lime and Bagasse Fibre Reinforced Expansive Soils', *19th International Conference on Soil Mechanics and Geotechnical Engineering (19th ICSMGE)*, ISSMGE, Seoul, Republic of Korea, pp. 2497-500.

10. Hasan, H., Dang, L., Khabbaz, H. & Fatahi, B. 2017, 'Swelling Pressure and Consolidation of Soft Clay Stabilized With Bagasse Ash and Lime', in I.A.-Q. Andreas Loizos, Tom Scarpas (ed.), *Bearing Capacity of Roads, Railways and Airfields*, CRC Press, London, UK pp. 1069-75.

Book Chapters

11. Dang, L.C., Dang, C.C. & Khabbaz, H. 2018a, 'Numerical Analysis on the Performance of Fibre Reinforced Load Transfer Platform and Deep Mixing Columns Supported Embankments', in M. Bouassida & M.A. Meguid (eds), *Ground Improvement and Earth Structures*, Springer, Cham, pp. 157-69.

12. Dang, L.C., Dang, C.C. & Khabbaz, H. 2018b, 'A Parametric Study of Deep Mixing Columns and Fibre Reinforced Load Transfer Platform Supported Embankments', in H. Khabbaz, H. Youn & M. Bouassida (eds), *New Prospects in Geotechnical Engineering Aspects of Civil Infrastructures*, Springer, Cham, pp. 179-94.

13. Dang, L.C. & Khabbaz, H. 2019, 'Experimental Investigation on the Compaction and Compressible Properties of Expansive Soil Reinforced with Bagasse Fibre and Lime', in J.S. McCartney & L.R. Hoyos (eds), *Recent Advancements on Expansive Soils*, Springer, Cham, pp. 64-78.

Journal Papers

14. Dang, L.C., Fatahi, B. & Khabbaz, H. 2016a, 'Behaviour of Expansive Soils Stabilized with Hydrated Lime and Bagasse Fibres', *Procedia Engineering*, vol. 143, pp. 658-65.

15. Dang, L.C., Hasan, H., Fatahi, B., Jones, R. & Khabbaz, H. 2016b, 'Enhancing the Engineering Properties of Expansive Soil Using Bagasse Ash and Hydrated Lime', *International Journal of GEOMATE*, vol. 11, no. 25, pp. 2447-54.

16. Hasan, H., Dang, L., Khabbaz, H., Fatahi, B. & Terzaghi, S. 2016, 'Remediation of Expansive Soils Using Agricultural Waste Bagasse Ash', *Procedia Engineering*, vol. 143, pp. 1368-75.

17. Dang, L.C., Dang, C.C. & Khabbaz, H., 'Modelling of Columns and Fibre Reinforced Load Transfer Platform Supported Embankments', *Proceedings of the Institution of Civil Engineers - Ground Improvement.* doi.org/10.1680/jgrim.18.00039

18. Dang, L.C., Dang, C.C. & Khabbaz, H., 'Numerical Investigation on the Effect of Columns and Fibre Reinforced Load Transfer Platform Supported Embankments', *(submitted)*.

19. Dang, L.C., Khabbaz, H. & Hasan, H., 'Geotechnical Characteristics of Expansive Soils Stabilised with Bagasse Ash and Hydrated Lime', *(submitted)*.

20. Dang, L.C. & Khabbaz, H., 'Assessment of the Engineering Characteristics of Lime Treated Expansive Soil with Bagasse Fibre', *(in preparation)*.

TABLE OF CONTENTS

LIST OF FIGURES

LIST OF TABLES

CHAPTER 1: INTRODUCTION

1.1. OVERVIEW

Reactive black soils are originated from decomposed rocks mainly containing fine-grained particles commonly known as expansive soils that show massive volume change when exposed to the fluctuations of moisture content. Evaporation, rainwater, dewatering, waste and supply water pipe leak phenomena, just to name a few, can be attributed to the principal reasons causing changes in the moisture content. Shrinkage and expansion of soil can commonly take place near the ground surface, where it is instantaneously subjected to seasonal and environmental variation ups and downs. The expansive soil is usually at unsaturated state and consists of montmorillonite clay minerals. Such clay minerals normally account for the main portion of the expansive soil, which highly yield the change in volume against the alteration of the moisture content. The severity of the damage induced by the expansive soil depends on the amount of monovalent cations absorbed in the clay minerals. Construction of civil engineering structures on expansive soils, such as highways, rail tracks, bridges, seaports, airports, and residential buildings, is highly risky, as this type of soil is susceptible to seasonal drying and wetting cycles, causing significant deformations. Frequent soil movements can generate cracks and damage buildings (Figure 1.1), roads (Figure 1.2), and other civil structures directly placed on this type of problematic soil.

The average annual cost of structural destruction associated with light structures and footings constructed on expansive soils was estimated and widely revealed in the previous findings reported by many researchers (Gourley et al. 1993; Jones & Jefferson

2012; Nelson & Miller 1997). For example, the average yearly destruction cost associated with expansive soils in the United States alone is roughly $US 15 billion (Jones & Jefferson 2012), which is tremendously greater than the combined damage cost of residential buildings and infrastructures induced by floods, hurricanes, tornadoes, and earthquakes. According to ASCE (the American Society of Civil Engineers), a quarter of houses have some sort of structural damage induced by expansive soils. Moreover, as reported by ABI (the Association of British Insurers) (Jones & Jefferson 2012), the average annual damage cost of structures related to expansive soils is estimated to be more than £400 million, which is currently the most costly geohazard in the UK. In Australia, the total damage cost due to shrink-swell of the ground is essentially enormous because expansive soil is widely distributed, and covering almost 20% of the ground surface of Australia. Additionally, six out eight of Australia's largest cities are considerably influenced by black soils as reported by Richards et al. (1983). Considine (1984) indicated that each year in Australia, a significant number of houses (around 50,000) were exposed to cracks accounting for approximately 80% of all housing insurance claims.

Figure 1.1 Structural damage due to ground heaving after (Al-Rawas et al. 2005)

A number of ground improvement techniques have increasingly been suggested for improving the engineering properties of expansive soil such as the application of granular pile-anchors (Phanikumar 1997), sand cushion technique (Satyanarayana 1966), and belled piers (Chen 1988). Additionally, chemical stabilisation is one of the most popular methods used to enhance the physical and mechanical characteristics of soft and expansive soils. The ground improvement technique using chemical agents such as lime and cement is a recognised practice in enhancing the engineering properties of problematic soils and this practice is highly applicable for lightly loaded structures such as low-rise residential buildings, road and highway pavements (Al-Mukhtar et al. 2012; Alsafi et al. 2017; Bahmani et al. 2016; Basha et al. 2005; Cardoso & Maranha das Neves

2012; Çokça 2001; Cong et al. 2014; Jha & Sivapullaiah 2015; Kamei et al. 2013; Millogo et al. 2012; Phanikumar 2009; Wong et al. 2013; Zhang et al. 2014).

Figure 1.2 A cracked road in Adelaide, Australia after (Considine 1984)

According to many researchers (Aldaood et al. 2014b; Bell 1996; Boardman et al. 2001; Celik & Nalbantoglu 2013; NLA 2004; Okyay & Dias 2010; Sherwood 1993; Wang et al. 2016; Zhang et al. 2015), lime stabilisation of subgrades can result in very effective improvement of engineering properties of clayey soils. Modification and stabilisation are essentially two forms of improvements (NLA 2004; Sherwood 1993).

Modification happens to some extent with almost all fine-grained soils, while the most considerable improvement takes place in clay soils of intermediate to high plasticity. Modification occurs primarily due to cation exchange between calcium cations supplied by the lime slurry, the quicklime (CaO) or the hydrated lime ($Ca(OH)_2$) and the existing cations absorbed into the clay mineral surfaces. The high pH environment induced by the lime-water system is required to promote the modification in that the hydrated lime reacts well with the clay mineral surfaces. In the high pH environment, the cation exchange reactions between the calcium ions and the clay minerals change the clay surface mineralogy as well as form new cementitious products. The process results in plasticity reduction, decrease in moisture holding capacity and swell, improved stability and the capability to construct a solid working platform. In contrast to lime modification, stabilisation (NLA 2004; Sherwood 1993) is a time-dependent pozzolanic reaction that occurs when a sufficient amount of lime is utilised to stabilise expansive soils. Obviously, stabilisation process improving a significant level of time-dependent strength gain due to the long-term pozzolanic reactions is of different nature to the modification process. While an increase in the lime content to improve expansive soils results in an increase in the pH of lime-soil mixture (i.e. pH≈12.4), the solubility of alumina and silica minerals from the surface of clay particles is likely to take place and at the same time, react with calcium from the lime in order to form new cementitious products such as calcium aluminate hydrates (CAH) and calcium silicate hydrates (CSH). Such CSH and CAH cementitious products of pozzolanic reactions contribute to the strength gain of soils stabilised with lime. Moreover, the pozzolanic reactions can not only occur within hours after mixing lime and soil but also continue for years. As a result, these long-term pozzolanic reactions of lime stabilised expansive soils promote notable strength gain with

time. According to a number of researchers (Aldaood et al. 2014a; Aldaood et al. 2014b; Basha et al. 2005; Celik & Nalbantoglu 2013; Kumar et al. 2007), expansive soil stabilisation and reinforcement using lime combined with agricultural and industrial waste by-products can extend the effectiveness of lime stabilised expansive soil behaviour such as the compressive and shear strength, the shrink-swell behavior, etc. In addition, the application of lime and waste by-products combination for expansive soil stabilisation can provide novel, low-cost, and green materials for sustainable construction development.

Agricultural and industrial (agro-industrial) waste by-products include silica fume, fly ash, bottom ash, rice husk ash, blast furnace slag, bagasse ash, bagasse fibres, coconut coir fibres, rubber crumbs, textiles, carpet fibre wastes and so on. These agro-industrial waste by-products have increasingly been identified to cause adverse effects on the environment, which requires public attention on their safe disposal and searching opportunities for utilisation as recycled materials in the areas such as construction and soil stabilisation. In practice, land-filling and incinerators are widely used to eliminate these by-products. Nonetheless, due to increasing costs of disposal and lack of readily available landfill spaces, the incinerator measure is generally regarded as an acceptable disposal solution of agricultural and industrial by-products. As a result of the incinerator process, the ashes and non-combustible residues are generated from the agro-industrial waste by-products, which are estimated to account for 10% of the total amount of the agro-industrial waste by-products (Punthutaecha 2002). Moreover, the production of the residues and ashes has increased over the years due to the development of industrial production. Taking sugar production in Brazil as an example, a double increase in sugar-

cane production from 568 million tons of sugar-cane in 2008 to 1000 million tons of sugar-canes in 2020 is forecasted (Frías et al. 2011). This implies that a significant landfill space would be required to dispose of the ashes and non-combustible residues. Therefore, to overcome the issue of disposal of agricultural and industrial waste by-products inducing the environment and health issues, utilisation of the agro-industrial waste by-products such as fly ash, bagasse ash and fibres in the areas of construction and soil stabilisation is indispensable to investigate. These methods are predicted to offer a better practical solution than simply landfilling the waste.

1.2. STATEMENT OF PROBLEM

Sugar-cane bagasse is obtained in abundant quantities from sugar-refining industry. After crushing of sugar-cane in sugar mills and extraction of juice from processed sugar-cane by milling, the discarded fibrous matter is called bagasse fibre (bagasse). Bagasse is employed as fuel in the cogeneration boiler in order to create steam for producing sugar as well as electricity. Bagasse is burnt at high temperature around 700~900°C in a controlled process to use its maximum fuel value, while producing bagasse ash with high amorphous silica, low carbon content and high specific surface area. Generally, bagasse ash is disposed in a landfill and now is becoming an environmental burden. It is estimated that more than 200,000 tons of bagasse ash are produced every year in Thailand (Chusilp et al. 2009a); 10,000 tons of bagasse ash produced every day in Brazil (Lima et al. 2012) and numerous amount of bagasse ash produced in other tropical countries worldwide.

As it is well reported in the literature, sugar-cane bagasse ash is classified as pozzolanic material because it is rich in amorphous silica, which is effectively used together with hydrated lime as a replacement for cement in improving the engineering

properties of concrete. Several studies on bagasse ash utilisation in concrete technology (Bahurudeen et al. 2014; Bahurudeen & Santhanam 2014; Chusilp et al. 2009b; Cordeiro et al. 2009; Cordeiro et al. 2008; Frías et al. 2011; Ganesan et al. 2007; Oliveira De Paula et al. 2010) indicated that well-burnt bagasse ash is most likely able to substitute up to 20% cement content in concrete admixtures without bringing adverse effects on the physical and mechanical characteristics of concrete. The main benefits of bagasse ash, replacing cement in concrete, are the enhancement of early high compressive strength, reduction in water permeability, considerable resistance to chloride permeation and diffusion, and increase in durability of reinforced concrete structures. Moreover, in high-performance concrete technology, Cordeiro et al. (2009) corroborated that replacing cement with up to 20% by ultrafine ground bagasse ash can produce high-performance concrete having similar mechanical properties compared with concrete produced using only cement as the cementitious material.

Although the potential use of bagasse ash as cement replacement material in concrete has become a focus of interest in recent years, only a few studies have been performed by researchers (Alavéz-Ramírez et al. 2012; Anupam et al. 2013; Faria et al. 2012; Jamsawang et al. 2017; Manikandan & Moganraj 2014; Sujjavanidi & Duangchan 2004) on the potential application of bagasse ash in soil stabilisation. Based on available literature, bagasse ash alone, and a combination of lime/cement and bagasse ash used in soil stabilisation can cause significant modification and improvement in the engineering properties of treated soil. However, more investigations are essential in order to have a better understanding of the geotechnical properties of expansive soils improved with the hydrated lime and bagasse ash.

Bagasse fibre is an abundant fibrous waste by-product of the sugar-cane industry, left after the crushing of sugar-cane for juice extraction as mentioned above. Bagasse fibre has been used for many purposes as a combustible material for energy supply in sugar-cane factories, a pulp raw material in paper industries, and building materials like bagasse-cement composites (Bilba & Arsene 2008; Onésippe et al. 2010; Tian & Zhang 2016; Tian et al. 2015), treated bagasse fibre reinforced biodegradable composites (Cao et al. 2006). Since bagasse fibres are renewable, environmentally friendly, low density and low-cost materials that have similarly physical and mechanical properties of other natural fibres such as jute, sisal, pineapple and coir fibres, bagasse fibre has the highly potential application in the area of construction as building materials and reinforcing component for soil reinforcement in support of subgrade beneath pavements and roads. However, very limited studies on bagasse fibres reinforced problematic soil have been performed so far. Therefore, further investigations of soil stabilisation and reinforcement are needed to comprehend the engineering properties of bagasse fibre alone, hydrated lime and bagasse fibres combination reinforced expansive soil.

1.3. RESEARCH OBJECTIVES AND SCOPE

Several goals are expected to be achieved in this study. However, the main goal is to utilise bagasse ash and fibre, an abundant fibrous waste by-product derived from sugar-refining industry, in road and railway construction as soil reinforcement materials and replacement materials of cement or lime. The application of these agricultural by-product materials has some potential benefits being that not only facilitates preventing the potential environment issues related to their disposal, but also alleviates the effect of

expansive soil inducing damage of highways and light loaded buildings. Moreover, it provides novel construction materials for sustainable development together with a tremendous amount of construction cost saving on the basis of decrease in dosages of conventional stabilisers such as lime, cement. Hence, the main objectives of this research are to investigate the influences of bagasse ash, bagasse fibre, hydrated lime, and their combination on the shrink-swell potential and the other engineering characteristics of treated expansive soil. The preparation of stabilised soil specimens was conducted by changing the bagasse ash contents from 0% to 25%, bagasse fibre contents from 0% to 2%, hydrated lime contents from 0% to 6.25%, and contents of bagasse ash combined with hydrated lime from 0% to 25% by the dry mass of expansive soil. Several series of laboratory experiments consisting of compaction, linear shrinkage, swell potential, swelling pressure, unconfined compressive strength (UCS), California bearing ratio (CBR), soil suction, consolidation tests have been performed on untreated and treated expansive soil samples with different additive contents in line with various curing time of 3, 7, 28, and 56 days. An array of comprehensive study on the microstructure development of untreated and treated expansive soils was carried out using scanning electron microscopy (SEM), pH measurements, and Fourier transform infrared (FTIR) techniques. The outcomes of this experimental investigation were analysed and discussed to obtain a better understanding of the effects of the hydrated lime, bagasse ash and fibre, and their combination on the shrink-swell behaviour. The compressive and shear strength, the stiffness, the bearing capacity, the brittleness and the ductility, the change of soil water retention, and the compressibility characteristics of the untreated and treated soil were also presented and discussed.

The pre-and-post failure behaviours of bagasse ash, bagasse fibre, hydrated lime alone, and their combination stabilised expansive soils were observed and evaluated. Such behaviours are mostly challenging geotechnical engineers and researchers in the field of ground improvement. Tang et al. (2007) reported that for cemented clayey soil, the peak stress increases dramatically with an increase in cement content, and the cemented soil exhibits a marked stiffness and brittleness. The axial strength increases with an increase in axial strain until the peak value is reached, then followed by a sudden drop to zero in cemented clayey soil. The failure strain of cemented soil is in a range of 0.5% to 0.75%, which is much smaller than that of untreated soil. However, based on the test results, they indicated that fibre inclusion could enhance the peak stress of untreated clayey soil to a certain level. The addition of fibre reinforced clayey soil shows more ductile behaviour and smaller loss of post-peak stress than untreated clayey soil. The reduction in the loss of post-peak stress is more noticeable for higher fibre content. Thus, one of the key objectives of this research is to precisely predict the post-failure behaviour of lime treated expansive clay with bagasse fibre and ash.

Another aim of this study is to propose numerical modelling that was conducted to assess a possible practical application of eco-friendly, inexpensive, and recycled fibre-lime reinforced soil as a replacement of geosynthetic reinforced traditional angular load transfer platform (LTP) layer combined with columns or piles supported embankments founded on soft soils. The application of lime-fibre reinforced soils to be used as fibre reinforced load transfer platform (FRLTP) is a feasible novel ground modification technique in combination with deep cement mixing (DCM) columns supported embankments placed over soft soils. The reasons are that the popular applications of the

geosynthetic reinforced traditional angular platform over columns supported embankments built on top of soft soils has come up with many geotechnical difficulties, namely intolerable total and differential settlements, larger lateral earth pressure and displacement, local or global instability, and potential failures due to over bearing or bending capacity of DCM columns. Therefore, a novel ground modification technique utilising green, low-cost and recycled materials as an FRLTP to be used as a replacement of geosynthetic reinforced traditional angular platform layer and DCM columns supported embankments is required to overcome those above-mentioned geotechnical difficulties.

To sum up, the specific objectives of the experimental and numerical investigations in this study are described as follows:

- Determining the optimum lime content based on pH measurements for expansive soils stabilised without or with bagasse ash as well as investigating the influences of addition of bagasse ash, bagasse fibre without or with hydrated lime combination on the compaction characteristics of treated soils.

- Better understanding of the shrink-swell behaviour such as the linear shrinkage, the swelling strain, the free swell potential and the swelling pressure, and the pre-and-post failure behaviour of lime treated expansive soil without or with bagasse ash and fibre inclusions.

- Studying the influences of additives (i.e. bagasse ash, bagasse fibre without or with hydrated lime combination) on the unconfined compressive strength of treated soils associated with different additive contents and curing periods.

- Evaluating the stiffness and the brittleness (ductility) of untreated soil and bagasse ash or bagasse fibre treated soils without or with hydrated lime inclusion when curing time and additive contents increased.

- Quantifying the bearing capacity of untreated soil and soils treated with bagasse ash, bagasse fibre in combination with or without hydrated lime, using California bearing ratio (CBR) tests when taking into consideration the influences of curing time and additive contents.

- Carrying out experimental investigations on the compressibility of soils stabilised with different contents of bagasse ash, bagasse fibre without or with hydrated lime combination, using one-dimensional consolidation tests.

- Investigating the indirect tensile strength and the soil water retention of untreated soils and hydrated lime treated soils without or with bagasse fibre reinforcement while considering the effect of bagasse fibre contents.

- Assessing the influence of bagasse fibre inclusion on the shear strength properties, the ductility, and the strain hardening behaviour of reinforced soils using triaxial compression apparatus.

- Evaluating the evolution of the microstructure of untreated and treated soils with bagasse ash or bagasse fibre without or with hydrated lime combination using scanning electron microscopy (SEM) and Fourier transform infrared (FTIR) techniques.

- Developing a numerical model analysis to simulate the behaviour of FRLTP and DCM columns supported embankment over soft soils. A few case studies available from the literature will be used to verify the proposed numerical model for predicting the performance of highway embankment supported by FRLTP and DCM columns reinforced soft soils.

- Performing an array of numerical analysis on the full geometry of a DCM columns-supported (CS) embankment reinforced without or with an FRLTP in a two-dimensional plane strain condition to examine the effectiveness of the FRLTP inclusion into the CS embankment system. Many important parameters of the embankment design such as maximum settlement and lateral displacement, generation and dissipation of excess pore water pressure or load transfer mechanism between columns and foundation soils will be investigated and discussed.

- Carrying out several series of extensive parametric studies on the influence of FRLTP properties (e.g., the FRLTP thickness, the elastic deformation modulus, etc.), the improvement depth of soft soils to investigate the performance of the DCM columns supported embankment with FRLTP regarding the differential and total settlements, the lateral displacement with depth, and the load transfer mechanism.

- Numerical findings and a guideline for a more accurate prediction of the differential and overall settlement, the lateral displacement, the stress transfer mechanism, the soil surface movement from the centreline of highway embankment, and variation of excess pore water pressure underneath highway embankment will be presented and proposed. Such findings and a guideline will definitely promote a reasonable analysis

and design procedure for practical engineers and practitioners in order to estimate the settlement of any given highway embankments placed on FRLTP and DCM columns improved multilayers of soft soils.

1.4. THESIS ORGANISATION

There are seven chapters in this thesis. An outline of these chapters is provided as follows:

- Chapter 1 presents a brief introduction with respect to the shrink-swell behaviour of expansive soil, chemical stabilisation of expansive soil without or with combination of agricultural and industrial waste by-products. Additionally, the statement of problem, the research objectives and scope of this investigation are also provided.

- Chapter 2 provides a comprehensive literature review of the behaviour of untreated and lime or cement treated expansive soil with agricultural and industrial waste by-products. They consist of the unconfined compressive strength and its influencing factors, the pH change, the bearing capacity, the linear shrinkage, the swelling potential and pressure together with various curing times and additive contents.

- Chapter 3 exhibits the detailed descriptions of the adopted materials, samples preparation, laboratory tests and their procedures, employed in this investigation. It can also be noted that the testing setups and apparatus are described in detail for interpretation. All experimental tests, used for this research, were carried out at the University of Technology Sydney.

- Chapter 4 represents the results of the laboratory experiment results to evaluate the influence of bagasse ash, hydrated lime, and their combination on the shrink-swell

potential and engineering characteristics of treated expansive soil. Soil specimens were prepared by varying bagasse ash contents from 0% to 25%, hydrated lime contents from 0% to 6.25% and combined hydrated lime-bagasse ash contents from 0% to 25% by the dry mass of expansive soil. Several series of laboratory experiments consisting of pH measurement, compaction, linear shrinkage, swell potential, swelling pressure, unconfined compressive strength (UCS), California bearing ratio (CBR), and consolidation tests have been performed on untreated and treated expansive soil samples while taking in to account the influence of additive contents and various curing times up to 56 days. A series of comprehensive study on the microstructure change was also conducted on untreated and treated expansive soils using scanning electron microscopy (SEM) and Fourier transform infrared (FTIR) techniques.

- Chapter 5 reveals the experimental investigation results on the mechanical characteristics of expansive soil reinforced with randomly distributed bagasse fibre and hydrated lime. The influences of bagasse fibre reinforcement on the behaviour of reinforced soils without or with lime stabilisation are investigated through several series of experimental tests. They comprise compaction, linear shrinkage, UCS, indirect tensile strength, CBR, free swell potential, swelling pressure, consolidation tests, soil suction, and shear strength tests. These laboratory tests were undertaken on untreated soil and soil samples treated with various contents of bagasse fibre from 0% to 2% and/or hydrated lime from 0% to 6%. SEM analysis was carried out on selected soil samples to examine the micromechanical reinforcement between fibre surface and soil particles.

- Chapter 6 presents numerical simulations of three case studies on a novel ground modification technique utilising fibre reinforced load transfer platform (FRLTP) and DCM columns supported (CS) embankment constructed on top of multilayers of soft soils that are proposed and investigated based on the finite element method incorporated in PLAXIS. Firstly, a series of numerical analysis is carried out on the full geometry of a CS embankment reinforced without or with an FRLTP in a two-dimensional plane strain condition to assess the effectiveness of the FRLTP inclusion into the CS embankment system. Subsequently, many design parameters of an embankment such as final settlement and lateral deformation, generation and dissipation of excess pore water pressure or load transfer mechanism between columns and soft soil foundation are analysed and examined. Consequently, another comprehensive series of parametric study on the influential factors such as the FRLTP thickness, Young's modulus, and the shear strength parameters of the FRLTP, the improvement depth of soft soils, are performed to comprehend the behaviour of the floating DCM columns supported embankment reinforced an with FRLTP.

- Chapter 7 presents a summary and conclusions derived from the experimental and numerical investigations. This chapter also highlights some recommendations for further investigations.

CHAPTER 2: LITERATURE REVIEW

2.1. INTRODUCTION

Reactive soil is originated from decomposed rocks or mainly contains fine-grained particles commonly known as expansive soil that shows massive volume change when exposed to the fluctuations of moisture content. Expansive soils have a tendency to swell when their moisture content is increased. The moisture change may come from rain flooding, leaking water, sewer lines, or reduction in surface evapotranspiration when an area is surrounded by pavements and buildings. Soils containing the majority of montmorillonite clay minerals (smectite) generally exhibit these properties (Chen 1988). Meanwhile, the kaolinite group is generally non-expansive. The mica-like group comprising of illinites and vermiculites can be expansive but generally does pose significant problems (Nelson & Miller 1997).

Excessive swelling, settlement, low bearing capacity, insufficient shear strength, high compressibility and internal erosion are known as some typical characteristics of expansive soils that result in damage due to volume change to many civil engineering structures including spread footings, roads, highways, railways, airport runways, earth dams founded on expansive soil. Expansive soils are usually found in abundance in semiarid regions of tropical and temperate climate zones, where annual evapotranspiration exceeds precipitation (Abduljauwad 1993; Nalbantoglu & Tuncer 2001). Swelling of expansive soils causes more damage to structures, particularly light buildings and pavements, than other natural hazards including earthquakes and floods (Jones & Holtz 1973).

One of the most common approaches of controlling volume changes is to stabilise expansive soils with chemical admixtures that prevent volume changes or effectively modify the volume change characteristics of expansive soils (Çokça 2001; Kehew 2006; Mokhtari & Dehghani 2012). Lime and cement have been used widely for expansive soil stabilisation to relatively shallow depth under footings and slabs for lightly loaded residential buildings, roads and highways, and industrial plants. Furthermore, the application of lime or cement combined with waste by-products for expansive soil stabilisation can decrease the construction costs by cutting down lime and cement usage, meanwhile facilitates effectively minimisation of the potential impacts on the environment for sustainable development and economic growth. This has recently become increasing interests from a number of researchers on the globe in carrying out research for utilisation of the waste by-products in the area of infrastructure foundations.

On the other hand, the industrial development has resulted in construction of many coal-fired power plants for energy demand, sugar-refining factories for sugar needs and so on. This development brought it with the problem of safe disposal or beneficial utilisation of large quantities of the by-products such as fly ash, bagasse ash and bagasse fibre. Only 0.5% to 1.75% of fly ash is productively employed, the rest is disposed in open stockpiles on land areas of sluiced to ponds at great expense (Çokça 2001). According to Frías et al. (2011), there were more than 568 million tons of sugar-cane generated yearly in Brazil for alcohol and sugar production. Referring to this industrial process, considerable volumes of bagasse wastes are generated, which are estimated to be about 25% of the total production of sugar-cane annually. However, the sugar industry development is planned to double in 2020 that will need 1000 million tons of sugar-cane

making a double increase in bagasse waste generation. These industrial by-products undoubtedly pose serious problems in terms of both land use and potential environmental pollution. Hence, effective utilisation of these industrial by-products must be regarded as economically and environmentally beneficial.

According to many researchers (Çokça 2001; Cordeiro et al. 2008; Frías et al. 2011; Nalbantoglu & Tuncer 2001; Osinubi et al. 2009a), waste by-products such as fly ash, bagasse ash and fibre have a high potential to be utilised in a variety of construction applications including filling materials, concrete, soil reinforcement materials, and liners. However, there is still a need to find new uses and to increase utilisation so less ash will be disposed. Very limited studies have been investigated to assess the possibility of using waste by-products as stabilisers for expansive soil stabilisation to an appreciable extent. This research reported herein addresses this possibility.

2.2. CHEMICAL AND MECHANICAL SOIL STABILISATION METHOD

Chemical Stabilisation method is an effective method to enhance soil properties by mixing chemical additives or stabilisers with soils (Bell 1996; Çokça 2001; Fatahi & Khabbaz 2013; Fatahi et al. 2012b; Mokhtari & Dehghani 2012; Nalbantoglu & Tuncer 2001; Osinubi et al. 2009a). Soil stabilisation by the chemical treatment such as lime and cement can improve shear strength properties and reduce the swelling and shrinkage potential of expansive clay soils, thereby offering a better foundation base to pavements, roads, railways and pipelines. Basically, there are two methods of chemical soil treatment. In the first method, the chemical simply forms a coating cover for the soil particles. They do not react with the soils, but bind the soil particles together and fill the soil pores. In the

second method, the chemicals are mixed with the soil and will actually react with soil to change the properties of the soil. There are several stabilising agents available in the market consisting of cement, lime, bitumen, emulsion, resin (e.g. epoxy resin, acrylic resin, solvinated resin), calcium silicates, calcium aluminates, sodium silicates, fly ash, rice husk ash, bagasse ash and so on.

2.2.1. Lime Stabilisation

The use of lime for stabilising plastic montmorillonitic clayey soils has been increasing in favour during the last few decades because it lowers volume change characteristics, prevents damage to structures, while improves workability and engineering properties of stabilised clayey soils. Generally, the amount of lime required to stabilise expansive soil ranges from 2% to 8% by the dry weight of soil (Bell 1996; Chen 1988). Addition of lime to clayey soil provides an abundance of calcium ions (Ca^{2+}) and magnesium (Mg^{2+}). These ions tend to replace other common cations such as sodium (Na^{+}) or potassium (K^{+}), in a process known as cation exchange. Replacement of sodium or potassium ions with calcium significantly reduces the plasticity index of clayey soils. A decrease in plasticity is usually accompanied by a reduction of the swelling and shrinkage potential of stabilised soils. The addition of lime increases the soil pH, which also increases the cation exchange capacity. A change of soil texture takes place when lime is mixed with clays. As the amount of lime is increased, there is an apparent reduction in clay content and consequently the percentage of coarse particles increases (Chen 1988). Moreover, the increase in lime inclusions causes the increase in pH in clayey soil, which facilitates taking place time-dependent and temperature pozzolanic reactions. When happening such

pozzolanic reactions, silica and alumina are dissolved out of the structures of clay minerals and then react with calcium to produce the new cementitious compounds, calcium silicate hydrates (CSH) and calcium aluminate hydrates (CAH), which contribute to the long-term strength gain in lime stabilisation of expansive soils (Bell 1996; Çokça 2001; Nalbantoglu & Tuncer 2001).

2.2.2. Cement Stabilisation

Cement is generally the best type of admixture to be used with soils; it is also commonly available but is often expensive. Mixing cement with expansive soil reduces the swelling potential. Normally, the amount of cement required for expansive soil stabilisation varies in a range from 2% to 6% by the soil (dry) weight (Chen 1988; Çokça 2001). The improvement in engineering properties of clayey soil when cement is added can be explained by three basic reactions as follows: dehydration process, ion exchange or flocculation and agglomeration, and pozzolanic reaction. According to several researchers (Chew et al. 2004; Lorenzo & Bergado 2006; Prusinski & Bhattacharja 1999), they explained that the hydration process rapidly occurs when cement is mixed with pore water of stabilised clayey soil to form primary cementitious compounds such as hydrated calcium silicates (C_2SH_x, $C_3S_2H_x$), hydrated calcium aluminates (C_3AH_x, C_4AH_x) and hydrated lime ($Ca(OH)_2$). Where C, S, A and H stand for Calcium (CaO), Silicate (SiO_2), Aluminate (Al_2O_3) and water (H_2O), respectively. According to Prusinski & Bhattacharja (1999), the hydrated calcium silicates (CSH) and hydrated calcium aluminates (CAH) play the most important role in enhancing the soil matrix, which consequently improve

the strength of stabilised clayey soil. The following chemical formulations describe the primary hydration reactions (Bergado et al. 1996; Prusinski & Bhattacharja 1999)

$$2C_3S + 6H \rightarrow C_3S_2H_3 + 3Ca(OH)_2 \quad (2.1)$$

$$2C_2S + 4H \rightarrow C_3S_2H_3 + Ca(OH)_2 \quad (2.2)$$

Moreover, according to Lea (1956), while the hydrated lime is deposited in a separate crystalline solid phase, the formation of above mentioned hydrated calcium aluminates and hydrated calcium silicates are the main cementing products. During hardening, the cement particles interact with the adjacent cement grains to form a hardened matrix, encasing soil particles (Bergado et al. 1996).

The second process involves the cation exchange, followed by flocculation and agglomeration of soil-cement particles. The bivalent calcium ion (Ca^{2+}) released from the hydrated lime, causes hydration of cement which subsequently rises the pH value of pore water in the soil (Fang 2006). It can be noted that a high pH value is important for further pozzolanic reactions. With cation exchange, flocculation of fine clay particles occurs, forming larger aggregate of clay particles. The cementitious compounds (i.e. CSH and CAH) serve as bridges and provides bonding between aggregates of clay particles through cementation (Prusinski & Bhattacharja 1999). Furthermore, the cementing products result in the dissociation of calcium ions which then react with silica and alumina in the soil to form pozzolanic products (Lorenzo & Bergado 2006). These secondary cementing products, stabilising the soil and increasing the strength of treated soil with time, are also reported by Porbaha et al. (2000a). The basic pozzolanic reactions are given below by Prusinski & Bhattacharja (1999).

$$Ca(OH)_2 + SiO_2 \rightarrow C-S-H \quad (2.3)$$

$$Ca(OH)_2 + Al_2O_3 \rightarrow C-A-H \quad (2.4)$$

2.2.3. Agricultural and Industrial By-products Used for Construction and Soil Stabilisation

Agricultural and industrial (agro-industrial) waste by-products include silica fume, fly ash, bottom ash, rice husk ash, blast furnace slag, bagasse ash, bagasse fibres, coconut coir fibres, rubber tires, textiles, carpet plastic waste and so on. These agro-industrial waste products are increasingly identified to cause negative effects on the environment, which requires public attention on its safe disposal and searching opportunities for utilisation as recycled materials in the areas of infrastructure construction and soil stabilisation. In practice, landfilling and incinerators are widely used to eliminate these by-products. Nonetheless, due to the increasing costs of disposal and lack of landfill space readily available, the only incinerator measure is regarded as an acceptable disposal solution of agricultural and industrial by-products. As a result of the incinerator process, the ashes and non-combustible residues are generated from the agro-industrial waste by-products, which are estimated to account for 10% of the total amount of the agro-industrial waste by-products (Punthutaecha 2002). Moreover, the production of the residues and ashes increases over years due to the development of industrial production, taking sugar production in Brazil as an example, estimate of a double increase in sugar-cane production from 568 million tons of sugar-cane in 2008 to 1000 million tons of sugar-canes in 2020 (Frías et al. 2011). This implies significant landfill is still required to dispose of the ashes and non-combustible residues. Therefore, to overcome the agricultural and industrial waste by-products inducing the environment and health issues,

utilisation of the agro-industrial waste by-products such as fly ash, bagasse ash and fibres in the areas of construction and soil stabilisation is critical to be investigated. These methods are predicted to offer a better practical solution than simply landfilling them.

The following sections summarise a variety of literature information on waste and recycled waste by-products that have been used in construction projects. A few of these materials are blast furnace slag, fly ash, bottom ash, bagasse ash and fibres, coconut coir, rubber tires.

2.2.3.1. Blast Furnace Slag

Iron ore, coke, and limestone are heated in the blast furnace to produce iron. Production taking place simultaneously in the blast furnace process is a material known as blast furnace slag. Selective cooling of the slag results in four distinct types of blast furnace slag (Punthutaecha 2002). They are summarised as follows:

- (1) Air-cooled form (solidification under ambient conditions), which finds extensive use in conventional aggregate applications;
- (2) Expanded or foamed form (solidified with controlled quantities of water), which is mainly used as light-weight aggregate;
- (3) Granulated form (solidified by quick water quenching to a vitrified state), which is mainly used in the manufacturing of slag cement;
- (4) Palletized form (solidified by water and air-quenching in conjunction with spinning drum), which is used both as a light weight aggregate and in the manufacturing of slag cement.

Granulated blast furnace slag, a by-product of the steel industry, consists of a substantial proportion of a glassy phase with a significant content of Ca, Si, Al, and Mg-based compounds. This is most likely to present as a solid form with high potential cementitious reactivity being that has been adopted in geotechnical engineering since it enhances soil properties similar to other available cementitious products (Punthutaecha 2002; Wild et al. 1999; Yi et al. 2015).

2.2.3.2. Fly ash

Fly ash is a major by-product of the combustion of pulverised coal. Fly ash mainly comprises of oxides of silicon, aluminium, iron, calcium, and unoxidised carbon. According to Çokça (2001), fly ash can be classified as non-plastic fine silt by the Unified Soil Classification System. The chemical compositions of fly ash vary considerably depending on the nature of coal burned and the power plan operational characteristics (Çokça 2001). There are two major classes of fly ash. Class F fly ash is produced from burning anthracite of bituminous coal. Meanwhile, class C fly ash is produced from burning lignite and sub-bituminous coal, which is classified as high calcium fly ash, having cementitious properties due to including more than 20% free lime according to ASTM (2015). Both classes of fly ash are pozzolans, which are defined as siliceous or siliceous and aluminous materials (Çokça 2001; Fatahi & Khabbaz 2014). Fly ash can provide an adequate array of divalent and trivalent cations (Ca^{2+}, Al^{3+}, Fe^{3+}, etc.) under ionised conditions that can promote flocculation of dispersed clay particles. Thus, expansive soils can be potentially stabilised effectively by cation exchange using fly ash.

2.2.3.3. Bottom ash

Bottom ash is an industrial by-product for the burning of coal produced in power generation plants. It is relatively suitable for the treatment of fine-drained soil in geotechnical applications that particularly require a large volume of material such as highway embankment construction, filling materials or backfills. These applications have become a promising solution to the problem of disposing bottom ash in terms of the environment because substantial economic savings can be obtained by the reduction of ash disposal costs and the conversation of natural soils and lands (Güllü 2014; Kim et al. 2005). Bottom ash colour ranges from gray to black and is generally angular with a porous surface. In addition, bottom ash is a relatively well-graded, sand-sized material. Table 2.1 shows the range of chemical composition of bottom ash.

López-López et al. (2016) carried out experimental work to investigate the chemical compositions of bottom ash by using scanning electron microscope (SEM). Based on the outcomes of SEM test, they reported that bottom ash has a high percentage in silicates and aluminates, and to a lesser extent, iron and calcium oxides, which are defined as cementitious characteristics. The remaining of the bottom ash components is unburnt residues. According to ASTM (2015), the bottom ash in their investigation can be classified as class F fly ash that is caused by calcination of anthracite or bituminous coal. According to many researchers (Gourley et al. 1993; Güllü 2014; Kim et al. 2005; López-López et al. 2016), bottom ash is currently being used as a construction material in artificial reefs, liners, and daily covers for landfill, concrete masonry blocks, lightweight and partial replacement of aggregate for highway embankment, construction of road and railway networks.

Table 2.1 Chemical compositions of fly ash and bottom ash after (Çokça 2001; Fatahi & Khabbaz 2013; Punthutaecha et al. 2006)

Chemical Composition (%)	Class F Fly ash	Class C Fly ash	Bottom Ash
MgO	0.69-1.60	1.01-1.66	0-0.80
Al_2O_3	19.70-25.50	19.44-22.13	13.00-15.10
SiO_2	54.8-64.2	44.18-58.62	39.60-43.30
CaO	2.27-9.8	2.18-18.98	2.04-3.50
Fe_2O_3	3.92-5.10	4.85-10.18	15.00-32.80
SO_3	0.10-0.60	0.36-3.96	0.36-3.96
K_2O	1.24	1.50-1.52	1.70-1.79
Na_2O	0.52	0.19-0.45	0.27-0.30
TiO_2	0.97	0.98-1.11	0-0.70
Loss in Ignition	-	1.10-1.19	0-2.10

2.2.3.4. Bagasse ash

Sugar-cane bagasse ash is obtained in abundant quantities from sugar-refining industry. After crushing of sugar-cane in sugar mills and extraction of juice from processed sugar-cane by milling, the remained fibrous matter is known as bagasse. Bagasse is subsequently used as fuel in the cogeneration boiler in generating steam for the production of sugar and electricity. Burning bagasse at high temperature from 700°C to 900°C in a controlled process is commonly adopted to use its maximum fuel value, meanwhile producing bagasse ash with high amorphous silica, low carbon content and high specific surface area. Generally, bagasse ash is disposed of in landfill and now is becoming an environmental burden. It is estimated that more than 200,000 tons of bagasse ash are produced every year in Thailand (Chusilp et al. 2009a); 10,000 tons of bagasse ash

produced every day in Brazil (Lima et al. 2012) and numerous amount of bagasse ash produced in other tropical countries worldwide. Thus, this agro-industrial by-product material is increasingly identified to pose a risk to the environment, which requires public attention and research on its safe disposal and for opportunities to use as recycled material in construction.

Bagasse ash, however, is considered as pozzolanic material rich in amorphous silica, which is effectively employed together with hydrated lime as a replacement for cement in improving the engineering properties of concrete. Several studies on bagasse ash utilisation in concrete technology (Bahurudeen et al. 2014; Bahurudeen & Santhanam 2014; Chusilp et al. 2009b; Cordeiro et al. 2009; Cordeiro et al. 2008; Frías et al. 2011; Ganesan et al. 2007; Oliveira De Paula et al. 2010) indicated that well-burnt bagasse ash is more likely able to substitute up to 20% cement content in concrete admixtures without bringing adverse effects on the physical and mechanical characteristics of concrete. The most benefits of bagasse ash replacing cement in concrete are the enhancement of early high compressive strength, reduction in water permeability, considerable resistance to chloride permeation and diffusion, increase in durability of reinforced concrete structures. Moreover, in high-performance concrete technology, Cordeiro et al. (2009) corroborated that cement replacement up to 20 percent by ultrafine ground bagasse ash can produce high-performance concrete having similarly mechanical properties when compared with concrete product prepared using only cement.

Table 2.2 Chemical compositions of sugar-cane bagasse ash after (Alavéz-Ramírez et al. 2012; Anupam et al. 2013; Bahurudeen et al. 2014; Bahurudeen & Santhanam 2014; Chusilp et al. 2009a; Osinubi et al. 2009a)

Chemical Composition (%)	Bagasse Ash
MgO	0.11-1.87
Al_2O_3	1.33-9.92
SiO_2	41.17-75.67
CaO	2.59-11.16
Fe_2O_3	1.50-6.98
SO_3	0.02-3.52
K_2O	2.10-9.59
Na_2O	0.12-0.22
TiO_2	0.74-1.10
Loss in Ignition	2.11-21.48

Although the potential use of sugar-cane bagasse ash as cement replacement material in concrete has become a focus of interest in recent years, only a few studies have been performed by researchers (Alavéz-Ramírez et al. 2012; Anupam et al. 2013; Manikandan & Moganraj 2014; Sujjavanidi & Duangchan 2004) on the potential application of bagasse ash in soil stabilisation. Nevertheless, based on the reliable experiment results, they indicated that bagasse ash alone, combination of lime and bagasse ash used in soil stabilisation caused significant modification and improvement in the engineering properties of treated soils. Table 2.2 reveals the range of chemical composition of sugar-cane bagasse ash.

2.2.3.5. Rubber Tires

Waste rubber tyres are challenging environmental concerns in many countries worldwide due to its disposal in landfill. In Australia, it is estimated more than 20 million tyres were accumulated in landfills by the year 2010 and the trend for accumulated rubber tyres is increasing at a rate of 2% (Mohammadi et al. 2014). Whole tyres are bulky with a lot of empty spaces internally. As a result, landfilling of waste rubber tyres occupies large landfill space and results in environmental issues such as fire, pollution, providing breeding sites for mosquito vectors of human disease (Kalkan 2013; Mohammadi et al. 2014; Tafreshi & Norouzi 2015). However, road construction applications, recycled rubber tyres are utilised in pavement concrete as a highly preferable option due to the high volume of recycles rubber, which can be incorporated in construction of road pavements. According to Mohammadi et al. (2014), although the reduction in the compressive strength of concrete manufactured limits use in most structural applications, rubberised concrete possible has some desirable characteristics such as lower density, higher toughness and ductility, better sound insulation and resistance against cracking, which make it a valid option for pavement applications. Additionally, Tafreshi & Norouzi (2015) reported that recycled tyres have the strong potentials being to be adopted in soft soil reinforcement in road construction, highway embankments, backfilling in retaining structures as lightweight materials. Despite the potential applications of recycled rubber types as construction materials, the special care should be taken for the potential of catching fire due to vandalism.

2.2.3.6. Coconut Fibres

Coconut fibre or coir fibre is an agro-waste by-product obtained from coconut plantations. Coconut plantations play an important role in the economy of tropical countries such as India, Sri Lanka, Brazil, Thailand, Vietnam, Malaysia and others. Coir fibre is suitable argo-waste material for soil reinforcement because of their availability, low-cost and environmentally friendly nature. Coir fibre contains more lignin than all other natural fibres such as jute, flax, linen, and cotton. It has a lignin content of 45.84%, which makes it as the strongest of all known natural fibres (Anggraini et al. 2016). According to Sivakumar Babu et al. (2008), the use of short coir fibre as randomly reinforcing material with expansive soil can result in improved engineering properties of treated soil. Despite many advantages, some modifications are useful to improve the performance of coir fibres as soil reinforcement.

2.2.3.7. Bagasse Fibres

Bagasse fibre is an abundant fibrous waste by-product of the sugar-cane industry, left after the crushing of sugar-cane for juice extraction. Bagasse fibre has been used for many purposes as a combustible material for energy supply in sugar-cane factories, a pulp raw material in paper industries, and building materials like bagasse-cement composites (Bilba et al. 2003), treated bagasse fibre reinforced biodegradable composites (Cao et al. 2006). Since bagasse fibre is a renewable, biodegradable, environmentally friendly, low density and low-cost material that has physical and mechanical properties similar to other natural fibres such as jute, sisal, pineapple and coir fibres. Hence, bagasse fibre has a high potential to be utilised in the area of construction as building materials and reinforcing components for soil reinforcement in support of subgrade beneath pavements and roads.

However, very limited investigations on bagasse fibre reinforced problematic soil have been performed so far. Therefore, further investigations are essential to comprehend the engineering properties of soft and reactive soils reinforced with bagasse fibre.

2.2.4. Behaviour of Cement, Lime Treated Expansive Soil with Agricultural and Industrial By-products

In this section, the engineering properties of expansive soils treated with fly ash, bagasse ash without or with lime or cement combination are reviewed. They are the unconfined compressive strength, California bearing ratio, the shrink-swell behaviour, and the pH change with various curing time and additive contents. Moreover, factors affecting the strength of treated soils, such as cement/lime content and curing time are also highlighted and discussed in detail.

2.2.4.1. Unconfined Compression Strength (UCS)

During preliminary soil investigations, foundation analysis and design for civil construction such as road and railway networks, residential buildings, the unconfined compression strength test is paramount and most likely used to determine the compressive strength and stiffness of natural soils as well as stabilised soils (Bahar et al. 2004; Bell 1996; Ene & Okagbue 2009; Lorenzo & Bergado 2006; Sharma et al. 2008). Overall, the peak shear strength of treated soil sample is greatly enhanced as compared to the untreated soil sample due to the effect of cementation bonds. Figure 2.1 displays a series of conventional unconfined compression strength tests on lime treated expansive soil performed by Sharma et al. (2008) with different lime contents ranging from 0% to 5% after 28 days of curing. The UCS values of treated expansive soil were also compared

with the UCS value of untreated sample. To be more specific, the untreated expansive soil failed at stress of 200 kPa and at a strain of 6%. However, upon addition of lime, the failure stress and the corresponding strain increased. It was observed that the failure stress and failure strain at 2% lime were 400 kPa and 7%, respectively, showing an increase of 100% in stress and 16.7% in strain. At 4% lime, the failure stress and failure strain were maximum at 650 kPa and 9%, respectively, showing a significant increase of 225% in stress and 50% in strain. This means that there was considerable improvement in the engineering behaviour of lime treated expansive soil when lime content was 4%. However, the failure compressive strength decreased when the lime content increased to 5%, indicating that 4% lime content was the optimum content.

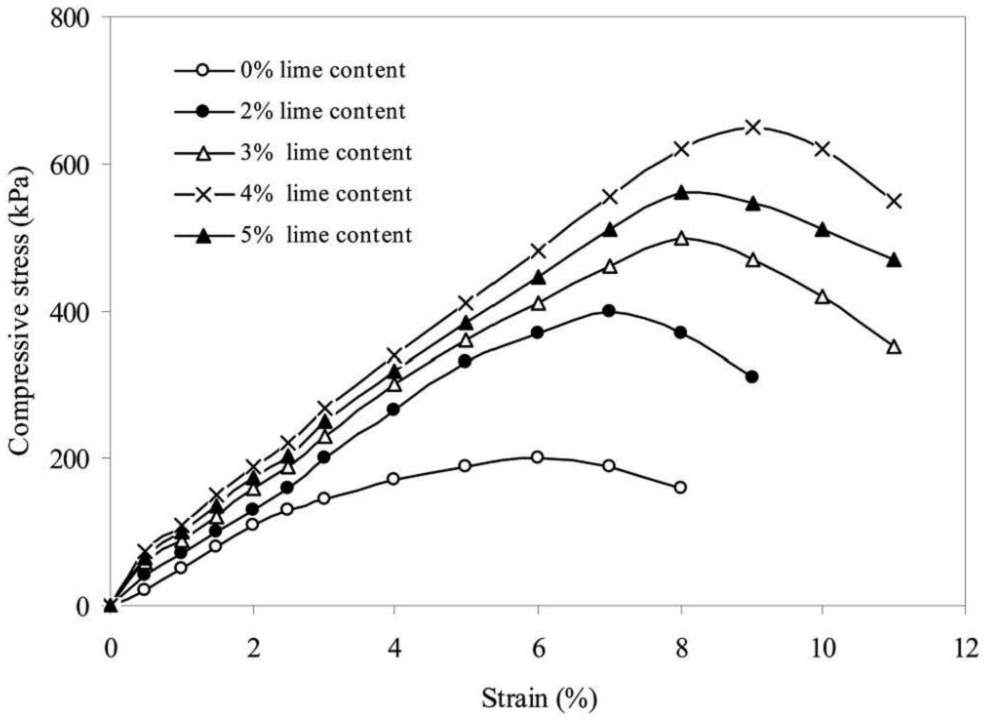

Figure 2.1 Stress-strain behaviour of lime treated expansive soil at 28 days curing after (Sharma et al. 2008)

Many researchers (Bell 1996; Dash & Hussain 2012; Kumar et al. 2007) indicated the similar trend observed for lime treated expansive soil. They explained that an excessive amount of lime added to treated expansive soil resulted in a reduction in its strength gain because lime has neither appreciable friction nor cohesion (Bell 1996), which serves as a lubricant to the soil particles and thereby decreases the strength. The decrease in the strength of limed soil may be attributed to the platy shapes of the unreacted lime particles in the soil admixture (Kumar et al. 2007). According to Dash & Hussain (2012), lime stabilisation of expansive soil produces cementitious gel that forms substantial volume of pores after reacting with soil particles. Then, with the increase in lime content, the soil structure tends to be increasingly porous to counteract the strength gain attributable to cementation. However, at very high lime content, an overall decrease in strength occurs due to excessive formation of lime induced cementitious gel. Meanwhile, the individual lime, cement addition to treated clayey soil or expansive soil exhibits more brittle behaviour and stiffness when increasing additive content as previous investigations presented by researchers (Basha et al. 2005; Fatahi et al. 2012b; Tang et al. 2007).

Several influencing factors of the compressive strength development of treated expansive soil with various additive types (i.e. fly ash, rice husk ash, lime, cement, etc.) have been identified. Such influence factors are additive content, curing time and types of soil (Porbaha et al. 2000b; Tan et al. 2002). Other factors such as the effect of stabilising reagent homogeneous mixing process, and the effect of curing temperature as well as humidity cannot be ignored. However, in the following parts, only the main impact factors including additive content and curing time contributing to the strength development of treated expansive soil are thoroughly discussed.

2.2.4.1.1. Effect of Additive Content

Sharma et al. (2008) conducted a series of laboratory tests to evaluate the influence of rice husk ash (RHA), an industrial by-product, in combination with lime to treat expansive soil with various additive contents after 28 days of curing as shown in Figure 2.2. They reported that the unconfined compressive strength increased with increasing lime content for given RHA contents. Particularly, the UCS increased by almost 127% when the lime content increased from 0% to 4% at an RHA content of 12%. However, the UCS decreased when lime further increased to 5%. This indicates that 4% was the optimum content for lime in RHA mixed with expansive clay. For a given lime content, the UCS increased with increasing RHA content. However, a content of 12% RHA gave the maximum UCS values for all lime content. This also indicates that 12% RHA was the optimum RHA content for lime treated expansive clays. They noted that the presence of high silica content (90%) in RHA increases pozzolanic reaction and the resistance to the applied compressive load of the RHA-soil admixture. The high pozzolanic reaction of RHA further increases the compressive strength of the blend in the presence of lime.

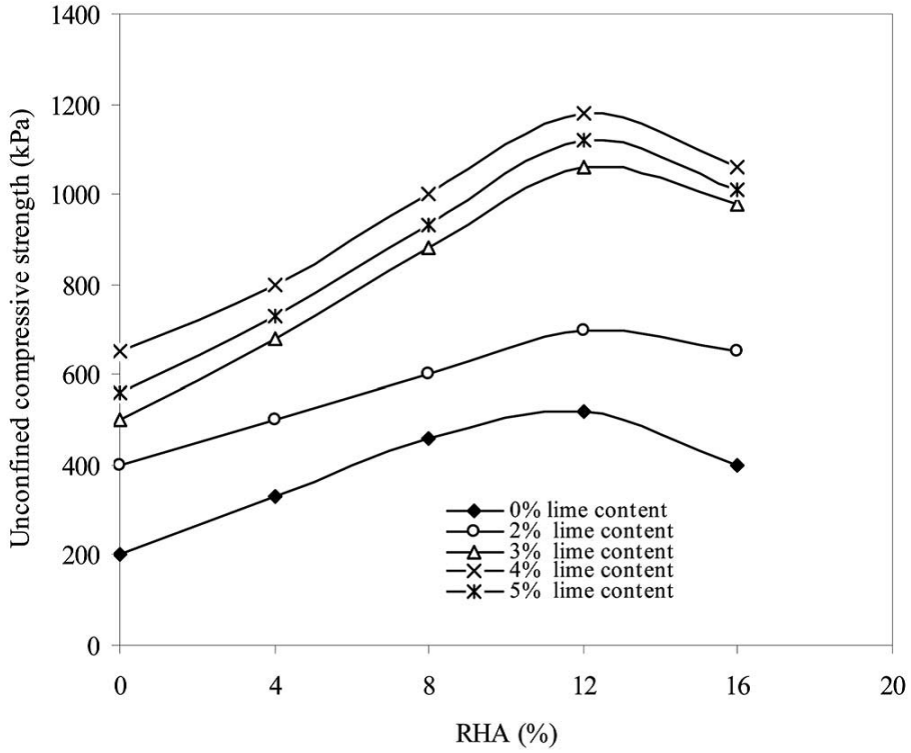

Figure 2.2 Effect of rice husk ash on UCS values of lime treated expansive soil at 28 days curing after (Sharma et al. 2008)

2.2.4.1.2. Effect of Curing Time

Bell (1996) carried out experimental studies on the effects of lime content and curing time on the unconfined compressive strength of montmorillonite and kaolinite soils. Based on the UCS test results, Bell (1996) reported that curing time plays a major important role in the development of the compressive strength of expansive soil treated with lime. In similar, Mitchell & Hooper (1961) indicated that the effect on the strength of lime stabilised expansive soil is a function of time, temperature and humidity. Referring to Bell (1996), the compressive strength increased rapidly at first 7 days of curing as illustrated in Figure 2.3 and Figure 2.4, and then increased more slowly at a more or less constant rate. As can be seen from Figure 2.3 and Figure 2.4, the unconfined compressive

strength of soil treated with lime developed rapidly with increasing addition of lime until an optimum lime content was reached and then began to decline for any further additional lime content. According to Bell (1996), the optimum line content represents the point of lime saturation and may move towards higher increments with increasing length of curing time. The strength gain associated with the optimum lime content tended to increase with longer curing time for kaolinite soils (Figure 2.3), meanwhile did not vary significantly with curing period for montmorillonite soils (Figure 2.4).

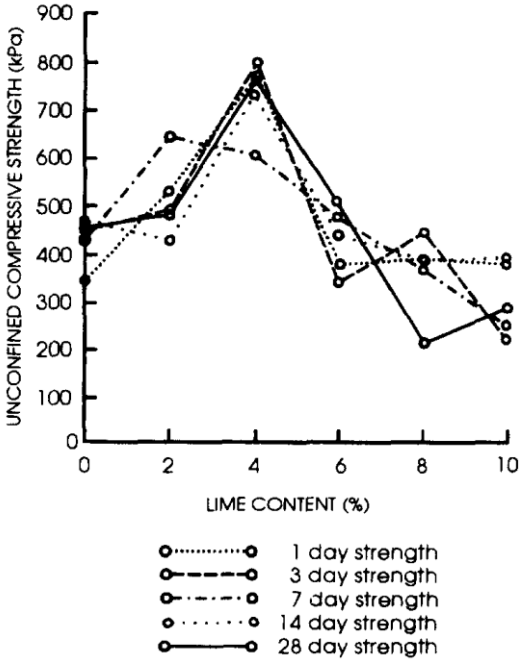

Figure 2.3 Effect of lime content and curing time on the UCS of expansive soil after (Bell 1996)

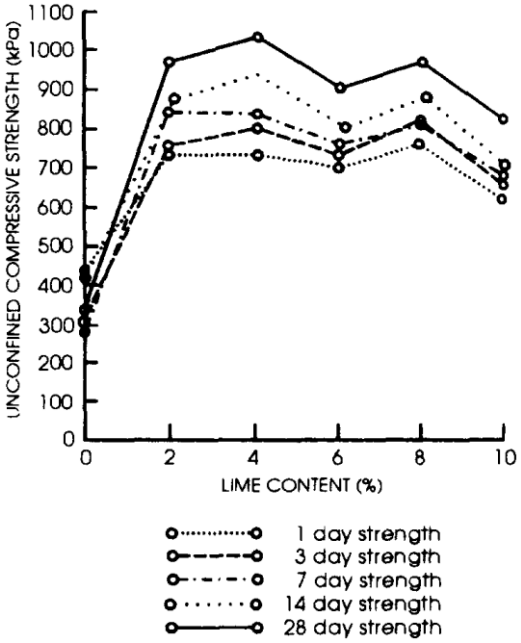

Figure 2.4 Effect of lime content and curing time on the UCS of clayed soil after (Bell 1996)

Zha et al. (2008) performed similar experiment studies on stabilised expansive soil using industrial by-product fly ash and lime inclusions. The findings of their study revealed that the properties of stabilised expansive soil were improved significantly with the increase

in additive content and curing time prolonged. As shown in Figure 2.5, the effect of 7 days of curing on the unconfined compressive strength was clearly observed, which displayed a significant increase in the unconfined compressive strength with increasing percentage of fly ash ranging from 9% to 12%. Then, there was a reduction in the unconfined compressive strength for any percentage of fly ash greater than 12% added to lime-expansive soil admixtures. Therefore, the optimum of fly ash content for improving the compressive strength of treated expansive soil was I a range of 9% to 12% as presented in Figure 2.5. This indicates that the quantity of fly ash up to optimum content can induce pozzolanic reaction and cemented material can effectively contribute to the development of the compressive strength, whereas the additional quantity of fly ash acts as unbounded silty particles, which has neither fiction or cohesion, causing the decrease in the strength (Bell 1996).

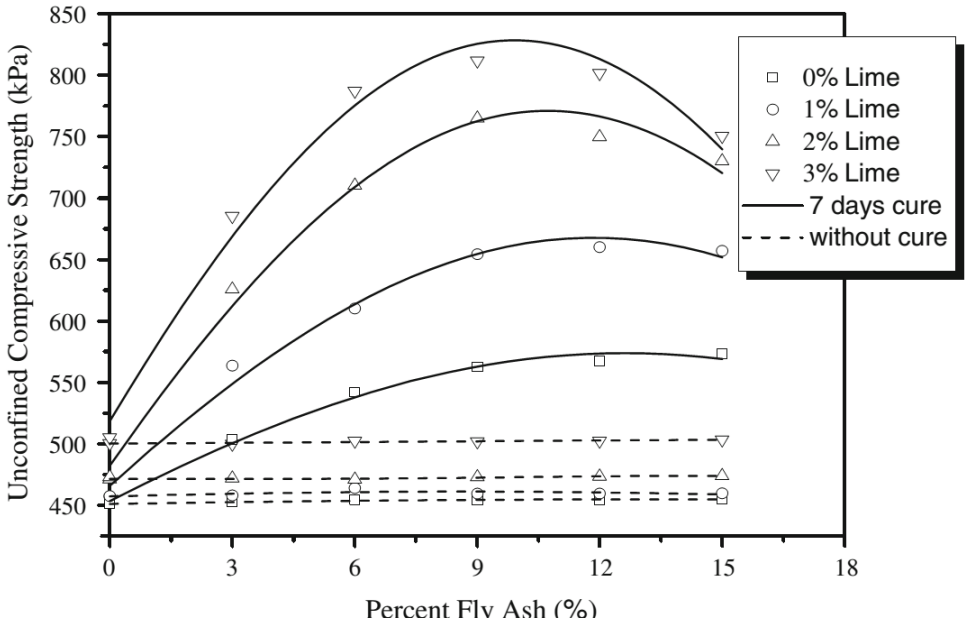

Figure 2.5 Effect of fly ash content and curing time on the UCS of lime treated expansive clay after (Zha et al. 2008)

2.2.4.2. Effect of pH Values on the Compressive Strength during Lime Stabilisation Process

Aldaood et al. (2014b) performed experimental investigations on the long-term stability of lime stabilised gypseous soils known as problematic soils, the effect of wetting-drying cycles on the mechanical behaviour of fine-grained soils with different curing times of 2, 7 and 28 days and various gypseous contents of 0, 5, 15 and 25% in combination with 3% lime. UCS test was of the main tests used to investigate the mechanical behaviour and the long-term stability of lime stabilised gypseous soils. After the end of the unconfined compression test, a 20 g portion of every failed untreated and treated UCS soil sample was used to determine the pH value in order to study the effects of curing time and additive contents on the compressive strength as well as the development of reactions at the microstructural level. Based on the reported laboratory test results, they indicated that the addition of lime increased pH, which promotes cation exchange of lime stabilised gypseous soils, whereas the increase in curing time resulted in the reduction of pH value as shown in Figure 2.6. Moreover, the increase in the pH values facilitates the dissolution of silica and alumina from clay particles, and then such silica and alumina combine with calcium to form cementitious compounds (i.e. CSH, CAH and ettringite) that support stronger soil samples. They also asserted that the pozzolanic reaction is a time and temperature-dependent reaction. Hence, the change in pH value depends on the reactions between soil, lime and gypsum inducing the formation of cementitious compounds. A high alkaline environment is frequently in favour of the dissolution, crystallization of ettringite (CASH) and the formation of new forms of hydrated silicates (CSH) and aluminates (CAH). They also reported that the pH reduction of lime stabilised gypseous soils with increasing curing time might be attributed to decrease in calcium (Ca^{2+}) and

hydroxyls (OH^-) ions due to pozzolanic reactions and the new formation of ettringite induced by the reactions between soil, lime and gypsum.

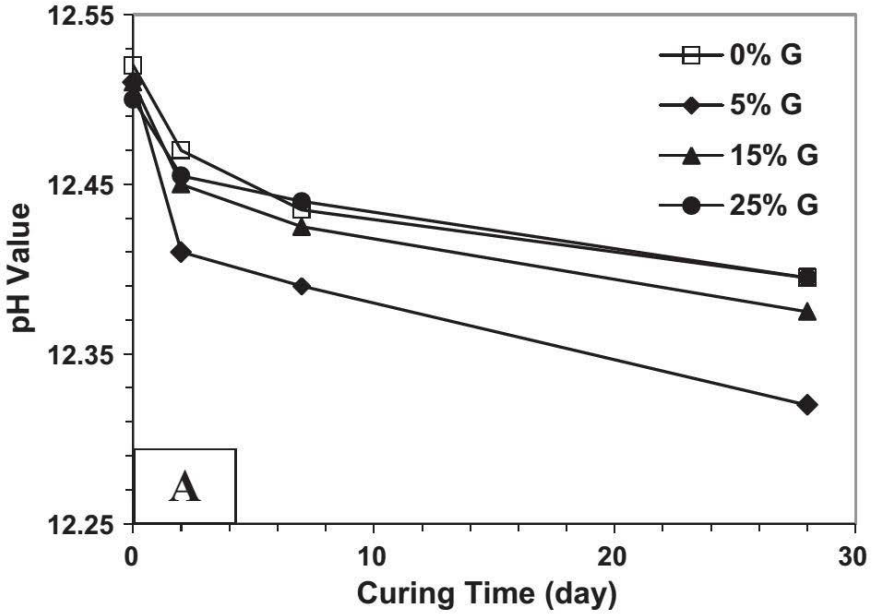

Figure 2.6 Variation of pH values of gypseous soil with curing time and additive content after (Aldaood et al. 2014b)

Chen & Lin (2009) also reported similar test results based on the experiment investigations undertaken on the variation of pH values with different curing time and incinerated sewage sludge ash-cement contents at a combination ratio of 4:1 as presented in Figure 2.7. Chen & Lin (2009) confirmed that the pH values increased with increasing amount of sludge ash-cement content from pH of 8.7 for untreated soil to a high pH level of 11.2 for 4% sewage sludge ash-cement combination treated soft soil. However, the pH values increased slightly to a certain extent for any sludge ash-cement admixture exceeded 4%. This phenomenon might be due to the calcium saturation principles of pH values and the mechanism of stabilisation. Moreover, they denoted that the pH values of treated soft soil decreased with the extension of curing age, which could be attributed to

the gradual decrease in the amount of calcium during the stabilisation progress. As a result of the stabilisation process, the new formations of cementitious products consisting of silica and calcium silicates, which assist better resistance to compressive load, were established corresponding to a weak alkaline environment as curing time increased.

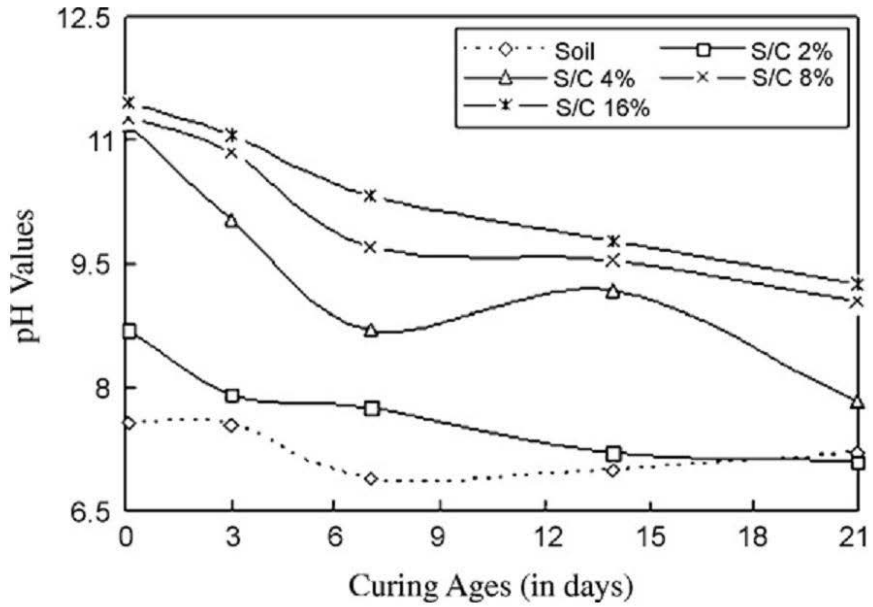

Figure 2.7 Relationship between pH values and curing ages with different amount of sludge ash-cement combination after (Chen & Lin 2009)

Solanki et al. (2009) conducted a laboratory study to evaluate the influence of different percentages of hydrated lime, cement kiln dust and fly ash on the pH values of stabilised silty clay. As can be seen in Figure 2.8, the pH values increased rapidly at lower additive contents. For example, only 2% lime content added to silty clay produced a high pH value of 12.3, meanwhile 10% cement kiln dust stabilised soil resulted in a pH level of 12.3. Adding 10% fly ash C into soil admixture gave a pH value of 11.5. Those pH values were determined to satisfy the sufficient lime requirement to make cation exchange

and pozzolanic reactions happen in accordance with ASTM D6276 (2006). However, the slight increase in pH values was clearly observed at higher additive content referring to Figure 2.8. At very high additive contents, the pH values approached to roughly 12.5. The increase in pH values with increasing additive content is due to the concentration of calcium (Ca^{2+}) ions surrounding clay particle surface, which results in the change in clay fabric due to flocculation and cation exchanges. A similar effect of pH on changes in clay matrix was also reported by Chew et al. (2004).

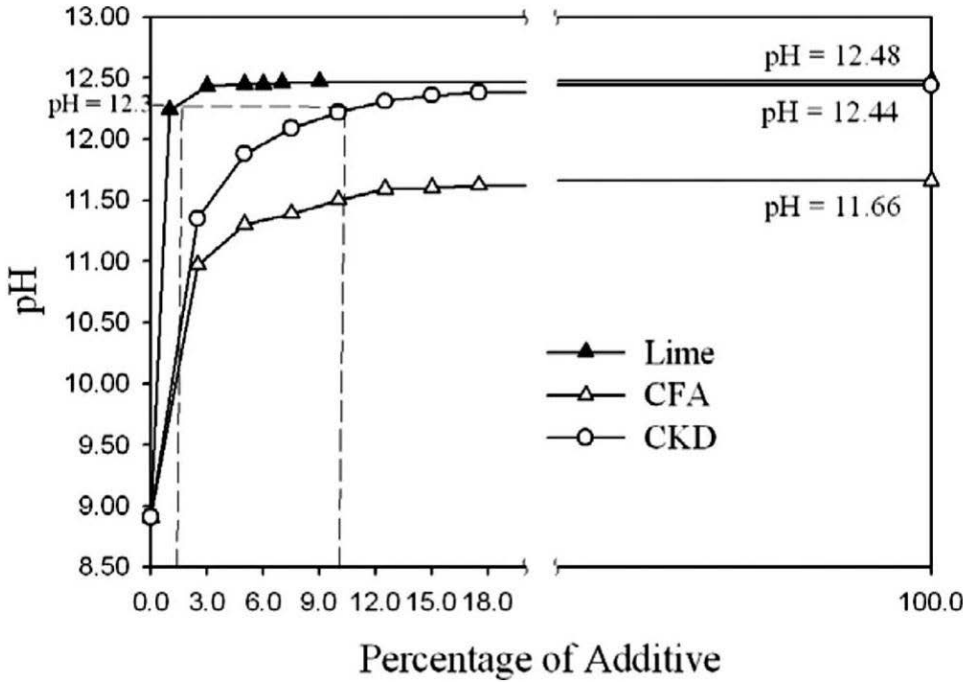

Figure 2.8 Variation of pH with the amount and types of additive after (Solanki et al. 2009)

2.2.4.3. California Bearing Capacity (CBR)

Anupam et al. (2013) investigated the influence of bagasse ash and fly ash additions on soaked CBR values of clayey soil with different fly ash and bagasse ash content from 0%

to 35% and various curing periods of 3, 7, 14, and 28 days. The test results shown in Figure 2.9 indicate that the soaked CBR values of treated clayed soil increased as the addition of fly ash and bagasse ash content increased up to 25% and thereafter these soaked CBR values started decreasing to 35%. Moreover, they mentioned that the CBR increased from 7.8% to 8.5% as the curing period increased from 3 to 28 days at 25% of fly ash mixed with clayey soil. In the case of bagasse ash, they reported that the CBR improved progressively up to 25% bagasse ash-clayey soil mixtures and then the CBR of treated clayey soil decreased with further addition of bagasse ash. They asserted that the CBR increase of treated soil was more pronounced for fly ash treated soil when compared to bagasse ash treated clayey soil. They also indicated that the low CBR of clayey soil was attributed to its inherent low strength, which was due to the dominance of the clay fraction. Meanwhile, the improvement of soaked CBR values observed for soils mixed with stabilisers was due to the frictional resistance contributed from the addition of fly ash and bagasse ash.

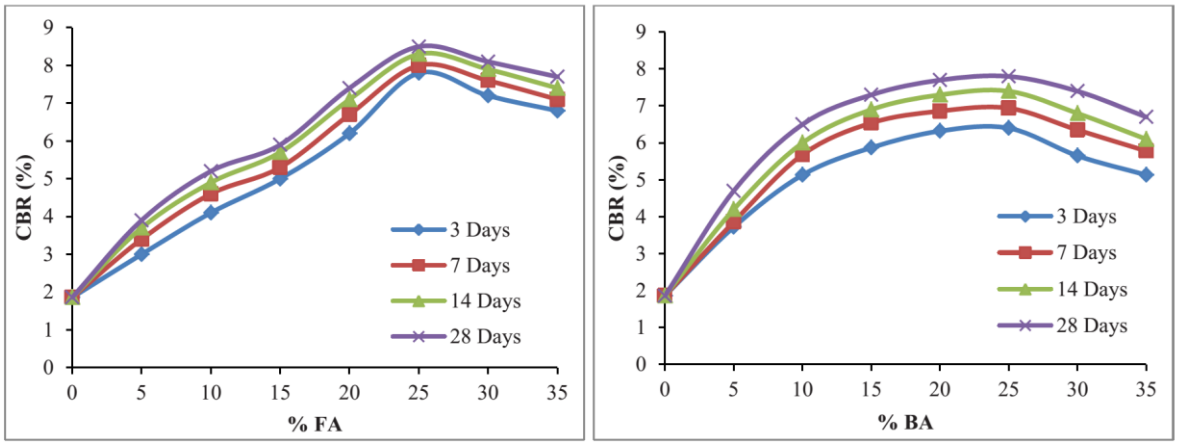

Figure 2.9 Effect of fly ash (FA), bagasse ash (BA) content and curing time on the CBR of treated clayey soil after (Anupam et al. 2013)

2.2.4.4. Linear Shrinkage (LS)

Bell (1996) studied the influence of lime on the shrinkage characteristics of expansive clayey soil by changing percentage of lime inclusion from 0% to 10%. As shown in Figure 2.10, it is clearly observed that the linear shrinkage of lime treated expansive soil decreased from almost 14% down to less than 3% as lime content increased from 0% to 10%. Therefore, Bell (1996) asserted that the addition of lime significantly improved the linear shrinkage of treated expansive clayey soil, meanwhile removed their swelling potential.

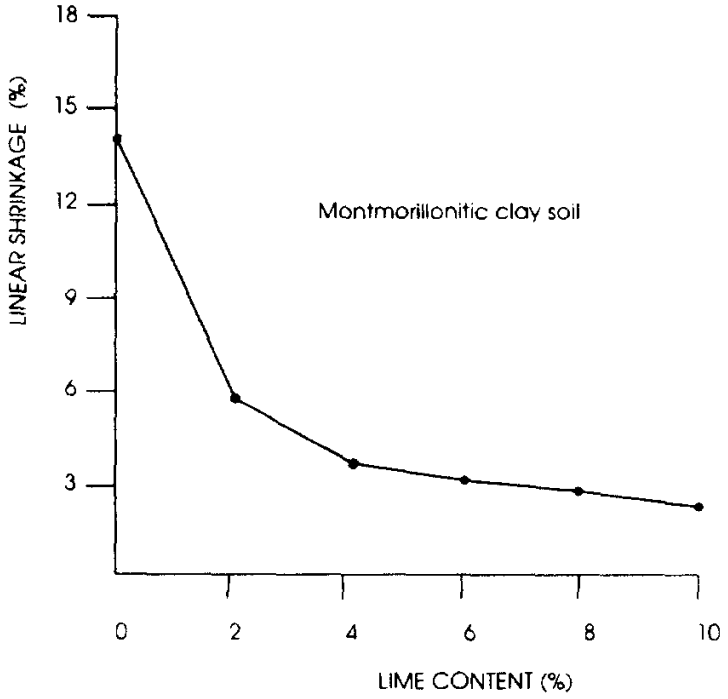

Figure 2.10 Effect of lime content on the linear shrinkage of montmorillonite clay soil after (Bell 1996)

Zha et al. (2008) conducted experimental study on the shrink-swell behaviour of expansive soil stabilised with fly ash and lime combination by varying lime content from 0% to 3% and fly ash content from 0% to 15%, referring to Figure 2.11 for more details.

Based on the experimental results of the axial shrinkage tests before and after the expansive treatment with fly ash and lime, they indicated that the values of axial shrinkage significantly decreased when fly ash and lime content increased. Moreover, they denoted that the addition of fly ash and lime known as non-expansive silt-size particles into the expansive soil could reduce the shrinkage-swell properties to some extent. They explained that fly ash has potential to provide multivalent cations, which promote flocculation of clay particles by cation exchange that was consistent with previous research reported by Mitchell (1993). As a result, the specific area and water affinity on the samples decrease, which indicate a reduction in the values of swell-shrinkage properties of stabilised expansive soil.

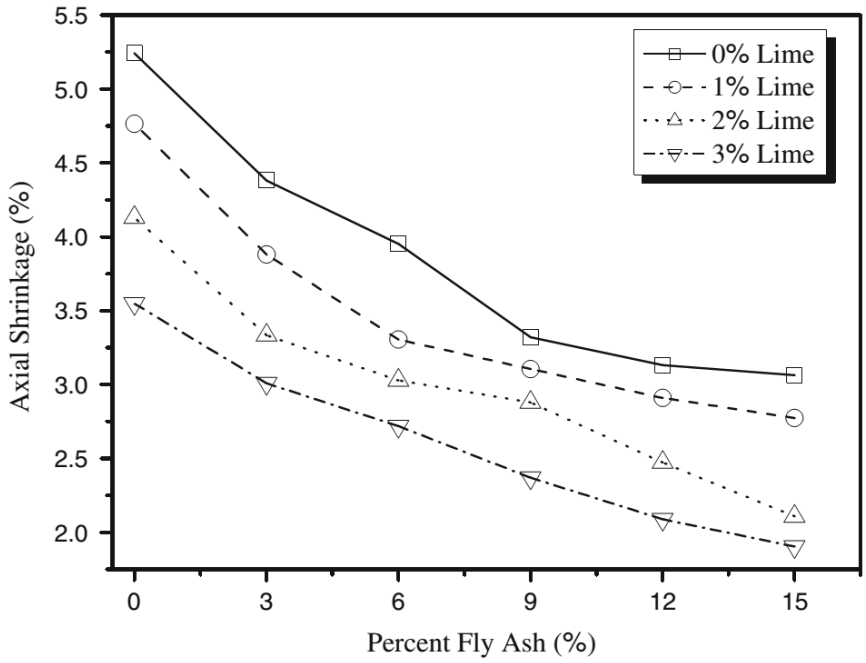

Figure 2.11 Variation of axial shrinkage of expansive soil mixed with various percentages of fly ash-lime after (Zha et al. 2008)

2.2.4.5. Swell Potential

Phanikumar et al. (2014) studied the variation of swell characteristics of lime-blended and cement-blended expansive clays as cement content increased from 0% to 20% and lime content increased from 0% to 4%. As can be seen in Figure 2.12, the swell potential decreased with increasing lime content (0, 1%, 2% & 4%) and cement content (0, 10%, 15% & 20%) in the blends. To illustrate the decrease in swell potential, they added that the swell potential of treated expansive clays decreased from 20% to 11.5% when lime content increased from 0% to 4%, and from 20% to 10.75% when cement content increased from 0% to 20%. Those values resulted in the decrease in the swell potential amount of 42.5% for 4% lime and 46.4% for 20% cement treated expansive clays, respectively, when compared with untreated expansive clay. They denoted that the decreased in the swell potential of expansive clays treated with lime or cement could be attributed to replacement of clay particles by lime or cement as well as due to flocculation. They also reported that the decrease in the swell potential was more noticeable for lime than cement inclusion for expansive soil treatment because lime is more pozzolanic in nature, and consequently, it controls swelling behaviour better than cement. Therefore, a lesser amount of lime would be sufficient to affect a certain percent reduction in the swell potential than cement.

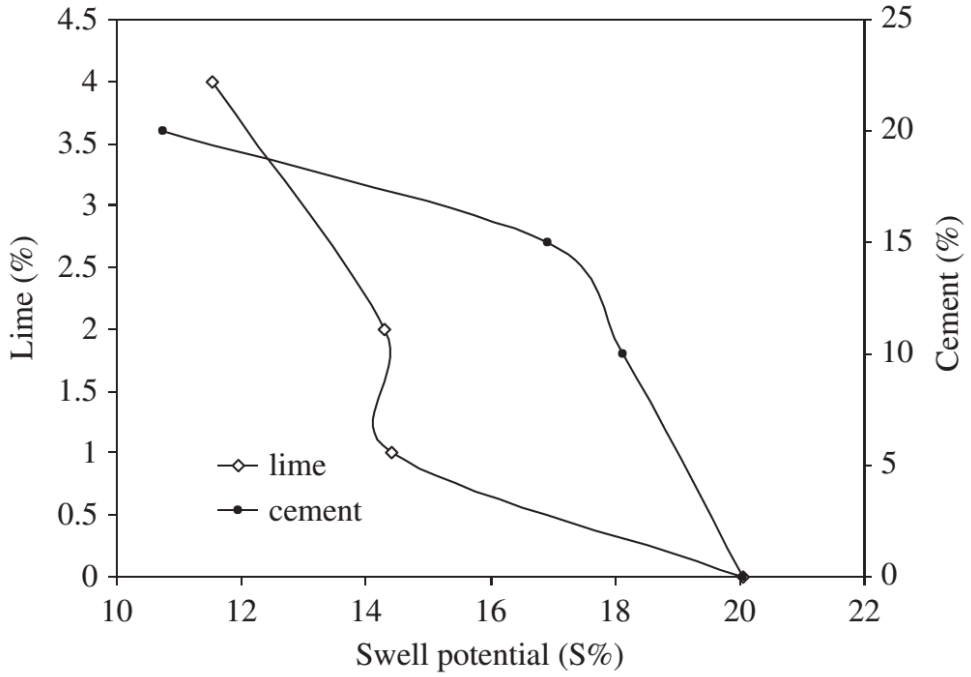

Figure 2.12 Effect of lime and cement on swell potential after (Phanikumar et al. 2014)

2.2.4.6. Swelling Pressure

Phanikumar (2009) carried out an experimental program to examine the influence of fly ash and lime inclusion on swelling pressure of expansive clays as presented in Figure 2.13. Based on the results of Oedometer test, Phanikumar (2009) indicated that the swelling pressure determined from e-logP curves decreased with increasing lime content from 0% to 6% and fly ash content from 0% to 20%. He stated that the influence of lime on the swelling pressure of stabilised expansive clays was more pronounced than fly ash. For example, with addition of 4% lime, the swelling pressure decreased from 330 kPa for untreated expansive soil to 160 kPa for expansive soil treated with lime. Meanwhile, the 20% fly ash inclusion into expansive soil resulted in the decrease in swelling pressure from 330 kPa for untreated expansive soil to 75 kPa. Phanikumar (2009) noted that

swelling pressure could not be measured at 6% lime treated expansive soil because the sample was very hard and could not be compressed to its initial void ratio.

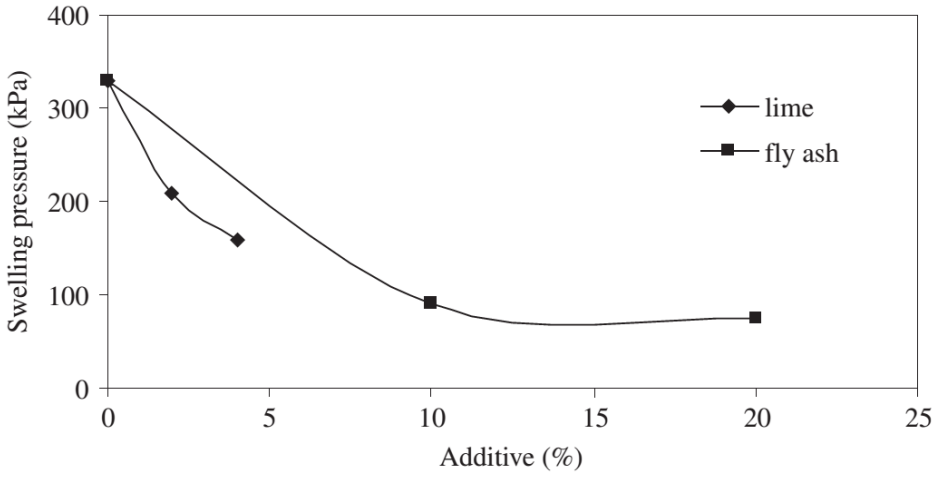

Figure 2.13 Effect of lime and fly ash on swelling pressure after (Phanikumar 2009)

Zha et al. (2008) performed an experimental investigation on the shrink-swell behaviour of expansive soil stabilised with fly ash and lime combination by changing lime content from 0% to 3% and fly ash content from 0% to 15% without curing as presented in Figure 2.14 and with 7 days of curing as shown Figure 2.15 for more details. From the experimental results of the swelling pressure tests before and after fly ash and lime treatment of expansive soil, they indicated that there was a significant decrease in the swelling pressure as combined lime-fly ash content and curing time increased. They explained that the reduction in swelling pressure with increasing combined lime-fly ash inclusions might be due to flocculation of clay particles by cation exchanges and decrease in specific areas of clay particles. Meanwhile, the increase in curing time induced the improvement in swelling pressure of expansive soil stabilised with lime-fly ash combination could be due to the pozzolanic reaction enhancement, which leads to formation of calcium silicate hydrate (CSH) and calcium aluminate hydrate (CAH).

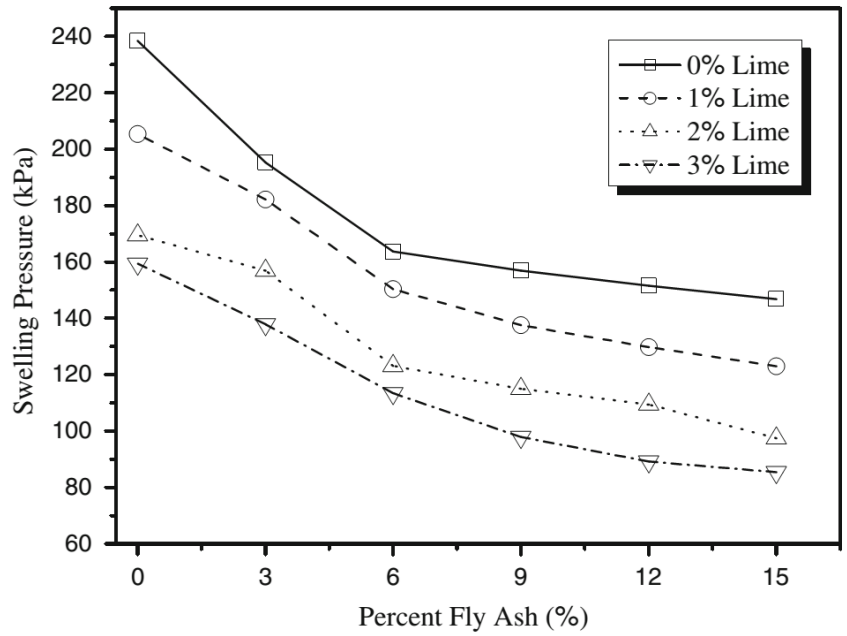

Figure 2.14 Variation of swelling pressure of expansive soil mixed with various percentages of fly ash-lime without curing after (Zha et al. 2008)

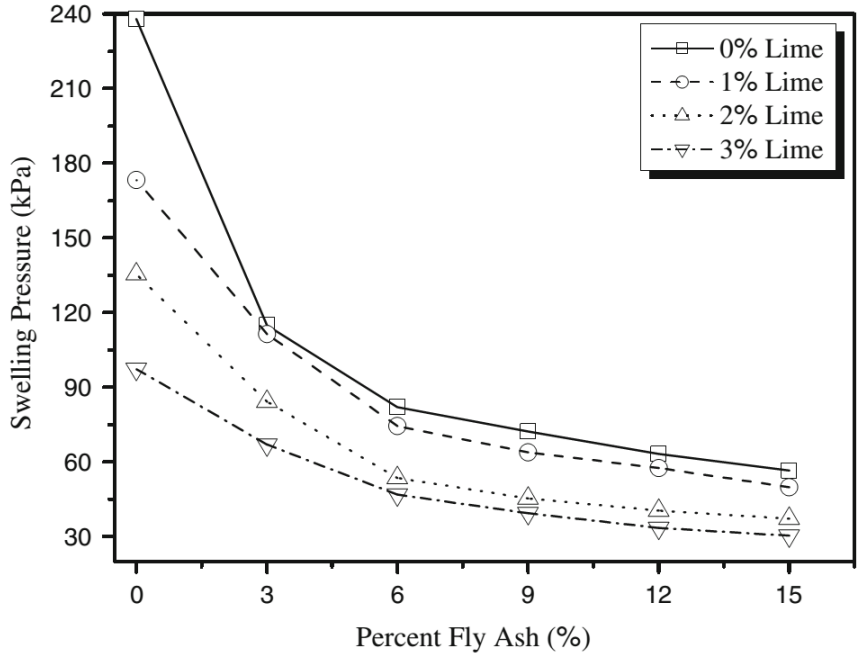

Figure 2.15 Variation of swelling pressure of expansive soil mixed with various percentages of fly ash-lime with curing for 7 days after (Zha et al. 2008)

2.2.5. Behaviour of Fibre Reinforcement of Expansive Soil without or with Cement, Lime Treatment

2.2.5.1. Volume or Linear Shrinkage (LS)

Bhadriraju et al. (2005) employed three different types of fibres, namely carbon fibre, nylon fibre, polypropylene fibre, reinforced expansive soils with various fibre contents of 0.4%, 0.6% and 1.0%. Based on the test results as shown in Figure 2.16, they indicated that the volumetric shrinkage strain decreased with increasing fibre contents, whereas it increased with increasing the compaction moisture content. Referring to Figure 2.17, the influence of fibre types on the shrinkage strain of reinforced expansive soils was observed and compared. They reported that carbon fibre was on the most effective fibre for minimising the volumetric shrinkage strain, followed by nylon fibre and polypropylene fibre, respectively. According to Bhadriraju et al. (2005), the improvement in the volumetric shrinkage strain might be due to the high tensile strength of fibres and the soil-fibre interaction as well as the interlocking mechanism of soil particles. Bhadriraju et al. (2005) asserted that when fibre reinforced soil sample is subjected to shrinkage, fibres in the soil matrix begin to mobilise the tensile resistance of fibres and consequently force soil particles coming into contact by cohesion to facilitate resistance to the shrinkage cracking. Moreover, they denoted that the dry unit weight reduction of soils reinforced with fibre addition could result in the enhancement of the swelling and shrinkage potential. That was consistent with previous investigations reported by Kota et al. (1996).

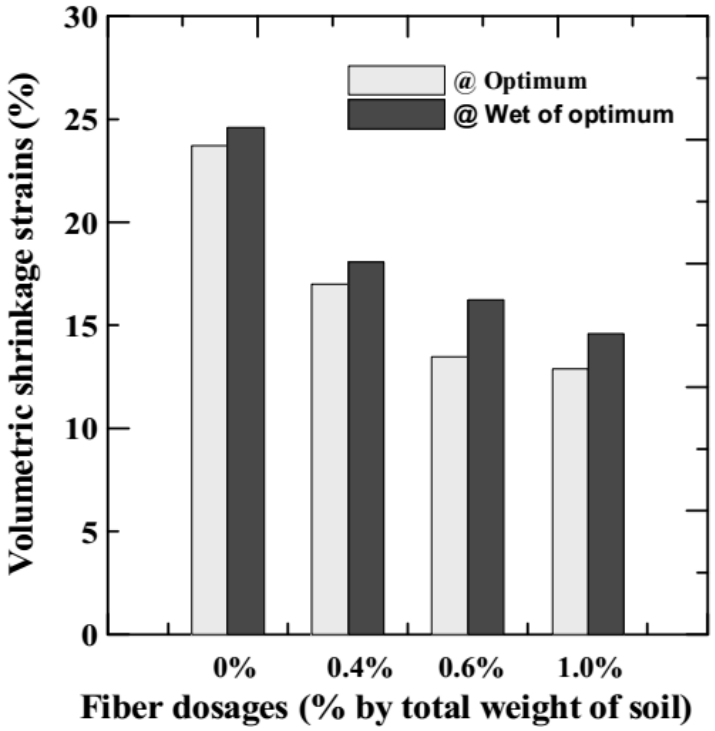

Figure 2.16 Influence of fibre contents and compaction moisture contents on the volumetric shrinkage strain of soils reinforced with carbon fibre after (Bhadriraju et al. 2005)

In addition, Jayasree et al. (2015) reported the volumetric shrinkage test results of expansive soils reinforced with two different lengths of coconut fibre: (1) coir pith fibre sieve passing 4.75 mm and (2) short coir fibre retained on 4.75 mm, along with increasing fibre content up to 3.0%. It was observed in Figure 2.18 that the introduction of coconut fibre decreased the volumetric shrinkage strain of reinforced expansive soils when coconut fibre content increased. They also indicated the reduction of the volumetric shrinkage strain varied with fibre length and the employed shrinkage tests. For example, as observed in Figure 2.18, for soil samples reinforced with coir pith fibre, the decrease in the shrinkage strain was ranging from 10% to 20% for the adopted 3D shrinkage strain test and from 13% to 29% from the used shrinkage limit test, respectively. Jayasree et al.

(2015) concluded that the volumetric shrinkage strain reduction could be attributed to the decrease in the plasticity of expansive soil reinforced with coir pith or short coir fibre.

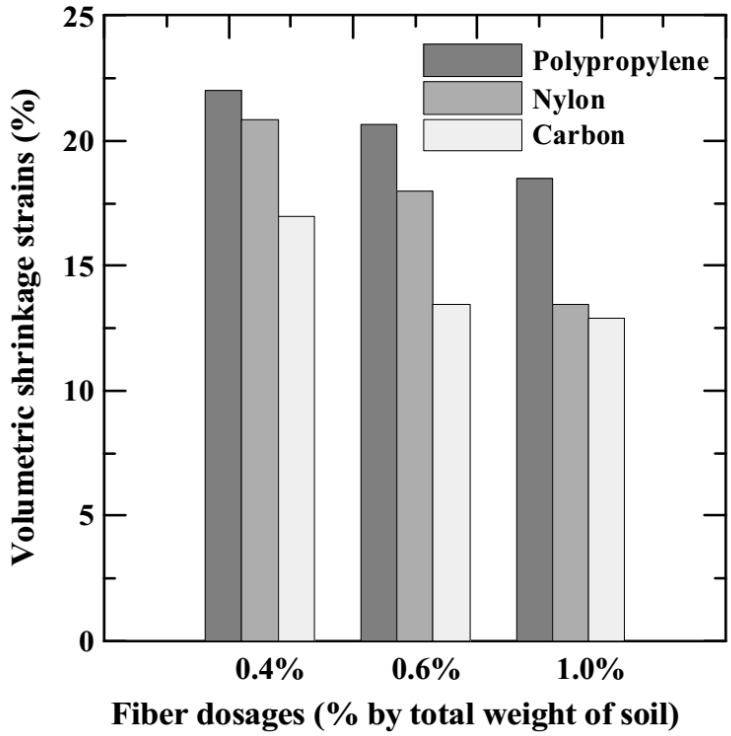

Figure 2.17 Influence of fibre types on the volumetric shrinkage strain of soils with fibre reinforcement after (Bhadriraju et al. 2005)

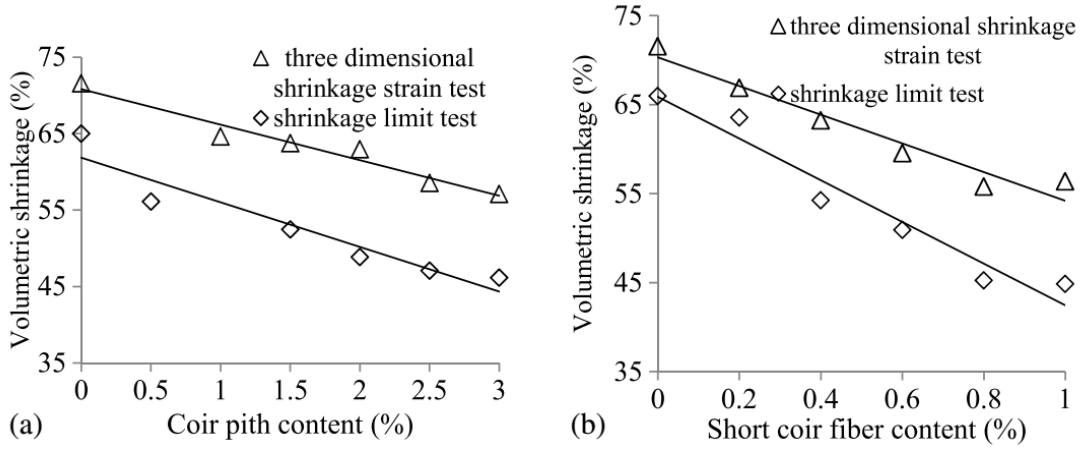

Figure 2.18 Effect of fibre length on the volumetric shrinkage strain: (a) coir pith fibre content; (b) short coir fibre content after (Jayasree et al. 2015)

2.2.5.2. Unconfined Compression Strength (UCS)

Ahmed et al. (2011) conducted experimental investigations to examine the influence of fibre length, fibre aspect ratio, and fibre contents on the unconfined compressive strength of 3% cement + 10% basanite (recycled gypsum) treated sandy soils with waste plastic trays fibre reinforcement. As observed in Figure 2.19, they found that the compressive strength of stabilised soils increased with waste plastic fibre contents and aspect ratios (fibre length) to a certain extent and then followed a slight decrease in the compressive strength with further increase in the fibre contents and the fibre length. Ahmed et al. (2011) indicated that the compressive strength development of stabilised soils reinforced with higher than 0.5% plastic fibre contents was insignificant or even the peak strength decreased slightly with further increase in the plastic fibre content up to 2%.

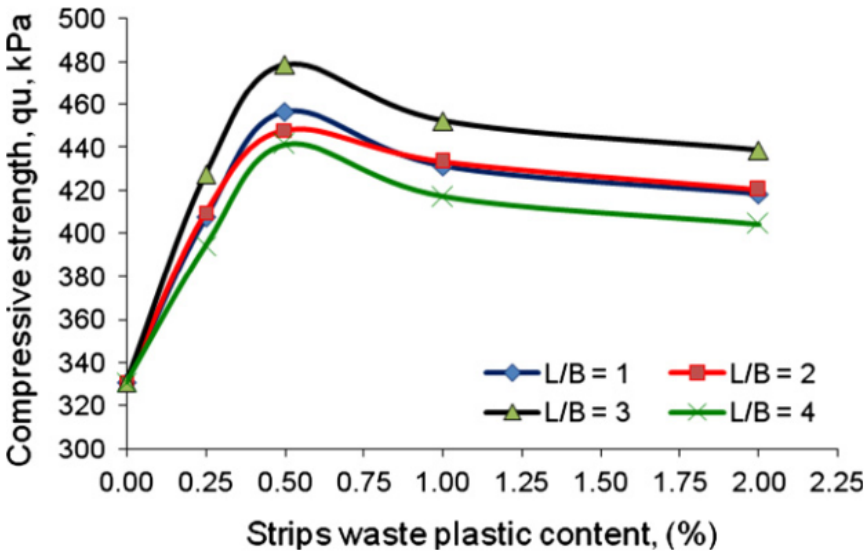

Figure 2.19 Effect of fibre contents and aspect ratios on the compressive strength of treated soils with strips waste plastic fibre reinforcement after (Ahmed et al. 2011)

Muntohar et al. (2013) revealed that the unconfined compressive strength of 12% rice husk ash (RHA) combined with 12% lime treated silty soils with polypropylene waste

plastic fibre reinforcement was influenced by the amount of plastic fibre inclusion. According to Muntohar et al. (2013), it was shown in Figure 2.20 that the peak compressive strength of combined RHA-lime treated silty soils reinforced with waste plastic fibre increased by 35% to 68% when the inclusion of fibre contents increased from 0% up to 1.2%. Investigations by Muntohar et al. (2013) and Ahmed et al. (2011) concluded that the improvement in the compressive strength was attributed to increasing the contact areas between soil particles and plastic fibres. When the waste plastic fibre content increased, the friction between plastic fibre elements and soils particles increased, and consequently enhanced the resistance to the applied loads. They also noted that the decrease in the compressive strength when an excessive fibre content was used to reinforce soils with chemical agents such as lime or cement in their investigations might be attributed to fibres-induced slippage of soil particles.

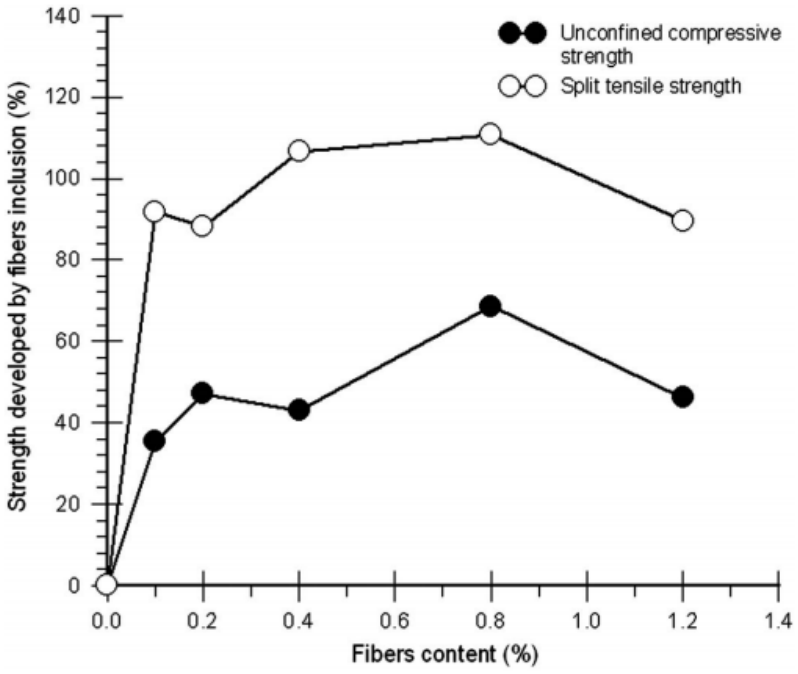

Figure 2.20 Effect of fibre inclusion on the unconfined compressive strength and the indirect tensile strength of 12% rice husk ash+12% lime treated soils reinforced with waste plastic fibres after (Muntohar et al. 2013)

Laboratory investigations by Sharma et al. (2005) found that the unconfined compressive strength of 2.5% cement treated sandy clay soils was significantly influenced with inclusions of two types of natural fibre including Pinus Roxburghii (PR) fibres and Grewia Optivia (GO) fibres, and curing times prolonged as presented in Figure 2.21. Sharma et al. (2005) reported that in comparison with unreinforced soil, the inclusion of PR fibres into the cement-soil mixtures (Figure 2.21a) increased the compressive strength by 137% as PR fibre content increased from 0.5% to 1% followed by a small decrease in the compressive strength with further increase in the PR fibre content to 2%. Whereas, the improvement in the compressive strength of 2.5% cement treated soil reinforced with GO fibres (Figure 2.21b) was ranging from 94% to 200% compared with the unreinforced soil strength of 190 kPa as GO fibres content increased in a range between 0.5% and 2%. It was obvious that the compressive strength improvement was more pronounced for stabilised soils reinforced with GO fibres than PR fibres. According to Sharma et al. (2005), the improvement in the compressive strength of cemented soil reinforced with natural fibres could be attributed to soil-fibres interaction resulting in the better fibres bond as PR fibre inclusions increased to 1%. However, the compressive strength decrease with additional fibre inclusions could be due to slipping of PR fibres over each other because of their fibre structure. They added that the reduction of the compressive strength was not observed for cemented soil reinforced with GO fibres as the inclusion of fibre content increased, which might due to the much better interaction between GO fibres and soil particles as well as the resultant GO fibres bonds did not allow slippage of fibres over each other. Sharma et al. (2005) found that the higher tensile strength of GO fibres could facilitate better fibres-soil bonds that promoted the more compressive strength of cemented soils reinforced with GO fibres.

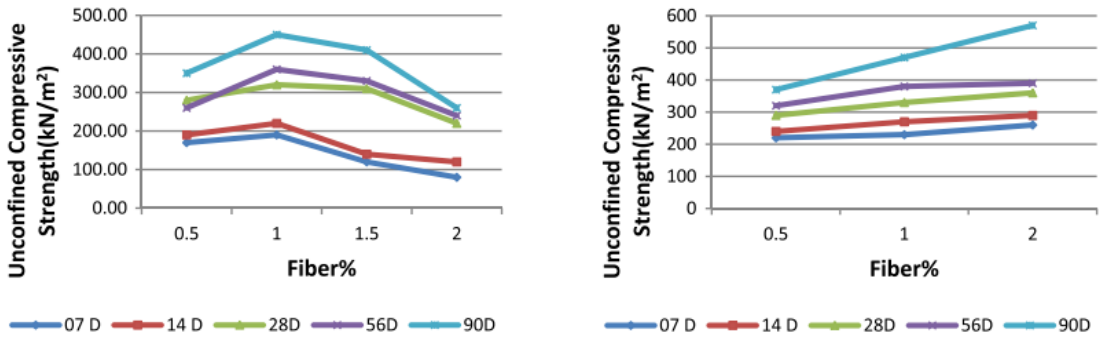

a. Pinus Roxburghii

b. Grewia Optivia

Figure 2.21 Effect of fibre contents and curing time on the compressive strength of cement treated clayey soils with natural fibre reinforcement: (a) Pinus Roxburghii fibres; (b) Grewia Optivia fibres after (Sharma et al. 2005)

2.2.5.3. Indirect Tensile Strength

Based on the results of the indirect tensile strength tests conducted on 3% cement combined with 10% recycled gypsum treated sandy soils with fibre reinforcement of waste plastic trays, Ahmed et al. (2011) revealed that the introduction of waste plastic fibre to reinforce soils caused an appreciable increase in the tensile strength as fibre content increased 0.25% to 1%. Then, it was followed by a slight decrease in the tensile strength with further increase in the fibre inclusions up to 2% as observed in Figure 2.22. That behaviour was clearly observed for every aspect ratio from 1 to 4, referring to Figure 2.22. Ahmed et al. (2011) indicated that the highest tensile strength was obtained for 1% waste plastic fibre reinforced soils stabilised with cement and recycled gypsum combination. Relations between aspect ratios (fibre length) and plastic fibre contents associated with the ratio of the tensile strength to the compressive strength were plotted in Figure 2.23. As seen from the figure, the average ratio of the tensile strength to the compressive strength of stabilised soils reinforced with waste plastic fibre increased from

0.20 to 0.25 as fibre content increased from 0% to 2%. The results reconfirmed that the presence of waste plastic fibre improved the tensile strength associated with the compressive strength of stabilised soils. Ahmed et al. (2011) concluded that the tensile strength improvement of stabilised soils with fibre inclusions was attributed to an increase in plastic fibre elements and orientation in favour of the tensile strain directions. Therefore, an increase of plastic fibre inclusion to a certain fibre content resulted in the corresponding increase in chances of a large number of fibre elements orientated in the principle tensile strain that facilitated the better resistance to tensile loads of stabilised soil with fibre reinforcement (Ahmed et al. 2011).

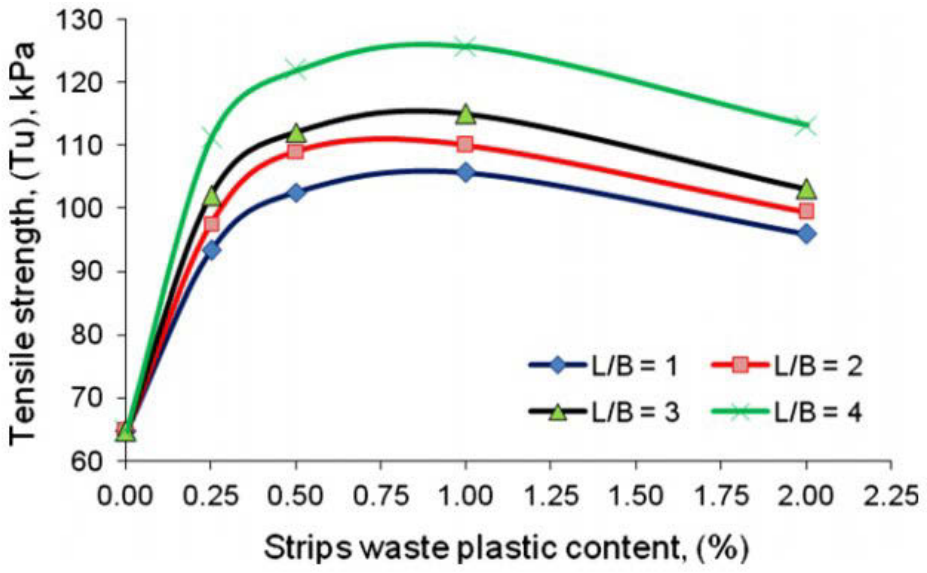

Figure 2.22 Effect of fibre contents and aspect ratios on the indirect tensile strength of treated soils with strips waste plastic fibre reinforcement after (Ahmed et al. 2011)

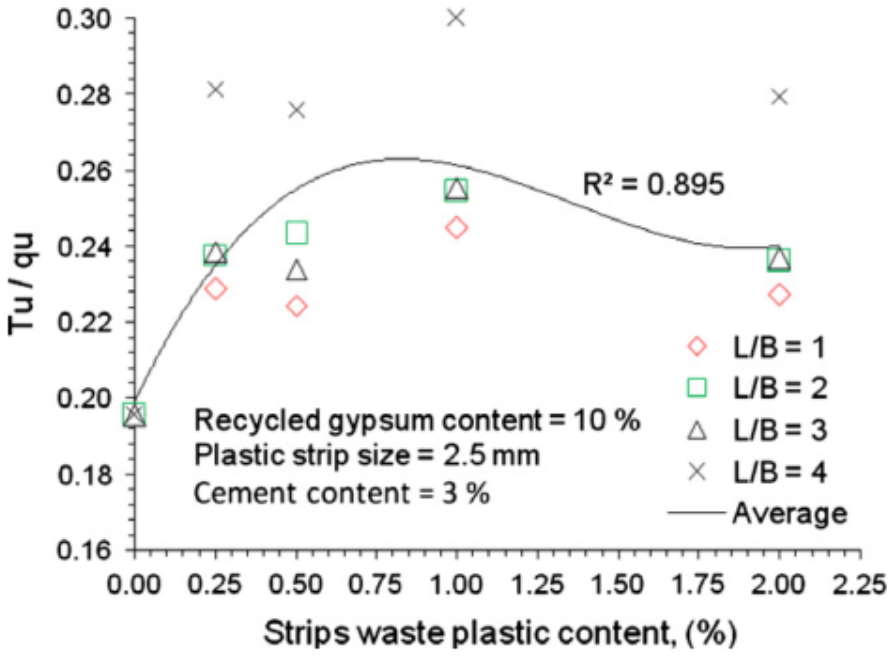

Figure 2.23 Effect of fibre contents on the ratio of indirect tensile strength and compressive strength after (Ahmed et al. 2011)

Investigations by Muntohar et al. (2013) as shown in Figure 2.20 confirmed that the indirect tensile strength of stabilised soils reinforced with waste plastic fibres increased by 88%-110% when the fibre content increased from 0% up to 1.2%. In addition, it was observed in Figure 2.20 that the increment of the tensile strength was more noticeable than that of the compressive strength of stabilised soils with fibre reinforcement. Thus, Muntohar et al. (2013) concluded that the inclusion of waste plastic fibres into the RHA-lime-soil mixtures played a more significant role in improving the tensile strength than the compressive strength of stabilised soils. Furthermore, Kumar & Gupta (2016) conducted an experimental study on the indirect tensile strength of cement-pond ash (PA)-rice husk ash (RHA) stabilised Kaolin clay soils with polypropylene fibres inclusion as presented in Figure 2.24. Their investigation showed that the presence of polypropylene fibres significantly increased the tensile strength of stabilised soils as the

fibre content increased from 0% to 1.5%. Kumar & Gupta (2016) asserted that the inclusion of fibres into the stabilised soils could reduce the further development of tension cracks subjected to the applied tensile loads. The total contact area between fibres and soil particles increased with increasing the fibre content and consequently increased the friction between them, contributing to the increased resistance to the applied tensile forces.

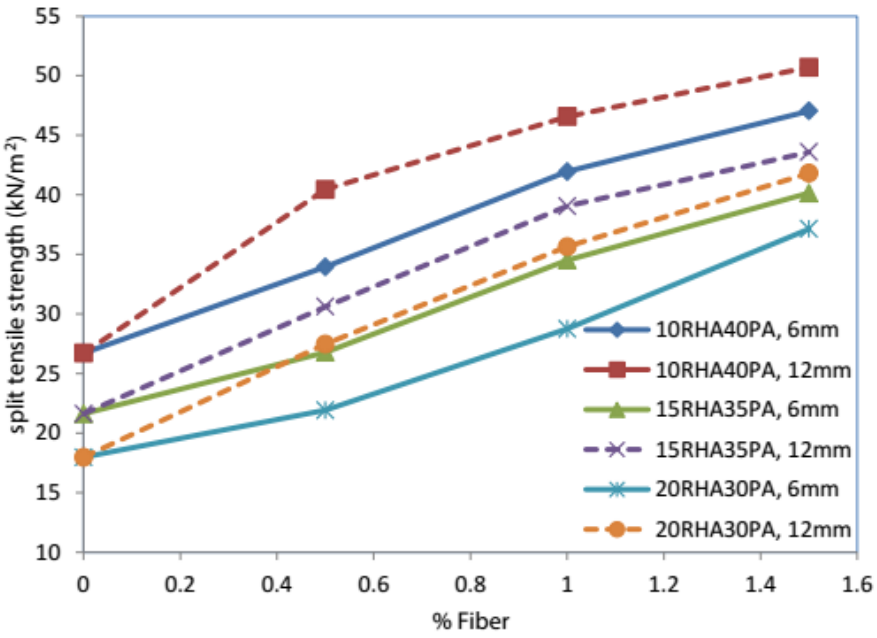

Figure 2.24 Effect of fibre contents on the indirect tensile strength of combined rice husk ash-pond ash stabilised soils reinforced with polypropylene fibres at 4% cement treatment after (Kumar & Gupta 2016)

2.2.5.4. California Bearing Capacity (CBR)

According to the experimental results of CBR tests on 12% RHA + 12% lime treated silty soils without or with polypropylene waste plastic fibre reinforcement, Bhadriraju et al. (2005) revealed that the inclusion of waste plastic fibre into the 12% RHA combined with

12% lime treated silty soil mixtures increased the CBR of treated soils. As observed in Figure 2.25, the soaked CBR increased with increasing waste plastic fibre content from 0% to 0.8%, and then followed by a small decrease in the CBR with further inclusions of fibre content up to 1.2%. Based on the CBR test results, Bhadriraju et al. (2005) suggested that adding a plastic fibre content of 0.8% into soil stabilised with RHA and lime resulted in the greatest CBR value of 53.8% that could meet the requirement for base course materials in accordance with the Indonesian standard SNI 03-1732-1989F.

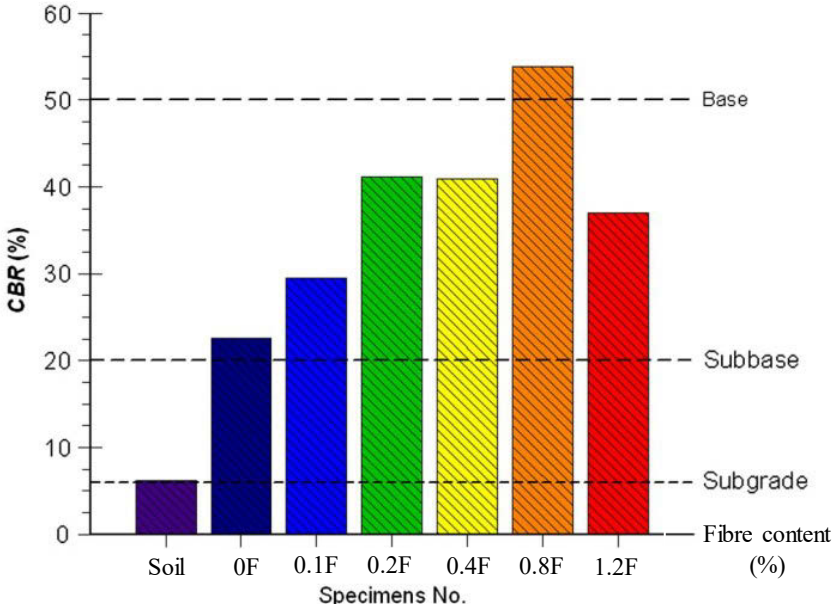

Figure 2.25 Effect of fibre contents on soaked CBR of 12% rice husk ash+12% lime treated soils with waste plastic fibre reinforcement after (Muntohar et al. 2013)

A correlation of the CBR and secant modulus of elasticity derived from the UCS tests on combined RHA-lime treated soils with plastic fibre reinforcement was also reported by Bhadriraju et al. (2005) as illustrated in Figure 2.26. By observation of Figure 2.26, they noted that the bilinear relationship between the secant modulus of elasticity and the CBR was a dominant mechanism for waste plastic fibre reinforcement of soils treated with RHA and lime combination. According to Bhadriraju et al. (2005), the

improvement in the CBR values could be attributed to the pozzolanic reactions between soils, lime and RHA material. In addition, the inclusion of the waste plastic fibre significantly contributed to the CBR enhancement of stabilised soils because of the interaction between the soils and the plastic fibres reinforcement subjected to compaction. Similarly, Nataraj & McManis (1997) also reported that the compaction resistance of fibre reinforcement due to the interaction of soils and fibres controlled the response of the fibres-soil mixtures to compaction.

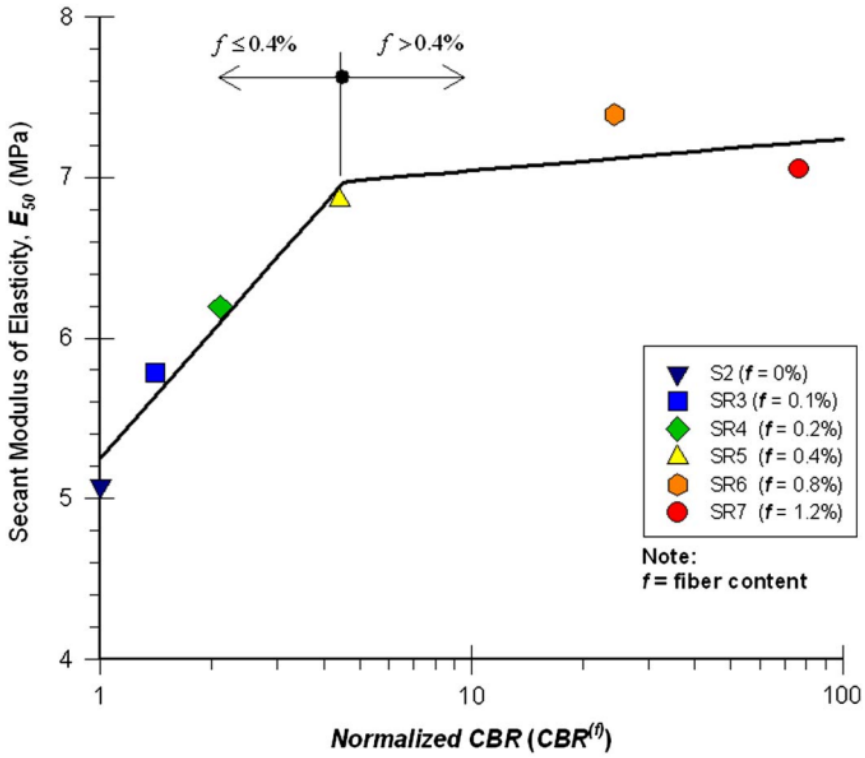

Figure 2.26 Correlation between secant modulus of elasticity and soaked CBR with fibre contents after (Muntohar et al. 2013)

2.2.5.5. Swell Potential

Experimental investigations by several researchers (Estabragh et al. 2014; Mohamed 2013; Viswanadham et al. 2009) found that the introduction of synthetic polypropylene fibre or natural hay fibre into expansive soils improved the swelling potential of stabilised

soil. As observed in Figure 2.27, Estabragh et al. (2014) reported that adding polypropylene fibre with a length of 30 mm and a width of 3 mm into soil resulted in the swelling potential reduction from 21.8% to 13.8% as the fibre content increased from 0.5% to 1.5%. In addition, as shown in Figure 2.28, they stated that increasing fibre length ranging between 10 mm and 30 mm, and fibre width from 0.3 mm to 5 mm while remaining the same fibre content of 1.5% reduced the swelling potential of reinforced soils. As can be seen in Figure 2.28, the most significant reduction of the swelling potential was observed for soil samples reinforced with the polypropylene fibre width of 5 mm. Estabragh et al. (2014) also reported that the addition of polypropylene fibre with a width of 5 mm, length of 30 mm, and fibre content of 1.5% into expansive soil was more effective in improving the swelling potential of treated soils in comparison with 5% and 8% lime treated soils without curing time.

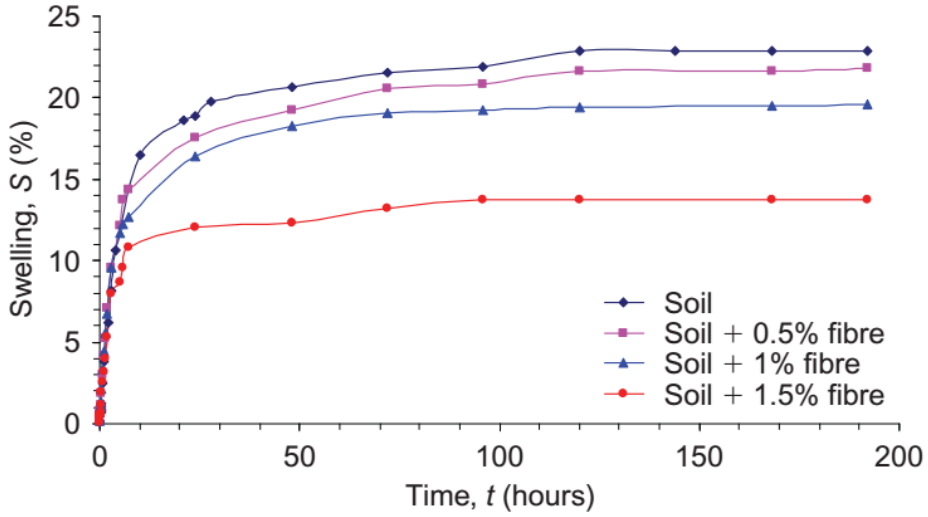

Figure 2.27 Effect of fibre contents on the free swelling strain of expansive soil reinforced with fibre after (Estabragh et al. 2014)

Similarly, Mohamed (2013) found that natural hay fibre reinforcement of expansive soil had a beneficial effect on the swelling behaviour of reinforced soils. As observed in

Figure 2.29, he reported the addition of 1% hay fibre content to reinforce expansive soil reduced the swelling potential by 23% compared with that of non-reinforced expansive soil. Mohamed (2013) also recommended that 1% hay fibre content could be the optimum fibre content for fibre reinforcement of expansive soil as observed in Figure 2.29.

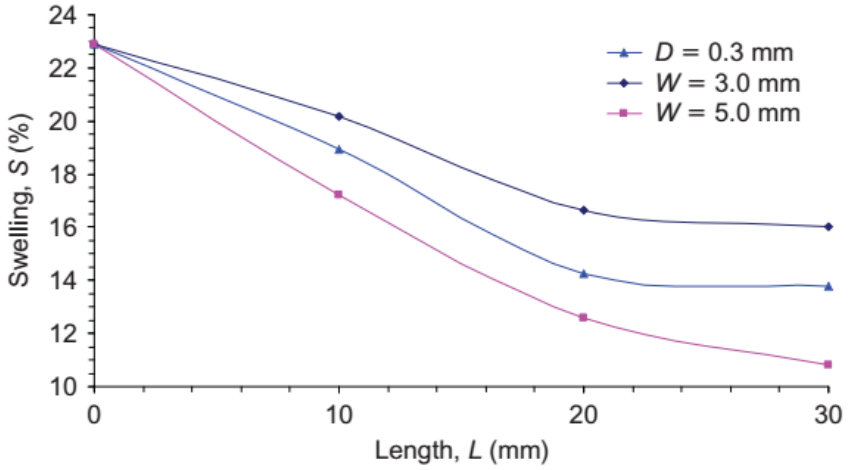

Figure 2.28 Effect of fibre length and diameter on the free swell potential of soil treated with 1.5% fibre content after (Estabragh et al. 2014)

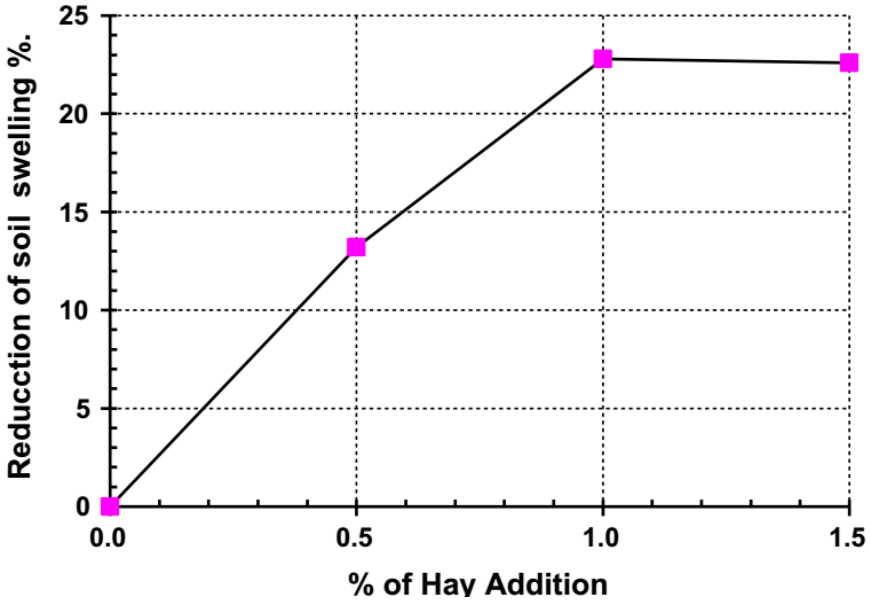

Figure 2.29 Effect of fibre contents on the swelling potential of expansive soil reinforced with hay fibre inclusion after (Mohamed 2013)

2.2.5.6. Swelling Pressure

Estabragh et al. (2014) reported the experimental results of polypropylene fibre inclusion for expansive soil modifications to examine the swelling pressure change of stabilised soils using conventional consolidation device. It was shown in Figure 2.30 that the swelling pressures of stabilised soil reduced from 355 kPa for unreinforced soil to about 60 kPa as the fibre content increased from 0% to 1.5%, resulting in the significant reduction of the swelling pressure by 83%. That behaviour revealed that polypropylene fibre reinforcement could effectively improve the swelling pressure of reinforced soil. In addition, as shown in Figure 2.31, the influence of fibre contents and fibre length on the swelling pressure of soils was observed for soil samples reinforced with polypropylene fibre with a width of 0.3 mm. Estabragh et al. (2014) found that the fibre length and fibre content had notable effects on the swelling pressures of stabilised soils. For example, with 1% fibre reinforced soil as illustrated in Figure 2.31, the swelling pressure reduced by 51% as the fibre length increased from 10 mm to 30 mm. According to Estabragh et al. (2014), the improvement in the swelling pressure with fibre inclusion could be due to replacement of expansive soil particles with non-swelling fibre materials in a given soil volume. Estabragh et al. (2014) presented another possible reason for the swelling pressure decrease was that due to contact between soil particles and fibres, the fibres in the fibre-soil matrix were starched and its tension strength was mobilised during swelling, and the high tensile strength of fibres promoted effective resistance to further swelling. A similar observation of the swelling pressure reduction with increasing fibre contents for expansive soils treated with short coir fibre was also reported by Jayasree et al. (2015).

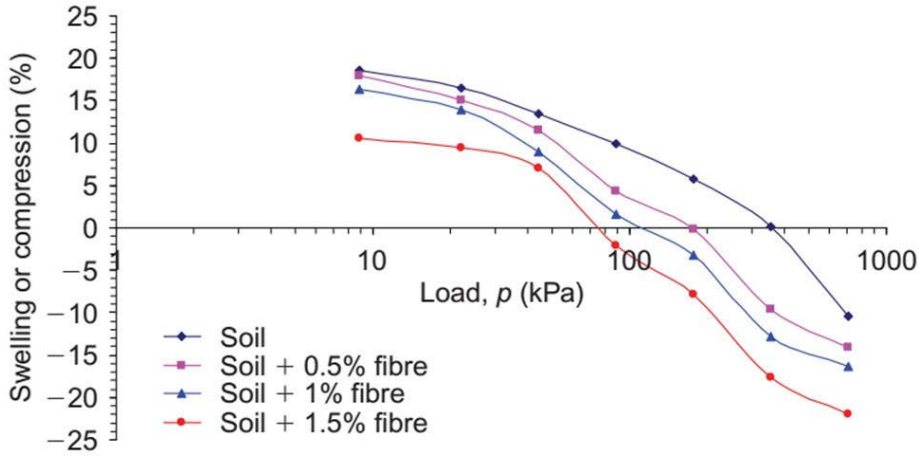

Figure 2.30 Effect of fibre contents on the swelling pressure of expansive soil reinforced with fibre after (Estabragh et al. 2014)

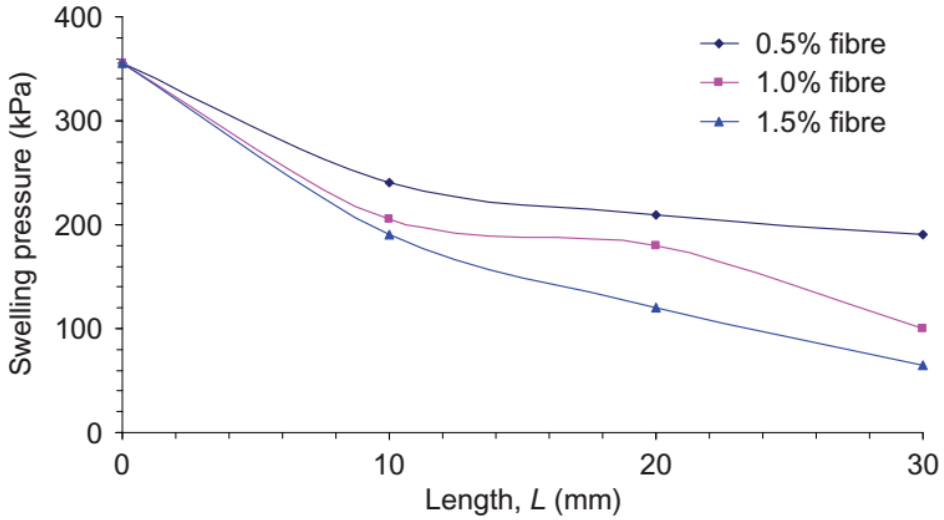

Figure 2.31 Effect of fibre length and fibre contents on the swelling pressure of soil treated with fibre width of 0.30 mm after (Estabragh et al. 2014)

2.2.5.7. Soil Water Characteristics Curves

In facts, field lime treatment of expansive soils is usually at unsaturated state. Therefore, suction is a primary parameter to describe the state of an air-water-soil system. In unsaturated soil, the relationship between water content and soil suction, which is defined

as soil water characteristic curve (SWCC) that can be determined using filter paper method (Bulut & Leong 2008; Bulut et al. 2001), is essential to assess the engineering properties of unsaturated soil. For example, the air entry value (AEV) can be estimated from the SWCC that facilitates predicting the shear strength (Khalili & Khabbaz 1998) on the basis of effective concept and a single stress variable defined in the following equation proposed by Bishop (1959)

$$\sigma' = (\sigma - u_a) + \chi(u_a - u_w) \tag{2.5}$$

In which σ' is the effective stress; u_a and u_w are pore air and pore water pressures, respectively; $(\sigma - u_a)$ is the net stress; $(u_a - u_w)$ is the matric suction; and χ is the effective stress parameter determined by using the unique linear relationship (Khalili & Khabbaz 1998) between χ and matric suction above the air entry value in a log-log scale.

$$\chi = \left(\frac{(u_a - u_w)}{(u_a - u_w)_b}\right)^{-0.55} \tag{2.6}$$

It is well known that lime treated clayey soil can gradually and eventually change the water retention capacity of soil to a certain extent due to cation exchange and flocculation taking place between calcium ions in lime and metal ions on the surface of clay particles (Elkady et al. 2015; Wang et al. 2016). These researchers indicated that the soil water retention capacity was under control of the pore size distribution and lime inclusion could effectively enhance the reduction of interconnection between pores. The larger amount of small size pores resulted in the better soil water retention capacity. Besides that, another explanation for the enhancement of water retention capacity of lime

stabilised clayey soil was that new cementitious products of lime-soil stabilisation were mainly coating the surface of clay soil particles, shortening and blocking the entrance of micro-pores, accordingly increasing the occluded pores of treated soil. In addition to that, hydration products more likely happening at the edges of clay particles could create the strong bonds holding all the soil particles together, altering the interconnection of macro-pores, and as a result, alleviating the macro-pores of the lime-soil matrix.

Having plenty of simulation models are readily available in the literature for use to best fit and transfer the experimental data of the SWCC into mathematical models. Previously studies on covering the mathematical models of SWCC were conducted by researchers (Elkady et al. 2015; Pasha et al. 2016; Puppala et al. 2006) in a more comprehensive manner. Of the many formulation models representing the SWCC, the model of Fredlund & Xing (1994) provides a best fitting and continuous SWCC as a function of either volumetric water content, degree of saturation or gravimetric water content covering a wide range of soil suction between 0 and 10^6 kPa. The Fredlund & Xing (1994) model equation can be expressed as follows:

$$\theta(\psi, a, n, m) = C(\psi)\frac{\theta_s}{\left[ln\left[e + \left(\frac{\psi}{a}\right)^n\right]\right]^m} \tag{2.7}$$

where $C(\psi)$ is a correction function defined as

$$C(\psi) = \frac{-ln\left[1 + \left(\frac{\psi}{\psi_r}\right)\right]}{ln\left[1 + \left(\frac{1000000}{\psi_r}\right)\right]} + 1 \tag{2.8}$$

where ψ = soil suction (kPa); ψ_r = soil suction corresponding to the residual water content (θ_r); θ_s = saturated water content; e = void ratio; and a, n, m = model parameters.

Experimental investigations by Puppala et al. (2006) were conducted on two type of expansive soils (A or D) stabilised with different types of fly ash (F1, F2) or bottom ash (B) combined with polypropylene fibres (P) reinforcement, which aimed to investigate the variation of soil water characteristic curves of stabilised expansive soils with fibre inclusion. In their investigation, relationships between volumetric water content change and soil suction were simulated using the proposed model of Fredlund & Xing (1994). According to the measured results of soil suction tests using pressure plate apparatus as potted in Figure 2.32, Puppala et al. (2006) reported that the volumetric water contents of fly ash stabilised soils reinforced with polypropylene fibres decreased in comparison with natural expansive soil. Whereas, the changes in the soil water characteristics of bottom ash stabilised soils with fibre reinforcement was minimal. Their investigations indicated that the influence of the fly ash stabilisation of expansive soils was more significant than bottom ash stabilisation, meanwhile the presence of polypropylene fibre had no notable influence on the SWCC of ash materials stabilised expansive soils. According to Puppala et al. (2006), the changes in the SWCC were expected to take place because the fly ash used in their investigation was fine and in powder form. Therefore, the fined fly ash altered the pore-size and the particle-size distribution of stabilised expansive soils by means of occupation the original voids of expansive soil and bonding fine clay particles together at their contact points. Those phenomena changed the SWCC of fly ash stabilised soils with fibre reinforcement to become flatter as observed in Figure 2.32. Whereas, since the particle-size of fibres and

bottom ash, and their distribution were coarser than fly ash, the introduction of combined bottom ash and fibre to stabilise expansive soils did not influence the volumetric water contents of stabilised soils that were mainly controlled by the fine fraction and the voids among them (Puppala et al. 2006).

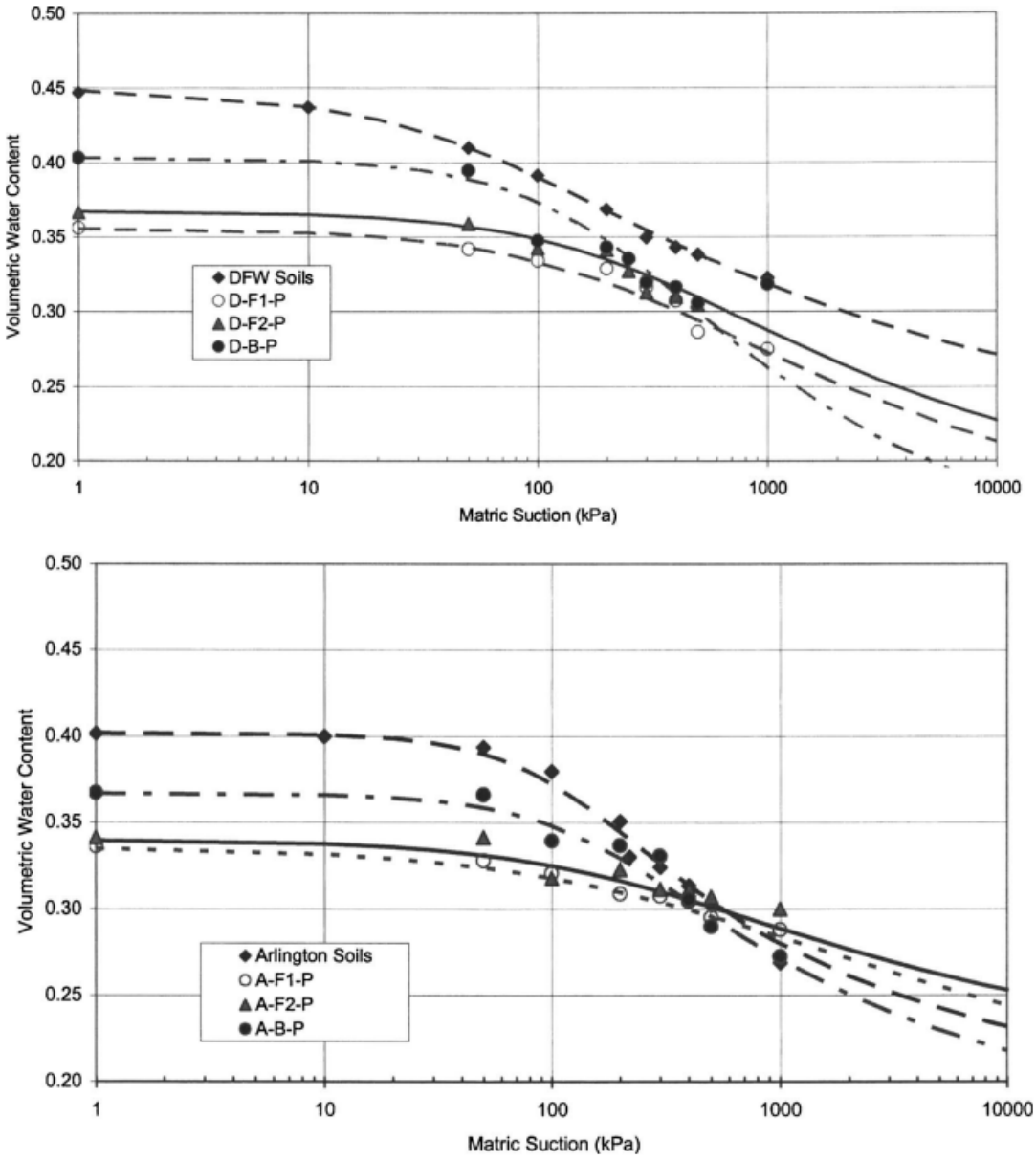

Figure 2.32 Soil water characteristic curves of untreated soils (A or D) and different types of fly ash (F1, F2) or bottom ash (B) treated expansive soils reinforced with polypropylene fibres (P) after (Puppala et al. 2006)

Another investigation by Malekzadeh & Bilsel (2014) carried out on polypropylene fibre reinforced expansive soils without chemical treatment such as lime, cement or fly ash found that the soil water characteristics of reinforced soils, simulated by a proposed model of van Genuchten (1980), increased with increasing fibre content from 0% to 2%. As observed in Figure 2.33, Malekzadeh & Bilsel (2014) concluded that the changes in the SWCC of expansive soils reinforced with propylene fibres could be attributed to a good bonding between the soils and the fibres that prevented the easy air access into the soils.

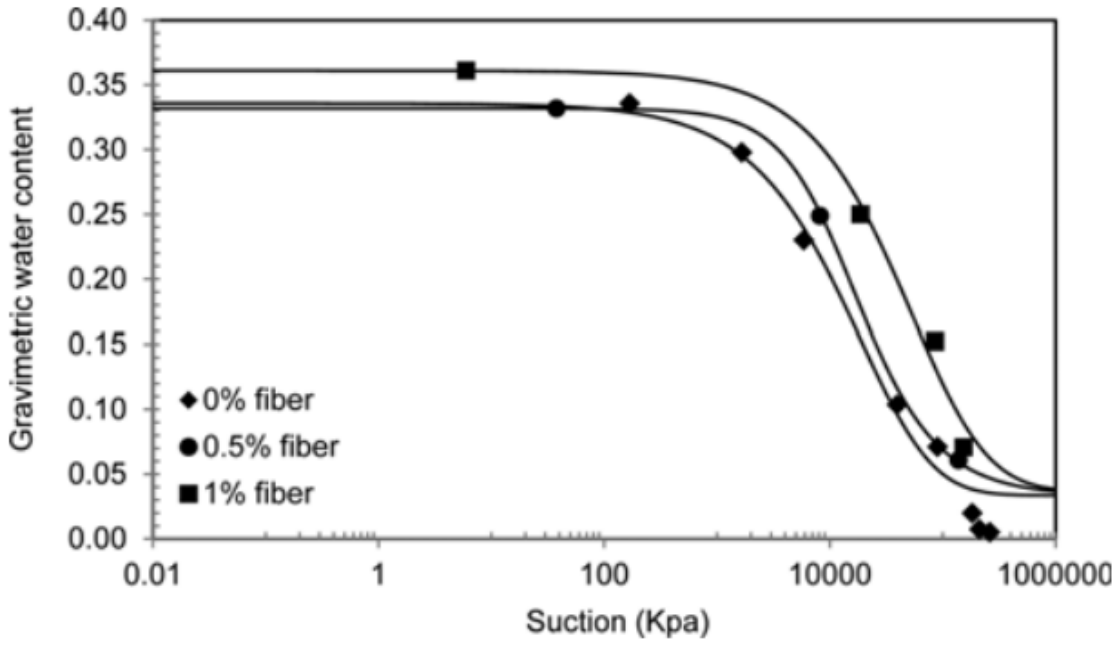

Figure 2.33 Soil water characteristic curves of untreated soil and expansive soils reinforced with polypropylene fibres after (Malekzadeh & Bilsel 2014)

2.3. SUMMARY AND GAP IDENTIFICATION

In this chapter, a comprehensive literature review of the behaviour of expansive soils and the modification techniques of expansive soils as well as the engineering properties of expansive soils treated with waste by-products such as fly ash, bottom ash, natural and synthetic fibres without or with lime or cement combination was carried out and presented. The engineering properties of waste by-products stabilised expansive soils without or with chemical treatment consisted of the unconfined compressive strength, California bearing ratio, the shrink-swell behaviour, the tensile strength, the soil water characteristics, and the pH change with various curing times and additive contents. In addition, many factors affecting the strength of treated soils such as cement or lime content, fibre length (aspect ratio), fibre width, water content, and curing time were thoroughly covered and discussed. From the comprehensive literature review, some conclusions and recommendations for waste by-products stabilised expansive clay soils without or with lime or cement treatment are summarised as follows:

- Investigations of expansive soil stabilisation with lime reported that the unconfined compressive strength of stabilised soils increased significantly by 100% - 225% with increasing lime content from 2% to 5%. It was found that the highest compressive strength was observed for soil samples treated with 4% lime, which implied that 4% lime content was the optimum additive content for expansive soil stabilisation. In addition, the introduction of waste by-products (e.g. rice husk ash, fly ash) into the lime-soil mixtures could extend the compressive strength development of the stabilised soils. It was reported that a combination of 12% rice husk ash (RHA) combined with 4% lime to stabilise expansive soils caused a significant increase in

the compressive strength about 90% compared with lime treated soil without RHA. The compressive strength increase was observed with the combined additive content and the curing time increased. The compressive strength development with increasing additive content and curing time could be due the cation exchange and pozzolanic reaction. The presence of high silica content in the ash materials (i.e. RHA, fly ash) when added in the lime-soil mixtures increased the pozzolanic reaction that promoted the further strength development of the combined ash-lime soil mixtures.

- Experimental studies were undertaken on gypseous soils treated with a combination of ash materials (e.g. sewage sludge ash) and cement to examine the variation of pH values with various curing times and combined additive contents. The pH test results indicated that the pH values increased with increasing additive contents, but decreased gradually with the extension of curing age. That behaviour could be attributed to the gradual reduction in the amount of calcium in the ash-cement-soil mixtures during soil stabilisation in progress, and consequently, the new cementitious products were being generated, which promoted the better resistance to the compressive loads.

- Laboratory investigations reported that combination of fly ash and lime treated expansive soils caused the significant improvement in the shrink-swell behaviour of treated soils as the additive content and curing time increased. It was concluded that the reduction in the shrink-swell potential when combined additive content increased could be due to flocculation of clay particles and decrease in the specific areas of clay particles by cation exchange. Meanwhile, as the curing time prolonged, the improved shrinkage and swelling behaviour might be attributed to the enhancement of the pozzolanic reaction contributed from the lime and fly ash combination, which resulted

in the more formations of new cementitious compounds such as calcium silicate hydrate (CSH) and calcium aluminate hydrate (CAH).

- This extensive literature noted that combination of lime or cement and ash materials (i.e. fly ash, rice husk ash) was highly effective in enhancing the mechanical properties of stabilised soils such as the compressive strength, the bearing capacity, the shrink-swell behaviour of expansive soil. Although several studies on the utilisation of bagasse ash in concrete technology indicated that well-burnt bagasse ash could replace up to 20% cement content in concrete admixtures without bringing adverse effects on the physical and mechanical characteristics of concrete, only few studies have been performed to examine the application of agricultural by-product of sugar-cane bagasse ash for soft soil stabilisation. In addition, the previous studies mostly focused on the improvement in the strength and the bearing capacity of soft soils stabilised with only bagasse ash application as an additive. Based on analysing the favourable test results, it was documented that the addition of bagasse ash to stabilise clayey soils improved the soil strength and bearing capacity when bagasse content increased up to 25%. However, investigations on the other geotechnical properties of soft soils such as the shear strength, the tensile strength, the compressibility as well as studying the utilisation of bagasse ash for problematic soil modification without or with lime or cement combination remain very limited.

- In comparison with untreated expansive soils, it is observed that the inclusion of synthetic fibres (e.g. carbon fibre, nylon fibre, polypropylene fibre) reinforced expansive soils without lime or cement stabilisation decreased the volumetric shrinkage strain with increasing fibre content from 0.4% to 1%, but it increased the

shrinkage potential when the moisture compaction content increased. Moreover, for expansive soil samples reinforced with natural fibres (i.e. coir pith coconut fibre, short coir fibre) without cement, the volumetric shrinkage strain gradually decreased as the fibre content increased from 0.5% to 3%, meanwhile the reduction in the shrinkage potential of reinforced soils varied with the fibre lengths and the applied shrinkage tests. The improvement of the volumetric shrinkage strain could be attributed to the fibre-soil interaction and the decrease in the plasticity of expensive soils stabilised with non-expansive fibre inclusion.

- Experimental investigations on ash materials (e.g. rice husk ash) combined with chemical treatment (i.e. lime or cement) of soils with fibre reinforcement revealed that the unconfined compressive strength and the bearing capacity were significantly improved with fibre inclusion, and they were affected by fibre contents, fibre aspect ratios (lengths) and so on. Overall, the compressive strength of stabilised soils reinforced with fibre inclusion increased to a certain fibre content at first followed by a slight decrease in the compressive strength with further increase in fibre content. It was concluded that at a given fibre content, the improvement in the compressive strength of stabilised soils with fibre reinforcement was attributed to the contact areas between soil particles and the fibre elements. When the amount of fibre inclusion increased, the contact areas and friction between the fibre elements and soil particles increased, and consequently improved the resistance to the applied load of stabilised soils with fibre reinforcement. However, it was noted that when excessive use of fibre content to reinforce soils with chemical stabilisation caused a small decrease in the

strength of stabilised soils, which could be due to fibres induced slippage over each other.

- Similar to the behaviour of the compressive strength of combined cement-ash material stabilised soils reinforced with fibre inclusion, the indirect tensile strength of stabilised soils showed an appreciable increase at first with increasing fibre content to a certain level and then exhibited a small decrease in the tensile strength with additional fibre inclusion into soils. It was observed that the relationships between fibre contents and the ratio of the tensile strength to the compressive strength of stabilised soils with fibre reinforcement increased slightly from 0.20 to 0.25 as the fibre content increased to around 1%. That behaviour confirmed that the improvement in the tensile strength of stabilised soils reinforced with fibre inclusion was more pronounced that of the compressive strength. In other words, the inclusion of fibres into soils stabilised with cement-ash material combination played a more important role in increasing the tensile strength than the compressive strength. It was important to note that the presence of fibre in the stabilised soils not only increased the tensile strength, but also improved the resistance to the tension cracks development of the stabilised soils with fibre reinforcement. The tensile strength development of stabilised soils reinforced with fibre inclusion was attributed to contribution of the total contact area between fibres and soil particles as well as fibre orientation in favour of the tensile strain directions when subjected to the tensile loading. As a result of the increased amount of fibre added into the stabilised soil matrix, the corresponding increase in the total contact areas and the chances of a larger number of fibre elements

orientated in the principle tensile strain directions promoted the better resistance to the applied tensile loads of the stabilised soils with fibre reinforcement.

- Experimentally investigating the swelling behaviour of fibre reinforcement of expansive soils without or with cement indicated that the introduction of polypropylene fibre significantly reduced the swelling potential of reinforced soils without cement stabilisation as fibre content increased from 0% to 1.5%. In addition, compared with 5% and 8% lime treated expansive soils without fibre reinforcement, the inclusion of only 1.5% fibre reinforced expansive soils without lime stabilisation was more effective in minimising the swelling potential than the counteracts treated soils without curing time. However, the influence of a combination of synthetic polypropylene fibres (or natural fibres such as bagasse fibre) and lime treated expansive soils on the swelling potential was not fully investigated and reported in the literature.

- The soil water characteristic curves (SWCC) of either lime stabilisation of expansive soil or ash materials (i.e. fly ash, bottom ash) stabilised expansive soils combined without or with synthetic polypropylene fibre reinforcement have experimentally been investigated and presented in the literature. However, laboratory investigations on the changes of the soil water characteristics of expansive soil stabilised with lime and natural fibre (e.g. bagasse fibre) remain limited. Thus, further investigations on the volumetric water content change of natural fibre reinforced expansive soils with lime combination are required for a better understanding of the SWCC.

- Based on this compressive review of the behaviour of expansive soils stabilised with waste by-products combined without or with cement or lime treatment, it was noted that the majority of the recent investigations have been focused on the geotechnical properties of fly ash, bottom ash stabilised soft soils or expansive soils without or with chemical stabilisation of lime or cement. However, very limited studies have been conducted to assess the engineering properties of agricultural waste by-products (e.g. bagasse ash, bagasse fibre) stabilised expansive soils without or with lime combination. Therefore, further investigations on the behaviour of expansive soil treated with bagasse ash or bagasse fibre without or with lime combination are carried out and presented the following chapters which aims to search for a practical possible solution of utilising the agricultural waste by-products such as bagasse ash and fibre in the field of infrastructure construction for sustainable development.

CHAPTER 3: MATERIALS, SAMPLE PREPARATION AND LABORATORY TESTING PROGRAM

3.1. INTRODUCTION

This chapter describes details of the materials, samples preparation, laboratory tests and their procedures, adopted in this research. It can be noted that the testing setups and apparatus are described in detail for interpretation. All experiment tests, employed for this investigation, were conducted at the University of Technology Sydney (UTS).

3.2. MATERIALS

3.2.1. Natural Expansive Soil

The soil samples used in this study were collected from a road construction site in Queensland, Australia. After removal of visible organic matters such as tree rootlets and leaves, the soil was air-dried and broken into pieces in the laboratory (Figure 3.1). Table 3.1 and 3.2 show the physical and mechanical properties, and the chemical composition of the soil used in this investigation, respectively. The soil was classified as high plasticity clay (CH) according to the Unified Soil Classification System (USCS), AS 1726 (AS 1993). The specific gravity of solids (G_s) was 2.64 ± 0.02. The grain size distribution showed that 0.06% of particles were in the range of gravel, 10.97% in the range of sand and 88.97% were fine-grained material (i.e., silt/clay). The particle size distribution curve of the employed soil is illustrated in Figure 3.2. Atterberg limits of the fine portion of

material were LL= 86% (liquid limit) and PL= 37% (plastic limit), which yielded to a plasticity index (PI) of 49%. The average linear shrinkage and natural moisture content of the soil samples were 21.67% and 30.76%, respectively. Based on the high linear shrinkage, swell potential, and plasticity index, the soil can be classified as highly expansive soil (Part 4: Pavement Materials 2007). It should be noted that for preparation of soil samples, as shown in Figure 3.3, particles larger than 2.36 mm were removed resulting in more consistent samples.

Table 3.1 Physical and mechanical characteristics of natural soil

Characteristics	Value
Gravel content (diameter > 2 mm, %)	0.06
Sand content (0.06 mm< diameter < 2 mm, %)	10.97
Silt content (0.002 mm< diameter < 0.06 mm, %)	78.00
Clay content (diameter < 0.002 mm, %)	10.97
Natural water content (%)	30.76
Liquid Limit (%)	86
Plastic Limit (%)	37
Plasticity Index (%)	49
Linear Shrinkage (%)	21.67
Swell potential (%)	9.80
Specific gravity	2.62-2.65
Specific surface area (m^2/kg)	1475
USCS classification of the soil	CH

Table 3.2. Chemical composition of natural soil

Chemical Composition	
Components	Content (%)
MgO	2.20
Al_2O_3	22.98
SiO_2	60.26
CaO	4.06
FeO	8.25
K_2O	0.60
Na_2O	0.39
TiO_2	1.26
-	-

Figure 3.1 Air-dried expansive soil

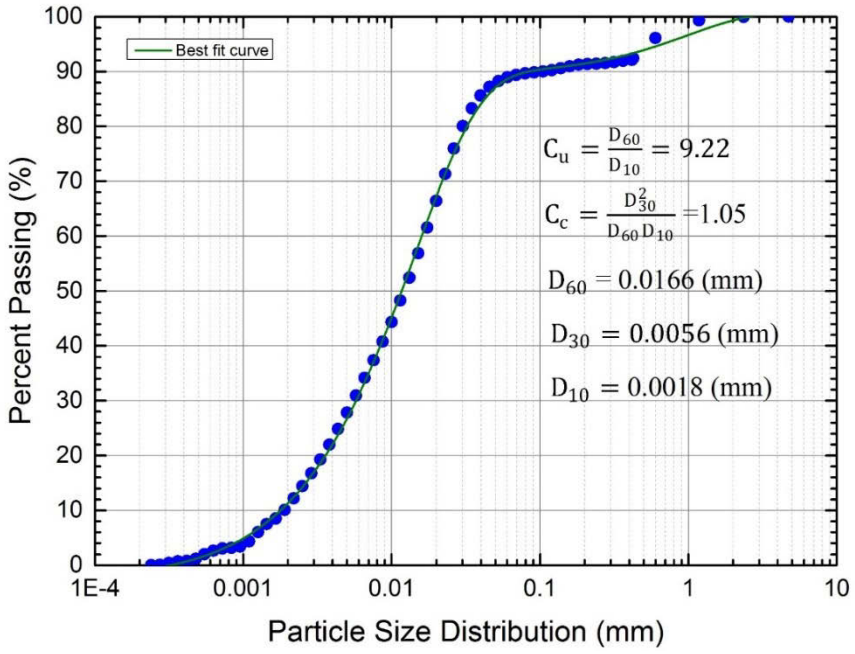

Figure 3.2 Particle size distribution curve for natural expansive soil

Figure 3.3 Selected expansive soil with particles smaller 2.36mm

3.2.1. Bagasse Ash

Bagasse ash (Figure 3.4) was collected during cleaning operation of boilers from ISIS Central Sugar Mill Ltd., Queensland, Australia. The bagasse ash was taken at burning temperatures ranging between 700-800°C, depending on the moisture content of bagasse. Table 3.3 provides the physical and chemical properties of typical bagasse ash utilised in this investigation. Figure 3.5 depicts a scanning electron microscope (SEM) image of the bagasse ash applied in this study. It should be noted that for preparation of bagasse ash samples utilised in this study, the bagasse ash (Figure 3.6) was carefully sieved and passed through 0.15mm aperture sieve to eliminate unburnt and oversize particles in order to enhance the pozzolanic reactivity of the bagasse ash, as recommended by Bahurudeen et al. (2016).

Figure 3.4 Sugar-cane bagasse ash

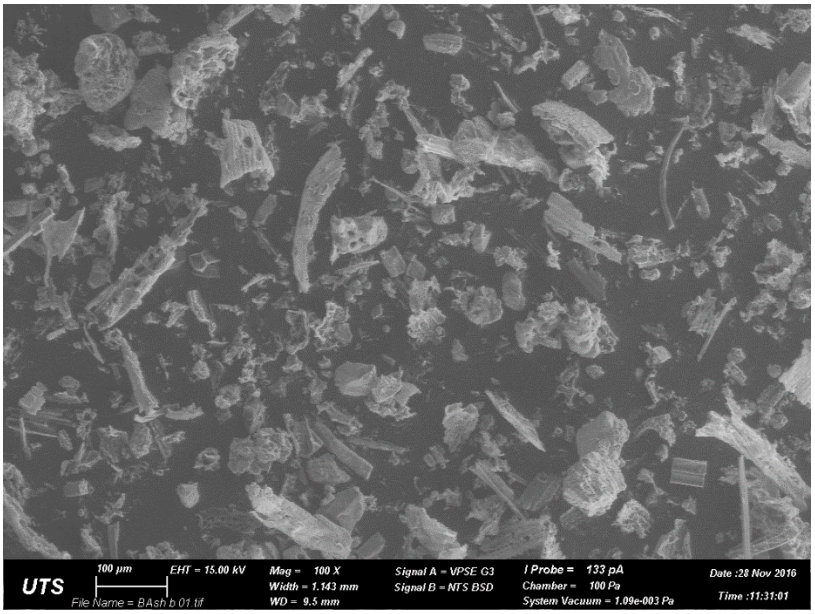

Figure 3.5 Scanning electron microscopy (SEM) image of sugar-cane bagasse ash

Figure 3.6 Selected sugar-cane bagasse ash employed in this study

Table 3.3. Physical and chemical characteristics of sugar-cane bagasse ash

Physical properties		Chemical Composition	
Property	Value	Components	Content (%)
Specific gravity	2.32	MgO	1.98
Specific surface area	228	Al_2O_3	5.95
(m^2/kg)		SiO_2	78.30
pH	8.64	CaO	2.43
		FeO	5.25
		SO_3	0.89
		K_2O	3.27
		Na_2O	0.54
		TiO_2	0.36
		P_2O_5	1.03
		-	-

3.2.2. Bagasse Fibre

Bagasse fibre used in this study was also obtained from the same source as bagasse ash, ISIS Central Sugar Mill Co. Ltd., Queensland, Australia. The bagasse fibre, as depicted in Figure 3.7, had a diameter ranging from 0.3 mm to 3.1 mm and a length ranging from 0.3 mm to 13.8 mm. The specific gravity of bagasse fibre (G_f) was about 1.25-1.55 and their average tensile strength was 96.24 ± 29.95 MPa. The obtained bagasse fibre was air dried at a controlled room environment with a temperature of 25°C and a relative humidity of 80% until its mass remained constant. Then, the dried fibres were carefully sieved and passed through 9.5 mm aperture sieve and retained on 300 μm aperture sieve, which were selected for this investigation.

Figure 3.7 Bagasse fibre used in this investigation

3.2.3. Hydrated Lime

Hydrated lime utilised in this study (Figure 3.8) has about 90% of calcium hydroxide. The hydrated lime was locally purchased in Sydney. Table 3.4 shows the physical and chemical properties of hydrated lime provided by the producer.

Figure 3.8 Hydrated lime

Table 3.4. Chemical composition and physical properties of hydrated lime

Physical properties		Chemical Composition	
Property	Value	Components	Content (%)
Specific gravity	2.2-2.3	Ignition loss	24%
Bulk density (kg/m^3)	400-600	SiO_2	1.8
pH	12.0	Al_2O_3	0.5
		Fe_2O_3	0.6
		CaO	72.0
		MgO	1.0
		CO_2	2.5

3.3. EXPERIMENTAL METHODS

3.3.1. Mixing of Materials

Soil samples were prepared by thoroughly mixing the pulverized natural soil with individual hydrated lime, bagasse ash, bagasse fibre or their combination as shown in Table 3.5 to become homogeneous mixtures before tap water was added at the target water content by the dry weight of each mixture. It should be noted that the hydrated lime-bagasse ash combination ratio of 1:3, which is considered as an optimum combination ratio, was derived from a number of preliminary unconfined compression strength tests conducted on treated expansive soil after 28 days of curing by changing the combination ratio of hydrated lime to bagasse ash from 1:1 to 1:5. Following this preparation, the mixtures were mixed thoroughly using a mechanical mixer. After mixing of the materials, soil specimens (Figure 3.9) were prepared for many conventional geotechnical experiments.

Figure 3.9 Additive-soil mixing

Table 3.5. Summary of mixes used in this study

Mix No.	Waste by-products (%)	Hydrated Lime (%)	Notes
1	0	0	Natural soil
2	6	0	Bagasse ash and soil
3	10	0	
4	18	0	
5	25	0	
6	0	1.5	Lime and soil
7	0	2.5	
8	0	4.5	
9	0	6.25	
10	4.5	1.5	Lime, bagasse ash and soil
11	7.5	2.5	
12	13.5	4.5	
13	18.75	6.25	
14	0.5	0	Bagasse fibre and soil
15	1.0	0	
16	2.0	0	
17	0.5	2.5	Lime, bagasse fibre and soil
18	1.0	2.5	
19	2.0	2.5	
20	0	4	Lime, bagasse fibre and soil
21	0.5	4	
22	1.0	4	
23	2.0	4	
24	0	6	Lime, bagasse fibre and soil
25	0.5	6	
26	1.0	6	
27	2.0	6	

3.3.2. pH Test

The approximate optimum lime content derived from the pH measurement (Eades & Grim 1966) required for expansive soil stabilisation using hydrated lime and waste by-products as additives was performed on the dry weight of the air-dried soil-additive-water mixtures in accordance with the procedure prescribed in ASTM D6276 (2006). The pH test was conducted using a pH meter and its probe (Figure 3.10) in accordance with the standard ASTM D6276 (2006). The pH meter and Probe were calibrated with 4, 7 and 10 buffer solutions at a controlled room environment of 25°C temperature. Samples were prepared at a solid-water ratio of 1:4. The air-dried soil was sieved through a 425 μm sieve. After that, 25g of the designated mixtures from the air-dried soil passing the 425 μm sieve mixed with various percentage of hydrated lime or waste by-products combined with hydrated lime were dispersed in 100ml distilled water, and continuously stirring the specimens for 30s at every 10 min for 1hour to ensure the homogeneous of the additive and soil mixtures. Subsequently, pH values of the slurries after 1 hour stirring were measured at a controlled room temperature of 25°C.

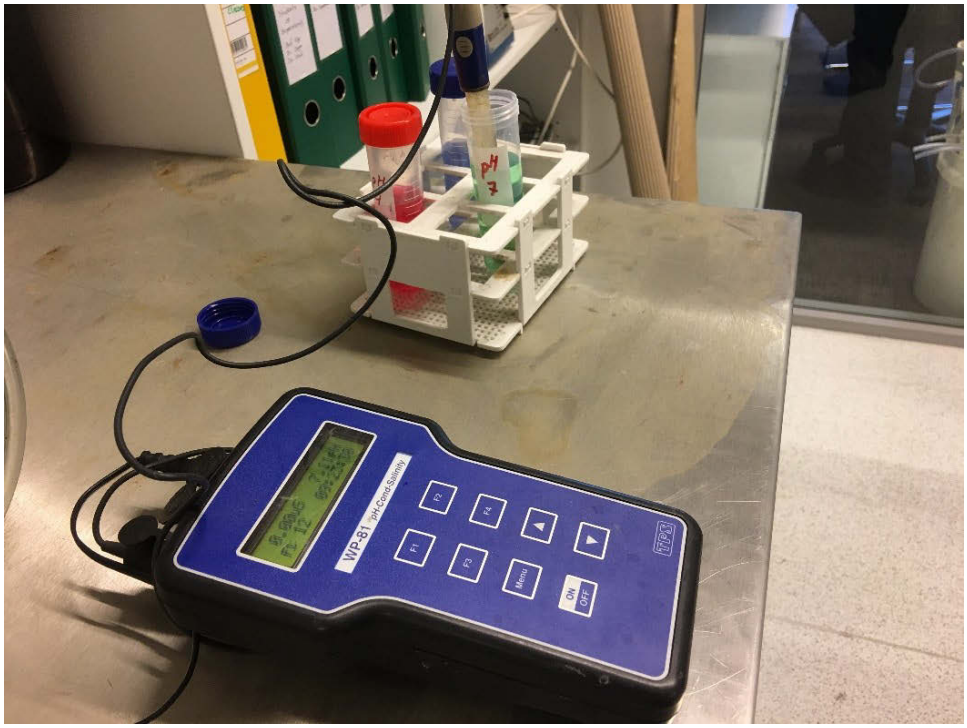

Figure 3.10 pH meter and the probe

3.3.3. Linear Shrinkage

In this investigation, portions of a soil sample of 250g from the material, passing the 425μm sieve by drying method were air-dried until they were dried enough to permit crumbling of the soil aggregation. The soil sample has been prepared in accordance with the procedure prescribed in AS 1289.1.1 (AS 2001) for the preparation of disturbed soil samples for Atterberg limits and linear shrinkage. Then, the linear shrinkage values of untreated and treated expansive soil specimens (Figure 3.11) with different contents of lime, bagasse ash and fibre as shown in Table 3.5 were determined as specified in accordance with the standard procedures, AS 1289.3.4.1 (AS 2008b).

(a)

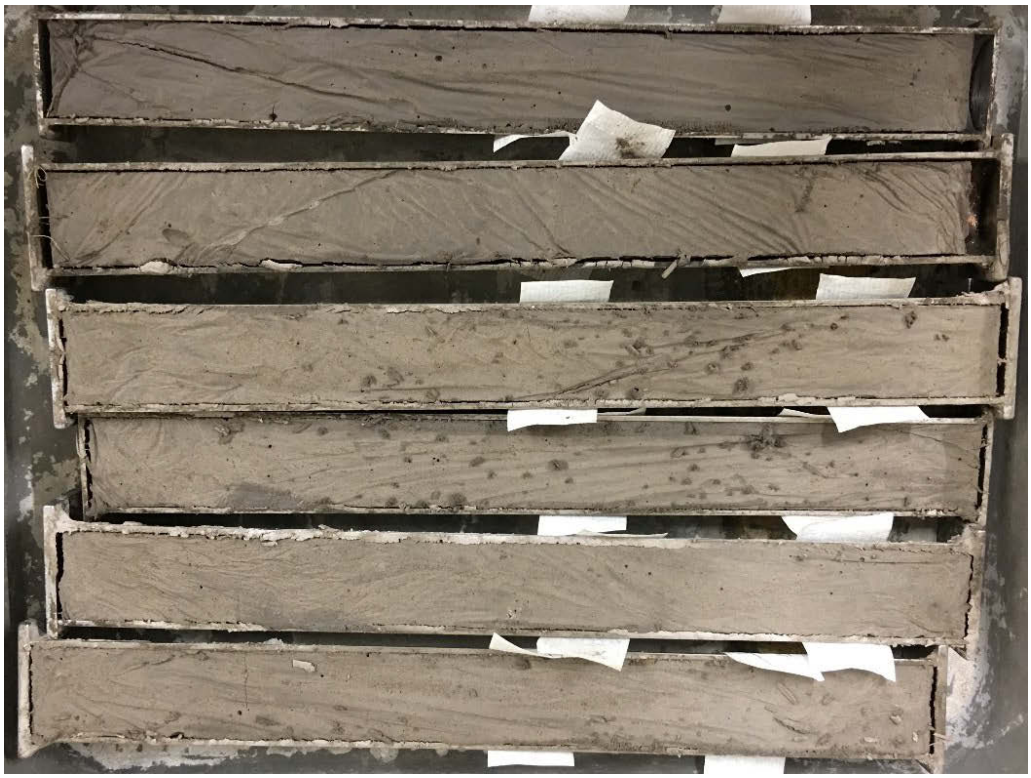

(b)

Figure 3.11 Linear shrinkage of (a) untreated soils and (b) 6% lime treated soils with 2% bagasse fibre

3.3.4. Standard Compaction Test

Standard compaction test was carried out to determine the maximum dry density (MDD) and the optimum water content (OMC) for untreated and treated soils in accordance with the procedures prescribed in AS 1289.5.1.1 (AS 2017). Different water contents were

added to the pulverised soils and thoroughly mixed to make them uniformly distributed through the soil mixtures. Then, the soil mixtures were placed in a cylindrical metal mould (Figure 3.12a), with an internal diameter of 105mm and height of 115.5mm and compacted in three layers by 25 uniformly distributed blows on the rammer falling freely from a height of 300 mm in accordance with the procedure of AS 1289.5.1.1 (AS 2017). The specimens (Figure 3.12b) were extruded, measured and weighed, and their moisture contents were determined. The dry density and water content of untreated soil for each specimen were calculated and recorded in accordance with AS 1289.5.1.1 (AS 2017). A total of eleven tests on samples with different water contents were conducted to determine the maximum dry density and the optimum moisture content of untreated soil. After that, different amounts of additives, as shown in Table 3.5, were added to the pulverised soil at the optimum moisture content of untreated soil. The blended mixtures were compacted in the same procedure applied to the untreated soil. The dry density of each mixture was achieved and used for carrying out other geotechnical tests.

(a)

(b)

Figure 3.12 Standard compaction test: (a) compaction tools; (b) compacted soil sample

3.3.5. Unconfined Compression Test

The unconfined compression tests were conducted in accordance with AS 5101.4 (AS 2008a). After mixing the expansive soil with waste by-product and hydrated lime, untreated and treated samples were compacted in a mould (Figure 3.13a) with 50 mm in diameter and 100 mm in height, at their dry density against the moisture content of 36.5% (the optimum moisture content of untreated soil). In order to ensure that each sample was compacted uniformly, the soil was placed in three equal layers using the tamping technique to obtain the target dry density. In addition, the samples were extruded prior to testing process, sealed by a proper plastic wrap (Figure 3.13b) to prevent moisture change, and then cured for different periods of 3, 7, 28 and 56 days at a controlled room environment of 25°C temperature and 80% relative humidity. After sample preparation

and curing, the samples were weighed and their dimensions were measured. Then the samples were set up in a conventional unconfined compression apparatus (Figure 3.14). The machine was set at a load rate of 1 mm/min, and this was kept consistent for all samples tested in accordance with AS 5101.4 (AS 2008a). An S-type load cell was used as a transducer to converting the force into an electrical signal, readable on the load cell display. A data logger was used to transfer the data from the load cell and a linear variable differential transformer (LVDT) to a readable output. The LVDT reading was used to calculate the strain of the samples. The axial stress at failure defined as the unconfined compressive strength (UCS) of the samples was then calculated. For each type of mixtures, the UCS value was obtained as the average of three unconfined compressive strength tests and should not deviate by more than 10% from the mean strength.

(a)

(b)

Figure 3.13 Unconfined compressive strength test: (a) a typical UCS mould; (b) selected soil samples prepared and sealed in vinyl plastic wrap for curing

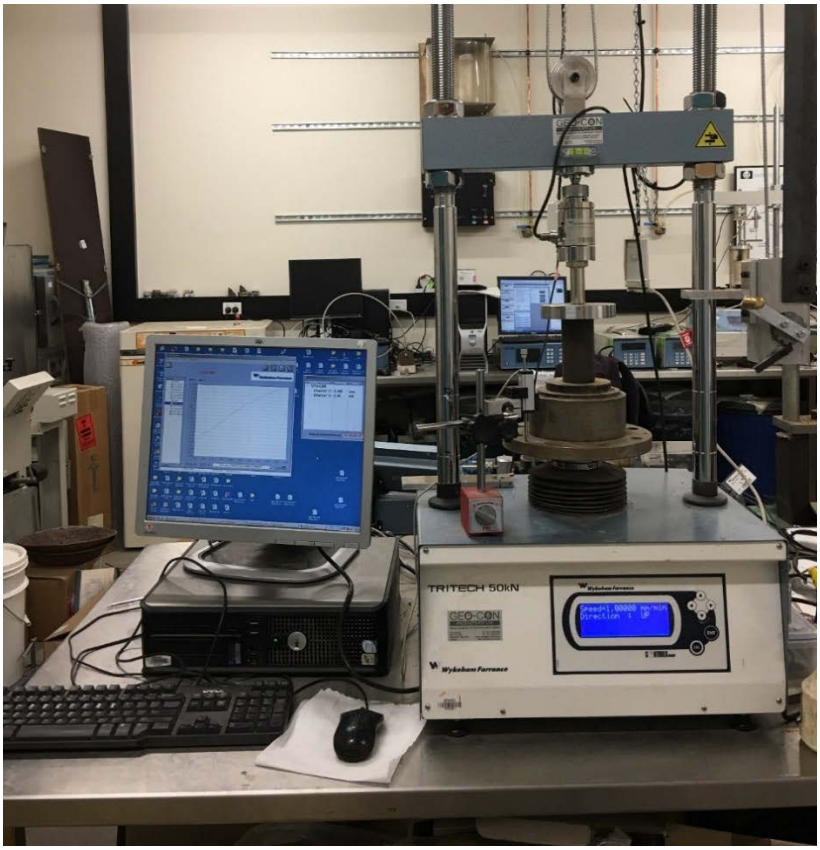

Figure 3.14 Conventional compression testing machine

3.3.6. Indirect Tensile Strength Test

The indirect tensile strength of samples was measured in accordance with AS 1012.10 (AS 2000). The relevant testing procedures for soil and rock samples have been well documented in the literature (Anggraini et al. 2015a; Fatahi et al. 2012b; Pourakbar et al. 2016). Soil samples with 50 mm in diameter and 100 mm in height, for the indirect tensile strength tests, were prepared by following the same procedure used for UCS sample preparation and in the same mould. After a 28 day-curing period at a controlled room environment of 25°C temperature and 80% relative humidity, the samples were weighed and their dimensions were measured. Then the samples were set up in a conventional compression apparatus (Figure 3.15). The machine was set at a load rate of 1 mm/min, and this was kept consistent for all samples tested in accordance with AS 1012.10 (AS 2000). Based on the peak load applied, the indirect tensile strength was calculated using the following Equation 3.1

$$\sigma_T = a\left(\frac{2P}{\pi DL}\right) \tag{3.1}$$

where P is the maximum load applied; D is the diameter of the sample; L is the thickness of the sample; and a is a shape parameter, which can be estimated as $a = 0.2621k + 1$, in which k is the ratio of the sample thickness to its diameter, as recommended by Yu et al. (2006). Figure 3.16 shows a selected soil sample treated with lime and bagasse fibre after completion of the indirect tensile strength test. It is noted that for each type of mixtures, the indirect tensile strength value was reported as the average of three samples and should not deviate by more than 10% from the mean strength.

Figure 3.15 Indirect tensile strength test (known as Brazilian or splitting test)

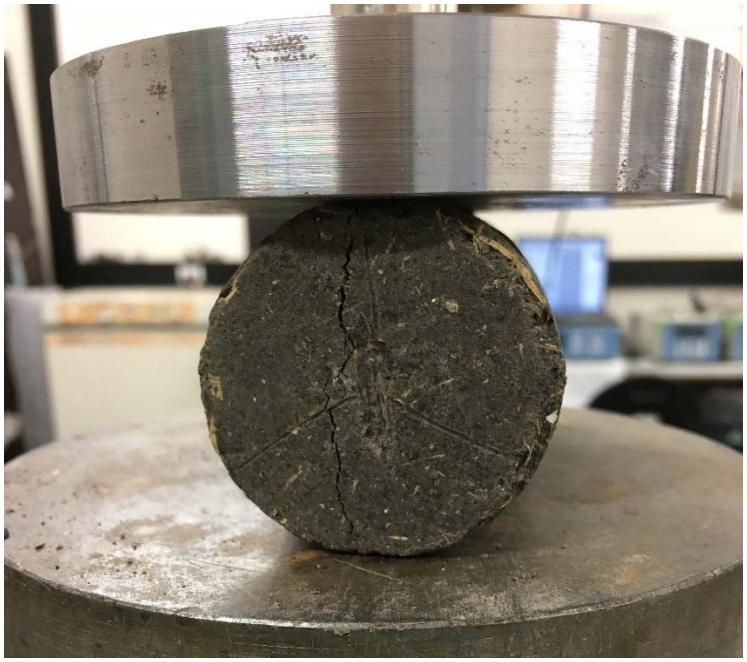

Figure 3.16 A selected soil sample after completion of the indirect tensile strength test

3.3.7. California Bearing Ratio Test

California bearing ratio (CBR) tests were conducted on untreated and treated expansive soil in accordance with the testing method specified in AS 1289.6.1.1 (AS 2014). After sample preparation, untreated and treated samples were compacted in a cylindrical metal mould, with 152 mm in internal diameter and 178 mm in height, at the dry density versus the optimum moisture content of untreated soil of 36.5%. In order to achieve uniform compaction, the samples were compacted in five equal layers by pressing the spacer disk of 61 mm in thickness with help of testing machine to obtain the target dry density. Then, the prepared samples were sealed in a plastic wrap to prevent moisture loss, and afterward curing for 7 and 28 days at a controlled room environment of 25˚C temperature and 80% relative humidity (Figure 3.17). After sample preparation and curing period, the samples were subjected to either soaking condition for 7 days (Figure 3.18) prior to testing in case of soaked CBR tests or an annular surcharge of 2.5 kPa put on the top as prescribed in AS 1289.6.1.1 (AS 2014) and immediately tested in the CBR testing machine without soaking (unsoaked CBR). The machine was set at a load rate of 1 mm/min according to the relevant standard and this was kept consistent for all samples tested. The LVDT and load cell readings were used to plot the load-penetration curve to be used to calculate the CBR values. The CBR values of untreated and treated expansive soil specimens were measured based on the greater values of 2.5 mm and 5 mm penetration. Figure 3.19 shows selected soil samples after completion of CBR tests. It can be noted that for each type of mixture, the CBR value was obtained as the average of three CBR tests and the standard deviation of the results should not be greater than 10%. If the standard deviation was greater than 10%, additional samples were prepared and tested before averaging.

Figure 3.17 CBR samples under curing condition

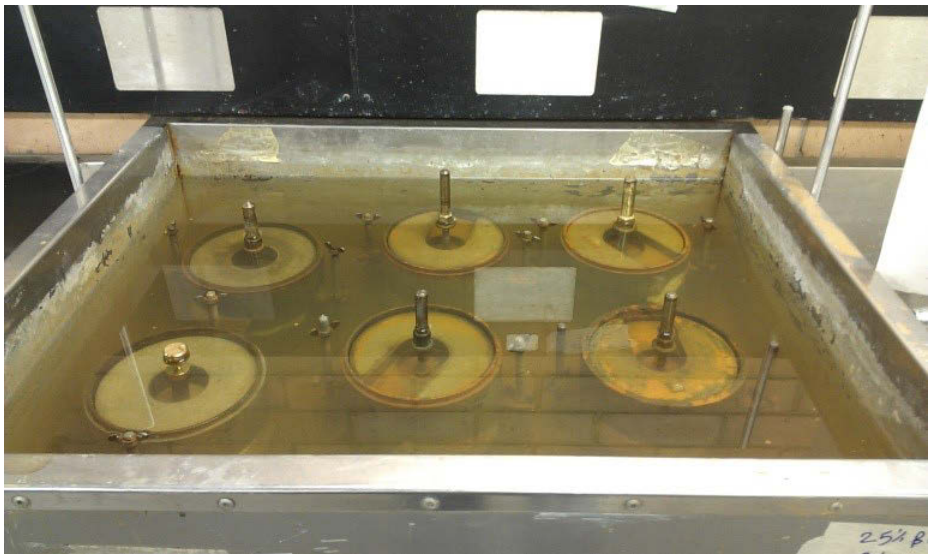

Figure 3.18 CBR samples under soaking condition

Figure 3.19 Selected samples after completion of CBR tests

3.3.8. Swell Potential Test

Samples for swell potential tests were prepared following the procedure used for CBR sample preparation and in the same mould, but having a shorter height (H) of 47 mm, to examine the free swell potential and swelling percentage versus elapsed time in addition to estimating the vertical ground surface heave due to fully wetting. After sample preparation and 3 days of curing, the soil samples were subjected to an initial seating load of 3 kPa on the top and soaked in water (Figure 3.20). The soil samples commenced swelling immediately after soaking and were allowed to swell freely. Swell deformations were measured, using a dial gauge, at regular time intervals until swelling stopped (i.e., less than 0.1% change per 2 days). The final swelling reading was used to determine the total swell (ΔH). The free swell potential of the soil samples (ΔH/H) was determined. It

should be noted that the free swell potential values reported were obtained as the average of duplicate swell tests. If the test results had significant variability, additional swell tests were carried out before averaging.

Figure 3.20 Swell potential test setup

3.3.9. One-dimensional (1D) Swelling Pressure and Consolidation Tests

A series of one-dimensional swelling consolidation tests were carried out on untreated and treated soil specimens after 3 days of curing using conventional oedometer apparatus following the testing procedure in accordance with AS 1289.6.6.1 (AS 1998). For sample preparation, soil specimens were compacted in a cylindrical metal ring, with an internal diameter of 50 mm and height (H) of 17 mm, at the MDD and OMC. After specimen preparation and curing, the compacted soils were extruded and put into the Oedometer ring of the same diameter and then standard Oedometer testing setup (Figure 3.21) was

followed (two-way drained setup). An initial seating load of 3 kPa was applied. Once proper loading contact was achieved, the samples were inundated with distilled water and remained for 4 days to get full saturation prior to compression. During the saturation stage of the consolidation tests, vertical swell deformation was measured using a dial gauge. Readings were taken at regular time intervals until swelling stopped (i.e., less than 0.1% change per 2 days). The final swelling readings were used to determine the total swell (ΔH). Accordingly, the free swell potential of each soil specimen ($\Delta H/H$) was determined. After completion of this stage, the soil specimens were subjected to additional pressure incrementally in accordance with the standard consolidation test procedure AS 1289.6.6.1 (AS 1998). At any level of pressure, the applied pressure was kept on the specimens for 24 hours to ensure the completion of consolidation. Swelling pressure was determined as the required pressure on the e-logP plot corresponding to the initial void ratio of the soil specimen prior to the saturation stage. For each type of mixtures, at least two samples were tested and then the average of the swelling pressure and compression test results were presented.

Figure 3.21 One-dimensional (1D) consolidation test (Oedometer test)

3.3.10. Triaxial Shear Test

Uniform soil specimens with 50 mm in diameter (D), 100 mm in height (H) and a same aspect ratio of H/D=2 were prepared for triaxial shear tests following the procedures used for UCS sample preparation in the same mould. The soil samples were then extruded, sealed by a plastic wrap to prevent moisture change, and then cured for 7 days. It can be noted that 7 days of curing was selected for bagasse fibre reinforced soil samples prior to testing in accordance with the early research reported by the research team at UTS, indicating that the improvement in the unconfined compressive strength of soils reinforced with bagasse fibre was nominal as curing time exceeded 7 days. After curing, the soil samples were weighed and their dimensions were measured prior to setting up in

triaxial compression apparatus (Figure 3.22) for an isotropically consolidated-undrained (CU) test in accordance with the standard procedures stated in AS 1289.6.4.2 (1998).

Low confining pressures of 50 kPa, 100 kPa and 200 kPa were used in this investigation to represent the field condition of typical subgrade soil under roads and highways in the investigated region. Prior to testing, the soil specimens were saturated to achieve Skempton's B value of 0.95 as a minimum and then consolidated isotropically at a given effective confining pressure. It should be noted that a relatively high back-pressure of 500 kPa was required to achieve the fully saturated conditions, achieving the minimum B value of 0.95, for every single sample. That is similar to the required back-pressure to get sandy silt soil samples to be fully saturated, recently reported in the literature (Chen & Indraratna 2014). The CU tests were conducted at a relatively small shearing rate of 0.017 mm/min to ensure the equilibrium of excess pore water pressure throughout the soil samples during shearing (Consoli et al. 2015). During the shear tests, all sensor reading data including confining pressure, excess pore water pressure and deviatoric load were automatically recorded using a special data logger to transfer the data to a readable output. The CU tests were continued to axial strains after the peak deviatoric stress for observation of the failure shape and shear plane of the tested samples as illustrated in Figure 3.23. It can be noted that for each type of mixtures, the shear strength value was reported as the average of three samples and should not deviate by more than 10% from the mean strength.

Figure 3.22 Triaxial compression test

Figure 3.23 A selected sample after completion of triaxial shear test

3.3.11. Microstructural Analysis

The microstructural evolution of the hydrated lime, bagasse fibre, and bagasse ash treated soil samples was investigated using scanning electron microscope (SEM) and Fourier transform infrared (FTIR) tests. The treated soil samples collected from fracture portions of the UCS tests after 28 days of curing at a controlled temperature of 25°C were utilised to carry out the microstructural analysis, while the similar tests were conducted on the untreated soil after the UCS tests without any curing.

SEM analysis was performed on the samples without coating and scanned using a high revolution scanning microscope (ZEISS EVO LS 15), as depicted in Figure 3.24, at an accelerating voltage of 15 kV. Prior to the tests, both untreated and treated soil samples were dried in an oven at a temperature of 40°C for 24 hours. Several SEM images at different magnifications were captured in order to evaluate the sample microstructural change as well as examine the formation of cementitious compounds of the stabilised soil.

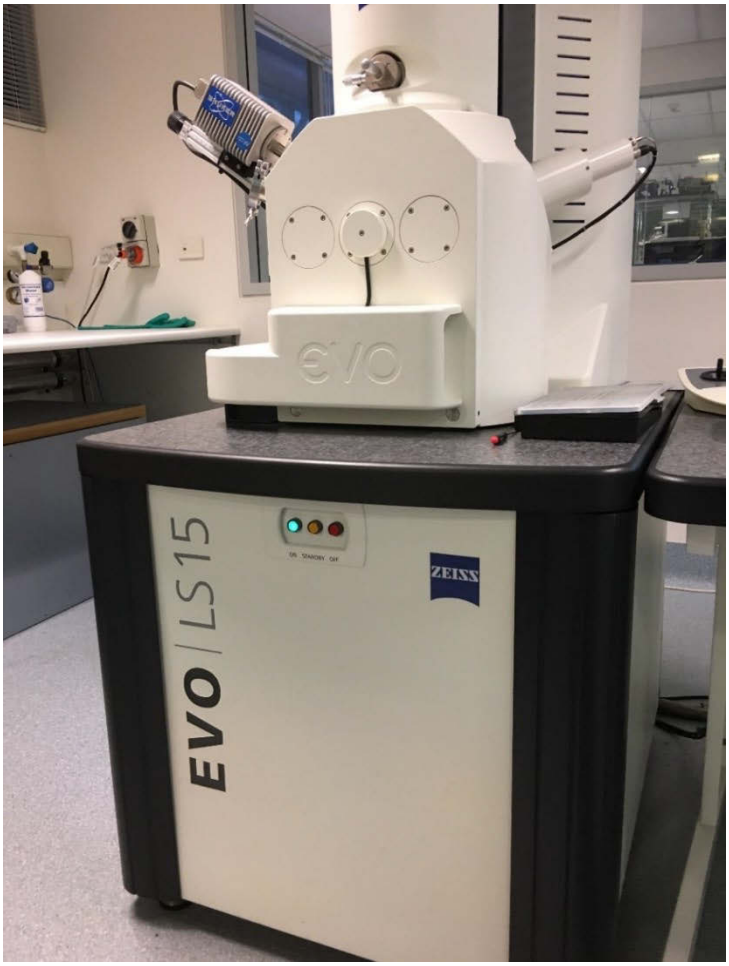

Figure 3.24 Scanning electron microscope (SEM) test

For the Fourier transform infrared (FTIR) tests, fracture portions of the samples remained after the UCS test were pulverized and passed through 425 μm sieve to be used for the FTIR tests. Prior to testing, both untreated and treated soil samples were dried in an oven at a temperature of 40°C for 24 hours. An FTIR pattern was recorded using a Shimadzu's MIRacle 10 Fourier transform infrared spectrometer at a resolution of 1cm^{-1}, over the range between 400 and 4000 cm^{-1}. The FTIR spectra were obtained as the average of 40 signal scans on each sample. The average results of two samples were analysed and reported. Figure 3.25 shows the setup used for FTIR tests.

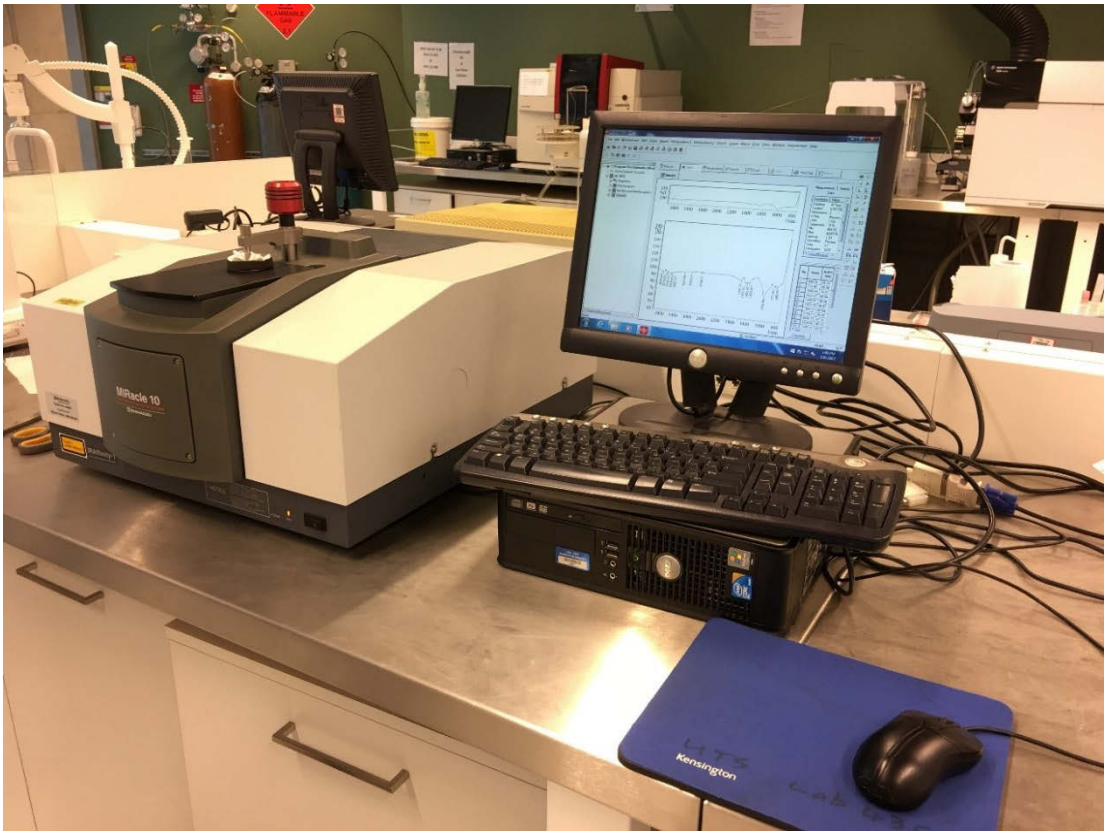

Figure 3.25 Fourier transform infrared (FTIR) test

3.3.12. Filter Paper Method

The drying soil-water characteristic curves (SWCC) of untreated and bagasse fibre-lime treated expansive soils were investigated using the filter paper method in accordance with the standard test procedure for measurement of soil potential suction using filter paper ASTM D5298 (ASTM 2016). Soil specimens were compacted in a cylindrical metal ring of 50 mm in internal diameter and 17 mm in height, at the MDD and OMC. After specimen preparation and curing for 7 days, soil samples were initially saturated under a minimal load of 3 kPa up to 7 days to get full saturation prior to testing and then the soil samples were weighed to ensure the full saturation condition obtained. The curing period of 7 days was selected based on the previous studies of lime-soil suction tests (Elkady et

al. 2015), who reported that the longer curing period had a negligible effect on the SWCC of lime treated expansive clay. By conducting the drying process for achieving SWCC, a number of untreated and treated soil samples were prepared and dried to various target water contents at a controlled room environment with a temperature of 25°C and a relative humidity of 80% for a period ranging from 1 to 7 days. However, some selected soil samples were introduced to over-dried in order to obtain a high suction value (e.g. close to 10^6 kPa). During the drying process, the target water contents were obtained by continuously measuring sample weight. After that, soil samples at the target water content were wrapped and stored in glass containers for 24 hours to get the water content uniformly distributed.

Soil samples with filter papers were placed and sealed in glass containers (desiccators) and then stored in an insulated chest for 7 days. After achieving equilibrium, the water contents of the soil and filter paper were measured and then the soil matric suction (simply called soil suction) was calculated using a typical calibration curve for filter papers (Whatman No. 42) presenting a relation between filter paper water content and suction in accordance with ASTM D5298 (ASTM 2016). During the suction tests, dimensions of untreated and treated soil samples were measured using a calliper and then the saturation degree of tested soil samples was determined and reported against soil suction. Figure 3.26 shows the samples and setup used for soil suction tests. It can be stated that for each suction point, the suction value was obtained as the average of three suction tests and the standard deviation of the results should not be greater than 10%. If the variation was greater than 10%, additional samples were prepared and tested before averaging.

(a)

(b)

(c)

Figure 3.26 Soil suction test: (a) sample preparation and tools; (b) and (c) placement of soil samples in a well-insulated container for suction equilibrium

3.4. SUMMARY

This chapter presents the materials, sample preparation, and the detailed experiment programs and procedures, used to investigate the influence of hydrated lime, bagasse fibre and bagasse ash additions on engineering properties of expansive soil. The preparation of stabilised soil specimens was conducted by changing the bagasse ash content from 0% to 25%, bagasse fibre content from 0% to 2%, hydrated lime content from 0% to 6.25%, and various contents of their combinations by the dry weight of expansive soil. Several series of laboratory experiments consisting of compaction, linear shrinkage, swell potential, swelling pressure, unconfined compressive strength (UCS), indirect tensile strength, California bearing ratio (CBR), and consolidation tests have been performed on untreated and treated expansive soil samples with different additive contents in line with various curing times of 3, 7,28, and 56 days. An extensive study on the microstructure development of untreated and treated expansive soils was also conducted using scanning electron microscopy (SEM), pH measurement, and Fourier transform infrared (FTIR) techniques. The outcomes of this experimental investigation were analysed and discussed to obtain a better understanding of the effects of the hydrated lime, bagasse ash, and their combination on the shrink-swell behaviour, the compressive strength and stiffness, the bearing capacity, the brittleness, the ductility, and the compressibility characteristics of the untreated and treated expansive soils.

CHAPTER 4: GEOTECHNICAL CHARACTERISTICS OF EXPANSIVE SOIL STABILISED WITH BAGASSE ASH AND HYDRATED LIME

4.1. INTRODUCTION

This chapter presents the results of the laboratory testing program in accordance with the testing methods and procedures specified in Chapter 3. This chapter aims to investigate the impacts of bagasse ash, hydrated lime, and their combination on the shrink-swell potential and engineering characteristics of treated expansive soil. The preparation of stabilised soil specimens was conducted by changing the bagasse ash content from 0% to 25%, hydrated lime content from 0% to 6.25% and combined hydrated lime-bagasse ash contents from 0% to 25% by the dry weight of expansive soil. Several series of laboratory experiments consisting of pH measurement, compaction, linear shrinkage, swell potential, swelling pressure, unconfined compressive strength (UCS), California bearing ratio (CBR), consolidation tests have been performed on untreated and treated expansive soil samples with different additive contents in line with various curing times of 3, 7, 28 and 56 days. A comprehensive study on the microstructure development of untreated and treated expansive soils was also conducted using scanning electron microscopy (SEM) and Fourier transform infrared (FTIR) techniques. A total of 468 specimens were prepared and employed to conduct many conventional geotechnical experiments as

summarised in Table 4.1. The outcomes of this experimental investigation were analysed and discussed to obtain a better understanding of the effects of the hydrated lime, bagasse ash, and their combination on the shrink-swell behaviour, the compressive strength and stiffness, the bearing capacity, the brittleness, the ductility, and the compressibility characteristics of the untreated and treated expansive soil. The results of the SEM and FTIR analysis were also presented and discussed to examine the change in microstructure of the stabilised soils and the formation of new cementitious compounds of Calcium-Silicate-Hydrate (C-S-H). Furthermore, the SEM results indicate the formation of new cementitious products (i.e., CSH, CAH or CASH) is primarily responsible for the improvement in the strength and stiffness of treated soils.

4.2. EXPERIMENTAL RESULTS AND DISCUSSION

4.2.1. Determination of Optimum Lime Content for Lime Soil Mixtures

Figure 4.1 shows the variation of pH values along with increasing hydrated lime alone and combined bagasse ash-hydrated lime content in the mixtures. It should be noted that the pH values in this study were determined using the testing method proposed by Eades & Grim (1966). Referring to Figure 4.1 and based on the analysed pH values, it is found that the approximately 5% hydrated lime can be considered as the optimum lime content for expansive soil stabilisation, while approximately 18% bagasse ash-hydrated lime combination (contained 4.5% lime in the mixture) can be considered as the optimum additive content for bagasse ash-hydrated lime to stabilise expansive soil. However, it can be noted that an increase in the pH value (>9) of stabilised soil may sometime create a corrosive environment to foundation structures. Therefore, special attention should be taken during the design stage of chemical treatment of expansive soil with lime.

Table 4.1 A number of tested specimens

No.	Test name	Curing time (days)	Natural soil	Bagasse ash	Hydrated lime	Lime-Bagasse ash	Summary
1	Compaction	0		12	12	12	47
		1	11				
2	Unconfined compressive strength (UCS)	3	3	12	12	12	123
		7		12	12	12	
		28		12	12	12	
		56			6	6	
3	Linear shrinkage (LS)	3	3	12	12	12	111
		7		12	12	12	
		28		12	12	12	
4	California bearing ratio (CBR)	3	3				51
		7		12			
		28		12	12	12	
5	Swell potential (SP)	3	3	12	12	12	39
		7					
		28					
6	Swelling pressure (PS)	3	3				39
		7		12	12	12	
		28					
7	1D consolidation (Oedometer)	3	3				15
		7				12	
		28					
8	Fourier transform infrared (FTIR)	3	3				9
		7					
		28			3	3	
9	Scanning electron microscopy (SEM)	3	1	1			4
		7					
		28			1	1	
10	pH	1 hr	3		15	12	30
		7					
		28					
						Total	**468**

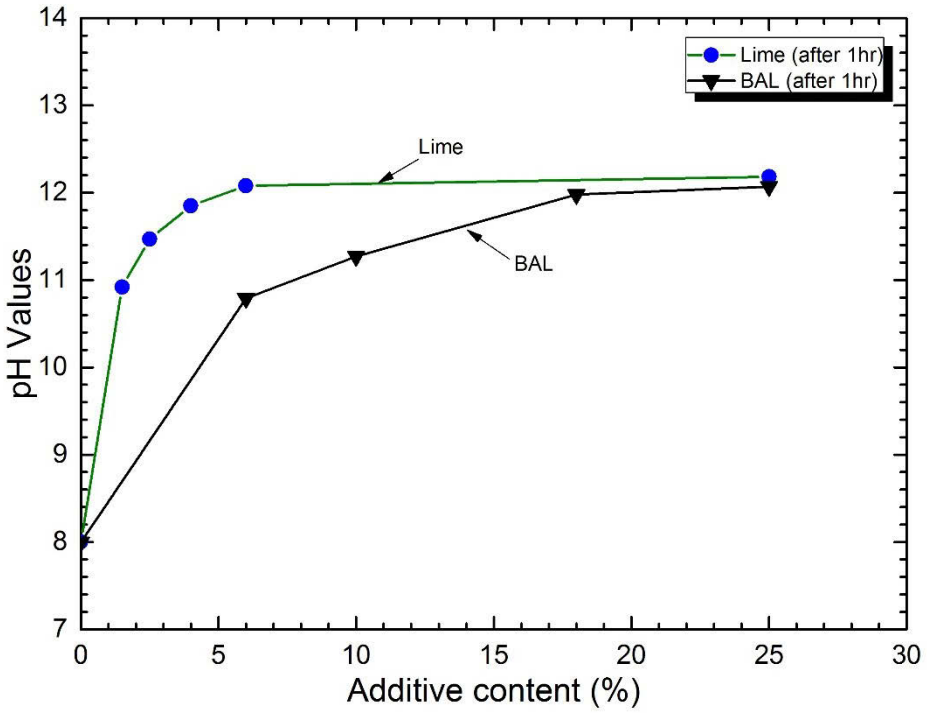

Figure 4.1 pH values of lime and bagasse ash-lime (BA+L) stabilised expansive soil after 1hour of mixing

4.2.2. Influence of Additive Content on Compaction Characteristics

The standard compaction tests were conducted on untreated expansive soil as a preliminary step to determine its maximum dry density (MDD) and optimum moisture content (OMC) as shown in Figure 4.2. Referring to Figure 4.2 and analyzing the results, the maximum dry density of 12.9 kN/m^3 and the optimum moisture content of 36.5% were achieved, respectively, for the untreated expansive soil. Subsequently, the 36.5% OMC of the untreated expansive soil was applied to the other additives and soil mixtures to evaluate the influence of the additive content on the so-called maximum dry density of the treated soil mixtures. The results of the standard compaction tests for various additive content treated expansive soil are depicted in Figure 4.3. Obviously, the MDD of the treated soil mixtures as illustrated in Figure 4.3a slightly decreased from 12.8 kN/m^3 to

12.2 kN/m^3 and from 12.6 kN/m^3 to approximately 12.0 kN/m^3 when bagasse ash (BA) and bagasse ash-lime (BA+L) content increased from 6% to 25%, respectively. Similarly, observation of the standard compaction results of the hydrated lime (L) treated soil mixtures as depicted in Figure 4.3b, the MDD of the lime treated soils reduced from 12.8 kN/m^3 to 12.6 kN/m^3 when the lime content increased from 1.5% to 6.25%. The decrease in the MDD of treated soil mixtures could be due to the flocculation and agglomeration, because of cation exchange processes between clay particles and additives, resulting in the coarser particles. The formation of the coarser particles occupying the lager spaces in the soil matrix, increases the void volume and hence reduces the dry density of the treated soil mixtures (Kinuthia et al. 1999; Millogo et al. 2012). Another reason that could be accounted for the phenomenon of the MDD reduction of the treated soil mixtures is essentially due to the lower specific gravity of the additives in comparison with that of untreated soil (Rahman 1986).

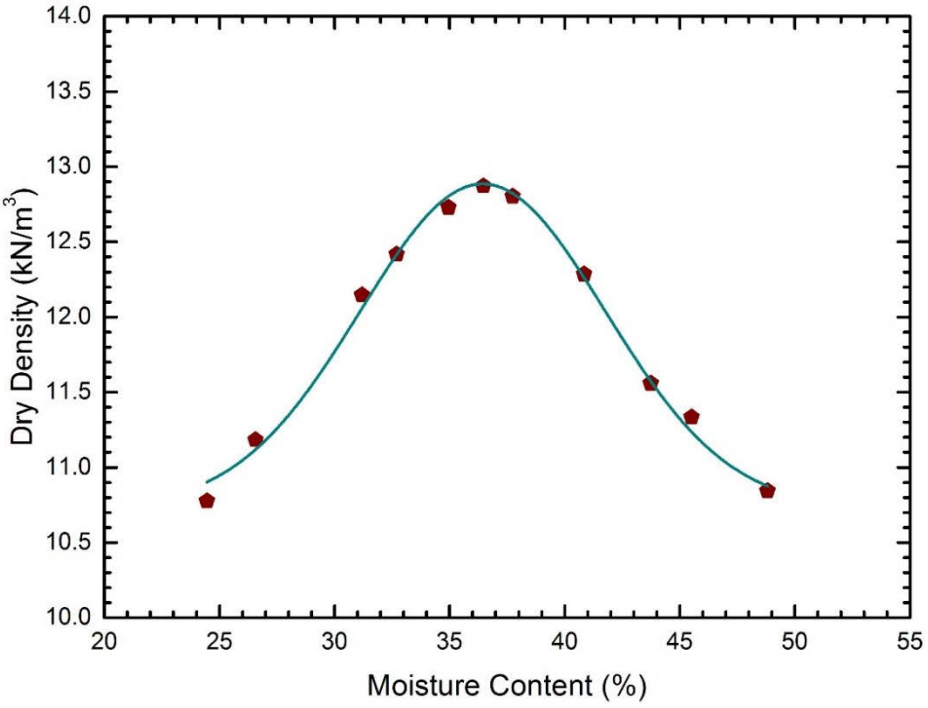

Figure 4.2 Compaction curve of natural expansive soil

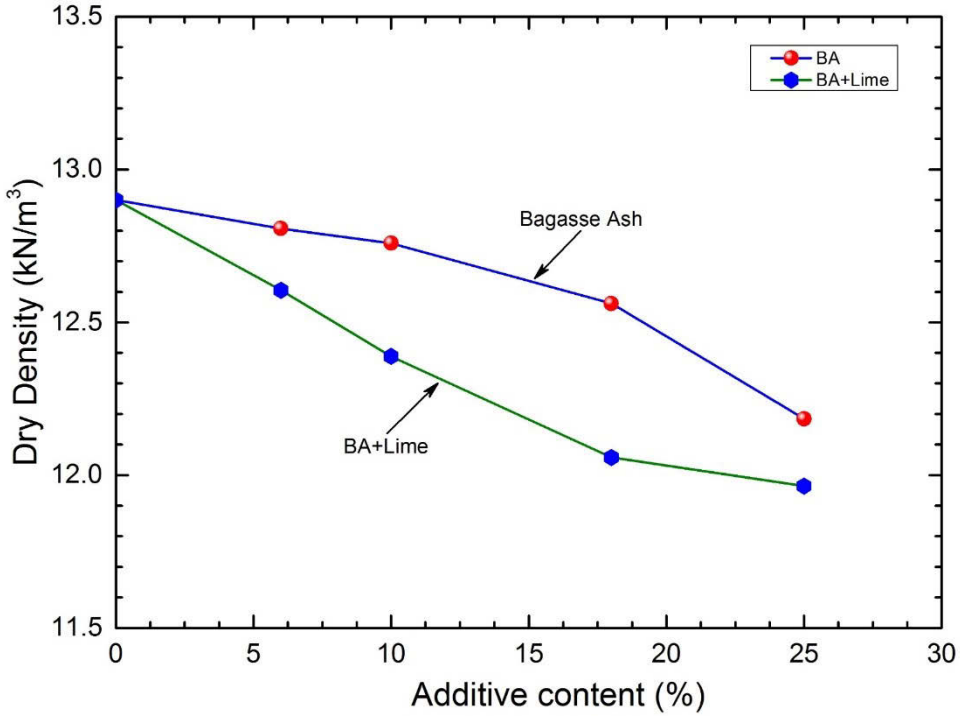

(a)

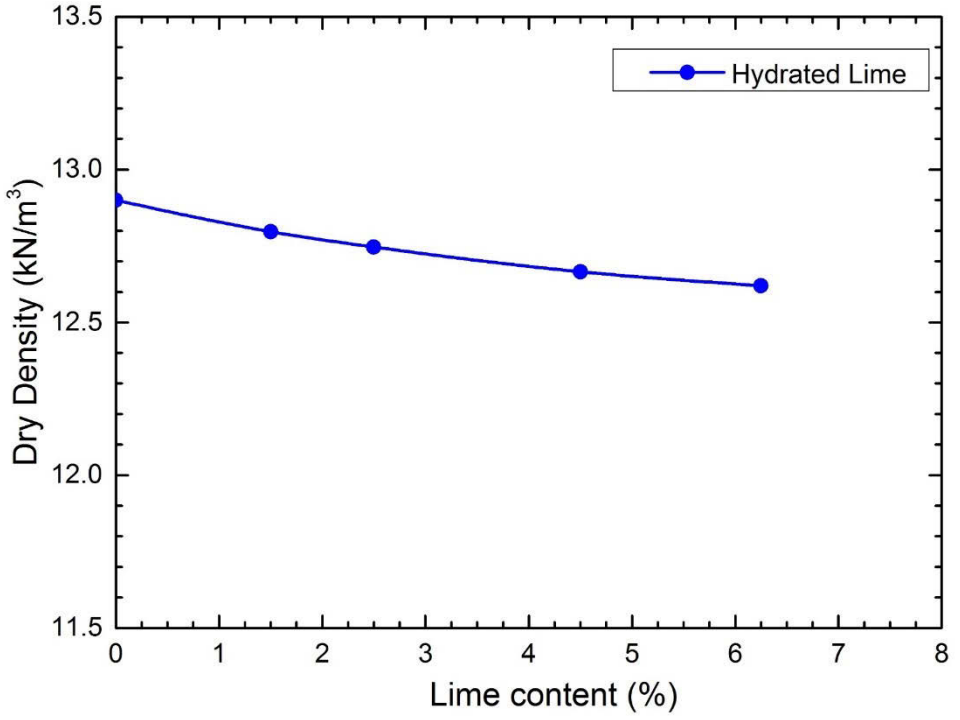

(b)

Figure 4.3 Influence of (a) bagasse ash and lime-bagasse ash, (b) hydrated lime content on the maximum dry density of treated expansive soil

4.2.3. Influence of Additive Content on Stress-Strain Behaviour

The stress-strain curves attained from unconfined compressive strength tests are depicted in Figure 4.4 for bagasse ash treated expansive soil and Figure 4.5 for hydrated lime-bagasse ash combination at a ratio of 1:3 treated expansive soil after 28 days of curing. As observed in Figure 4.4, the stress-strain behaviour of untreated expansive soil is compared with that of bagasse ash treated expansive soil when bagasse ash content increased up to 25%. The untreated expansive soil reached a peak stress of 138 kPa at an axial strain of 3.5%. However, the peak stress and strain increased progressively with the increasing bagasse content up to 18% followed by a slight drop as bagasse ash content increased to 25%. It can be noted that the peak stress and corresponding axial strain at 18% bagasse ash were 203 kPa and 4.9%, respectively, which reveal a remarkable increase of 48% and 40%, respectively, compared to those of untreated soil. Thus, the material ductility and compressive stress were enhanced due to the addition of bagasse ash. In general, there was a considerable improvement in mechanical properties of bagasse ash treated expansive soil. Nonetheless, the unconfined compressive stress of treated expansive soil reduced slightly when the bagasse ash content was greater than 18%, which indicates that 18% bagasse ash content could be the optimum bagasse ash content achieving the highest compressive stress.

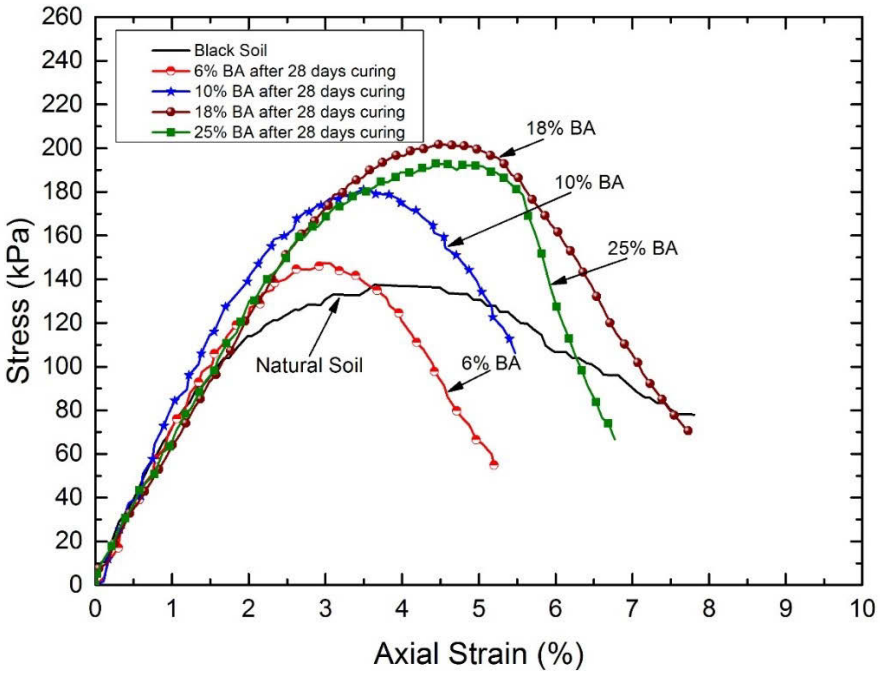

Figure 4.4 Influence of different bagasse ash content on stress-strain behaviour of expansive soil

In addition, Figure 4.5 illustrates the influence of different hydrated lime-bagasse ash combinations on stress-strain behaviour of expansive soil after 28 days of curing. As expected, the peak stress increased dramatically with an increase of combined hydrated lime-bagasse ash content and the stabilised expansive soil also displays a marked stiffness and brittleness in comparison with the untreated expansive soil. For example, at 25% hydrated lime-bagasse ash addition, the failure stress and corresponding axial strain of treated expansive soil were about 1255 kPa and 1.35%, respectively, which show a substantial increase of 815% in the peak stress but a significant reduction of 61% in the corresponding peak strain in comparison with those values of untreated expansive soil. However, in comparison with the expansive soil treated with 6.25% hydrated lime as shown in Figure 4.5, the addition of 25% hydrated lime-bagasse ash combined yielded a considerable increase of approximately 58% in the peak stress together with resulting in

81% corresponding axial strain. This implies that the addition of combined hydrated lime-bagasse ash exhibits more ductile behaviour, axial stress and strain-hardening characteristics than individual hydrated lime treated expansive soil. According to several researchers (Cai et al. 2006; Fatahi et al. 2012b; Tang et al. 2007), the failure strain for cement/lime treated clayey soil is typically ranging from 0.5% to 0.75% which is significantly less than the corresponding values in this research for lime/bagasse ash treated soil. Hence, the failure strain of soil treated with bagasse ash-hydrated lime obtained in this investigation ranging from 1.22% to 1.52% could be considered the remarkable improvement in ductility of stabilised expansive soil.

Generally, it can be expressed that the additions of bagasse ash, hydrated lime, and their combination to expansive soils result in chemical reactions in forms of cation exchange, pozzolanic reaction, carbonation, and cementation. During cation exchange, flocculation of clay particles occurs giving rise to agglomeration into coarser particles helping resist the compressive stresses much more effectively in comparison with those of virgin soil. In addition, the cementation process plays a key role in binding the clay particles together and consequently increasing the compressive stress. Results in this investigation are a good agreement with the findings of published research by other researchers (Ganesan et al. 2007; Goyal et al. 2007; Manikandan & Moganraj 2014; Osinubi et al. 2009a; Sharma et al. 2008).

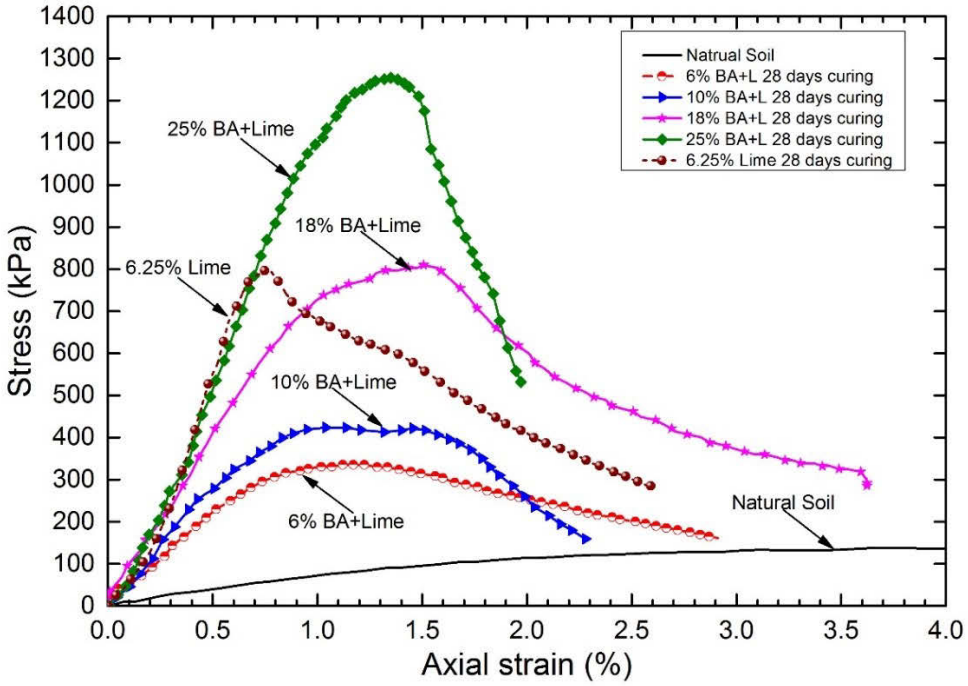

Figure 4.5 Influence of different hydrated lime-bagasse ash content on stress-strain behaviour of expansive soil after 28 days of curing

4.2.4. Influence of Additive Content on UCS Values

Figure 4.6 presents the influence of bagasse ash contents on the unconfined compressive strength of treated expansive soil after various curing periods including 3, 7 and 28 days. The UCS (unconfined compressive strength) of stabilised expansive soil increased steadily with an increasing amount of bagasse ash up to 18% and then followed by a slight drop to 25% bagasse ash inclusion regardless of any given curing periods of 3, 7 and 28 days. Hence, this obviously confirms that 18% bagasse ash content can be considered as the optimum content required for expansive soil stabilisation. Furthermore, a nonlinear relationship between unconfined compressive strength and bagasse ash content was clearly observed in Figure 4.6.

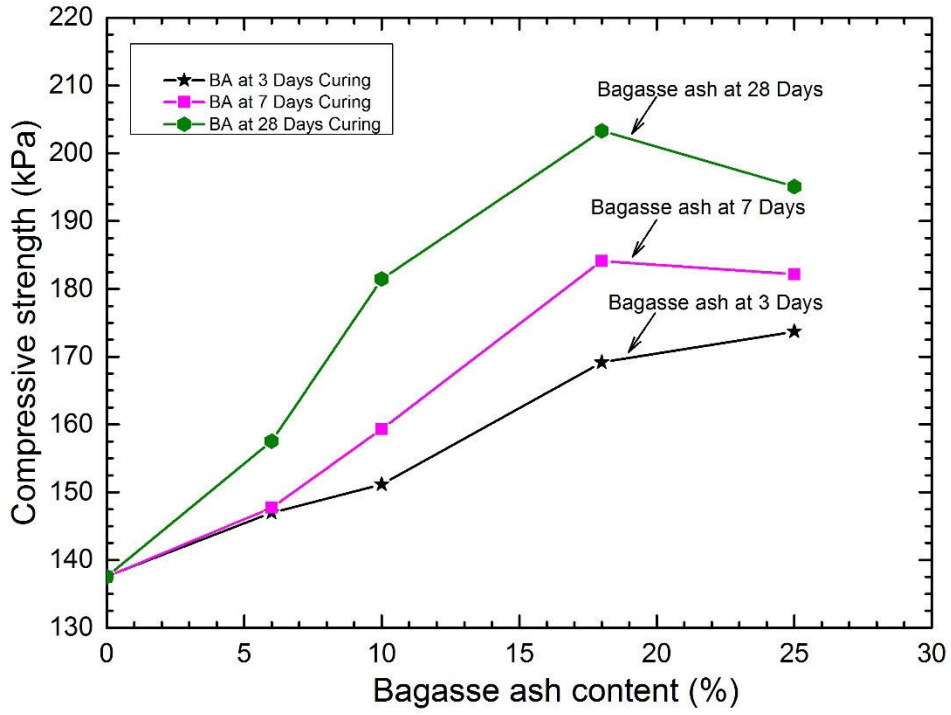

Figure 4.6 Influence of bagasse ash addition on average UCS value of treated expansive soil with various curing times

The influence of hydrated lime and bagasse ash-hydrated lime content on the UCS values of stabilised expansive soil along with various curing times is displayed in Figure 4.7 and Figure 4.8, respectively. Overall, the unconfined compressive strength increased significantly with hydrated lime (L) content as well as hydrated lime-bagasse ash combined (BA+L) content. As plotted in Figure 4.7 and Figure 4.8, the general trend obviously showed a steady increase in the unconfined compressive strength with the additive content irrespective of the curing time. Referring to Figure 4.7 and Figure 4.8, there was a sharp increase in UCS values (i.e., 480%) when the hydrated lime content increased from 0% up to 6.25%. Meanwhile, with an increase in the BA+L content from 0% to 25%, the UCS values significantly increased by almost 815%. Moreover, in

comparison with the individual BA (bagasse ash) treated expansive soil at the same curing time, the 28 days-curing UCS value of 25% BA+L content was significantly greater than that of 25% BA treated expansive soil by 545% referring to Figure 4.6. These comparisons reveal that the combination of hydrated lime-bagasse ash at a ratio of 1:3 was more effective in enhancing the unconfined compressive strength of stabilised expansive soil than the other additives used alone.

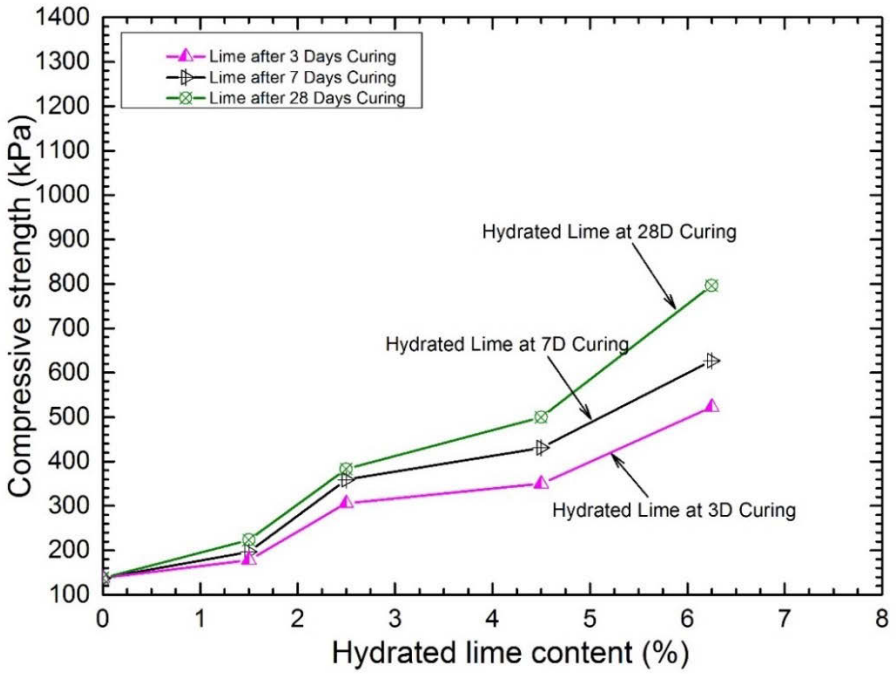

Figure 4.7 Influence of hydrated lime addition on average UCS value of treated expansive soil with various curing times

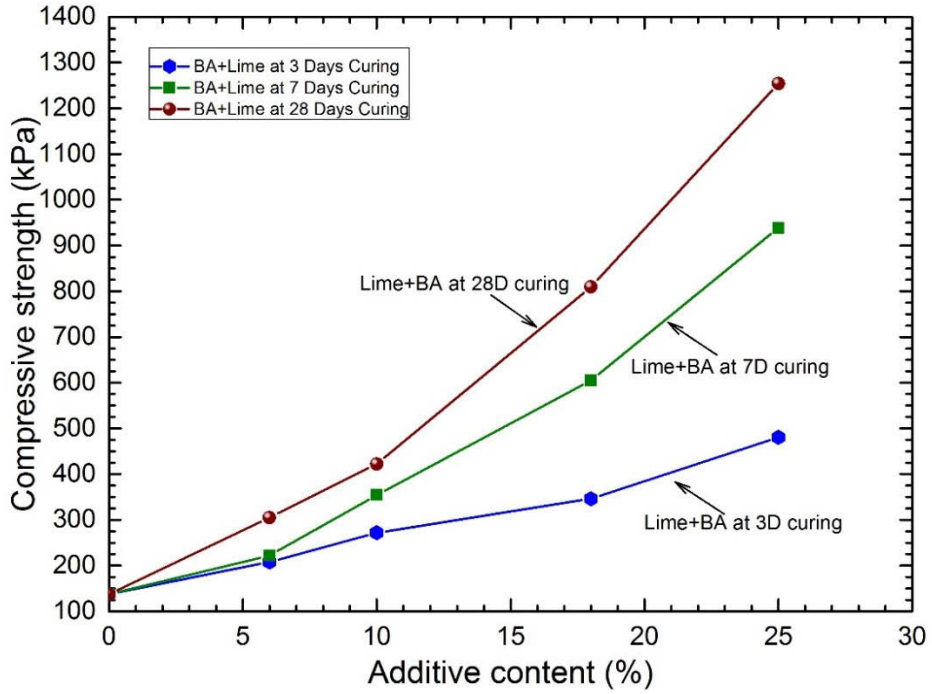

Figure 4.8 Influence of hydrated lime and bagasse ash admixtures on average UCS value of treated expansive soil with various curing times

It is noteworthy to state that the additions of bagasse ash, hydrated lime, and their combination effectively contribute to the expansive soil stabilisation. The improvement is more pronounced when the combination of hydrated lime and bagasse ash stabilised soil is used. The substantial improvement in compressive strength could be attributed to cation exchange, pozzolanic reactions due to a high amount of alumina, silica, and lime available in bagasse ash. When such minerals are exposed to water, alumina and silica chemically react with free lime in bagasse ash and form cementitious compounds distributed between clay particles, enhancing the compressive strength of bagasse ash treated soil. Correspondingly, the addition of hydrated lime aids in accelerating the reactivity of the pozzolan available in further enhancing the compressive strength of the treated soil. The more pozzolanic reactions of hydrated lime-bagasse ash admixture, the

better compressive strength of the admixture would be. These interpretations are in good conformity with the previous research results available in the literature (Osinubi et al. 2009b; Usman et al. 2014).

4.2.5. Influence of Curing Time on Unconfined Compressive Strength

Figure 4.9-4.12 exhibit the effect of different curing periods of 3, 7, and 28 days on the unconfined compressive strength of stabilised soils. Overall, as illustrated in these figures, the unconfined compressive strength of treated expansive soil increased with increasing curing time. For example, as observed in Figure 4.9, for the soil specimens treated with 18% bagasse ash and cured for 28 days, there was almost 20% and 10% increase in the UCS observed in comparison with 3 days, 7 days curing, and 48% increase compared with the UCS value of untreated expansive soil, respectively. As observed in Figure 4.9, when bagasse ash content is more than 6%, the compressive strength of treated soil increases significantly with curing time, which reveals the higher increase in additive content stabilised expansive soil produced the larger impact on the compressive strength of treated soils.

Figure 4.10 and 4.11 show the effect of curing time on the unconfined compressive strength for hydrated lime and combined hydrated lime-bagasse ash stabilised expansive soil, respectively. Generally, the curing time has a notable impact on the strength gain of treated soil. As evident in these figures, the unconfined compressive strength of treated expansive soil samples was significantly higher than that of untreated soil samples. For example, as illustrated in Figure 4.10 for the soil treated with 4.5% lime as the curing time increased from 3 days to 28 days, the UCS showed a remarkable

increase of 43%. The time-dependent increase in compressive strength of soil treated with lime might be due to lime-soil reactions, which facilitates the formation of cementitious bonds linking soil aggregates as a result of pozzolanic reactions. Nevertheless, the effect of time on the strength improvement was more pronounced when additive content exceeded 10%, as plotted in Figure 4.11. For example, for the samples treated with 6% hydrated lime-bagasse ash admixtures, an increase of 47% in compressive strength was observed when curing time increased from 3 days to 28 days, while the corresponding increase for samples treated with 18% combined additives was 135%. In addition, it is observed that the increase in compressive strength of BA+L stabilised soil was more significant during the first 7 days of curing period. Inspection of UCS results as shown in Figure 4.11 reveals a gradual increase in compressive strength of stabilised soil as the curing time increased from 7 days to 28 days. To be more specific, the addition of 25% hydrated lime-bagasse ash admixtures resulted in the remarkable increase in UCS values by 585% corresponding to 7 days curing, while the UCS values increased further by 230% as curing time increased from 7 days to 28 days. A similar trend can be observed in Figure 4.9 for bagasse ash and Figure 4.10 for hydrated lime stabilised expansive soils.

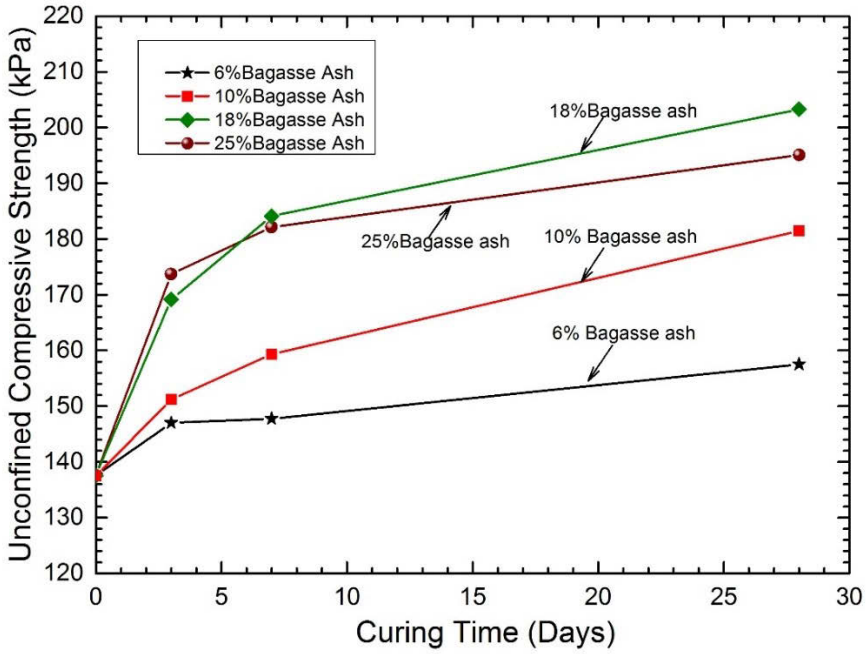

Figure 4.9 Influence of curing time on unconfined compressive strength of treated expansive soil with various bagasse ash contents

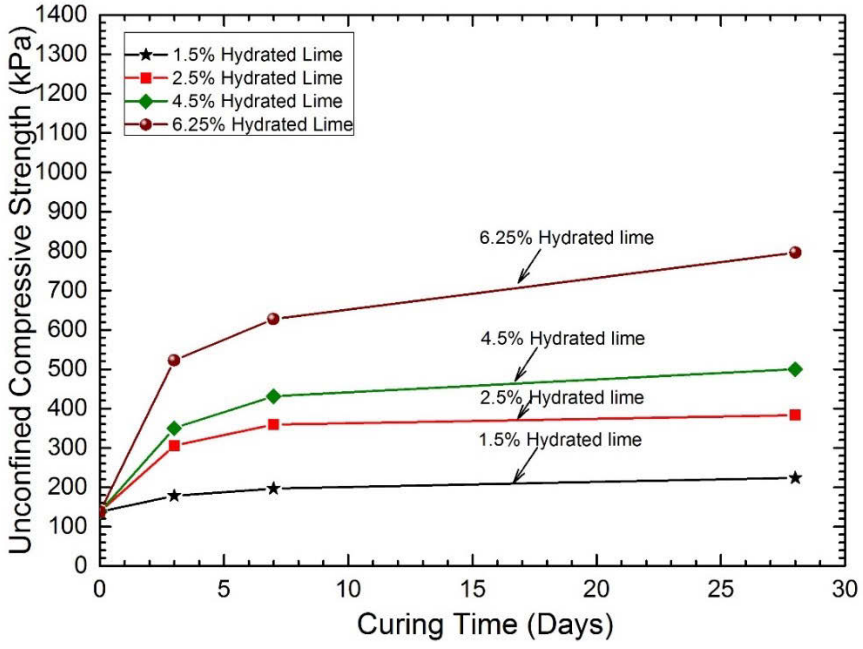

Figure 4.10 Influence of curing time on unconfined compressive strength of treated expansive soil with various hydrated lime contents

Referring to Figure 4.12 for further comparing the strength development in the BA+L and hydrated lime admixtures with longer curing time, the remarkable strength development of soil treated with BA+L was observed not only at the initial stage of 28 days of curing but also at the subsequent 28 days irrespective of additive content. However, for samples treated with hydrated lime alone, the predominant strength gain was obtained at the initial stage of 28 days of curing, the compressive strength remained almost constant when curing time exceeded 28 days. This trend manifests the BA+L admixtures are more effective in enhancing the compressive strength of treated soil than hydrated lime in the longer curing time. This behaviour is attributable to the higher pozzolanic materials such as silica (SiO_2), alumina (Al_2O_3), and ferric oxide (Fe_2O_3) containing in the mixtures of lime treated soil combined with bagasse ash, which promote the higher pozzolanic reactivity and hence enhance the higher strength in the long term. This behaviour is consistent with the similar phenomenon reported by other researchers (Jiang et al. 2015; Kampala & Horpibulsuk 2013) when studied silty clay stabilised with calcium carbide residue and hydrated lime, and (Wu et al. 2016) when stabilized solid waste using fly ash, bottom ash and paper sludge with cement.

It can be concluded that the curing time influences the compressive strength of stabilised expansive soil significantly attributed to hardening process of soil modification due to cation exchange reactions between calcium (Ca^{2+}) ions and the existing negative ions on the clay mineral lattice. This process contributes considerably to the initial strength gain followed by a period of steady growth with a low rate of the pozzolanic reactions. Such pozzolanic reactions generate cementitious bonds surrounding clay particles that enhance the compressive strength of treated soil with time. Furthermore, the

notable strength gain with increasing curing time may also be due to further crystallization of cementitious compounds instead of the instant soil-lime modification as reported by Boardman et al. (2001). However, as observed in Figure 4.9-4.12, the low threshold of lime addition has little impact on the strength gain of stabilised expansive soil. This may be due to insufficient lime available in low dosage additive required to make cation exchange reactions happen while accelerating pozzolanic reactions. Such modification and pozzolanic reactions are essential to contribute to flocculation and agglomeration of clay particles taking place and then improving the compressive strength of the treated expansive soil with time.

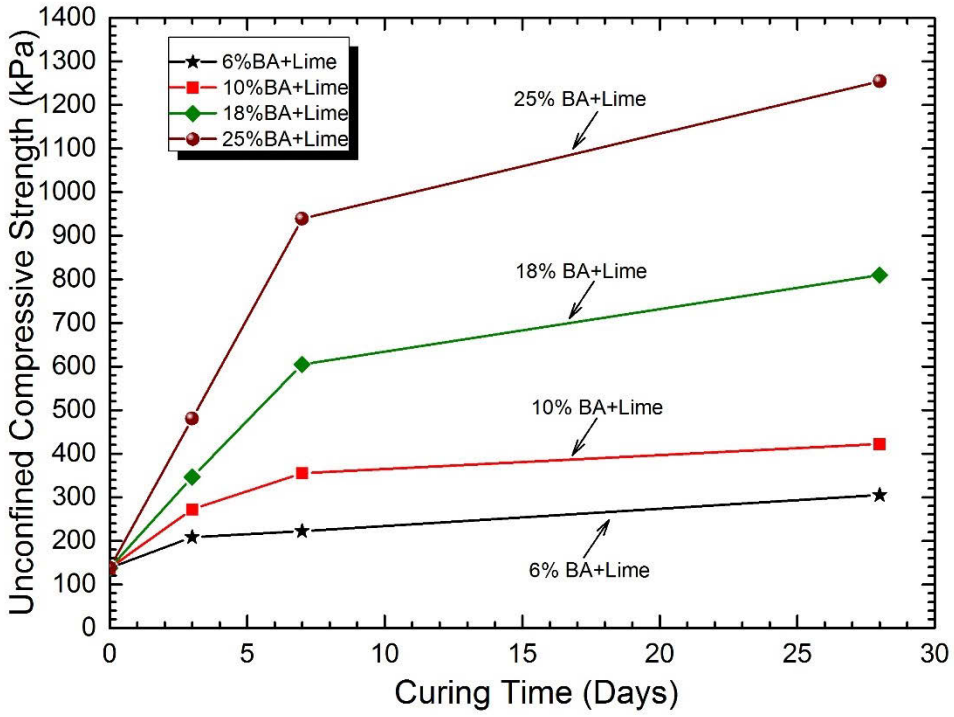

Figure 4.11 Influence of curing time on unconfined compressive strength of treated expansive soil with various hydrated lime-bagasse ash contents

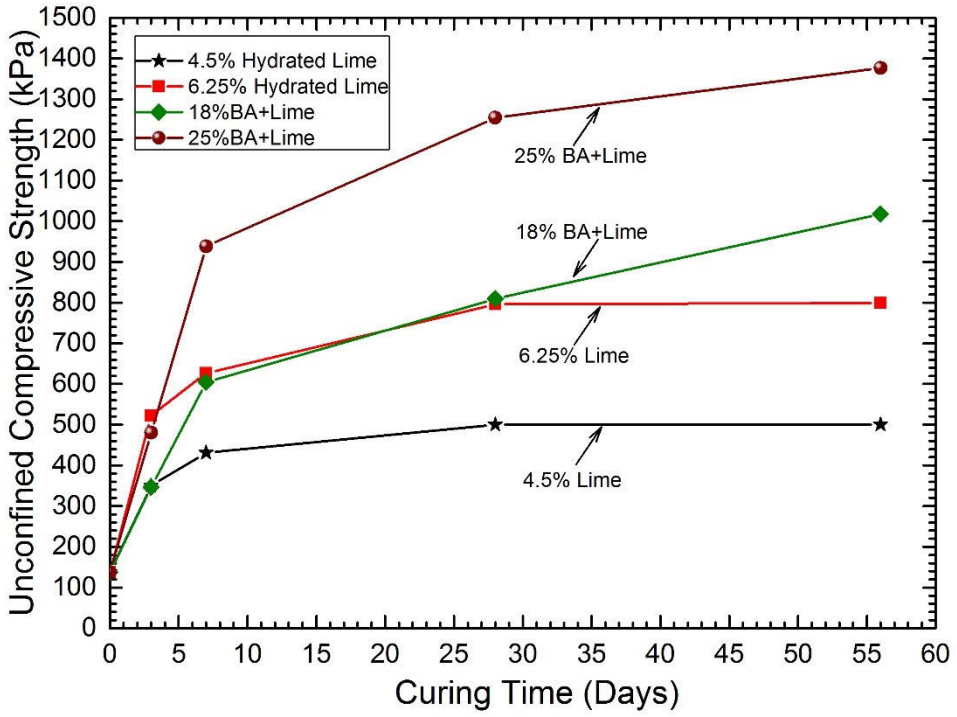

Figure 4.12 Influence of longer curing time on unconfined compressive strength of treated expansive soil with various hydrated lime and lime-bagasse ash contents

4.2.6. Influence of Additive Content on California Bearing Ratio

The strength and bearing capacity of subgrade materials are essential design criteria in pavement engineering. California bearing ratio (CBR) test is one of the most common tests used to assess the quality of base and subgrade materials for highway and road construction and design purposes. Figure 4.13 represents variations of the CBR value of expansive soil specimens stabilised with different bagasse ash contents up to 25% along with various curing periods up to 28 days. In general, as shown in this figure, an appreciable improvement in CBR value was observed with an increase in additive content as well as the curing time. For instance, in comparison with the untreated soil, the CBR value of bagasse ash stabilised expansive soil after 7 days of curing increased from 7.1%

to 11.5% with increasing bagasse ash (BA) content from 0% to 25%, respectively (i.e. 62% increase in CBR). In addition, with the curing time increased from 7 days up to 28 days, the CBR value of expansive soil treated with 25% BA increased significantly (approx. 83%). This obviously demonstrates that the surge of CBR value was not only with increasing BA content but also with curing time. The increase in CBR value with curing time may be due to hydration and pozzolanic reactions inducing the improvement in strength contributed from bagasse ash, which is in good agreement with the early researchers observation (Anupam et al. 2013; Osinubi et al. 2009a).

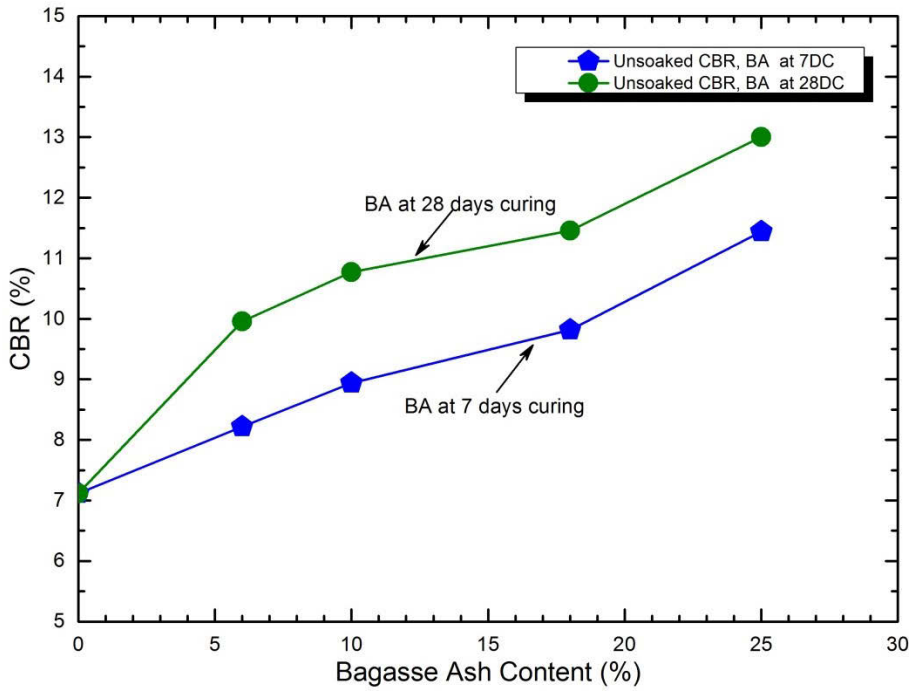

Figure 4.13 Influence of bagasse ash admixtures on average unsoaked CBR of treated expansive soil with various curing times

Figure 4.14 indicates the general effect of additions of hydrated lime and BA+L combined on the CBR gain of treated expansive soil after 28 days of curing. As illustrated

in Figure 4.14, the CBR values of treated expansive soil increased drastically as additive content increased up to 4.5% and then followed by either a slight drop for hydrated lime alone or a slight increase for combined hydrated lime-bagasse ash. In comparison with the untreated soil, the addition of 6% of BA+L (with 1.5% hydrated lime in this mixture) contributed to the increase in CBR by a factor of 2.8, whereas the addition of 18% BA+L (with 4.5% hydrated lime in the mixture) resulted in 8.2 times increase of CBR. However, there was an insignificant increase in CBR with further increase in BA+L content up to 25% (with 6.25% hydrated lime in the mixture). This 18% BA+L can be considered as optimum additive content for CBR enhancement. A similar trend was observed in Figure 4.14 for the hydrated lime alone reconfirming that 4.5% hydrated lime content could be the optimum lime content for CBR improvement. It can be observed that the CBR value of soil improved with BA+L was closed to the corresponding mixture, which implies that the addition of bagasse ash would not produce the adverse effect on the strength and bearing capacity of the lime stabilised soil. As evident in Figure 4.14, bagasse ash is more effective in enhancing CBR when more hydrate lime is utilised to treat the soil (e.g. 6.25% hydrated lime). Hence, it is important to note that the combinations of BA+L resulted in the more significant improvement in CBR value as the more BA+L additive is utilised. It should be noted that even 1.5% hydrated lime combined with 4.5% bagasse ash (1:3 combination) could result in a CBR of 20%, which could easily satisfy the minimum 15% CBR requirement adopted by most of the design guidelines for selected subgrade (Section4-Flexible Pavement Construction 2010; Muntohar et al. 2013). With the higher addition of BA+L, the obtained CBR value could meet the subbase course materials requirement fairly easily (Part 4A: Granular Base and Subbase Materials 2009; Muntohar et al. 2013). The increase in CBR value might be due to the flocculation and

agglomeration phenomena in the short term as well as attributable to the hydration process and pozzolanic reactions in the long term to form new cementitious compounds contributed from bagasse ash and hydrated lime.

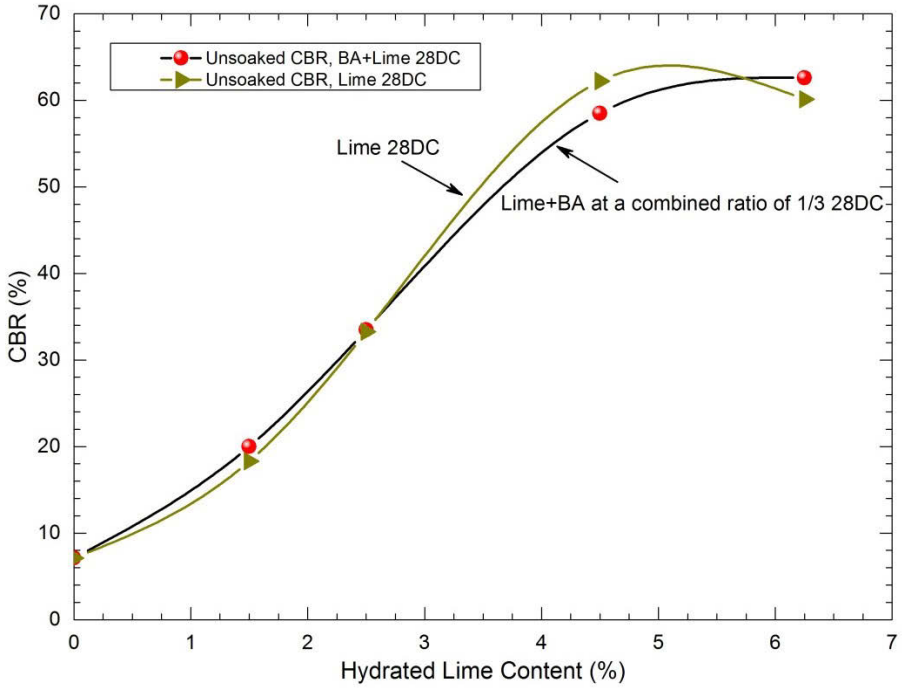

Figure 4.14 Influence of hydrated lime, combined hydrated lime-bagasse ash admixtures on unsoaked CBR of treated expansive soil after curing for 28 days

4.2.7. Influence of Additive Content on Linear Shrinkage

Variations of linear shrinkage of the treated expansive soil along with BA, hydrated lime, and BA+L contents as well as curing time are presented in Figure 4.15-4.17, respectively. In general, the increase in additive content resulted in the improvement in linear shrinkage of the treated soil. The significant and rapid reduction in linear shrinkage was observed during the first 7 days of curing period for any given additive contents. Subsequently, there was a less notable reduction in the linear shrinkage beyond 7 days of curing. For example, as plotted in Figure 4.15, by increasing BA content from 0% to 25%, the linear

shrinkage of treated expansive soil after 7 days of curing decreased by 45%; However, with further increase in curing time up to 28 days, marginal improvement (less than 2%) in the linear shrinkage at the same amount of bagasse ash was observed. The similar trend can be observed for the hydrated lime and BA+L treated soils. For example, referring to Figure 4.16, when hydrated lime content increased from 0% to 6.25%, about 64% reduction in the linear shrinkage for 7 days cured samples was observed, whereas the decrease in linear shrinkage was approximately 68% with longer curing time up to 28 days. Correspondingly, the increase in BA+L content from 0% to 25%, as plotted in Figure 4.17, produced a significant reduction in the linear shrinkage after 7 days by almost 79%. Meanwhile, the further increase in curing time up to 28 days resulted in a minor decrease in the linear shrinkage (by 5%). It should be noted that the results of linear shrinkage tests indicate that the combination of BA+L (bagasse ash-hydrated lime) was much more effective than the individual bagasse ash or hydrated lime alone in improving the linear shrinkage of expansive soil regardless of any particular additive content and curing time.

Consequently, the use of either BA or BA+L for expansive soil treatment could be likely beneficial since these stabilisers could provide considerably positive impacts on the engineering characteristics of expansive soil in terms of alleviating linear shrinkage and cracking. The observed significant improvement in linear shrinkage could be attributed to the flocculation and aggregation phenomena of clay particles induced by the presence of free lime in bagasse ash contributing to the formation of coarser particles, and eventually enhanced the strength of the treated soil. In other words, the finer clay particles were replaced by relatively stronger and coarser particles that could be the key factors

resulting in the considerable decrease in linear shrinkage with the increase in the additive content and curing time.

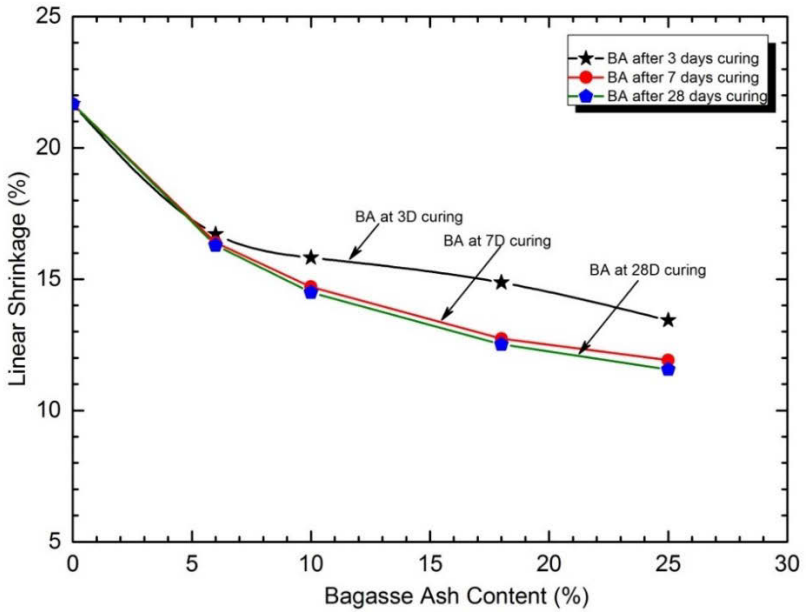

Figure 4.15 Linear shrinkage of expansive soil mixed with various bagasse ash contents for different curing times

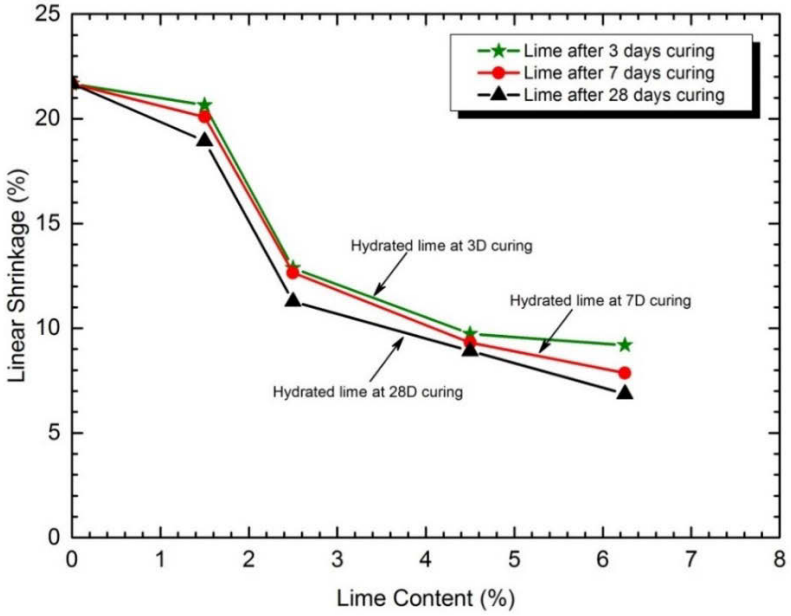

Figure 4.16 Linear shrinkage of hydrated lime treated expansive soil with different additive contents and curing times

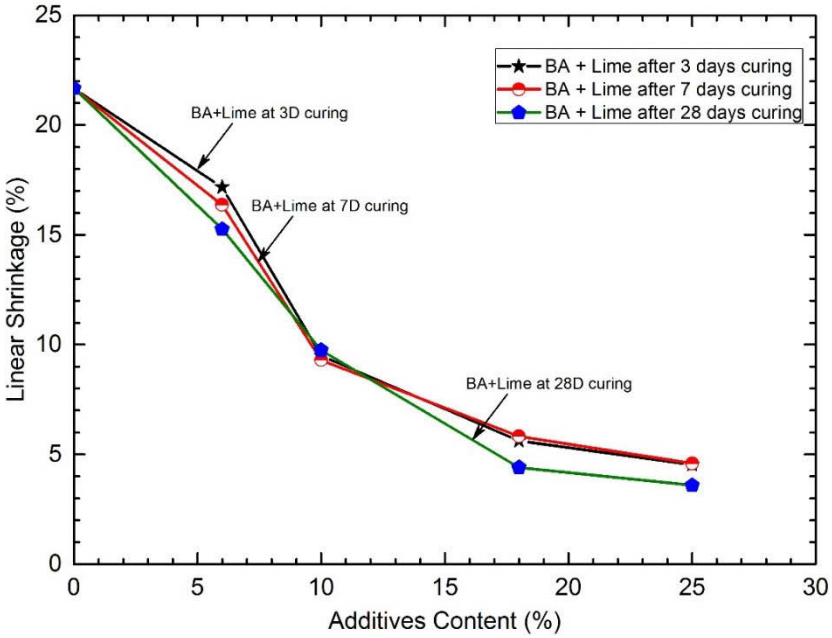

Figure 4.17 Linear shrinkage of hydrated lime-bagasse ash treated expansive soil with different additive contents and curing times

4.2.8. Influence of Additive Content on Time-Dependent Swelling

Figure 4.18 shows the time-dependent swelling variations of untreated and treated expansive soils for varying bagasse ash contents from 0% to 25%. It can be observed that swelling percentages (swelling strain) of bagasse ash stabilised soil decreased substantially with increasing bagasse ash content. In the adopted experiments reported in Figure 4.18 for bagasse ash treated expansive soil, the swelling strain approximately reached equilibrium state after 7 days of testing regardless of any given bagasse ash content. For example, the application of 18% bagasse ash treated soil resulted in the swelling strain of 2.5% after 7 days of testing, while the swelling strain increased further by 0.4% as testing time increased from 7 days to 28 days.

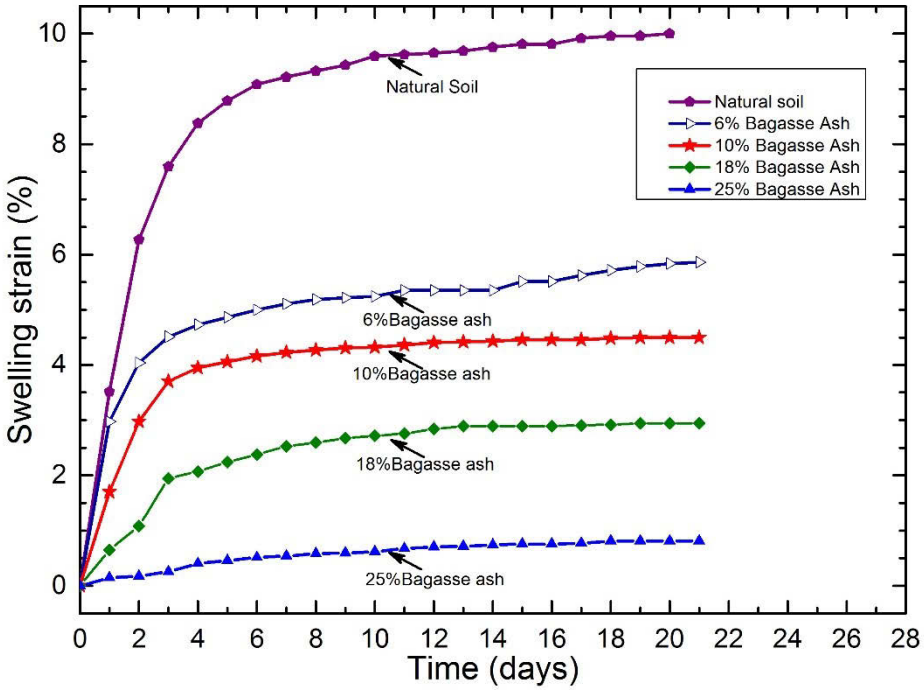

Figure 4.18 Influence of bagasse ash on swelling strain with time of expansive soil

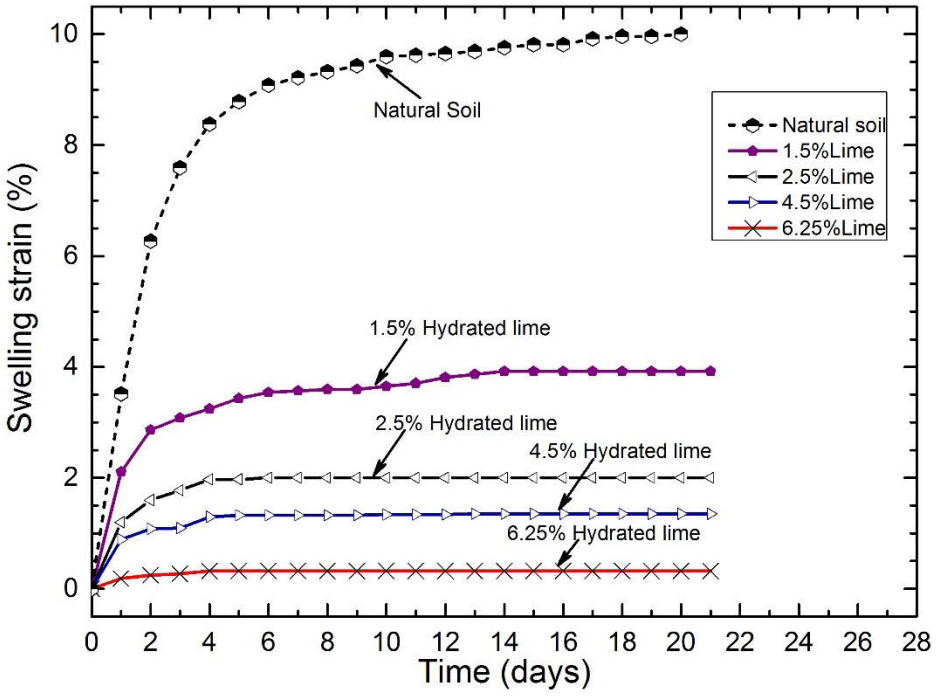

Figure 4.19 Influence of hydrated lime on swelling strain with time of expansive soil

Similar to the swelling trend of bagasse ash treated soil, the majority of swelling strain was measured in the short-term (i.e. first 4 days of testing) of the 21 days of testing period as illustrated in Figure 4.19 for hydrated lime stabilised soils. Meanwhile, a further increase in testing time resulted in a very slow increase in swelling strain observed or even zero swelling strain recorded for the higher content of the hydrated lime treated soil. For example, as evident in Figure 4.19, the swelling strain of 2.5%, 4.5% and 6.25% hydrated lime treated soils approached the approximate equilibrium state after 4 days of testing, apart from the case of 1.5% hydrated lime stabilised soil that required longer duration to obtain the equilibrium. The similar behaviour was observed by Punthutaecha et al. (2006) when investigating vertical swelling strain of expansive soil stabilised with recycled ashes and fibres; Rezende et al. (2017) when swelling tests were conducted on tropical soil mixed with Phosphogypsum and cement/lime. The possible reasons for the hydrated lime-soil admixtures attained the equilibrium state of swelling earlier compared to those of untreated and bagasse ash treated soil could be mainly attributed to instantaneously flocculation and agglomeration happening in the shorter term while partially due to time-dependent pozzolanic reactivity in the long-term. Such time-dependent reactivity of lime-soil admixtures can enhance the swelling resistance notably and effectively of the treated soil in comparison with bagasse ash used alone. Nonetheless, the insufficient amount of hydrated lime treated soil (e.g. 1.5% hydrated lime) could result in not only the accomplished interval of the equilibrium state gradually slow but also the higher maximum swelling strain (total swelling).

In order to further compare the time-dependent swelling strain of soil treated with hydrated lime, Figure 4.20 displays variations of the swelling strain of hydrated lime

treated soil with bagasse ash versus testing time. It is clearly observed in Figure 4.20 that with the presence of bagasse ash in the lime-soil admixtures, the swelling strain of treated soil reached a practically negligible level within the first 4 days of testing and remained almost zero swelling strain with a further increase in testing time. But it is except for the case of 1.5% hydrated lime treat soil with 4.5% bagasse ash (6%BA+L), which took approximately 12 days to reach the equilibrium state. To illustrate this, the latter sample of 6%BA+L obtained the equilibrium state at 1.4% swelling strain during the first 12 days of testing, whereas the other admixtures of hydrated lime treated soil with bagasse ash from 10% to 25% obtained the equilibrium state at approximately 0.1% swelling strain or below as can be seen in Figure 4.20. These experimental results reveal that the addition of bagasse ash into the lime treated soil admixtures is more effective in controlling the swelling strain than bagasse ash or hydrated lime alone treated soils. In other words, the soil treated with hydrated lime and bagasse ash become more stable when exposed to water than the soils stabilised with bagasse ash or hydrated lime alone. In addition, the more combined bagasse ash-hydrated lime content, the better-controlled swelling strain would be. That could be the reason why 1.5%lime treated soil with 4.5% bagasse ash remained relatively high swelling strain compared to the higher BA+L content treated soils as presented in Figure 4.20. As previously discussed, the substantial improvement in swelling strain of hydrated lime soils with bagasse ash is primarily attributable to immediately flocculation and agglomeration taking place in the shorter term while partially due to time-dependent pozzolanic reactivity in the long-term contributed from bagasse ash addition into the lime-soil admixtures.

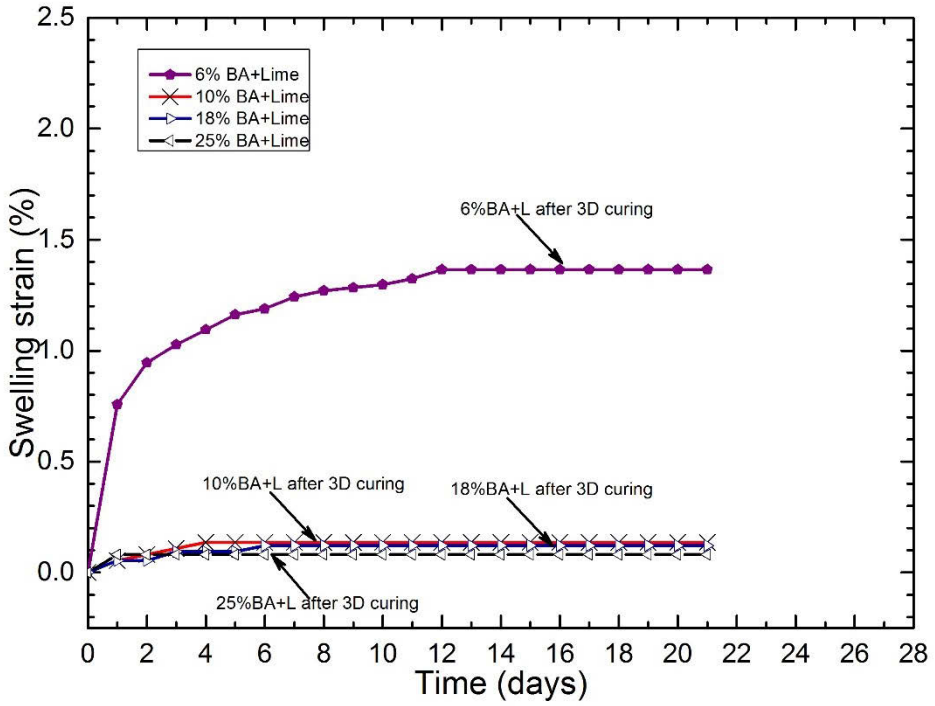

Figure 4.20 Influence of hydrated lime-bagasse ash combination on swelling strain with time of expansive soil

4.2.9. Influence of Additive Content on Swell Potential

Figure 4.21 and 4.22 display alternation of the swell potential of expansive soil treated with bagasse ash, hydrated lime, and BA+L in association with an increase in additive content. Overall, the swell potential of treated soil reduced with increasing additive content. As observed in Figure 4.21, the swell potential value of expansive soil treated with bagasse ash decreased steadily from roughly 10% to less than 1% when bagasse ash content increased up to 25%. Meanwhile, the additions of BA+L content up to 25% resulted in the significant decrease in swell potential of treated soil from almost 10% to less than 0.5%. It should be noted that the reduction of the swell potential was more noticeable for the combination of bagasse ash and hydrated lime treated expansive soil than bagasse ash alone treated soil. For example, with the increase in bagasse ash content

from 0% to 25%, the swell potential of treated soil samples gradually decreased to less than 1%, in such case, the treated expansive soil can be considered as non-expansive soil. Whereas, with a small increase in the BA+L content treated soil from 0% to merely 10%, the swell potential of soil treated with BA+L reduced drastically to less than 1%.

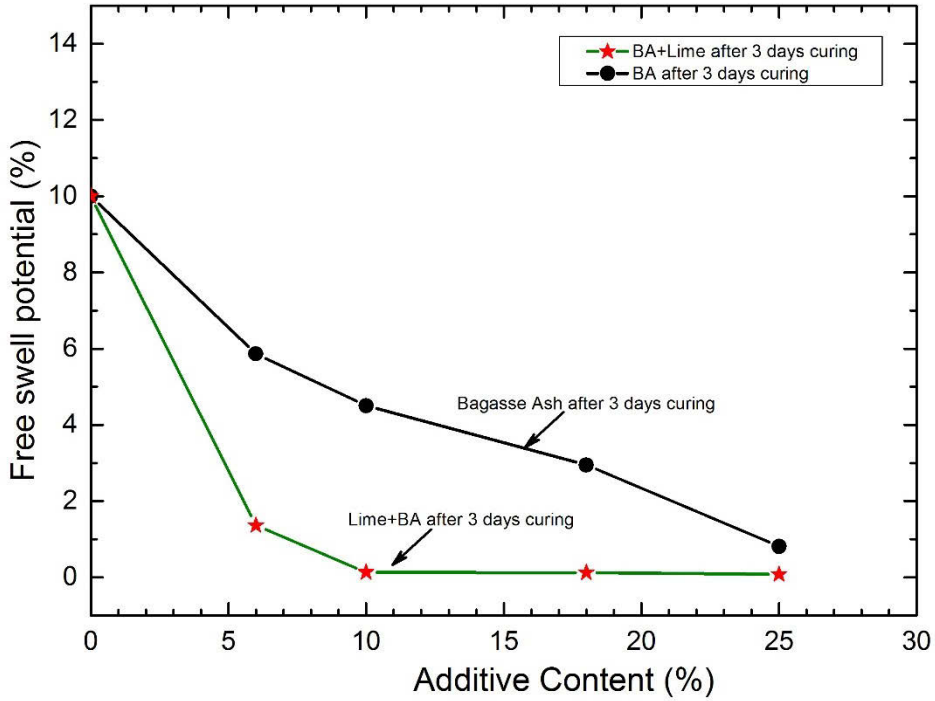

Figure 4.21 Influence of bagasse ash and hydrated lime-bagasse ash additions on the free swell potential of treated expansive soil

Likewise, Figure 4.22 indicates the swell potential of expansive soil treated with hydrated lime alone significantly reduced with an increase in hydrated lime content from 0% to 6.25%. For example, the increase in hydrated lime treated soil up to 6.25% resulted in a gradual drop of swell potential to an insignificant level of less than 0.5%. It is noteworthy to state that with the marginal swell potential of 0.5% obtained after stabilisation of expansive soil with hydrated lime, the treated soil can be considered as non-expansive soil. However, in comparison with bagasse ash or BA+L treated soils as illustrated in Figure 4.21, the improvement in the swell potential was again more effective

for BA+L than bagasse ash or hydrated lime alone treated soils. It can be expressed that the addition of 25% bagasse ash, 5% hydrated lime and only 7% BA+L stabilised expansive soil induced a comparable effect on the swell potential as visually seen in Figure 4.21 and 4.22. This implies that a prominent mount of the swell potential of treated expansive soil dropped to a certainly marginal level of less than 1%. The decrease in swell potential in line with the increase in the amount of bagasse ash, hydrated lime and its combination may be mainly due to taking place cation exchange phenomenon in that sodium, magnesium ions in original soil are most likely to be replaced by almost calcium ions of hydrate lime or free lime present in bagasse ash, which consequently enhance the swell potential of treated expansive soil. Results in this investigation are consistent with the previous investigations well-documented in the literature (Brooks et al. 2011; Yilmaz 2015).

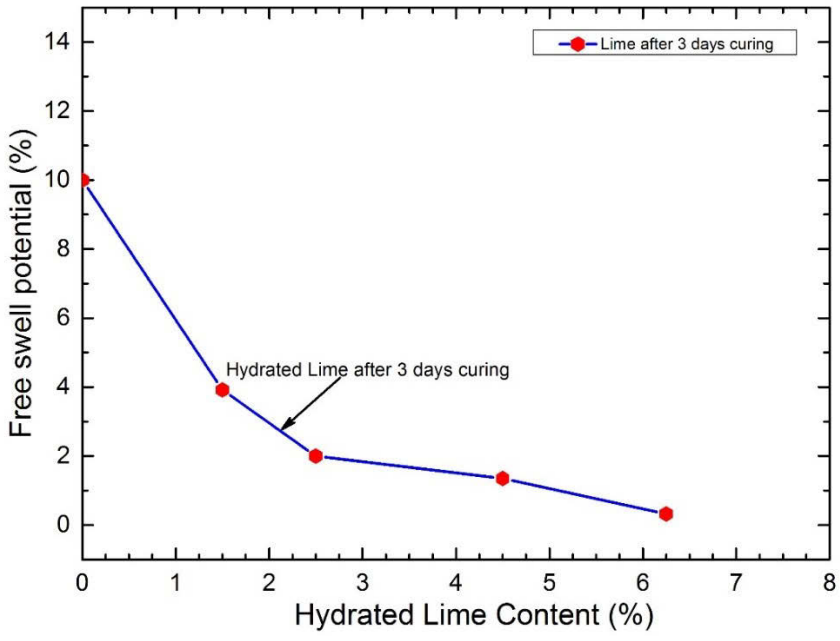

Figure 4.22 Influence of hydrated lime only and hydrated lime-bagasse ash additions on the free swell potential of treated expansive soil

4.2.10. Influence of Additive Content on Swelling Pressure

Swelling pressure tests were firstly carried out on untreated soil specimens and then conducted on treated expansive soil specimens using conventional dimensional consolidation apparatus to determine the swelling pressure of expansive soil so as to evaluate the influence of individual bagasse ash, hydrated lime, combined hydrated lime-bagasse ash inclusions on the fluctuation of swelling pressure of treated soil. The average swelling pressure of untreated soil specimen was primarily determined about 80 kPa. Following, Figure 4.23 and 4.24 display the variation of swelling pressure associated with increasing bagasse ash and BA+L, hydrated lime content, respectively. As observed in Figure 4.23, the addition of bagasse ash alone treated soil resulted in the steady reduction in swelling pressure from 80 kPa for natural soil to 31.5 kPa when bagasse ash content increased from 0% to 25%. The swelling pressure reduction amount for soils treated with bagasse ash was approximately 60% compared to that of untreated soil. Moreover, the BA+L combination showed a significant decrease in swelling pressure with an increase in additive content from 0% up to 10% followed by a gradual decrease in swelling pressure to approach a certain value of 10 kPa with further increase in BA+L content up to 25% as illustrated in Figure 4.23. This leads to an amount of swelling pressure reduction of approximately 88% as BA+L content treated soil increased from 0% to 25%. It is worthy to note that the decrease in swelling pressure was more pronounced for the combination of hydrated lime and bagasse ash treated soil than bagasse ash alone treated soil. Furthermore, the variation in swelling pressure of treated soil along with the increase in hydrated lime content is presented in Figure 4.24. This figure shows that the swelling pressure of soil treated with hydrated lime drastically dropped when hydrated lime content increased from 0% up to 4.5% followed by a minimal decrease in swelling

pressure with a further increase in hydrated lime content exceeded 4.5%. However, in comparing with BA+L treated soils as plotted in Figure 4.23, the addition of bagasse ash into the corresponding lime soil mixtures resulted in the lower swelling pressure observed at any given additive content, which confirms the combination of hydrated lime and bagasse ash was more effective in improving the swelling pressure of stabilised soil.

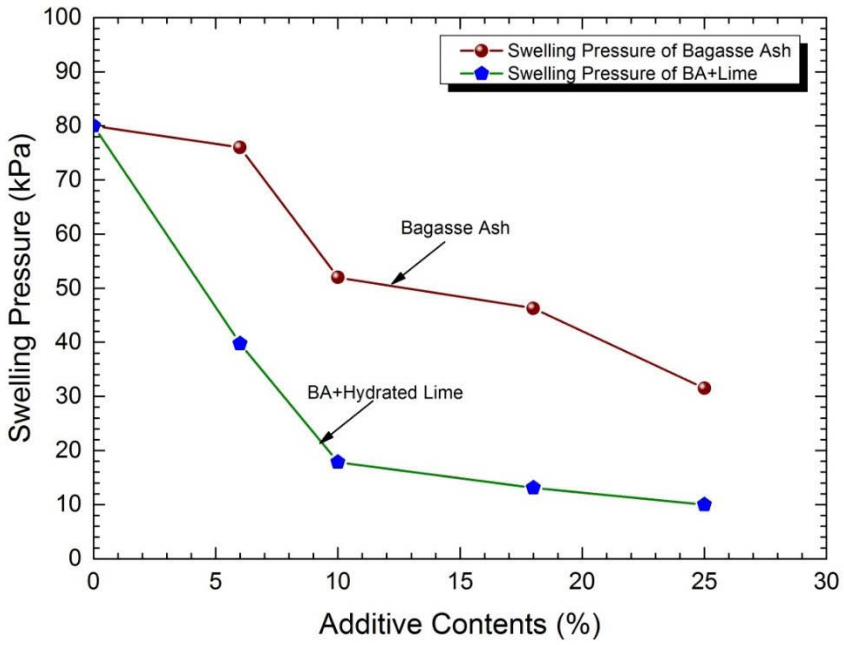

Figure 4.23 Influence of bagasse ash and hydrated lime-bagasse ash additions on the swelling pressure of treated expansive soil

In general, the swelling pressure depicts a similar trend of the free swell potential for the same additives of the stabilised soil samples. It can clearly be observed from the test results that the reduction in swelling pressure was more noticeable for hydrated lime-bagasse ash combination stabilised soils. Meanwhile, bagasse ash alone has less notable impact on swelling pressure resistance among the three adopted additives to treat expansive soil. As discussed in the previous section, the decrease in the swelling pressure

of treated soil in line with the increasing additive content could be attributed to cation exchange phenomenon in that alumina, silica, and sodium ions in untreated expansive soil are most likely to be replaced by almost readily available calcium ions of hydrated lime and free lime presenting in bagasse ash, which hinders the swell potential and swelling pressure of treated expansive soil.

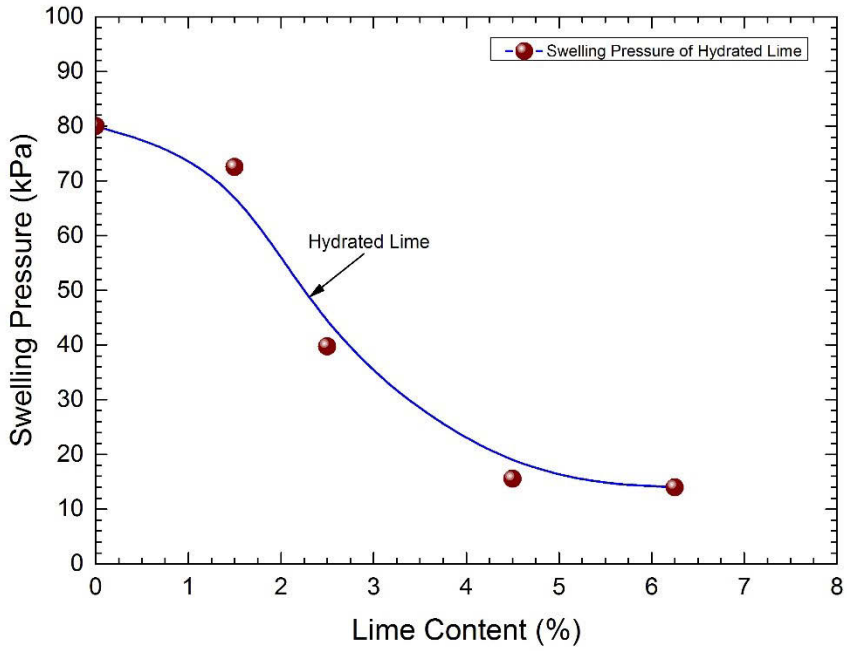

Figure 4.24 Influence of hydrated lime alone and hydrated lime-bagasse ash additions on the swelling pressure of treated expansive soil

4.2.11. Influence of Bagasse Ash and Hydrated Lime on Secant Modulus

Figure 4.25-4.27 depict the influence of the additions of bagasse ash, hydrated lime, and a combination of hydrated lime and bagasse ash, respectively, on secant modulus of treated expansive soil with different curing times. The secant modulus ($E_{50\%}$) also known as the initial Young's modulus (Fatahi et al. 2012b; Kim et al. 2008) indicate the slope of a line between the origin and the point of 50% failure stress on the stress-strain curve as

calculated in Equation (4.1). The overall behaviour exhibits that the secant modulus of stabilised expansive soil increased with the increase in additive contents and curing time prolonged, except for the case of soils stabilised with bagasse ash.

$$E_{50\%} = \frac{0.5q_u}{\varepsilon_{50\%}} \tag{4.1}$$

where q_u is the failure stress derived from the unconfined compressive strength tests and $\varepsilon_{50\%}$ is the axial strain when the normal stress is equal to $0.5q_u$.

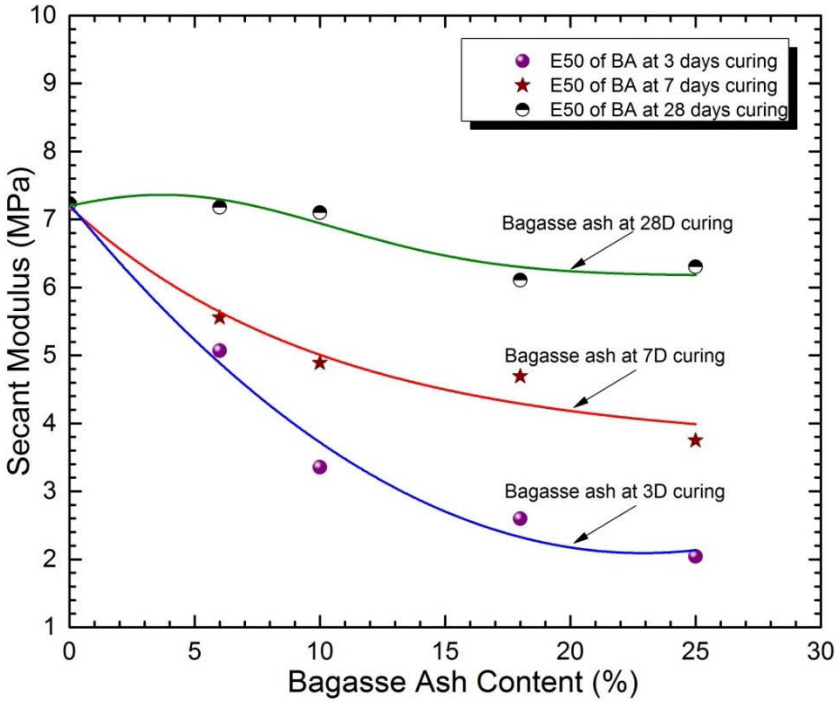

Figure 4.25 Influence of bagasse ash additions on Young's modulus of treated expansive soil with different curing times

It can clearly be seen in Figure 4.25 that the secant modulus of stabilised soils decreased with the increase in bagasse ash content but increased with an increase in curing

time. Specifically, when the addition of bagasse ash treated expansive soil increased from 0% to 25%, the secant modulus decreased from 7.2 MPa to a certain level of 2 MPa after 3 days of curing, which implies that the bagasse ash inclusion induced the decrease in stiffness of stabilised soil to a certain extent. This stiffness reduction may be due to using pozzolanic material such as bagasse ash that changes the original soil to become more ductile. However, the secant modulus of bagasse ash treated expansive soil increased with the curing time increase from 3 days to 28 days. For example, the secant modulus value of 25% bagasse ash stabilised expansive soil surged significantly from 2 MPa to 6.3 MPa when the curing duration increased from 3 days to 28 days as presented in Figure 4.25.

Figure 4.26 and 4.27 reveal the influence of hydrated lime alone and BA+L combination on the secant modulus of treated soils, respectively, associated with the increase in curing time from 3 days to 28 days. It is clearly observed in these figures that the stiffness of stabilised expansive soil significantly increased with an increase in the content of both additives in line with curing period extended. The nonlinear relationship between secant modulus and additives content was clearly depicted as the dominant mechanism. These figures also exhibit that the addition of bagasse ash into the hydrated lime-soil admixtures resulted in the similar impact on the stiffness improvement of treated expansive soil in comparison with those of expansive soils stabilised with hydrated lime alone. Referring to Figure 4.27, for example, with the addition of BA+L content increased from 0% to 25% after 28 days of curing, the secant modulus of treated soil significantly increased from 7.2 MPa to 107.2 MPa (approximately 14.9 times higher than that of untreated soil), meanwhile the secant modulus of soils treated with hydrated lime at the same curing time derived from Figure 4.26 was almost 13.6 times higher that of natural

soil when lime content increased from 0% to 6.25%. This demonstrates that the addition of bagasse ash into the lime treated soil specimens would not reduce the stiffness of treated soil; thus, bagasse ash can be utilised as a filling material in support of road and highway embankment construction without causing adverse effects in terms of stiffness and settlement. In fact, according to Ghosh & Dey (2009), the secant modulus is a key factor in predicting the settlement of foundations or highway embankments constructed on subgrade soils stabilised with recycled filling materials such as fly ash, bagasse ash.

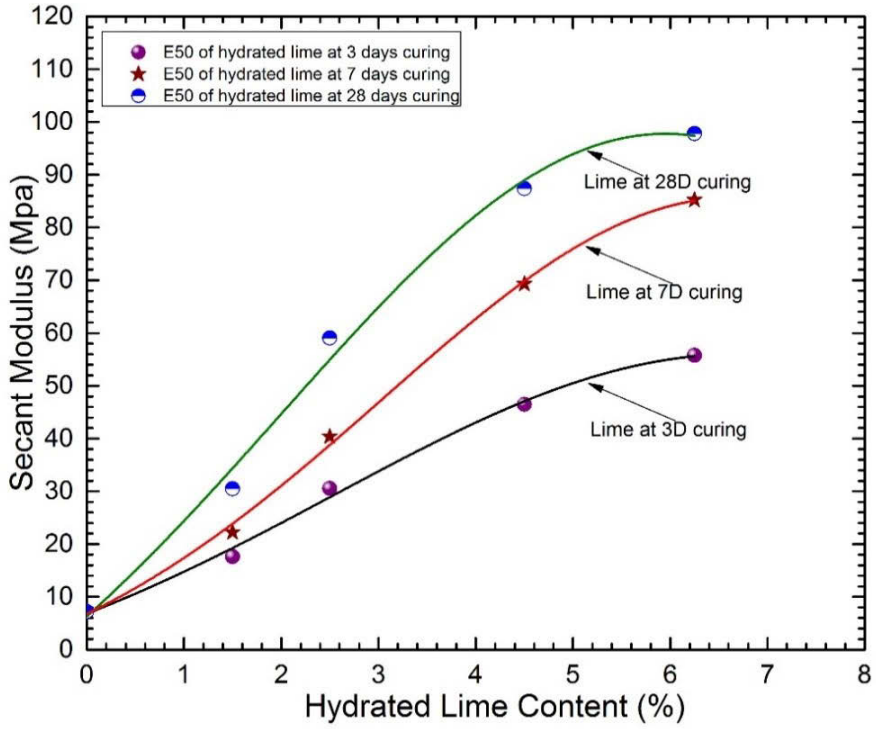

Figure 4.26 Influence of hydrated lime additions on Young's modulus of treated expansive soil with different curing times

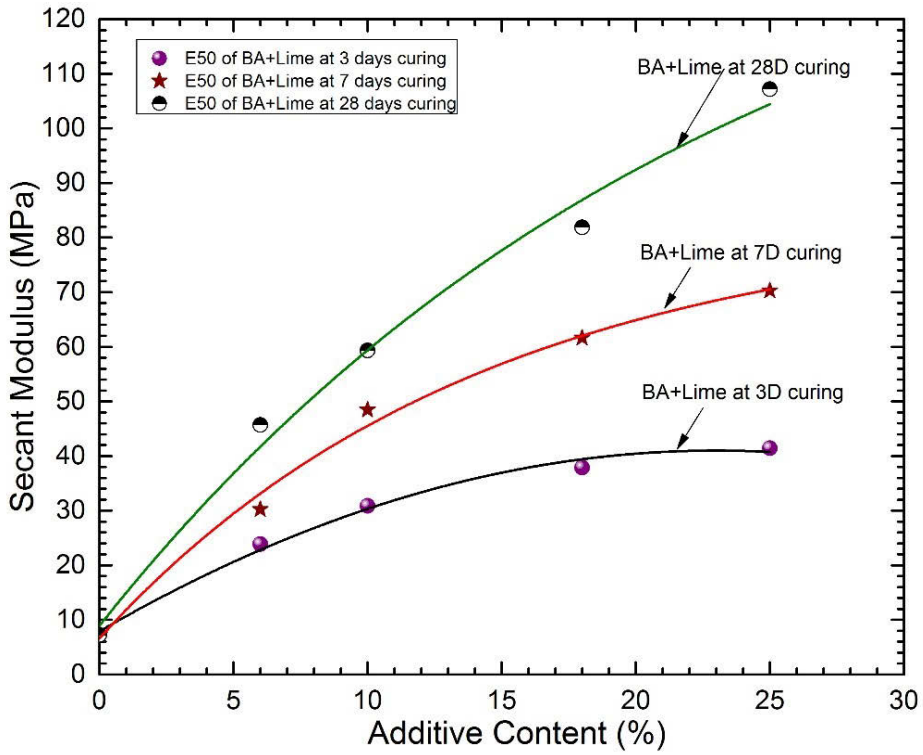

Figure 4.27 Influence of hydrated lime-bagasse ash additions on Young's modulus of treated expansive soil with different curing times

Furthermore, referring to Figure 4.26 and 4.27, the secant modulus development of soils treated with hydrated lime alone and BA+L, respectively, was most likely similar each other in both its pattern and value but considerable with curing time. However, the significant increase in the secant modulus during the first 7 days of curing is clearly seen from Figure 4.26 for hydrated lime alone treated soils followed by a relatively slow increase in secant modulus as curing time increased from 7 to 28 days. Meanwhile, the significant improvement in the secant modulus of hydrated lime treated soil with bagasse ash evenly continued as curing time increased up to 28 days as illustrated in Figure 4.27. The early improvement of soils treated with only hydrated lime could be attributable to the required setting time of limed soil is not quite long compared to pozzolanic materials

(bagasse ash) stabilised soil with hydrated lime. Moreover, bagasse ash contains higher pozzolanic materials such as silica, alumina, and ferric oxide as mentioned earlier, which facilitates the higher pozzolanic reactivity of lime treated soil with bagasse ash and hence enhance the higher stiffness and strength gain as curing time extended.

4.2.12. Influence of Bagasse Ash-Lime Addition on Compression Characteristics

A review of the recent investigations on the application of hydrated lime stabilised expansive soil combined with bagasse ash reveals that very limited work has been carried out on the compressibility of stabilised soil. Therefore, this investigation is conducted to provide insight into the influence of BA+L addition on the compressibility characteristics of stabilised soil. Figure 4.28 exhibits that the relationship of void ratio against effective compression pressure obtained from the one-dimensional (1D) consolidation tests after 3 days of curing followed by another 4 days of soaking, briefly saying a total of 7 days of curing. The 1D consolidation test results display that the addition of BA+L stabilised expansive soil tended to decrease the compression characteristics of stabilised soil with increasing additive content from 0% to 25% at the same given curing period of 7 days. A decrease in the slope of the virgin curves was clearly observed in the figure for all combined additive admixtures of stabilised soil. However, the reduction of virgin curves was more noticeable for higher BA+L content (e.g. 18% and 25%) stabilised soils as illustrated in Figure 4.28. The improvement in the compressibility of hydrated lime stabilised soil with bagasse ash might be attributed to cation exchange reactions. An increase in hydrated lime combined with bagasse content resulted in a corresponding increase in the flocculation and aggregation because of cation exchange reactions

between calcium cations and other exchangeable cations including sodium, magnesium and so forth, which are responsible for the improvement on the compressibility characteristics of stabilised expansive soil.

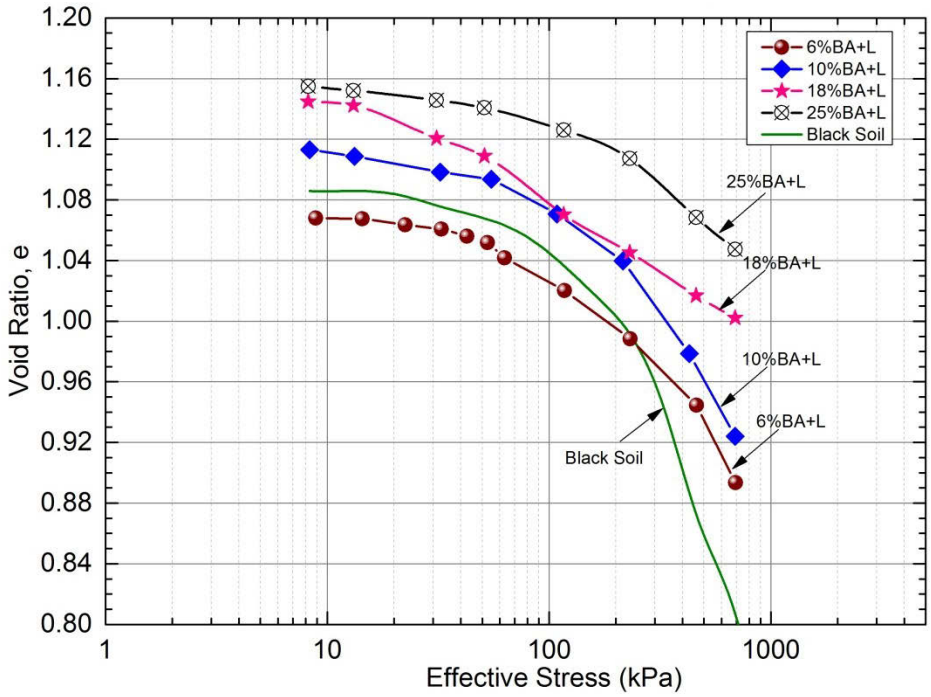

Figure 4.28 Influence of hydrated lime-bagasse ash addition on compression curves of treated expansive soil after 7 days of curing

Figure 4.29 indicates the effect of the combination of hydrated lime and bagasse ash on the compression index of stabilised soil after 7 days of curing at the range of effective pressure applied from 400 kPa to 600 kPa. The compression index (C_c) of BA+L stabilised soil was plotted against additive content as seen in Figure 4.29. The figure exhibits the considerable decrease in C_c with an increase in the BA+L content from 0% to 18% followed by a marginal increase in C_c up to 25%. This reveals a general tendency that the compressibility of expansive soil stabilised with hydrated lime and bagasse ash

combination was improved as BA+L additive content increased. The most improvement on the compression index was noticeably observed for the admixture of expansive soil stabilised with 18% BA+L. The significant reduction in the compression index of BA+L stabilised soils as plotted in Figure 4.29 could be due to the flocculation and aggregation formations of expansive soil stabilised with hydrated lime and bagasse ash combination as explained in the above session.

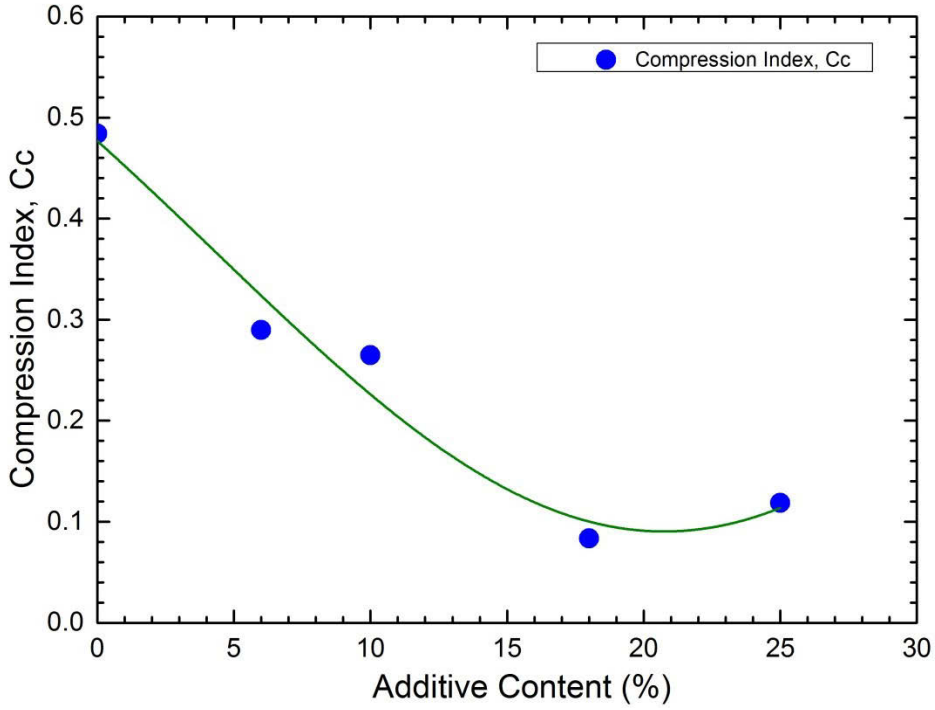

Figure 4.29 Influence of hydrated lime-bagasse ash addition on compression index of treated expansive soil for effective stress ranging from 400 kPa to 600 kPa

4.2.13. Influence of Bagasse Ash and Hydrated Lime on Microstructural Evolution

Figure 4.30 displays the comparative FTIR spectra of natural expansive soil, 6.25% hydrated lime treated soil, and 25% hydrated lime treated soil with bagasse ash at 28 days of curing to confirm the presence of Si-O-Si and Al-O-Si bands in the treated soil samples.

The FTIR spectra of the treated soil samples exhibit a broad band of Si-O-Si in the range between 600 and 1500 cm^{-1}. This band may be associated with the complicated FTIR spectra of C-S-H (Bahmani et al. 2014; Hou et al. 2012; Jo et al. 2007; Pourakbar et al. 2016). As observed in Figure 4.30 for more details, the symmetrical stretching vibrations of Si-O-Si and Al-O-Si groups appear at around 680 cm^{-1}, meanwhile observation of the peak at around 773 cm^{-1} confirms the presence of Al-O stretching vibration (Fasihnikoutalab et al. 2017; Salih et al. 2015a; Yunsheng et al. 2007), which becomes weak in the FTIR spectra of 6.25% lime treated soil and 25% lime treated soil with bagasse ash. This means that the Al-O group may transform into other formations in the hydration process. The dominant peak represents the symmetrical stretching vibration bands of Si-O, which can be observed in the range between 950 and 1100 cm^{-1} (Fasihnikoutalab et al. 2017; Pourakbar et al. 2016; Salih et al. 2015b; Yunsheng et al. 2007). The strong peak at approximately 1001 cm^{-1} presented in the FTIR spectrum of the untreated soil shifts towards the wave number at round 1004 cm^{-1} for the 6.25% lime treated soil and at around 1006 cm^{-1} for the 25% lime treated soil with bagasse ash. The transition in the wave number of the Si-O bands may be attributed to the transition of symmetric to asymmetric stretching mode of the Si-O bands in that the partial replacement of SiO_4 tetrahedron by AlO_4 tetrahedron, resulting in a change in the local chemical environment of Si-O groups (Salih et al. 2015a; Yunsheng et al. 2007). The prominent difference in the transmittance percentages at around 1000 cm^{-1} of the untreated soil and the hydrated lime, BA+L treated soil samples may also confirm the change in microstructure or the formation of new cementitious compounds of C-S-H (Bahmani et al. 2016; Salih et al. 2015b).

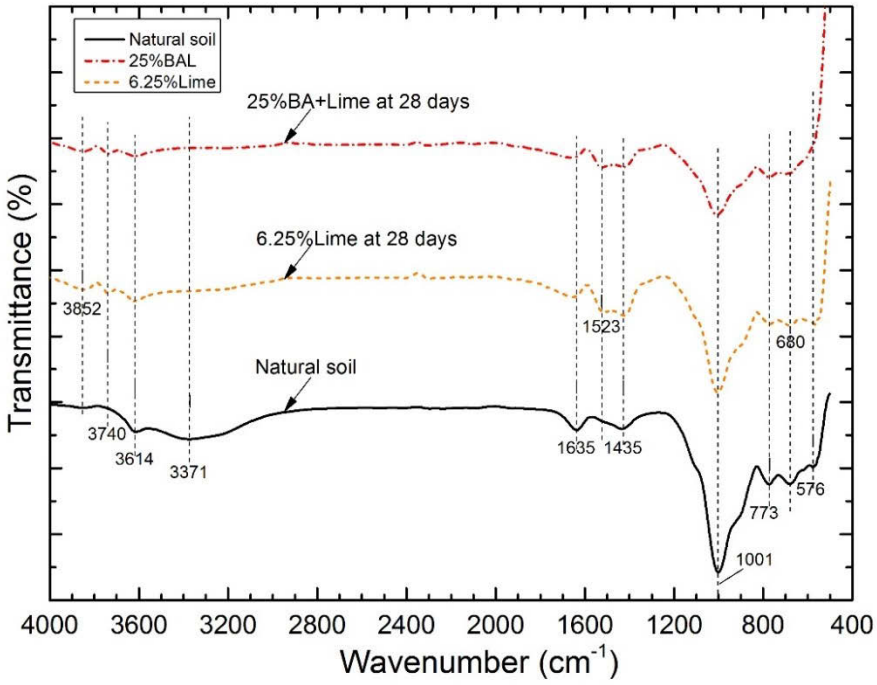

Figure 4.30 Fourier transform infrared (FTIR) spectra of untreated soil and hydrated lime, lime-bagasse ash treated soil after 28 days of curing

The other peaks are observed in Figure 4.30 ranging from 1400 to 1450 cm^{-1} and centred at around 1435 cm^{-1}, which indicate the stretching vibrations of O-C-O. This peak may be attributed to the carbonation reaction (Bahmani et al. 2014; Fasihnikoutalab et al. 2017; Salih et al. 2014). Appearance on the peaks centered at around 1635 cm^{-1} and 3371 cm^{-1} may represent the bending vibration of H-O-H and the stretching vibration of -O-H groups from weakly bound water molecules, which may be absorbed in the surface or entrapped in the large cavities between rings of C-S-H chains (Panias et al. 2007; Pourakbar et al. 2016; Salih et al. 2014). Visibly, observation on the decrease in the magnitude of these bands in the FTIR spectra of the stabilised soil samples indicates the decrease in the amount of molecular water after 28 days of curing related to an increase

in the higher crystalline degree of C-S-H chains (Mozgawa & Deja 2009; Salih et al. 2015a).

Scanning Electron Microscope (SEM) images of natural soil and soils treated with 6.25% hydrated lime, 25% hydrated lime and bagasse ash combination (BA+L) are illustrated in Figure 4.31a-4.31c, respectively, aimed to evaluate the microstructure evolution of stabilised soils. It should be noted that the SEM images of selected soil samples were obtained after UCS tests at the same curing period of 28 days and then followed by drying process in an oven at a temperature of 40°C for 24 hours. Observation of the microstructure of compacted soil without chemical stabilisation as shown in Figure 4.31a looks like wet-state morphology and highly plastic material representing typical formation of expansive clay as previously observed by Aiban (2006). Whereas, the additions of hydrated lime and BA+L chemically treated soils changed the wet condition of untreated soil to become drier and less plastic as visually seen in Figure 4.31b-4.31c. The plates like cementitious products (e.g. CSH, CAH or CASH) derived from the time-dependent pozzolanic reactions are clearly observed in the pore space between clay particles from soil samples treated with hydrated lime alone as shown in Figure 4.31b. Meanwhile referring to Figure 4.31c, the cementitious products were attached to the bagasse ash stabilised clay particles with hydrated lime. As such formation of cementitious products, the stabilised particles become not only larger than the original clay and bagasse ash particles but also stronger due to crystallization with curing time. In order words, the formation of cementitious products is responsible for the development of particle bonds in the stabilised soil mixtures, promoting the improvement in soil strength, stiffness and other geotechnical properties. This interpretation of the

microstructure change of stabilised soils effectively proves that the addition of hydrated lime or BA+L has significant impacts on the stiffness and strength gain, the compressibility characteristics as well as the shrink-swell behaviour of treated soils.

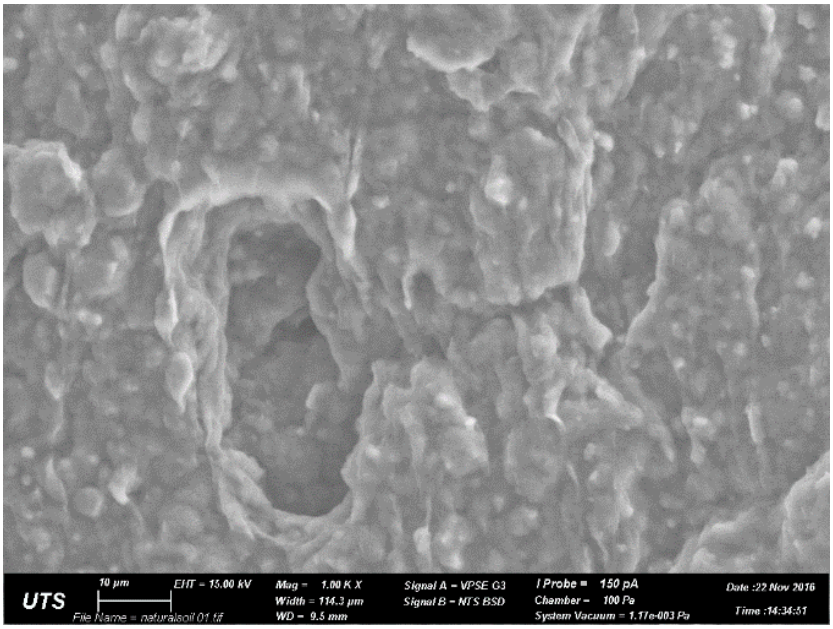

(a) Natural soil

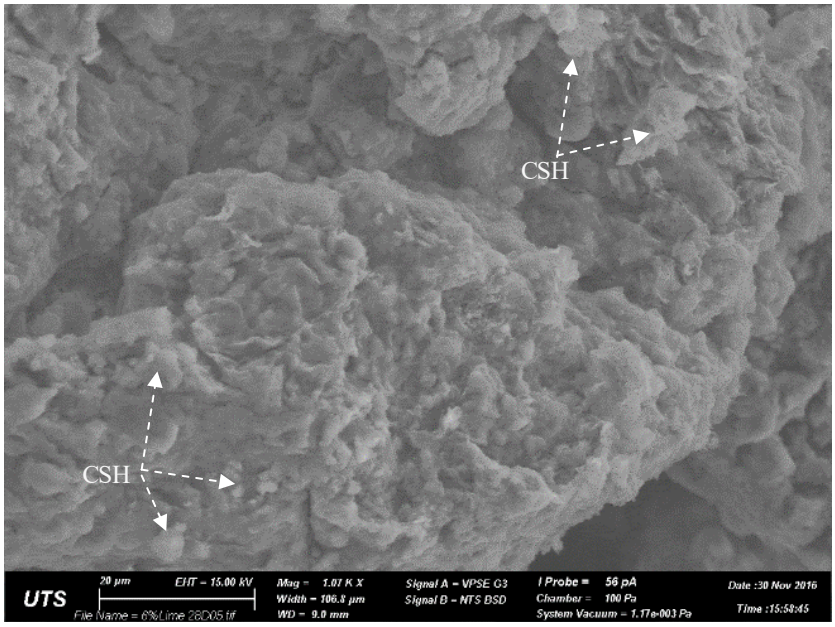

(b) 6.25% Hydrated lime

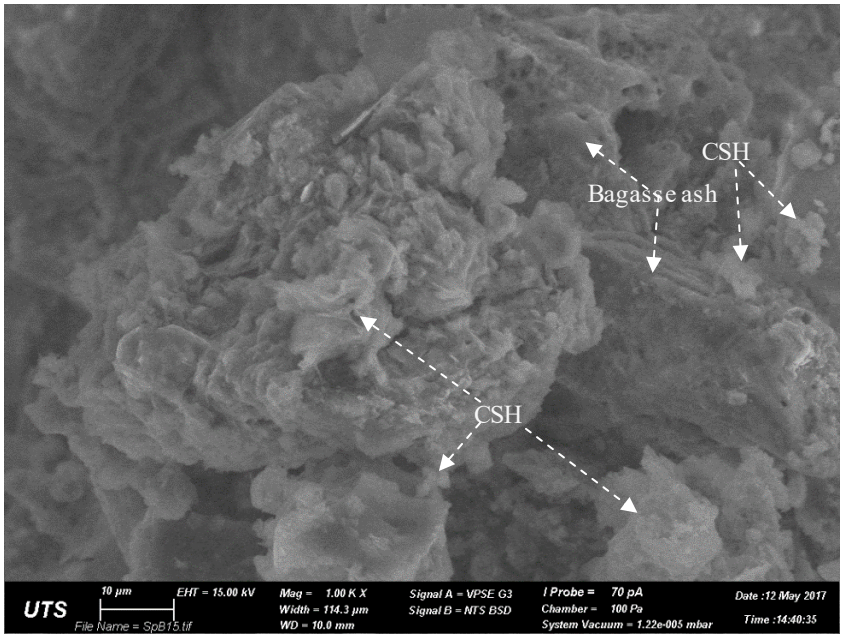

(c) 25% BA+Lime

Figure 4.31 SEM images of (a) untreated expansive soil and expansive soil treated with (b) 6.25% hydrated lime and (c) 25% BA+Lime after 28 days of curing

4.3. SUMMARY

This chapter presents an experimental investigation that has been carried out to explore the effects of adding bagasse ash, hydrated lime, and combined hydrated lime-bagasse ash on the engineering properties of expansive soil. The laboratory tests were conducted to quantify the stress-strain behaviour, the unconfined compression strength (UCS), the influence of curing time on UCS values, California bearing ratio, linear shrinkage, swell potential, swelling pressure, secant modulus and compression index of untreated and treated expansive soils. Furthermore, an array of microstructure study on the evolution of untreated and treated expansive soils was carried out using scanning electron microscopy (SEM), pH measurement, and Fourier transform infrared (FTIR) techniques. The key findings of this study, based on the experimental results are summarised as follows:

The pH measurement shows that about 5% hydrated lime content was sufficient for the short term reactions (i.e. cation exchanges between soil particles and lime) to take place, defined as the optimum lime content to stabilize expansive soil, while 18% hydrated lime-bagasse ash combination was experimentally determined as the optimum additive combination for expansive soil stabilisation.

The expansive soil stabilisation by bagasse ash (BA), hydrated lime (L), and the BA+L combination resulted in the decrease in the maximum dry density (MDD) of stabilised soils. The MDD reduction of stabilised soils could be due to the flocculation and agglomeration because of cation exchange processes between clay particles and additives resulting in the coarser particles, which occupies the larger spaces in the soil matrix, increases the void volume and consequently reduces the MDD of treated soils. Another possible reason could explain for the MDD reduction of the treated that might be attributable to the lower specific gravities of the additives in comparison with that of untreated soil.

The unconfined compressive strength (UCS) of treated expansive soil considerably increased with the increase in additive content along with curing time. The strength development of soils treated with BA+L was definitely more noticeable than that of bagasse ash, hydrated lime alone treated soils. In addition, hydrated lime treated soils with bagasse ash exhibits more ductile behaviour than hydrated lime alone treated soils. Inspection of the UCS results of treated soils with curing time reveals that the increase in strength was more significant during the first 7 days of curing and then followed by a gradual increase in strength with further curing time up to 28 days. While the strength development of soils mixed with BA+L continued smoothly after 28 days of curing, the

compressive strength remained almost constant for hydrated lime alone treated soils. It is important to note that the low quantity of employed stabilisers has a little effect on the strength gain of stabilised soil with time. The low compressive strength gain with time might be due to inadequate free lime available in bagasse ash or BA+L admixtures necessarily to accelerate the activity of pozzolan to form cementitious compounds that play a key role in binding clay aggregates together as well as improving the strength of stabilised soils with time.

Similar to the UCS test results, the increase in additive content in line with curing time resulted in the significant improvement in CBR value of stabilised expansive soil. It is noteworthy to state that the 4.5% hydrated lime treated soil could be the optimum content for CBR improvement. The addition of bagasse ash would not produce the adverse effect on the strength and bearing capacity of lime stabilised soil, even if BA+L combination resulted in the more significant improvement in CBR value as the more BA+L additive is utilised. In general, the 6% BA+L stabilised soil could easily satisfy the minimum 15% CBR requirements adopted by most of the selected subgrade design guidelines, meanwhile the higher addition of BA+L stabilised soil could meet the CBR requirement for subbase course materials fairly easily.

The improvement in linear shrinkage, swelling strain, free swell potential, and swelling pressure of hydrated lime stabilised soils with bagasse ash was more pronounced than that of bagasse ash or hydrated lime alone stabilised soils. The flocculation and aggregation phenomena of modified clay particles in the short-term together with the cementitious products attached to the bagasse ash and clay particles due to pozzolanic reactions in the long-term tended to form the coarser particles, less specific surface area,

and eventually enhance the strength of the treated soil. In other words, the finer clay particles were replaced by relatively stronger and coarser particles that could be the key factors resulting in the considerable decrease in the linear shrinkage and the swelling properties of treated soil with time.

Adding bagasse ash alone to stabilise soils without lime combination appeared to decrease the stiffness of treated soil, which indicates the addition of bagasse ash changed the brittleness of treated soil to become more ductile. On the contrary, the introduction of hydrated lime treated soil had a more notable effect on the secant modulus increase, obtained during the first 7 days of curing, than the effect on the secant modulus gain with the further increase in curing time up to 28 days. Moreover, the secant modulus of soils treated with bagasse ash alone or BA+L increased smoothly during the 28 days curing period. The increase in the content of hydrated lime alone or BA+L likely resulted in the similar increase in secant modulus of treated soils, representing that bagasse ash introduced into lime-soil mixtures would produce the same stiffness as soil mixed with hydrated lime alone.

The addition of hydrated lime stabilised expansive soil combined with bagasse ash resulted in the remarkable influence on the compression curve and compression index of stabilised soil. An increase in BA+L content led to a significant decrease in compressibility characteristics of treated soils. The lowest slope of the compression curve was visually observed for 25% BA+L treated soil, while the highest reduction in compression index (C_c) was achieved for the 18% BA+L stabilised soils within the high pressure applied ranging between 400 kPa and 600 kPa. This interpretation confirms the addition of pozzolanic material such as bagasse ash into lime-soil mixtures is very

effective in improving the compressibility characteristics of treated expansive soil, which could be an advantage to use bagasse ash combined with hydrated lime as a filling material constructed under embankments.

The FTIR spectra of untreated soil and soil samples treated with hydrated lime or BA+L confirm the appearance of a broad band of Si-O-Si in the range between 600 and 1500 cm^{-1}. The prominent difference in the transmittance percentages at around 1000 cm^{-1} of the untreated soil, hydrated lime, and BA+L treated soil samples reveals the change in microstructure or the formation of new cementitious compounds of C-S-H. Furthermore, the SEM results indicate the formation of cementitious products (i.e. CSH, CAH or CASH) as a result of the time-dependent pozzolanic reactions between clay and/or bagasse ash particles together with hydrated lime is primarily responsible for the improvement in the strength and stiffness as well as other geotechnical properties of treated soils.

The utilisation of hydrated lime-bagasse ash combination for stabilising expansive soil can highly be effective not only in improving the geotechnical properties of expansive soil but also in minimising the influence of industrial waste by-products on the environment. This investigation has explored the potential use of an eco-friendly waste material, bagasse ash for sustainable infrastructure development by means of reducing the consumption of conventional stabilisers, such as lime or cement, commonly adopted in expansive soil treatment.

CHAPTER 5: ENHANCING GEOTECHNICAL PROPERTIES OF EXPANSIVE SOIL USING RANDOMLY DISTRIBUTED BAGASSE FIBRE AND HYDRATED LIME

5.1. INTRODUCTION

In this chapter, the results of an experimental investigation on the engineering characteristics of expansive soil reinforced with randomly distributed bagasse fibre and hydrated lime in accordance with the testing methods and procedures specified in Chapter 3 are presented. Bagasse fibre, an agricultural waste by-product left after crushing of sugar-cane for juice extraction, was employed in this investigation as a reinforcing component for expansive soil reinforcement. To comprehend the effects of bagasse fibre reinforcement on the geotechnical properties of reinforced soils without or with lime stabilisation, several series of experimental investigations were carried out. They included a number of different geotechnical tests such as compaction, linear shrinkage, unconfined compressive strength (UCS) tests using a conventional compression machine, indirect tensile strength, California bearing ratio (CBR), free swell potential, swelling pressure, consolidation, soil suction, and shear strength tests using advanced triaxial compression apparatus. Those laboratory tests were conducted on untreated soils and soil samples treated with different percentages of randomly distributed bagasse fibre from 0% to 2% and hydrated lime from 0% to 6%. Following the compression tests, scanning electron microscopy (SEM) analysis was performed on selected soil samples to evaluate the

micromechanical reinforcement between soil particles and fibre surface. The findings of this experimental investigation are analysed and discussed to have a better understanding of the effects of the hydrated lime, bagasse fibre, and their combination on the shrink-swell behaviour. Results of the compressive strength and stiffness, the tensile strength, the shear strength, the bearing capacity, the brittleness, the ductility, the soil-water retention characteristics as well as the compressibility properties of the untreated and treated expansive soils are also presented and discussed in detail.

5.2. EXPERIMENTAL RESULTS AND DISCUSSION

5.2.1. Effect of Bagasse Fibre and Lime Content on Compaction Characteristics

The standard compaction curve of untreated expansive soil as a preliminary step to determine the maximum dry density (MDD) and the optimum moisture content (OMC) of the soil only is presented in Figure 5.1a. Analysis of the compaction results of natural soil found the MDD and the OMC to be 12.9 kN/m^3 and 36.5%, respectively. Subsequently, several series of soil samples mixed soils with different contents of hydrated lime and bagasse fibre were prepared at the OMC of the untreated soil (36.5%) to investigate the influence of the additive content on the so-called maximum dry density of the treated soil mixtures. The results of the standard compaction tests for various contents of lime treated expansive soil with bagasse fibre reinforcement are depicted in Figure 5.1b. It is observed that with bagasse fibre inclusion into soils without lime treatment, the MDD of the reinforced soil mixtures gradually decreased from 12.9 kN/m^3 to 11.4 kN/m^3 as bagasse fibre content increased from 0% to 2%. The MDD reduction could be due to the lower specific gravity of bagasse fibre in comparison with that of untreated soil. Furthermore, addition of hydrated lime into bagasse fibre reinforced soil

mixtures as observed in Figure 5.1b shows that the MDD of stabilised soils decreased with an increase of hydrated lime content from 0% to 6%. It is noted that the MDD of each lime-bagasse fibre-soil mixture was obviously lower than that of the bagasse fibre reinforced soils without lime treatment. The MDD decrease of lime treated soils with bagasse fibre might be attributed to the lower specific gravity of bagasse fibre together with the flocculation and agglomeration because of cation exchange processes between clay particles and lime that change the soil particles to become coarser particles. As mentioned earlier, the formation of the coarser particles occupying the larger spaces in the soil matrix, increases the void volume and hence reduces the dry density of the treated soil mixtures. In addition, tiny air gaps trapped into fibre surface could be another possible reason that explains the reduction of the MDD of lime-fibre-mixtures. An increase in bagasse fibre content leads to a corresponding increase in the tiny air gaps and hence reduces the MDD of stabilised soil composites. Results of this investigation are consistent with other researcher observations (Ayeldeen & Kitazume 2017; Kinuthia et al. 1999).

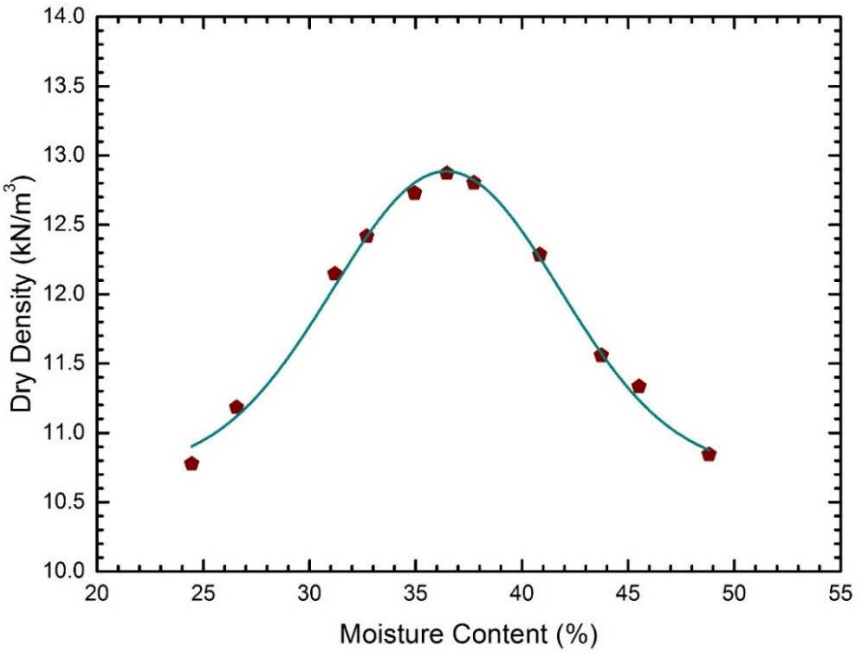

(a)

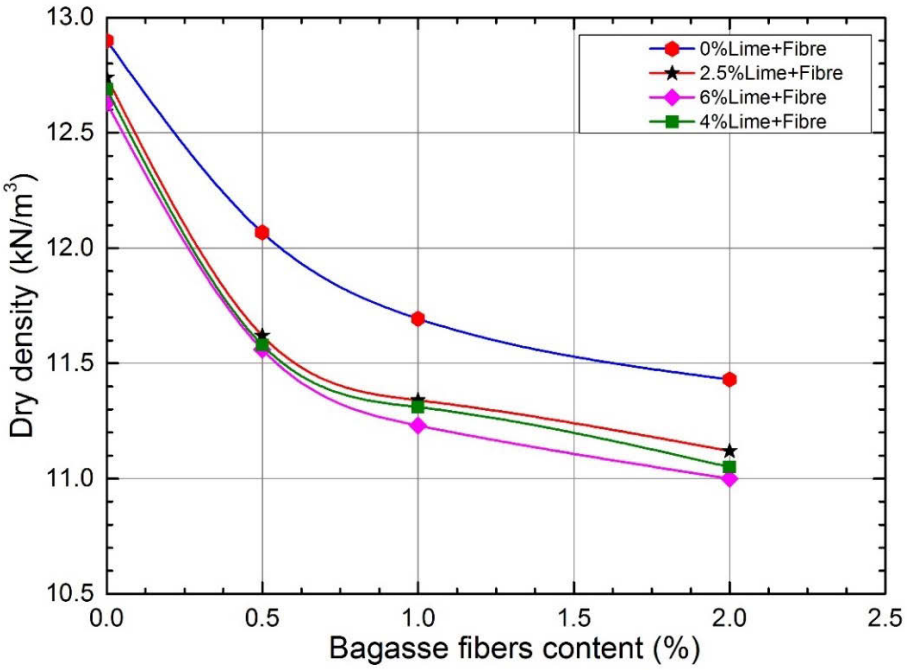

(b)

Figure 5.1 Compaction curves of (a) natural expansive soil and (b) expansive soil reinforced with different bagasse fibre and hydrated lime contents

5.2.2. Effect of Bagasse Fibre and Lime Content on Linear Shrinkage

Figure 5.2 displays the effects of bagasse fibre addition on linear shrinkage with different curing days. It can be noted that when bagasse fibre content increased from 0% to 2%, the linear shrinkage decreased gradually with increasing curing time. Specifically, with the addition of 2% bagasse fibre after 3 days of curing, the linear shrinkage of reinforced expansive soil reduced by almost 40% compared with that of virgin soil specimen. When the curing time increased from 0 to 28 days, the linear shrinkage of bagasse fibres reinforced expansive soil decreased to 7 days of curing and then remained almost constant with a longer curing period. In addition, Figure 5.3 demonstrates the effects of combined hydrated lime-bagasse fibre addition on the linear shrinkage of expansive soil after curing for 7 days. According to Figure 5.3, similar trends of linear shrinkage of bagasse fibre

reinforced expansive soil can be found that the linear shrinkage reduced with the increase in bagasse fibres and hydrated lime percentages. For example, when the individual addition of hydrated lime content was increased from 0% to 6.25%, the reduction of linear shrinkage of treated expansive soil was approximately 63%. Meanwhile, the linear shrinkage of 6.25% hydrated lime combined with 2% bagasse fibres treated expansive soil decreased significantly by almost 86% in comparison with the linear shrinkage of untreated expansive soil. As observed in Figure 5.2 and 5.3, it is noteworthy to state that the combinations of hydrated lime and bagasse fibres yielded a higher reduction of linear shrinkage than only bagasse fibres reinforced expansive soil. The significant improvement of linear shrinkage could be attributed to the flocculation and aggregation phenomena of clay particles induced by the presence of free lime dosage that caused a decrease in surface of clay particles, and then the clay particles become coarser and less plastic. As a result, the finer clay particles were replaced with relatively coarser particles that could be one of the key factors resulting in the considerable decrease in linear shrinkages with increasing the additive content. The addition of bagasse fibre reinforcement, moreover, resulted in the further decrease in linear shrinkage of lime treated expansive soils that may be due to the development of interaction between bagasse fibre surface and soil matrix with time, which could be essentially beneficial from fibre reinforcement.

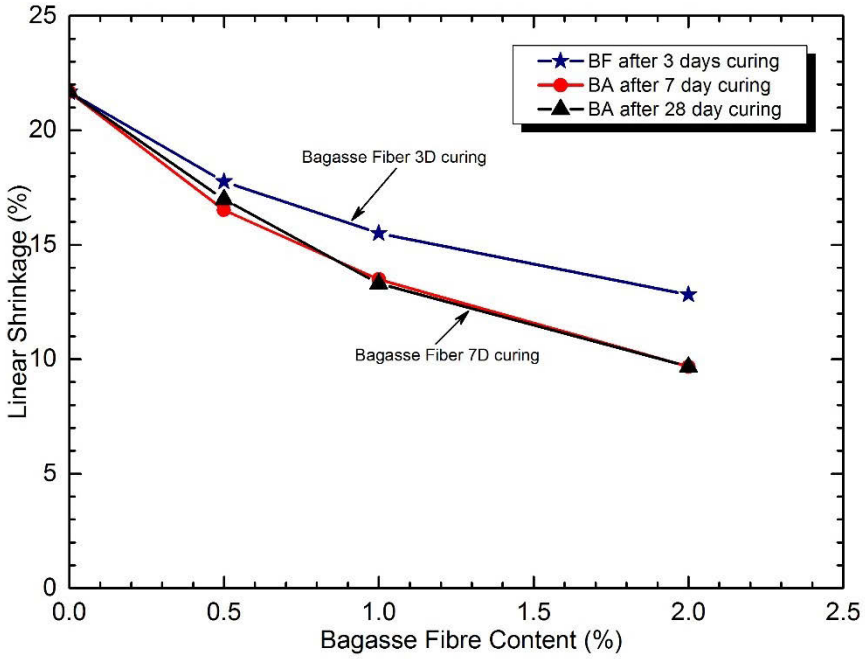

Figure 5.2 Linear shrinkage of expansive soil mixed with various bagasse fibre contents along with different curing periods

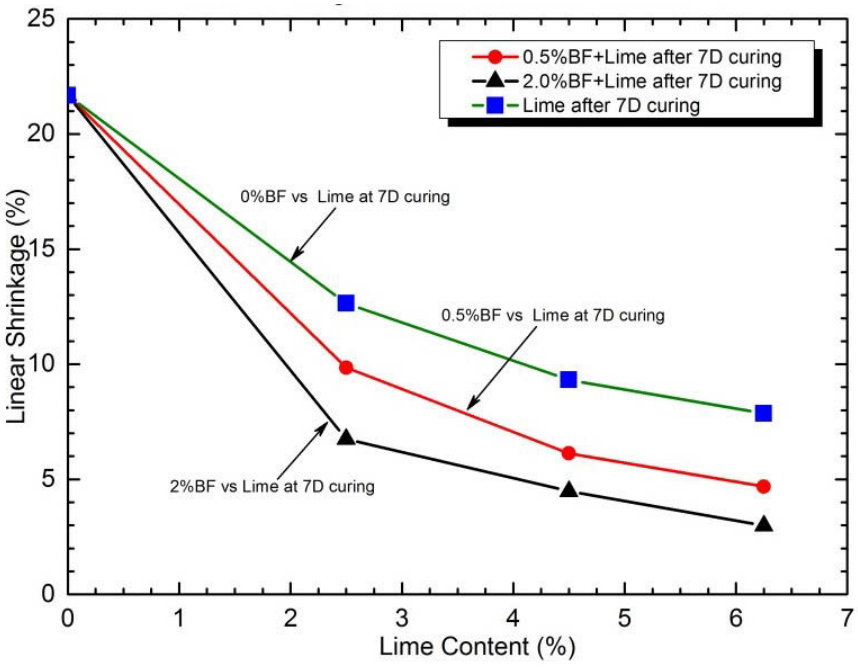

Figure 5.3 Linear shrinkage of expansive soil mixed with various contents of bagasse fibres-lime combination after 7 days of curing

5.2.3. Effect of Bagasse Fibre and Hydrated Lime on Stress-Strain Behaviour

Figure 5.4 displays the effects of bagasse fibre reinforcement on the axial stress-strain behaviour of expansive soil, derived from the UCS tests. As illustrated in Figure 5.4, the peak stress of reinforced soils significantly increased with an increase in bagasse fibre content from 0% to 2%. For example, the peak axial stress considerably increased from 137 kPa for 0% bagasse fibre reinforced soil (non-reinforced soil) to around 194 kPa for soil reinforced with 2% bagasse fibre at the same curing period of 7 days, resulting in the corresponding improvement in the peak stress of approximately 41%. As expected, the post-peak stress also increased with an increase in bagasse fibre content up to 2% as clearly depicted in Figure 5.4. The highest post-peak stress (residual strength) was visually observed for the soil reinforced with 2% bagasse fibre. The improvement in the residual strength corroborates that bagasse fibre reinforcement could transform the behaviour of reinforced soils from strain softening to strain hardening by reducing the loss of the post-peak strength. This behaviour confirms the beneficial effect of bagasse fibre reinforcement on the axial stress-strain relationship of expansive soil.

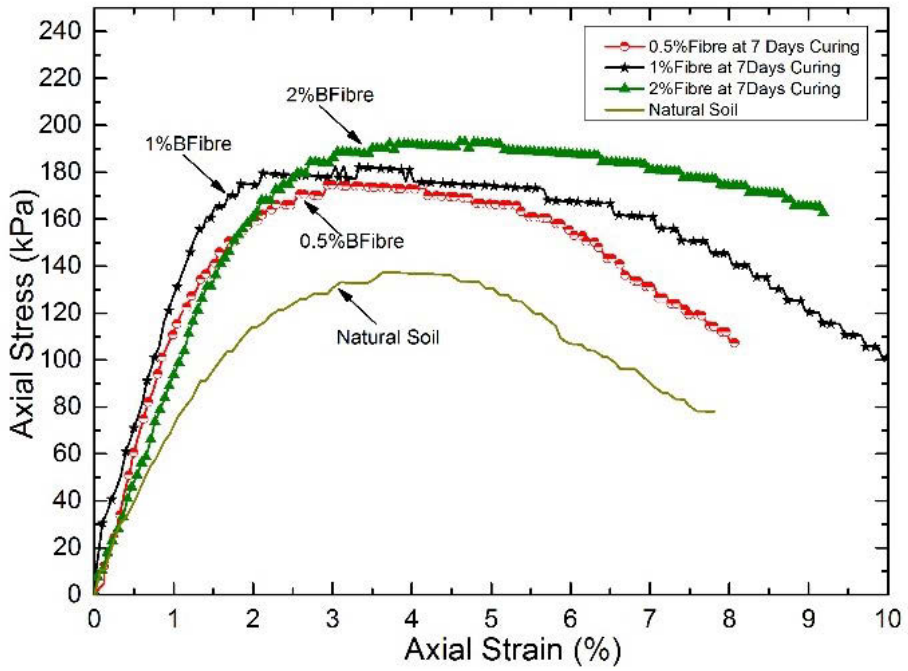

Figure 5.4 Axial stress-strain relationship of expansive soil reinforced with different bagasse fibre contents

Since the effect on the peak compressive strength (peak strength) of soils reinforced with different bagasse fibre contents is not clearly captured in Figure 5.4. Hence, the peak strength and the initial deformation modulus (secant modulus) of reinforced soils are plotted in Figure 5.5 against bagasse fibre content for further evaluation and comparison. It is noted that the secant modulus is defined as the slope of initial stress-strain curve between the origin and the point of 50% failure stress. As observed in Figure 5.5, the peak strength increased significantly with a small amount of 0.5% bagasse fibre first introduced into the soil matrix. This was followed by a slight increase in the peak compressive strength as fibre reinforcement increased up to 2%. Meanwhile, the secant modulus of the reinforced soil increased considerably from about 7.2 MPa to 14 MPa (i.e. resulting in the corresponding increment of about 94%) with an increase in bagasse fibre content from 0% to 1%. However, the secant modulus of soils

reinforced with bagasse fibre decreased slightly as the further increase in fibre content exceeded 1%. This phenomenon indicates that excessive use of bagasse fibre reinforced soil reduced the stiffness of the fibre-soil matrix.

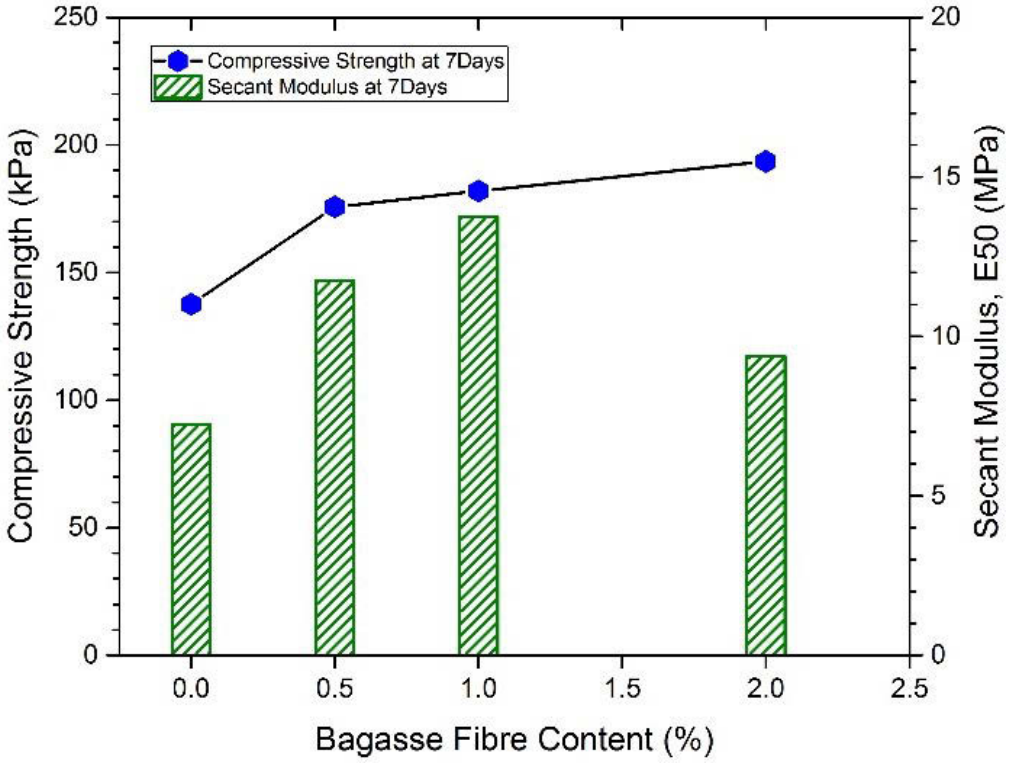

Figure 5.5 Variations of the unconfined compressive strength and secant modulus of expensive soil reinforced with different bagasse fibre contents

Figure 5.6 depicts the stress-strain relationships of hydrated lime treated expansive soil with bagasse fibre after curing for 28 days, obtained from the UCS tests. As it can be seen in Figure 5.6a and 5.6b, for lime treated soil samples without fibre reinforcement, the peak compressive strength increased dramatically with an increase of hydrated lime content from 0% to 4% and 6%, but the compressive strength reached a peak at a low axial strain (i.e. around 0.85%). Additionally, the stabilised soils display a marked stiffness and high brittleness compared with that of original soil. For instance, with additions of hydrated lime content of 4% and 6% to expansive soils as illustrated in

Figure 5.6a and 5.6b, respectively, the corresponding failure (peak) compressive strength of treated soils increased significantly to about 580 kPa and 850 kPa. These correspond to the significant increase of approximately 320% and 515% in the peak strength in comparison with that of untreated soil, respectively. However, the corresponding failure strain of lime treated soils abruptly decreased by approximately 76%, which indicates the brittle behaviour of lime-soil composite. Especially, as evident in Figure 5.6b, the post-peak strength of soil sample treated with 6% lime without fibre reinforcement was suddenly lost.

With bagasse fibre reinforcement of lime-soil mixtures, as observed in Figure 5.6a and 5.6b, the peak strength and the corresponding strain continued to increase, the brittle behaviour and the loss of the post-peak strength were improved. However, the deformation stiffness of treated soils with bagasse fibre reinforcement decreased with increasing bagasse fibre content as the lower slope of the initial stress-strain curves was visibly observed in comparison with that of stabilised soil without fibre reinforcement. For example, as can be seen in Figure 5.6b for 6% lime treated soils with bagasse fibre reinforcement, the peak strength increased from 850 kPa to approximately 1070 kPa and the corresponding strain increase from 0.85% to 2.40%, which result in the peak strength increased by 26% and the axial failure strain increased by 182%, respectively. According to Tang et al. (2007), the axial failure strain for typical cemented clayey soil is ranging from 0.5% to 0.75% that is very much smaller in comparison with the axial failure strain of lime treated expansive soils reinforced with bagasse fibre. Hence, the axial failure strain of bagasse fibres-hydrated lime combination stabilised expansive soil obtained in this experimental investigation ranging from 1.1% to 2.4% could be considered as the

remarkable improvement in ductility of fibres reinforced expansive soil. This also agrees well with the previous research reported by Fatahi et al. (2012b).

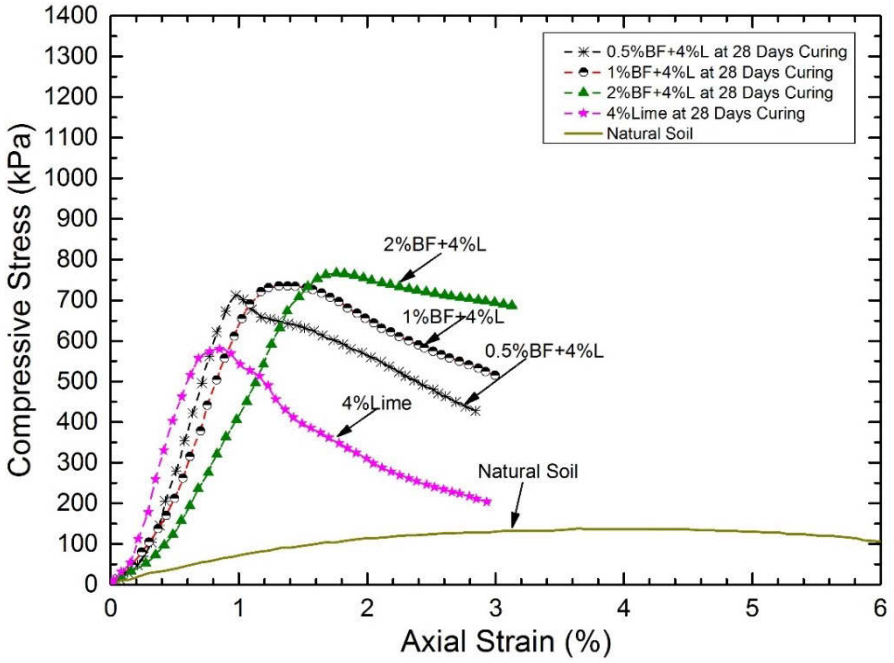

(a) 4% Lime-fibre-soil mixture at 28 days of curing

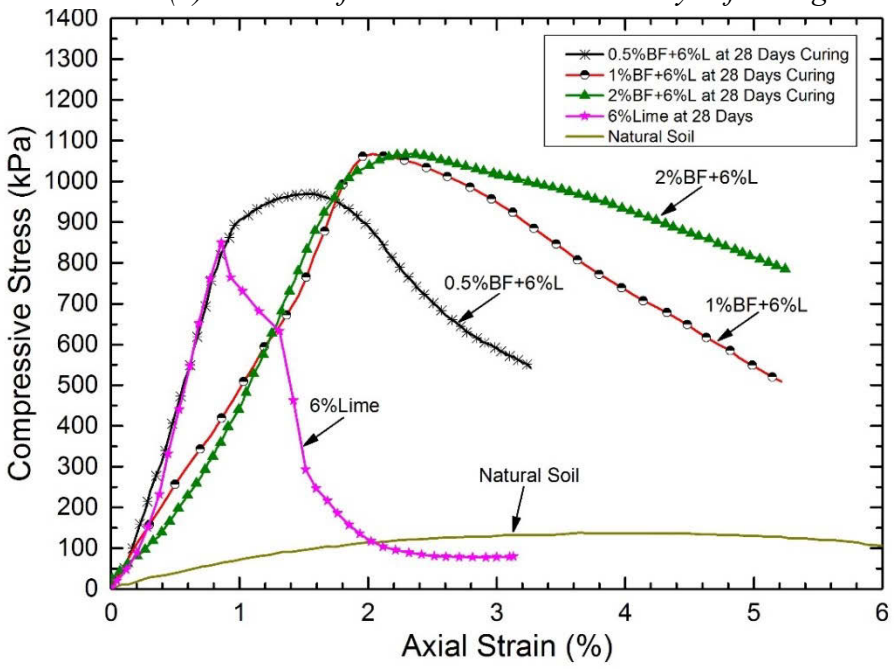

(b) 6%Lime-fibre-soil mixture at 28 days curing

Figure 5.6 Stress-strain behaviour for untreated soil and bagasse fibre reinforced soils with (a) 4% lime and (b) 6% lime after 28 days of curing

5.2.4. Effect of Bagasse Fibre Reinforcement on the Failure Characteristics

Figure 5.7 exhibits the effects of bagasse fibre reinforcement on the failure characteristics of expansive soils stabilised with hydrated lime. As observed in Figure 5.7a, lime treated soil without bagasse fibre reinforcement shows the extremely brittle behaviour, and remarkable tension cracks are wide and long, which tend to appear from the top half of the treated soil specimen. However, with the addition of bagasse fibre into lime-soil mixtures as shown in Figure 5.7b-5.7d, the tension cracks became narrower and shorter as bagasse fibre content increased. This phenomenon reveals that bagasse fibre reinforcement of soils treated with hydrated lime transformed the brittle behaviour of lime treated soil to more ductile material and as a result, the post-peak strength of stabilised soils was enhanced. In other words, bagasse fibre inclusion can enhance the lime treated soil behaviour from strain softening to strain hardening by curtailing the loss of post-peak strength. Observation of these failure samples is consistent with the stress-strain behaviour of stabilised soils illustrated in Figure 5.6a and 5.6b. According to many researchers (Olgun 2013; Tang et al. 2007), the improvement in tension cracks of stabilised soil specimens with fibre reinforcement could be due to contributions of bagasse fibre with high tensile strength that serve as bridges. Such bridges efficiently resist the further opening and the development of tension cracks, and hence prevent stabilised soil specimens from the sudden loss of compressive strength or complete failure.

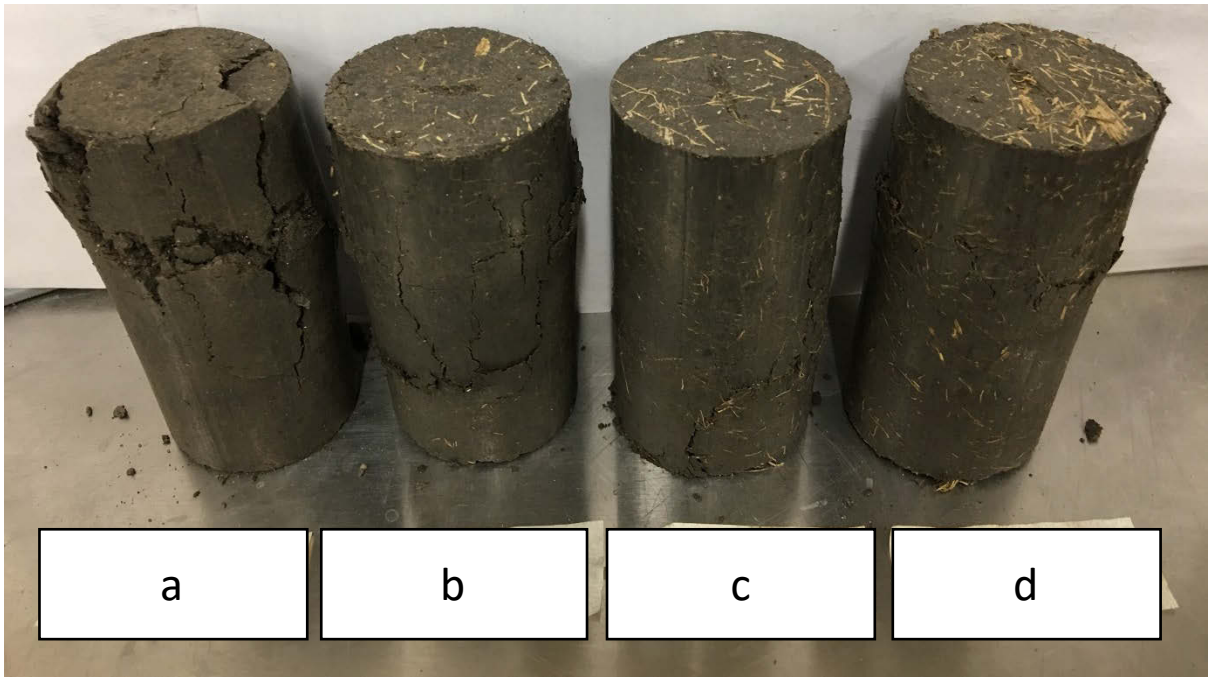

Figure 5.7 Effect of bagasse fibre (BF) addition on failure characteristics of 4% lime treated soils with: (a) 0% BF; (b) 0.5% BF; (c) 1% BF and (d) 2% BF

5.2.5. Effect of Bagasse Fibre Reinforcement and Hydrated Lime on UCS Values

Figure 5.8 exhibits fluctuations of the unconfined compressive strength of expansive soil specimens mixed with various contents of bagasse fibre after different curing periods of 3, 7, and 28 days. Overall, as illustrated in the figure, the unconfined compressive strength in all treated expansive soil specimens increased with increasing additive content and curing time. According to in Figure 5.8, for example, when the bagasse fibre content increased from 0% to 2% at the same curing period of 3 days, the gradual increase in UCS value was approximately 20%. The comparable trend can be observed with longer curing times of 7 and 28 days. Correspondingly, there was a relative increase in UCS with curing time prolonged. To take 2% bagasse fibre reinforced expansive soil as an example, the UCS value was found to improve slightly by another 20% as compared to that of the same fibre content after 3 days of curing. However, it is obviously observed that the UCS

increase with longer 7-day curing was insignificant. The strength improvement of bagasse fibre reinforced expansive soil could be attributed to the interaction and interlocking mechanism between clay particles and fibre surface developed during specimen preparation process by the compactive effort and with curing age.

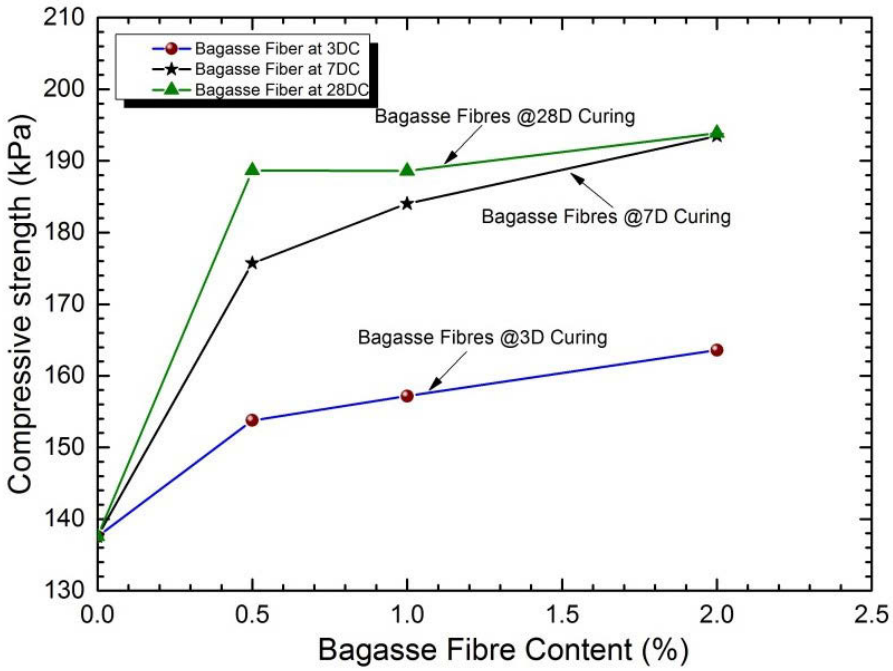

Figure 5.8 Effect of bagasse fibre addition on average UCS values of treated expansive soil with various curing times

Figure 5.9 displays the results of the unconfined compressive strength tests of 4% and 6% lime treated expansive soils reinforced with various bagasse fibre contents after curing for 28 days. Overall, as illustrated in this figure, the unconfined compressive strength of stabilised soils increased with increasing both hydrated lime and bagasse fibre contents. The trend line of the peak compressive strength for 4% lime treated soils with bagasse fibre reinforcement is parallel with its counterpart for 6% lime treated soils

reinforced with bagasse fibre. Referring to Figure 5.9, the compressive strength increased promptly with the addition of 0.5% bagasse fibre into 4% lime treated expansive soil, but then it increased gradually with further addition of bagasse fibre content up to 2%. However, for soil samples treated with 6% lime, the peak compressive strength increased gradually with the increase in bagasse fibre addition from 0% to 1% and subsequently remained unchanged with a further increase in bagasse fibre content exceeded 1%.

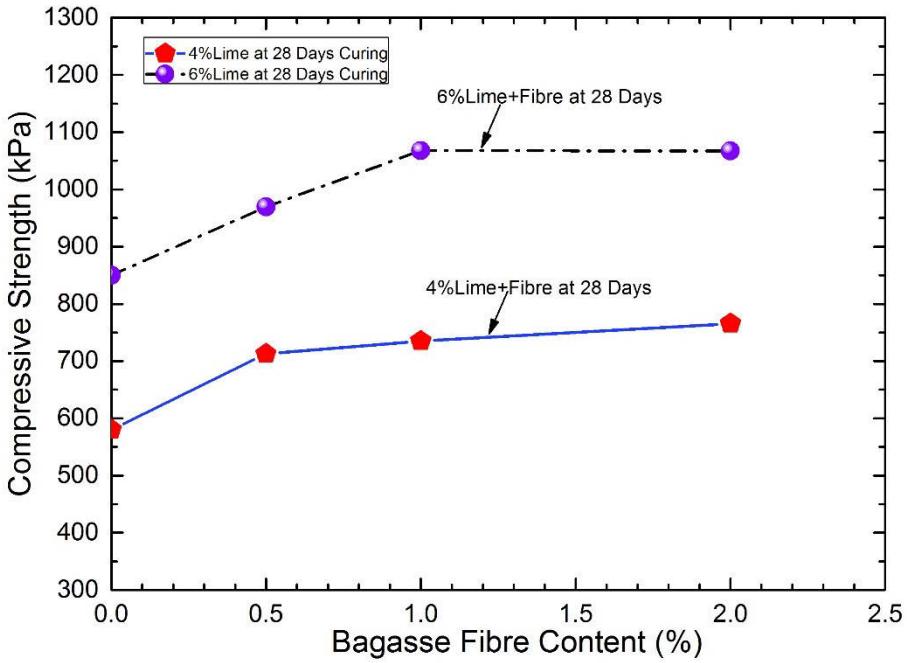

Figure 5.9 Variation of UCS values for 4% lime and 6% lime treated expansive soils with bagasse fibre reinforcement after 28 days of curing

5.2.6. Effect of Bagasse Fibre Reinforcement on Brittleness Index (I_B)

The effect of bagasse fibre reinforcement on the ductility (or brittleness) can be investigated by determining and analysing the brittleness index (I_B), which is defined in Equation 5.1 proposed by Oliveira et al. (2016) as follows:

$$I_B = 1 - \frac{q_r}{q_u} \quad (5.1)$$

where q_u and q_r are the peak compressive strength and the residual compressive strength, respectively. When $I_B = 1$ implies that the material behaviour is completely brittle, meaning that the compressive strength is totally lost after peak failure; whereas, $I_B = 0$ denotes the material behaviour is perfectly ductile.

Figure 5.10 shows the influence of bagasse fibre reinforcement on brittleness index (I_B) of 4% and 6% lime treated expansive soils after 28 days of curing. As observed in Figure 5.10, the brittleness index (I_B) of lime-soil mixtures increased with the increase in hydrated lime content from 4% to 6%, but significantly decreased when bagasse fibre content increased from 0% to 2%. For example, in lime treated soil samples without bagasse fibre reinforcement, I_B increased from 0.58 to 0.90 as lime content increased from 4% to 6%, respectively. However, observation of the brittleness index presented in Figure 5.10 shows the substantial reduction of approximately 45% and 70% in the I_B value for 4% and 6% lime treated soils, respectively, when only 0.5% bagasse fibre was introduced into the lime-soil mixtures. As observed in Figure 5.10, although the introduction of 0.5% bagasse fibre resulted in the almost same brittleness index for these two different lime-soil mixtures, the reduction of I_B was more noticeable for 6% lime treated soils with fibre reinforcement due to its extremely high brittleness index without fibre reinforcement. Moreover, the I_B value tended to approach zero when a further increase in bagasse fibre content up to 2% was introduced into lime-soil mixtures. This phenomenon clearly corroborates that the bagasse fibre reinforcement had a notable influence on the ductility of lime treated soils, which transformed the stabilised soil behaviour from brittle to more and more ductile, by reducing the brittleness index (I_B) significantly. As a result of the

reduction of the brittleness index, the loss of the post-peak compressive strength of lime treated soil reinforced with bagasse fibre was significantly improved as illustrated in Figure 5.6. Results of this laboratory investigation are in good agreement with previous studies with respect to inclusions of steel fibre, recycled carpet fibre and polypropylene fibre to cement treated clay soils (Fatahi et al. 2012b; Olgun 2013; Oliveira et al. 2016), available in the literature.

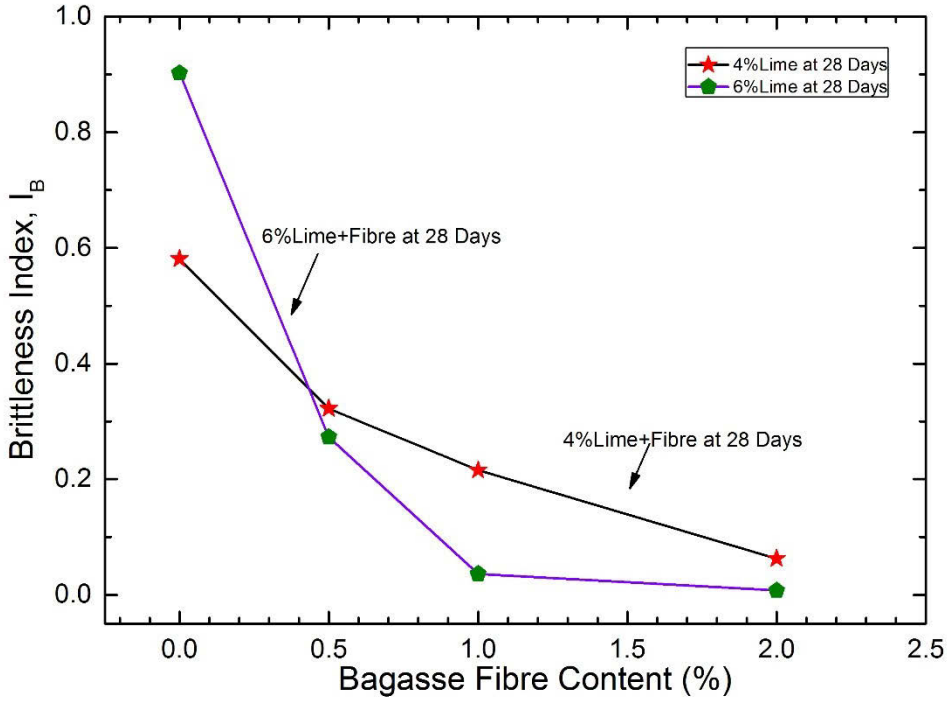

Figure 5.10 Effect of bagasse fibre reinforcement on brittleness index (I_B) of lime treated expansive soil after 28 days of curing

5.2.7. Effect of Hydrated Lime and Bagasse Fibre on Indirect Tensile Strength

5.2.7.1. Effect of bagasse fibre and hydrated lime on stress-strain behaviour

Figure 5.11 displays the tensile load-displacement behaviour of natural expansive soil and lime treated soils with bagasse fibre reinforcement after 28 days of curing. It is

observed in the figures, the linear relationship was the predominant mechanism between tensile load and vertical displacement for lime treated soils without or with bagasse fibre reinforcement. As expected, the introduction of lime treated soils significantly increased the tensile strength of stabilised soils in comparison with that of untreated soil. Moreover, the addition of bagasse fibre into the 4% lime-soil mixtures generally enhanced the tensile strength but decreased the stiffness of treated soils as observed in Figure 5.11a. Adding bagasse fibre transformed the treated soil behaviour from brittle to more ductile by enhancing the loss of post-peak tensile strength as clearly depicted in Figure 5.11a for 4% lime treated soil with bagasse fibre. However, with addition of the higher lime content to stabilise expansive soils as shown in Figure 5.11b, the bagasse fibre reinforcement of soils stabilised with 6% lime indicates the same behaviour of lime treated soil without fibre reinforcement, which means the brittle behaviour appeared to be a dominant mechanism for 6% lime stabilised soil with bagasse fibre. In this case, as depicted in Figure 5.11b, the bagasse fibre reinforcement of 6% lime-soil mixture improved the tensile strength, but the stiffness of stabilised soils was almost unchanged. In other words, the fibre reinforcement of 6% lime-soil mixtures appeared not to contribute to the transformation of stabilised soils from brittle behaviour to ductile behaviour. Results in this investigation show good agreement with the previous results of lime/cement treated soils with fibre reinforcement well documented in the literature (Correia et al. 2015).

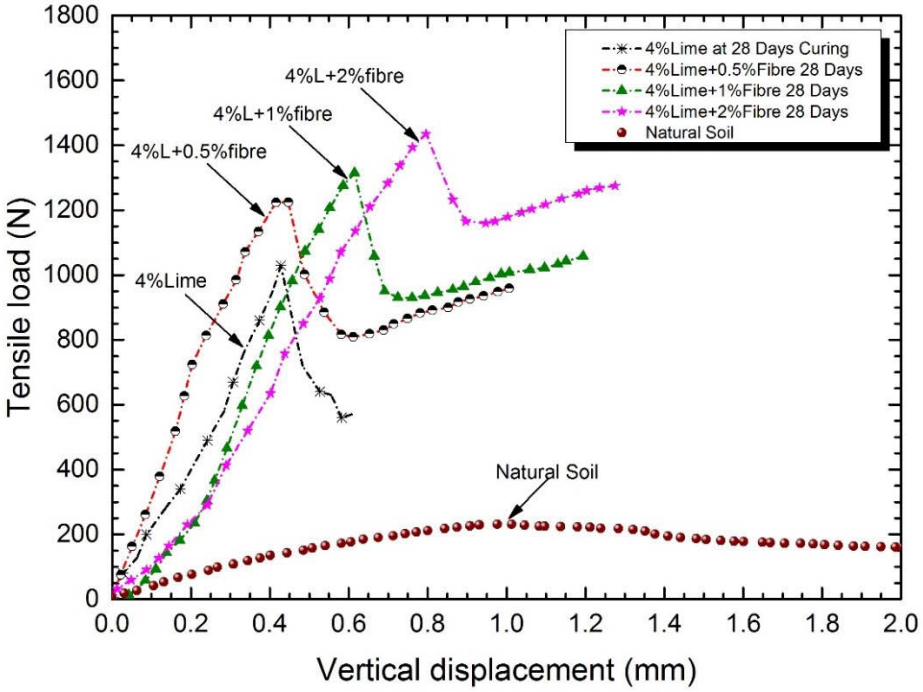

(a) *4% Lime-bagasse fibre-soil mixture*

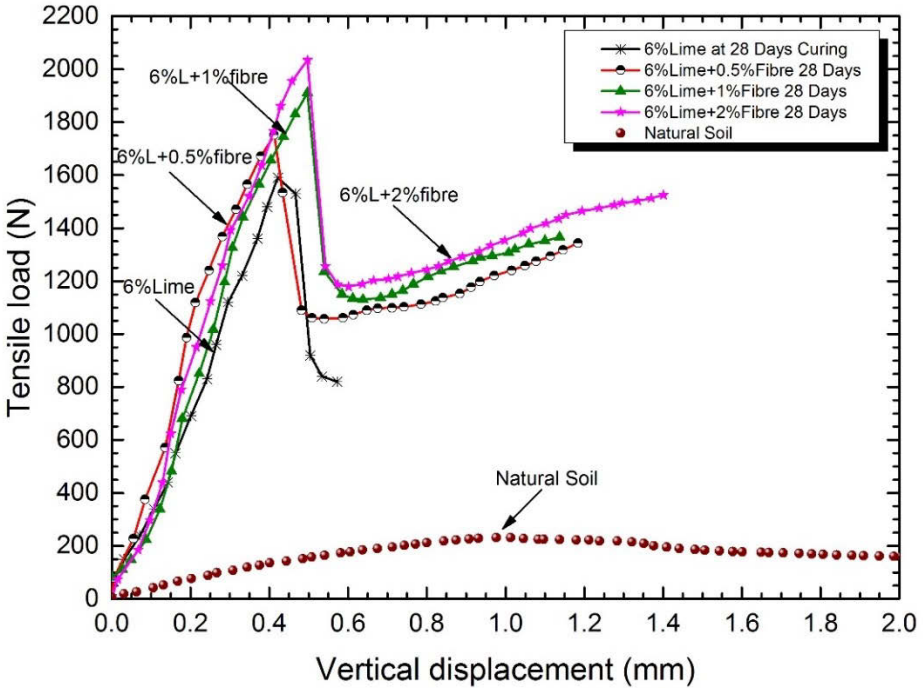

(b) 6% Lime-bagasse fibre-soil mixture

Figure 5.11 Tensile load-displacement curves for untreated soil and bagasse fibre reinforced soils with (a) 4% lime and (b) 6% lime after 28 days of curing

The improvement in the tensile strength of lime treated soils could be attributable to formation of cementitious bonds between clay particles as a result of cation exchange and pozzolanic reactions. The addition of bagasse fibre into lime-soil mixtures resulted in the additional improvement in the tensile strength of stabilised soils due to interaction between soil aggregates and fibre surface as well as contribution of high tensile strength from bagasse fibre. The reduction in the stiffness and the change in the stabilised soil behaviour from a brittle material to more ductile one for a certain amount of lime stabilised soil with bagasse fibre may be attributed to inclusion of bagasse fibre as a more ductile and deformable material into the lime-soil matrix. However, the stiffness of bagasse fibre reinforced soils stabilised with high additive content (i.e. 6% lime) remained almost unchanged because the addition of high lime content to stabilise soils produces the high stiffness lime-soil matrix mainly contributed by lime stabilisation. The high lime content required for expansive soil stabilisation may lessen the effectiveness of fibre reinforcement in improving the ductility of reinforced soils because its peak tensile strength is typically obtained at a low axial strain level. However, many researchers (Consoli et al. 2009b; Correia et al. 2015) recently reported that a high strain level is required for better mobilisation of the tensile strength of fibre reinforcement of cemented soils to take place.

5.2.7.2. Effect of bagasse fibre and hydrated lime on the development of indirect tensile strength

Figure 5.12 shows variations of the peak tensile strength of various contents of lime treated soil with different contents of bagasse fibre reinforcement. It can be observed that the tensile strength of soils stabilised with two different lime contents of 4% and 6%

linearly increased with an increase in bagasse fibre content from 0% to 2%. As expected, the improvement in the tensile strength was more pronounced for 6% lime treated soil with bagasse fibre reinforcement than 4% lime treated soil with the same amount of fibre reinforcement. For example, with 6% lime treated soil, the inclusion of bagasse fibre from 0% to 2% significantly increased the tensile strength from approximately 310 kPa to 400 kPa, resulting in the increment of 29% in the tensile strength compared with that of 6% lime treated soil without bagasse fibre reinforcement. The improvement in the tensile strength of lime treated soil samples reinforced with bagasse fibre indicated the effectiveness of bagasse fibre reinforcement, which might be contributed from the enhancement of interaction and interlocking between fibre surface and new cementitious products in the lime-soil matrix as well as the high tensile strength of bagasse fibre as discussed earlier.

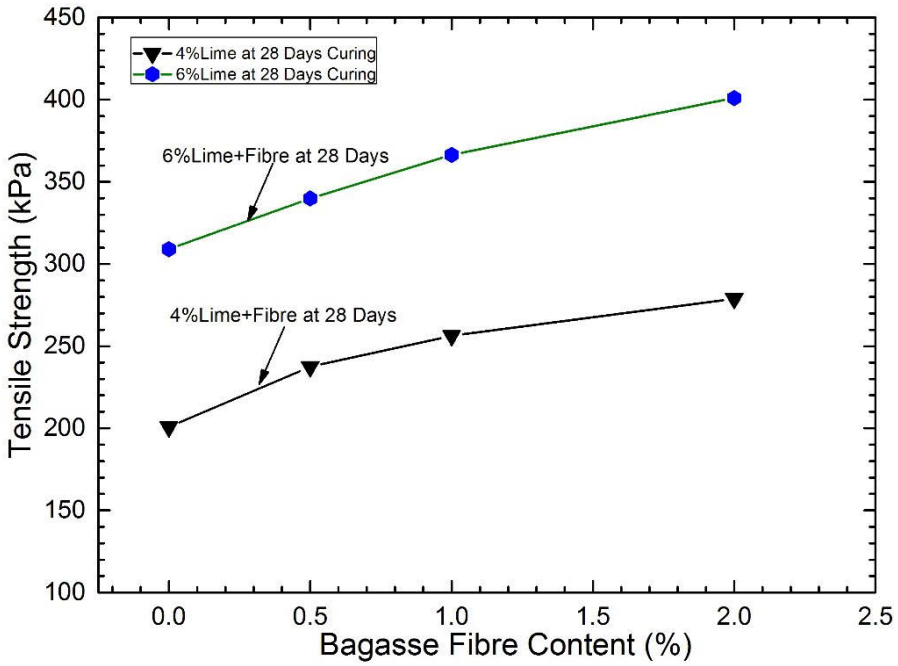

Figure 5.12 Effect of bagasse fibre content on the tensile strength of lime treated soil

5.2.8. Effect of Bagasse Fibre and Hydrated Lime on California Bearing Ratio

Figure 5.13 represents the variation of soaked CBR values of randomly distributed bagasse fibre reinforced expansive soil after 7 days of curing and 7 days of soaking. As can be seen in Figure 5.13, the smallest CBR value of 3.5% is associated with untreated expansive soil. Then, the CBR values increased slightly from 3.5% to 4.7% with an increase in bagasse fibre content from 0% to 2.0%. As discussed earlier, the increase in CBR values of bagasse fibre reinforced expansive soil could be attributed to the interaction and interlocking mechanism between clay particles and fibres developed during specimen preparation process by the compactive effort and with the extension of curing age. Increasing fibre content resulted in an increase in the fibre surface area, exposed to soil matrix, which facilitated better resistance to penetration load.

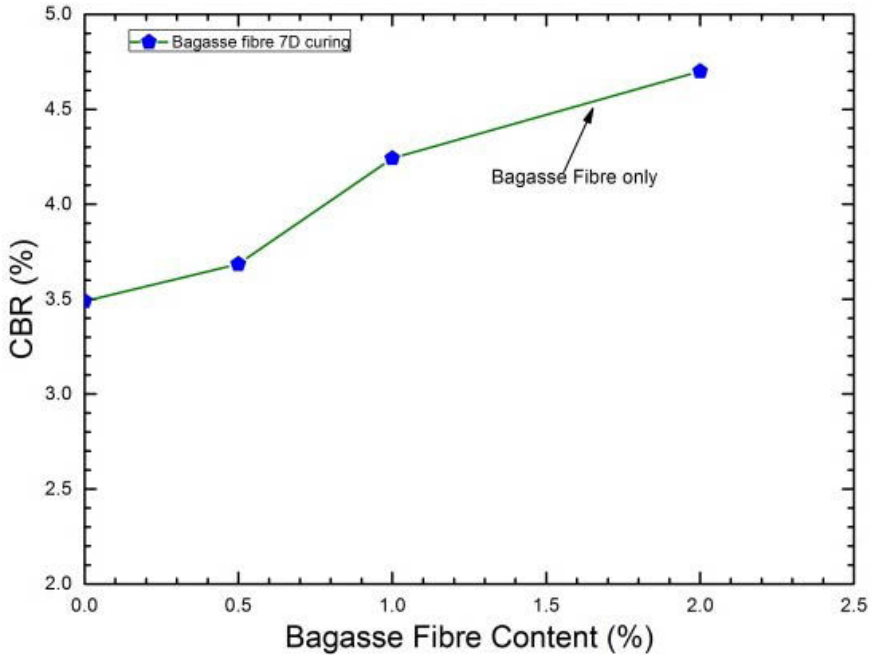

Figure 5.13 Variation of the soaked CBR of randomly distributed bagasse fibre reinforced expansive soil after 7 days of curing

Figure 5.14 displays the influence of various contents of bagasse fibre and hydrated lime treated expansive soil after 7 days of curing and 7 days of soaking. As illustrated in Figure 5.14, the CBR values of treated expansive soil increased steadily with increasing bagasse fibre content from 0.5% to 2% in combination with increasing lime content from 4% to 6% (based on the dry mass of soil). To illustrate this, the increase in bagasse fibre content from 0.5% to 2% when added to 4% lime treated expansive soil caused the soaked CBR value increased by approximately 40%. Likewise, a significant increase in amount of approximately 39% for the soaked CBR value was found when an increase in bagasse fibre content from 0.5% to 2% was added into 6% lime treated expansive soil. As expected, the increase in CBR value was more noticeable for the 6% lime combined with different percentages of bagasse fibre treated expansive soil. It can be explained that the significant improvement in CBR value could be attributed to the cation exchange between calcium ions in lime and metal ions on surfaces of clay particles. Then, such physical effects and chemical reactions form agglomeration and flocculation of clay particles, make the clay particles to be coarser, more brittle and less plastic, which promote friction resistance of lime-soil matrix. The next justification is associated with the time-dependent pozzolanic reactions. Such pozzolanic reactions take place quite slowly and are facilitated by high alkaline soil. The pH value of around 12.4, produced by lime-soil mixtures, gives rise to the dissolution of silica and alumina from clay mineral lattice. The dissolved silica and alumina from the lattice of clay minerals react with calcium available in the lime in order to establish new cementitious compounds, calcium silicate hydrate (CSH) and calcium aluminate hydrate (CAH). These cementitious compounds crystallize with time and give rise to the compressive strength of treated expansive soil. The addition of bagasse fibre reinforcement, moreover, contributed to the

development of interaction between bagasse fibre surface and soil matrix with time, which could be essentially beneficial of fibre reinforcement with lime treated expansive soil. Similar behaviour was well documented in the literature by researchers (Bell 1996; Dang et al. 2016b).

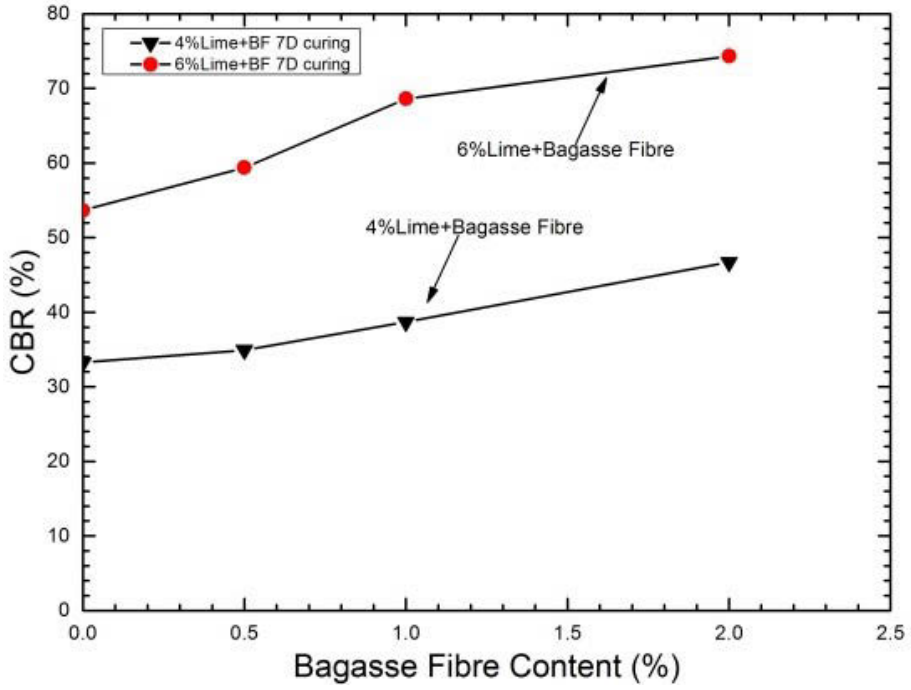

Figure 5.14 Variation of the soaked CBR of randomly distributed bagasse fibre and lime reinforced expansive soil after a curing period of 7 days

5.2.9. Effect of Bagasse Fibre and Lime on the Swell Potential

5.2.9.1. Results of CBR tests

Figure 5.15 and 5.16 exhibit the fluctuation of swell potential of randomly distributed bagasse fibre reinforced expansive soil and bagasse fibre-lime treated expansive soil, respectively, after 3 days of curing. Overall, the swell potential decreased with increasing bagasse fibre and lime contents. To be more specific, Figure 5.15 shows that a significant reduction of the swell potential of only bagasse fibre reinforced expansive soil was

observed as fibre content increased up to 1%. For example, the swell potential reduction of expansive soil reinforced with 1% bagasse fibre was about 48% in comparison with that of untreated expansive soil. Then, this was followed by a slight increase in the value of swell potential with increasing bagasse fibre content greater than 1%. However, the amount of swell potential measured was lower than that of untreated expansive soil. It is of interest to note that the swell potential reduction of reinforced expansive soil indicated the enhancement of bagasse fibre in heaving resistance.

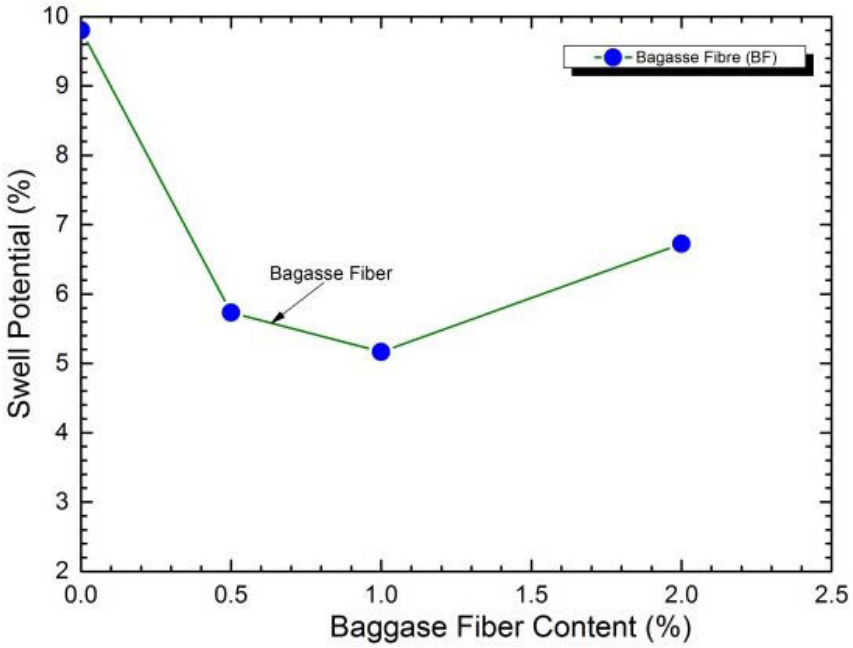

Figure 5.15 Variation of swell potential of randomly distributed bagasse fibre reinforced expansive soil

Figure 5.16 presents the enhancement of 0.5% and 2% bagasse fibre combined with different hydrated lime treated expansive soil. Observation of the results of swell potential tests plotted in Figure 5.16 depicts that adding bagasse fibre-lime combination resulted in a significant reduction of swell potential of treated soils. For example, the swell potential value significantly reduced from 9.8% to less than 0.5% with merely

adding 2.5% lime plus 0.5% bagasse fibre to the soil samples. A further increase in bagasse fibre and lime content gave rise to the swell potential of reinforced soil down to almost zero. The significant improvement in the swell potential could be attributed to cation exchange between calcium ions in lime and metal ions on surfaces of clay particles. As discussed earlier, when lime adopted to treat expansive soil, some physical and chemical changes happen to form flocculation and agglomeration of clay particles, alter the clay particles to be coarser, more brittle and less plastic, which promote better resistance to swelling behaviour. More importantly, with the addition of bagasse fibre to lime-soil mixtures, expansive clay replaced with non-expansive bagasse fibre and development of interaction and interlocking mechanism between clay particles and fibre surface could provide the effective resistance to the swell potential of lime-bagasse fibre-soil mixtures.

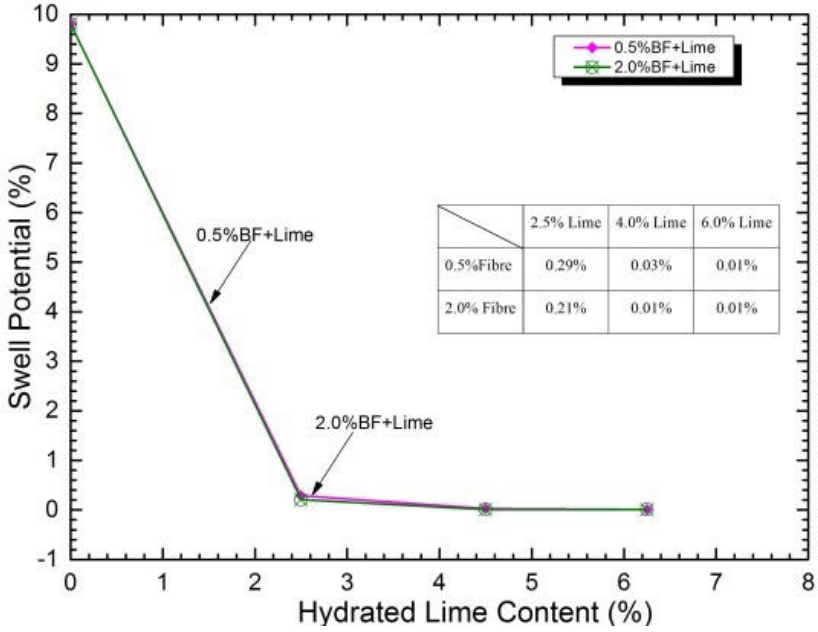

Figure 5.16 Variation of swell potential of various percentages of randomly distributed bagasse fibre and lime reinforced expansive soil (from CBR tests)

5.2.9.2. Results of Oedometer tests

Swell potential tests were conducted on untreated and treated samples using conventional Oedometer device in order to examine the free swell potential versus elapsed time in support of estimating the vertical ground surface heave of expansive soil due to fully wetting. Figure 5.17 exhibits the improvement of 2.5% lime combined with different bagasse fibre contents ranging from 0% to 2% for reinforcement of expansive soil. It is observed in Figure 5.17, lime treated expansive soils reinforced with bagasse fibre yielded the significant decrease in the swell potential. For instance, the swell potential of stabilised soils significantly decreased from approximately 10.5% to less than 0.5% when addition of 2.5% lime combined with an increase in bagasse fibre content from 0% to 1%. A further increase in bagasse fibre greater than 1% plus 2.5% lime content caused a slight increase in the free swell potential. However, the obtained swell potential value was very much lower than that of untreated expansive soil. Hence, the free swell potential results obtained from the Oedometer tests reconfirm the improvement of lime-bagasse fibre inclusion in heaving resistance, which shows a good agreement with the free potential results derived from the CBR swell tests.

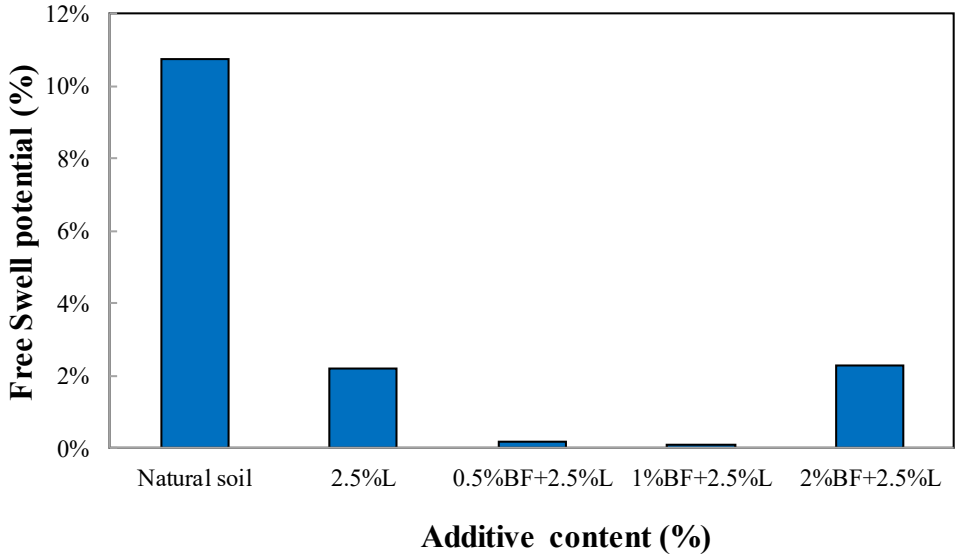

Figure 5.17 Variation of free swell potential of various percentages of randomly distributed bagasse fibre and lime reinforced expansive soil (from Oedometer tests)

5.2.10. Effect of Bagasse Fibre and Lime on Swelling Pressure

The influence of lime-bagasse fibre inclusions on the fluctuation of swelling pressure of treated expansive soil is presented in Figure 5.18. The measured swelling pressure of untreated expansive soil was about 80 kPa as illustrated in Figure 5.18. Following the swelling pressure measurements of untreated expansive soil, a series of experimental tests were conducted to examine the swelling pressure of expansive soil treated with different additive contents. It is clearly observed in Figure 5.18 that the addition of a relatively small percentage of 2.5% lime treated expansive soil reduced the swelling pressure significantly from 80 kPa for natural soil to approximately 25 kPa. The substantial reduction amount of swelling pressure was approximately 69% for only 2.5% lime treated expansive soil. Moreover, a combination of 2.5% lime with bagasse fibre content increasing from 0% to 1% showed the most effective improvement in swelling pressure of treated soil to less than 5 kPa. This was followed by a trivial increase in the swelling

pressure approached a certain value of 15 kPa with a further increase in bagasse fibre content higher 1% plus 2.5% lime. In general, the swelling pressure depicts a similar trend of the free swell potential for the same amount of additives stabilised expansive soil. As discussed in the previous section, the swelling pressure decrease in line with increasing the amount of lime and bagasse fibre treated expansive soil could be attributed to taking place the cation exchange phenomenon in that alumina, silica, and sodium ions in untreated expansive soil are most likely to be replaced by almost readily available calcium ions of hydrated lime. Meanwhile, by adding bagasse fibre into lime-soil mixtures, non-expansive bagasse fibre partially replaced expansive clay and the evolution of interaction and interlocking mechanism between clay particles, new cement products, and fibre surface could promote the effectiveness of the application of lime-bagasse fibre-soil mixtures in enhancing the swelling behaviour. Furthermore, the high tensile strength of bagasse fibre could be a possible reason for the effective improvement in the swelling resistance of bagasse fibre reinforced soils with lime stabilisation.

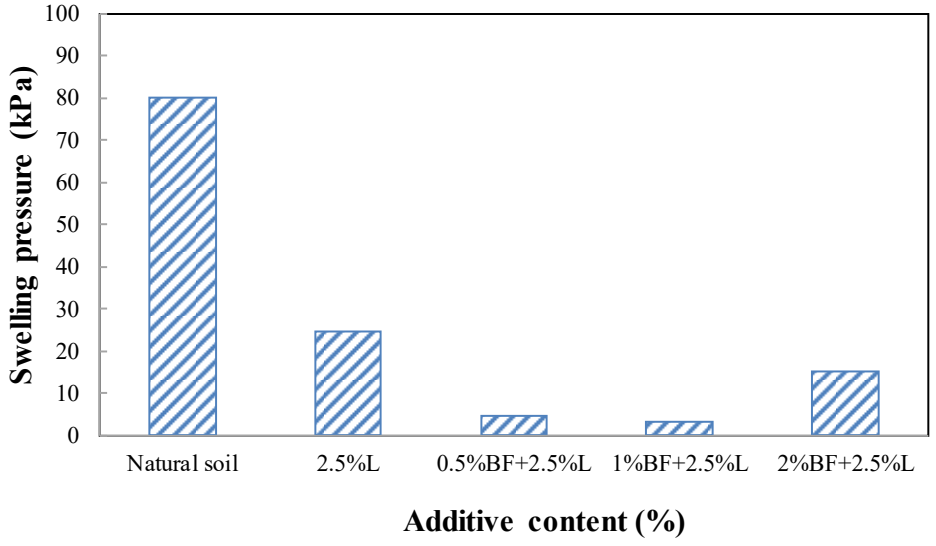

Figure 5.18 Variation of swelling pressure of various percentages of randomly distributed bagasse fibre (BF) and lime (L) reinforced expansive soil

5.2.11. Effect of Bagasse Fibre and Lime on the Compression Characteristics

To investigate the influence of hydrated lime and bagasse fibre inclusion on the compressibility characteristics of stabilised expansive soil, several series of 1D consolidation tests were undertaken on untreated soil and treated expansive soils with different contents of bagasse fibre combined with various percentages of lime from 2.5% to 6%. In the first experiment series, to comprehend the effect of hydrated lime on the compressible properties of expansive soils reinforced with bagasse fibre, only 0.5% bagasse fibres were added to lime-soil mixtures, meanwhile the hydrated lime content was changed from 0% to 6%. The relationship of void ratio against effective compression pressure, obtained from the 1D-consolidation tests after 3 days of curing, was clearly depicted in Figure 5.19. The compression test results indicate that 0.5% bagasse fibre reinforced soils combined with various lime contents tended to decrease the compression characteristics of treated expansive soil when increasing lime content from 0% to 4%. This trend was followed by a light increase in the compressibility with higher lime inclusion (e.g. 6%). A decrease in the slope of the virgin curves was obviously observed for all combined additive mixtures of treated expansive soil. However, the reduction of virgin curve was more noticeable for soil sample treated with 4% lime-0.5% bagasse fibre combination. The compressibility improvement of combined lime-bagasse fibre reinforced expansive soil might be attributed to cation exchange reactions between calcium ions in lime and metal ions on surfaces of clay particles and contribution of interaction between bagasse fibre surface and lime-soil matrix with curing time. An increase in lime content results in an increase in the flocculation and aggregation because of cation exchange reactions between calcium cations and other exchangeable cations

including sodium, magnesium and so forth, which are responsible for the improvement of compressibility characteristics of treated expansive soil.

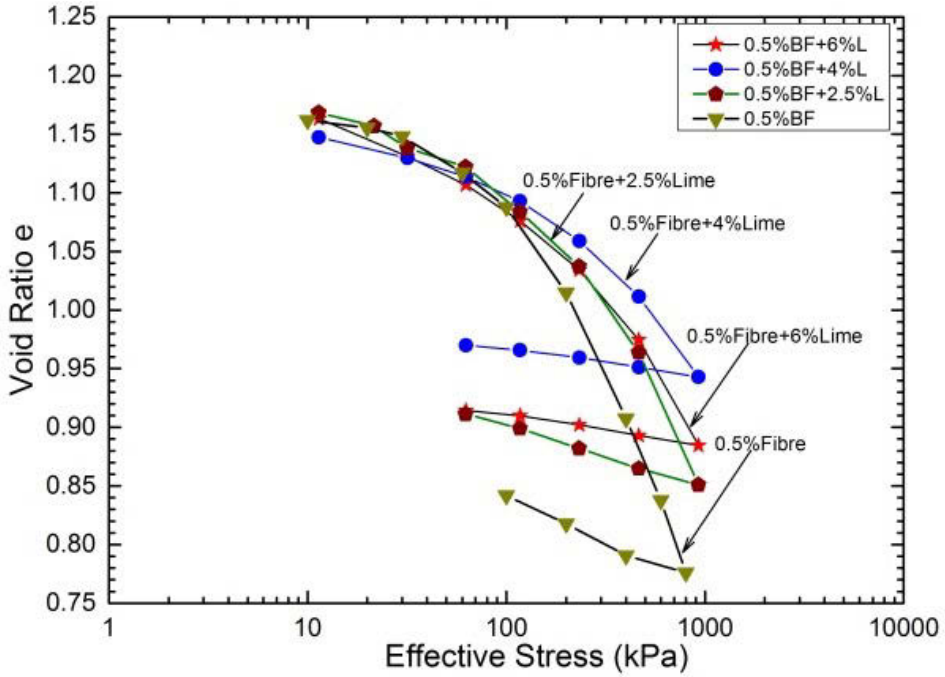

Figure 5.19 Variation of effective stress-void ratio curves of 0.5% randomly distributed bagasse fibre and various contents of lime reinforced expansive soil

In the second experiment series, to study the influence of bagasse fibre on the compression properties of lime treated expansive soil, an amount of 2.5% hydrated lime was added to lime-soil admixtures, while the bagasse fibre content was varied from 0% to 2%. Figure 5.20 depicts the influence of different fibre content combined with 2.5% lime on the compressibility of stabilised soils. The experimental results reveal that the bagasse fibre and lime treated soil appeared to decrease the compression characteristics of treated soil as bagasse fibre content increased from 0% to 1% and then followed by a slight increase in the compressibility with bagasse fibre inclusion greater than 1%. The slope reductions of the virgin compression curves were found for all combined additive

mixtures of treated expansive soil. However, the most reduction of a virgin curve was observed for soil treated with 2.5% lime-1% bagasse fibre combination.

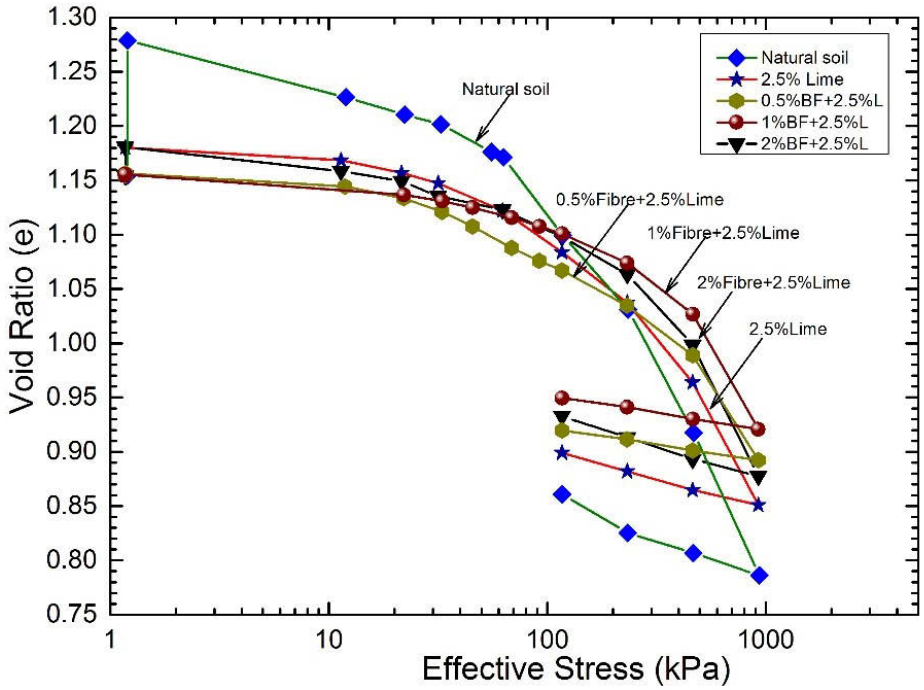

Figure 5.20 Variation of effective stress-void ratio curves of various content of randomly distributed bagasse fibre and 2.5% lime reinforced expansive soil

The influence of bagasse fibre reinforcement on the preconsolidation pressure of lime treated expansive soil is illustrated in Figure 5.21. It is noted that the preconsolidation pressures of 2.5% lime treated soils with various bagasse fibre contents were derived from Figure 5.20 using a proposed method of Boone (2010). Observation of the preconsolidation pressures presented in Figure 5.21 notes that the increase in bagasse fibre content from 0% to 1% in order to reinforce soils with 2.5% lime resulted in the corresponding increase in the preconsolidation pressure from 165 kPa to around 240 kPa (approximately 45% improvement). When an additional increase in bagasse fibre

content beyond 1% exhibited a marginal decrease in the preconsolidation *pressure* of reinforced soils to a certain value of 215 kPa. However, by comparing with untreated soil and only 2.5% lime treated soils, the preconsolidation pressure of 2.5% lime treated soil with 2% bagasse fibre reinforcement significantly increased by 38% and 30%, respectively. This behaviour reveals that bagasse fibre reinforcement was very effective in improving the preconsolidation pressure of lime-soil mixture, whereas an excessive inclusion of bagasse fibre content exceed 1% tented to reduce its positive impact on the improvement in the preconsolidation pressure of reinforced soils with lime.

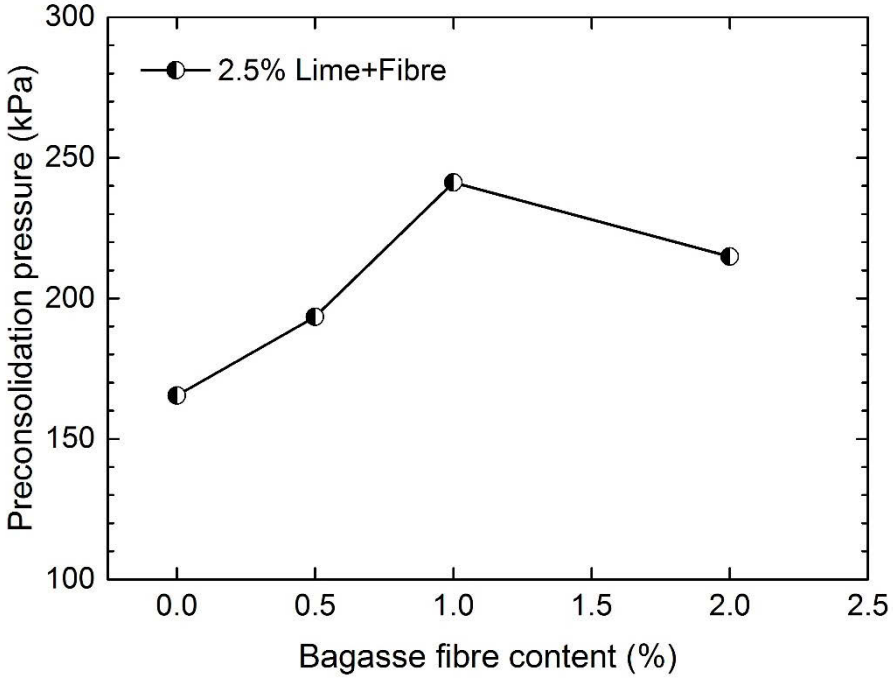

Figure 5.21 Variation of preconsolidation pressure of expansive soil reinforced with various contents of bagasse fibre and 2.5% lime

Figure 5.22 indicates the influence of bagasse fibre reinforcement on the variation of compression index (Cc) and swelling index (Cs) of 2.5% lime-soil mixtures after curing and soaking for 7 days. It can be noted that Cc is defined as the slope of the straight

line portion (virgin compression portion) of the effective stress-void ratio curve, meanwhile Cs is the slope of the unloading compression curve. As can be seen in Figure 5.22, the value of Cc appeared to reduce with increasing bagasse fibre inclusion from 0% to 1%. However, an increasing trend of the compression index was observed when the bagasse fibre inclusion into the lime-soil mixture increased beyond 1%. Similar behaviour can be found for the swelling index of lime treated soils with bagasse fibre reinforcement as bagasse fibre content increased up to 2%. As observed in Figure 5.22, the change of Cc was more pronounced than the Cs variation of reinforced soils with lime stabilisation. The reduction of both the Cc and Cs indices confirms that the addition of bagasse fibre can effectively reduce the compressibility of lime treated soils.

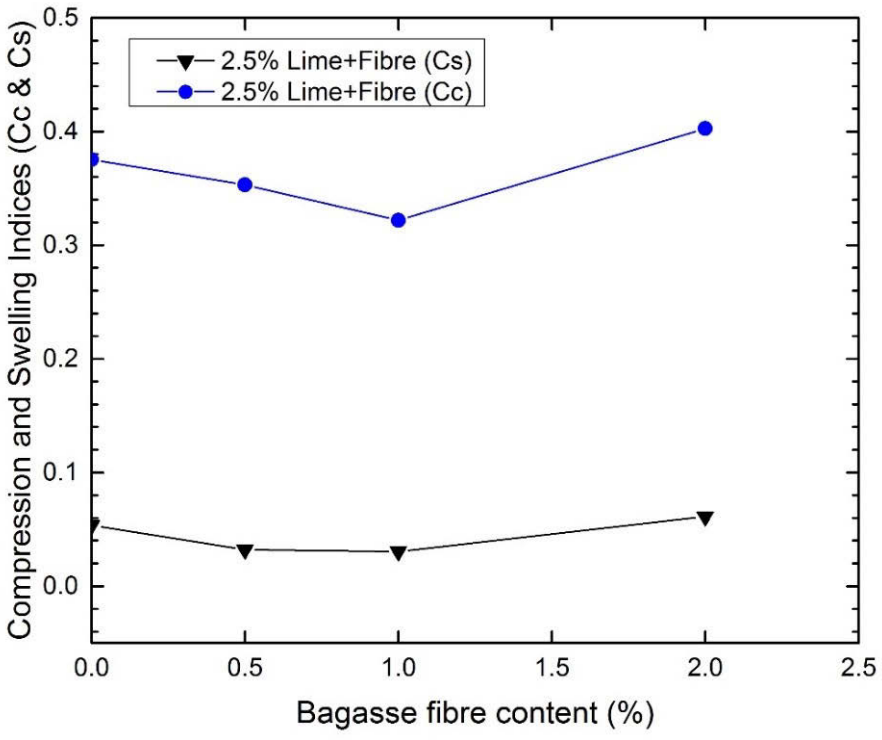

Figure 5.22 Variation of compression and swelling indices of expansive soil reinforced with various contents of bagasse fibre and 2.5% lime

The compressibility decrease of combined lime-bagasse fibre reinforced expansive soil might be attributed to cation exchange reactions between calcium ions in lime and metal ions on surfaces of clay particles as well as contribution of interaction between bagasse fibre surface and lime-soil matrix with curing time as discussed earlier. An increase in fibre content resulted in the increase in the fibre surface area, exposed to soil matrix, which facilitated better resistance to the compression load, whereas an excessive fibre content inclusion could increase the compressibility of treated soil to a certain extent due to the relatively high compressibility of natural fibre compared with soil particles.

5.2.12. Effect of Bagasse Fibre and Lime on Soil-Water Characteristic Curves

The effect of lime and lime-fibre inclusions on soil-water characteristic curves (SWCC) of stabilised expansive soil is shown in Figure 5.23a and 5.23b. The SWCC for untreated and treated soils was plotted by using the curve fitting model Equations 2.7 and 2.8 proposed by Fredlund & Xing (1994) to simulate the SWCC by means of a nonlinear, least square regression analysis. It should be noted that the best fitting parameters of Equations 2.7 and 2.8 were derived from the experimental data using Microsoft Excel and Solver.

$$\theta(\psi, a, n, m) = C(\psi)\frac{\theta_s}{\left[ln\left[e + \left(\frac{\psi}{a}\right)^n\right]\right]^m} \quad (2.7)$$

where $C(\psi)$ is a correction function defined as

$$C(\psi) = \frac{-ln\left[1 + \left(\frac{\psi}{\psi_r}\right)\right]}{ln\left[1 + \left(\frac{1000000}{\psi_r}\right)\right]} + 1 \quad (2.8)$$

where ψ = soil suction (kPa); ψ_r = soil suction corresponding to the residual water content (θ_r); θ_s = saturated water content; e = void ratio; and a, n, m = model parameters.

Generally, the predicted SWCC data showed a good relationship with the measured SWCC data for both untreated and lime–bagasse fibre treated soils. It can be seen in Figure 5.23a and 5.23b that the lime and bagasse fibre inclusions had significant influences on the SWCC of stabilised expansive soil. The SWCC tended to increase with the additions of 4% lime combined with increasing bagasse fibre content from 0% to 2%. To be more specific, the SWCC slopes of lime-fibre treated soil were steeper in comparison with that of untreated soil. This phenomenon is expected to happen because expansive soil stabilisation using lime and bagasse fibre tends to improve water retention capacity of stabilised soil by effectively enhancing pore size distribution of the soil. The lime powders and hydration products of lime-soil reactions facilitate occupying the original void among finer clay particles. Moreover, the improvement of soil water retention capacity can be attributed to the flocculation and pozzolanic reactions that help alter the microstructure of treated soil. Results of this investigation agree well with the results earlier reported by researchers (Elkady et al. 2015; Wang et al. 2016).

Table 5.1 displays the variations of air entry values (AEV) of lime-fibre treated soil. The AEV_S was derived from the SWCC regarding the degree of saturation (SWCC_S) plotted in Figure 5.23a in a semi-log plane, meanwhile the AEV_w was

resulted from the SWCC between matric suction of soil and gravimetric water content (SWCC_ w) plotted in Figure 5.23b in a log-log scale as proposed by Pasha et al. (2016). Observation of the results of AEV_S and AEV_w reveals that the air entry values were more pronounced for bagasse fibre-lime treated expansive soil and the AEV_w estimated from the SWCC_w was much greater than that of AEV_S derived from SWCC_S regardless of untreated or treated soils. This behaviour could be due to the different scales were adopted and an interrelationship between air entry value and preconsolidation pressure was not taken into accounts in this investigation because of unavailable consolidation test data. Therefore, to have a better understanding of the fluctuation of AEV, the AEV_S was compared and discussed in detail. For example, the AEV_S of untreated soil was about 200 kPa, whereas the addition of 4% lime into soil resulted in the AEV_S of 490 kPa. The increased amount of 4% lime stabilised soil was approximately 145% compared to that of natural soil. However, the combination of 4% lime and different fibre contents from 0% to 2% caused a slight decrease in AEV_S ranging from 490 kPa to 375 kPa. This implies that the presence of bagasse fibre showed no notable impacts on the water retention capacity of treated soils. The improvement of AEV_S might be mainly due to alteration of a small fraction of clay caused by lime-soil stabilisation. This is consistent with the observations reported by Puppala et al. (2006) studying on the influence of fly ash and recycled plastic fibres stabilised expansive soil.

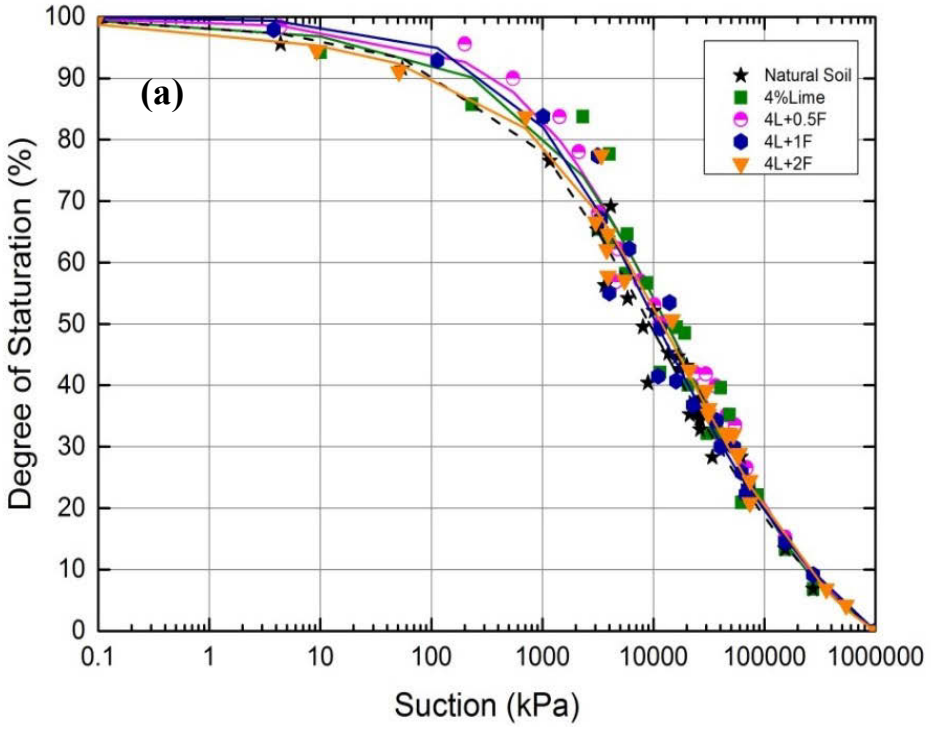

(a)

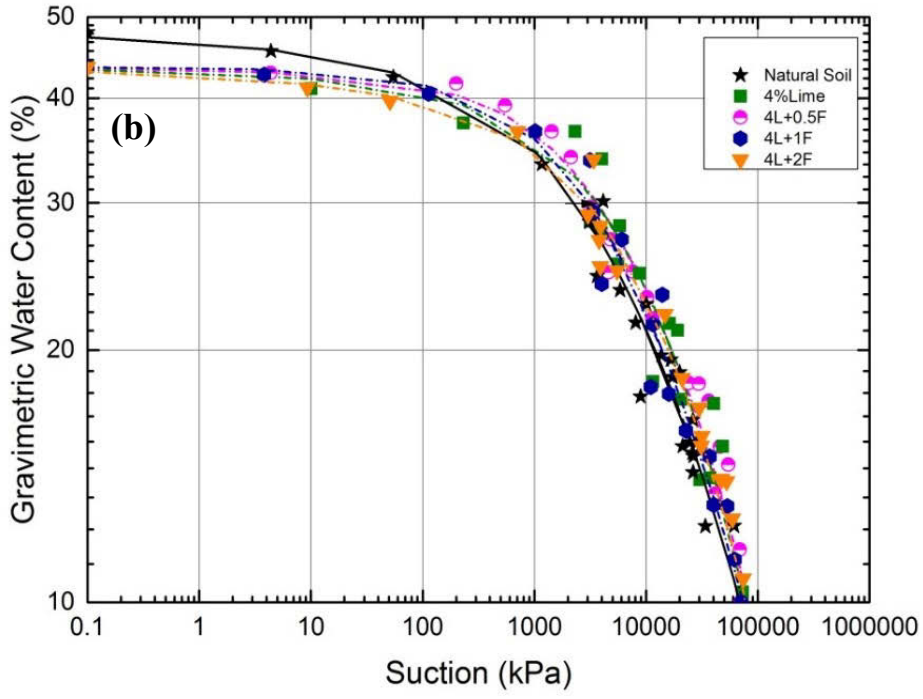

(b)

Figure 5.23 Variation of soil-water characteristic curves of various percentages of randomly distributed bagasse fibre and lime reinforced expansive soil as a function of (a) degree of saturation; (b) gravimetric water content

Table 5.1. Variation of air entry values of natural soil and bagasse fibre-lime stabilised soils

Additive content (%)		AEV_S (kPa)	AEV_*w* (kPa)
Lime content (%)	**Fibre content (%)**		
0	0	200	3115
4	0	490	5005
4	0.5	475	5130
4	1	430	4990
4	2	375	4785

*Notes: **AEV_S** is air entry value derived from a relationship between soil suction and degree of saturation (S); **AEV_*w*** is air entry value derived from a relationship between soil suction and gravimetric water content (*w*).

5.2.13. Effect of Bagasse Fibre Reinforcement on the Shear Strength Characteristics

5.2.13.1. Effect of bagasse fibre on stress-strain behaviour

Figure 5.24a-5.24c exhibit the effects of bagasse fibre content on the undrained deviatoric stress-strain behaviour of reinforced expansive soil associated with different confining pressures from 50 kPa to 200 kPa. As illustrated in Figure 5.24, the peak deviatoric stress of reinforced soil significantly increased with an increase in bagasse fibre content from 0% to 2%. For example, as shown in Figure 5.24c, the peak deviatoric strength increased from 136 kPa for 0% bagasse fibre reinforced soil (non-reinforced soil) to 193 kPa for 2% bagasse fibre reinforced soil at the same confining pressure of 200 kPa, which results in the corresponding improvement in the peak deviatoric strength of approximately 41%. As expected, the peak deviatoric stress also increased with increasing confining pressures from 50 kPa to 200 kPa as illustrated in Figure 5.24a-5.24c. To take 2% bagasse fibre reinforced soil as an example, the peak deviatoric strength increased from around 98 kPa

at confining pressure of 50 kPa to 193 kPa at confining pressure of 200 kPa, resulting in the corresponding increase in the peak deviatoric strength of almost 97%. A similar trend of the peak deviatoric strength increase was visually observed for 0.5% and 1% bagasse fibre reinforced soils. In addition, the improvement in the initial deformation modulus of reinforced soils is clearly observed in Figure 5.24a-5.24c as the slope of initial deviatoric stress-strain curves became steeper when bagasse fibre content increased up to 2%. This behaviour indicates that adding bagasse fibre improved the stiffness of reinforced soils. Moreover, it can be noted that with the addition of bagasse fibre reinforced soils, as plotted in Figure 5.24a-5.24c, the deviatoric strength reached a peak in a low range of axial strain between 0.5% and 1% at a low confining pressure of 50 kPa. Meanwhile, the peak deviatoric strength was found in a range of 1% to 3% axial strain with a further increase in the confining pressure exceeded 50 kPa. More importantly, the post-peak deviatoric strength of bagasse fibre reinforced soils, as shown in Figure 5.24a-5.24c, was significantly enhanced in comparison with the typically post-peak shear strength of soil stabilised with conventional stabilisers (e.g. lime, cement and fly ash). According to many researchers (Chen & Indraratna 2014; Lo & Wardani 2002; Zhang et al. 2015), the shear strength of lime/cement treated soils is suddenly lost after peak shear strain. This phenomenon implies that bagasse fibre reinforcement could enhance the reinforced soil behaviour from strain softening to strain hardening by diminishing the post-peak shear strength loss.

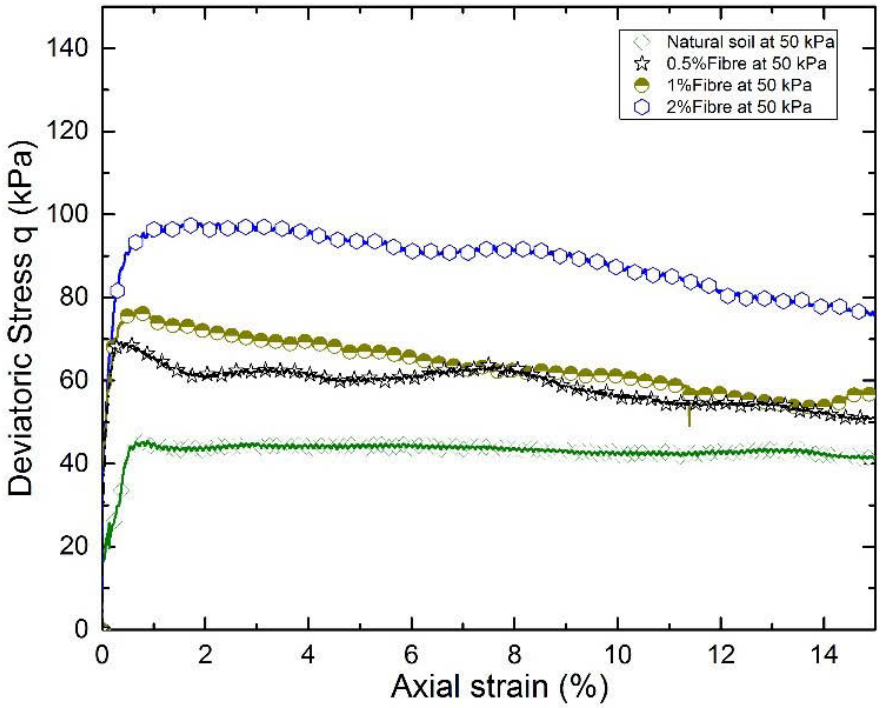
Natural soil at 50 kPa
0.5%Fibre at 50 kPa
1%Fibre at 50 kPa
2%Fibre at 50 kPa
Deviatoric Stress q (kPa)
Axial strain (%)
0
20
40
60
80
100
120
140
0
2
4
6
8
10
12
14

(a)

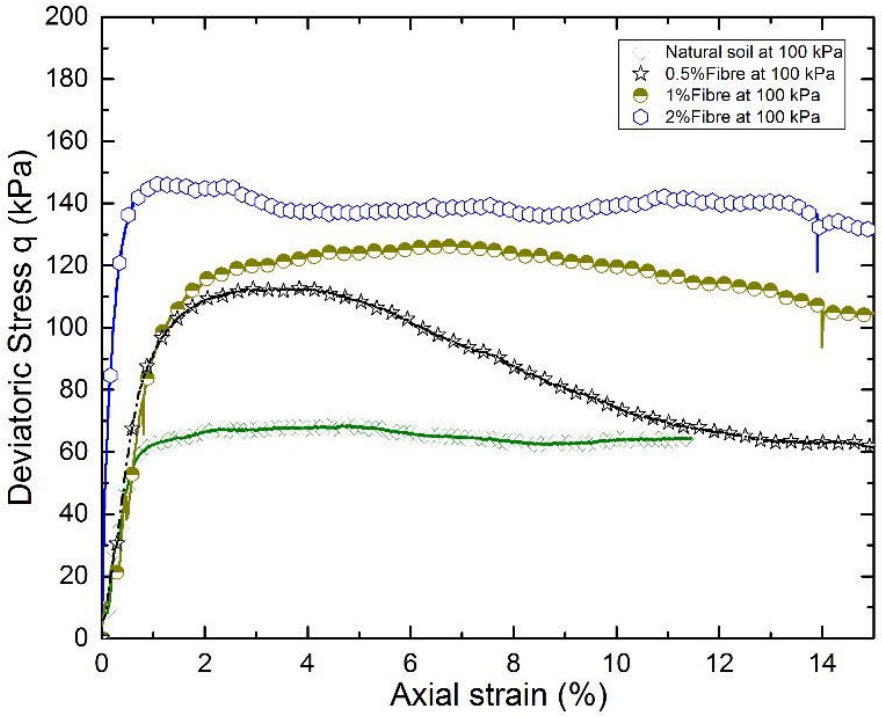
Natural soil at 100 kPa
0.5%Fibre at 100 kPa
1%Fibre at 100 kPa
2%Fibre at 100 kPa
Deviatoric Stress q (kPa)
Axial strain (%)
0
20
40
60
80
100
120
140
160
180
200
0
2
4
6
8
10
12
14

(b)

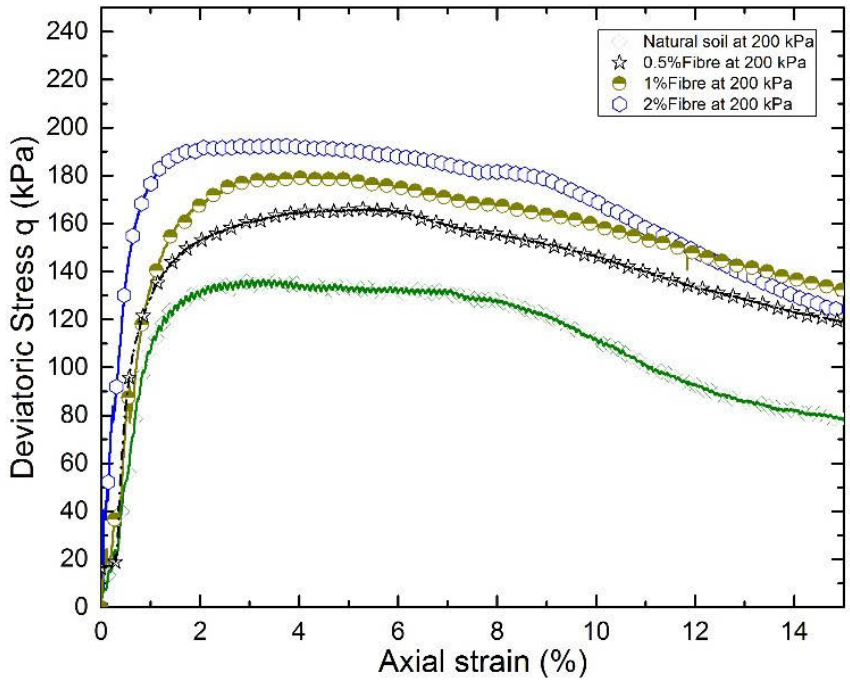

(c)

Figure 5.24 Deviatoric stress-axial strain behaviour of expansive soil reinforced with bagasse fibre at different confining pressures of (a) 50 kPa, (b) 100 kPa and (c) 200kPa

5.2.13.2. Effect of bagasse fibre on excess pore water pressure

The variations of excess pore water pressure of non-reinforced soil and soils reinforced with different bagasse fibre contents associated with axial deviatoric strain for various confining pressures from 50 kPa to 200 kPa are illustrated in Figure 5.25a-5.25c. It is observed in Figure 5.25a that the excess pore water pressure reached a peak at a low axial deviatoric strain range between 0.3% to 1% followed by a gradual drop to either a certain marginal value or even negative excess pore water pressure along with increasing bagasse fibre content from 0.5% to 2%. However, the post-peak excess pore water pressure of non-reinforced soil decreased slightly, then followed by a small increase again and remained unchanged up to 15% axial shear strain. Furthermore, the increase in excess pore water pressure was pronounced for non-reinforced soil. Nevertheless, as evident in

Figure 5.25b-5.25c, when the confining pressure increased beyond 50 kPa, the peak excess pore water pressures of reinforced soils are observed in a range of 1% to 3% axial shear strain and then the excess pore water pressure exhibited a slight decrease or remained almost constant up to the maximum axial shear strain of 15% tested. Moreover, the excess pore water pressure of bagasse fibre reinforced soils showed a similar pattern with that of non-reinforced soil. However, the values of excess pore water pressure were higher for bagasse fibre reinforced soils than non-reinforced soil. In opinion of the authors, the reduction in the post-peak excess pore water pressure observed in Figure 5.25a for bagasse fibre reinforced soils at low confining pressure (pre-shear consolidation pressure) of 50 kPa seems to indicate that the reinforced soils were most likely to be lightly overconsolidated clay soils where negative excess pore water pressure appears to develop with further straining after peak deviatoric strength. According to Lorenzo et al. (2006), such reinforced clay soils when sheared under low pre-shear consolidation pressure would dilate similarly to lightly overconsolidated clay soils if they were subjected to drained loading conditions. Nonetheless, this dilative behaviour would not take place if reinforced soils were sheared under higher confining pressures (e.g. 100 kPa or 200 kPa confining pressure as presented in Figure 5.25b-5.25c, in this investigation), which induced higher effective stresses. As a result, the negative excess pore water pressure would not occur due to the application of the higher pre-shear consolidation pressures, which resulted in the higher shear resistance as well as the greater peak and post-peak shear strength as evident in Figure 5.24a-5.24c.

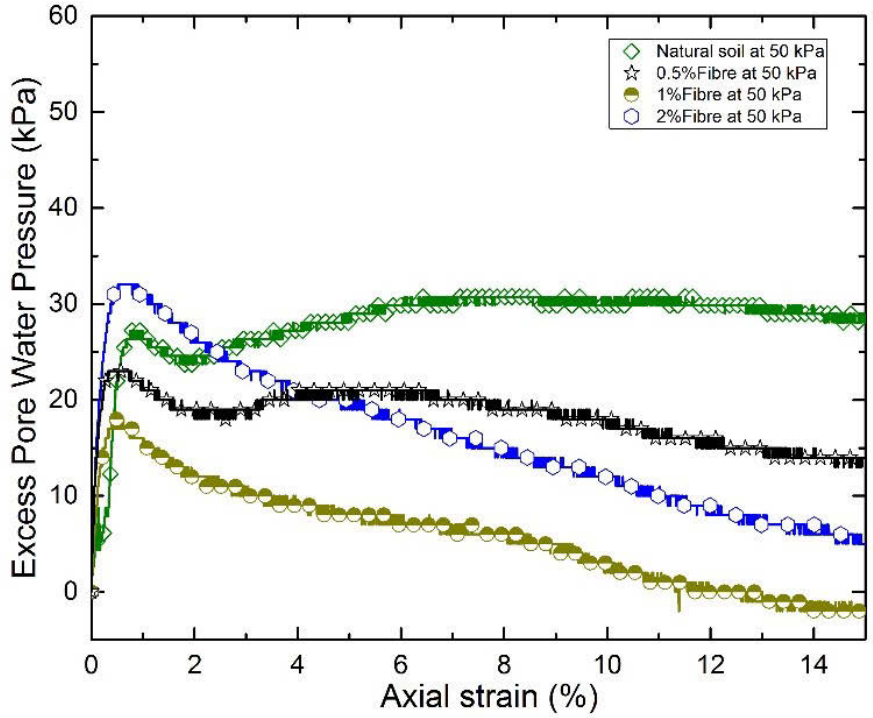
Natural soil at 50 kPa
0.5%Fibre at 50 kPa
1%Fibre at 50 kPa
2%Fibre at 50 kPa
Excess Pore Water Pressure (kPa)
Axial strain (%)
0
10
20
30
40
50
60
0
2
4
6
8
10
12
14

(a)

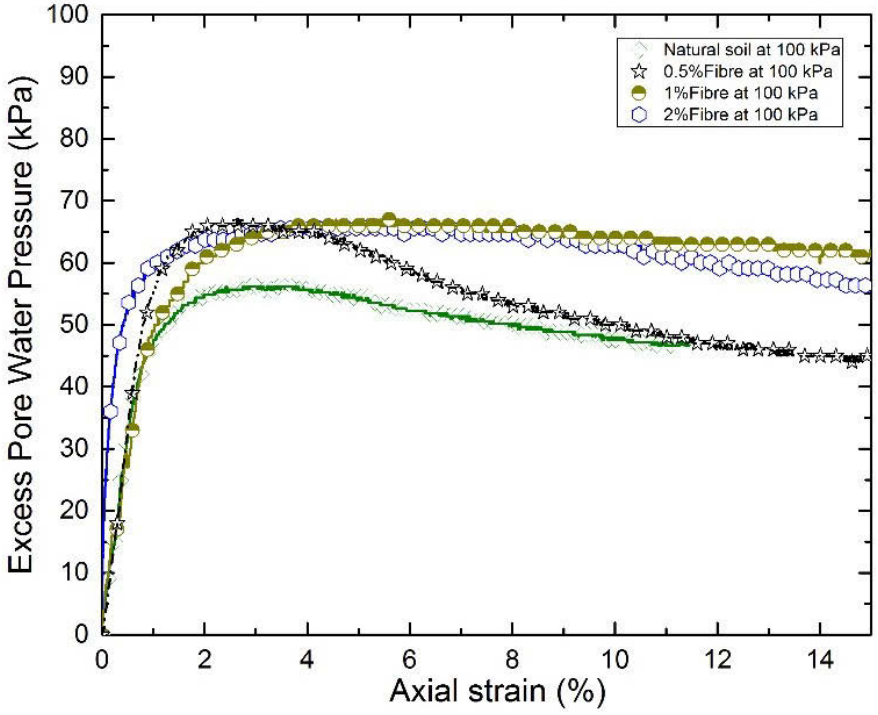
Natural soil at 100 kPa
0.5%Fibre at 100 kPa
1%Fibre at 100 kPa
2%Fibre at 100 kPa
Excess Pore Water Pressure (kPa)
Axial strain (%)
0
10
20
30
40
50
60
70
80
90
100
0
2
4
6
8
10
12
14

(b)

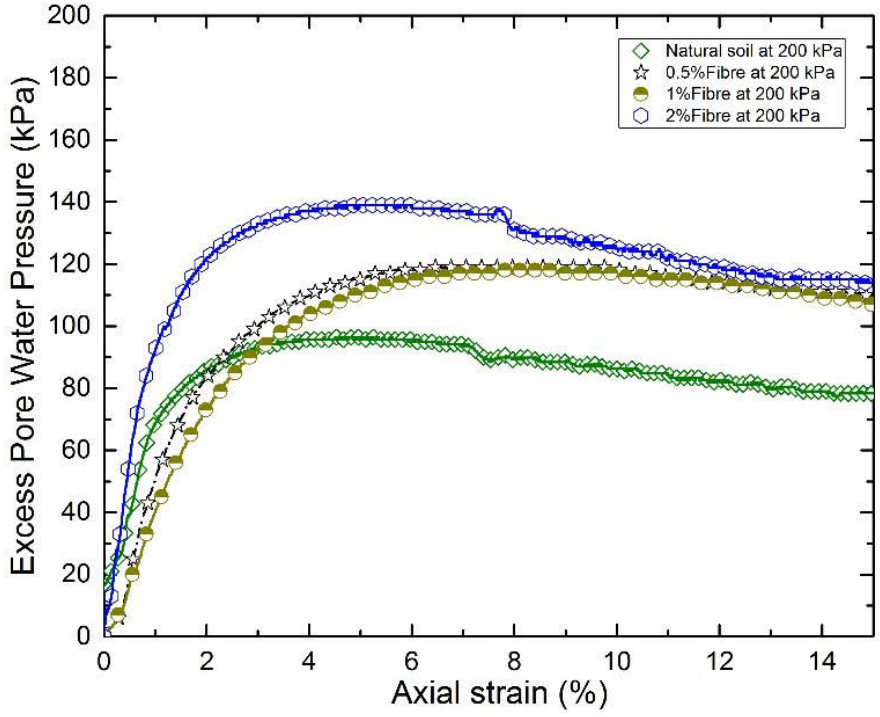

(c)

Figure 5.25. Excess pore water pressure change of expansive soil reinforced with bagasse fibre at different confining pressures of (a) 50 kPa, (b) 100 kPa and (c) 200kPa

5.2.13.3. Effect of bagasse fibre on ultimate shear strength

Figure 5.26 displays the variation of ultimate deviatoric strength versus bagasse fibre content at different confining pressures. As illustrated in Figure 5.26, the ultimate deviatoric strength positively and significantly depended on the bagasse fibre content to reinforce soils. An increase in the bagasse fibre content resulted in the ultimate deviatoric strength increase of reinforced soils as shown in Figure 5.26, irrespective of any given confining pressures. This confirms the effectiveness of bagasse fibre for expansive soil reinforcement in terms of the ultimate shear strength. The shear strength improvement of bagasse fibre reinforced soils compared to that of non-reinforced soil specimen may result from the interaction effect between fibre surface and clay particles due to compaction energy. Such interaction effect improves with increasing bagasse fibre content, which is

a key factor resulting in the increase in the ultimate shear strength of reinforced soils. It should be noted that a nonlinear relationship between the ultimate deviatoric strength and the bagasse fibre content was clearly depicted as the predominant mechanism for soils reinforced with bagasse fibre. Moreover, the ultimate deviatoric strength appears to be significantly influenced by the applied confining pressures varying from a relatively low pressure level of 50 kPa to a high pressure level of 200 kPa. As expected, increasing the confining pressure ranging from 50 kPa to 200 kPa caused an increase in the ultimate deviatoric strength regardless of adopted bagasse fibre content. The ultimate shear strength improvement visually observed for non-reinforced and reinforced soil specimens could be attributable to the effective stress increase induced by the corresponding confining pressure increase as discussed in the previous section.

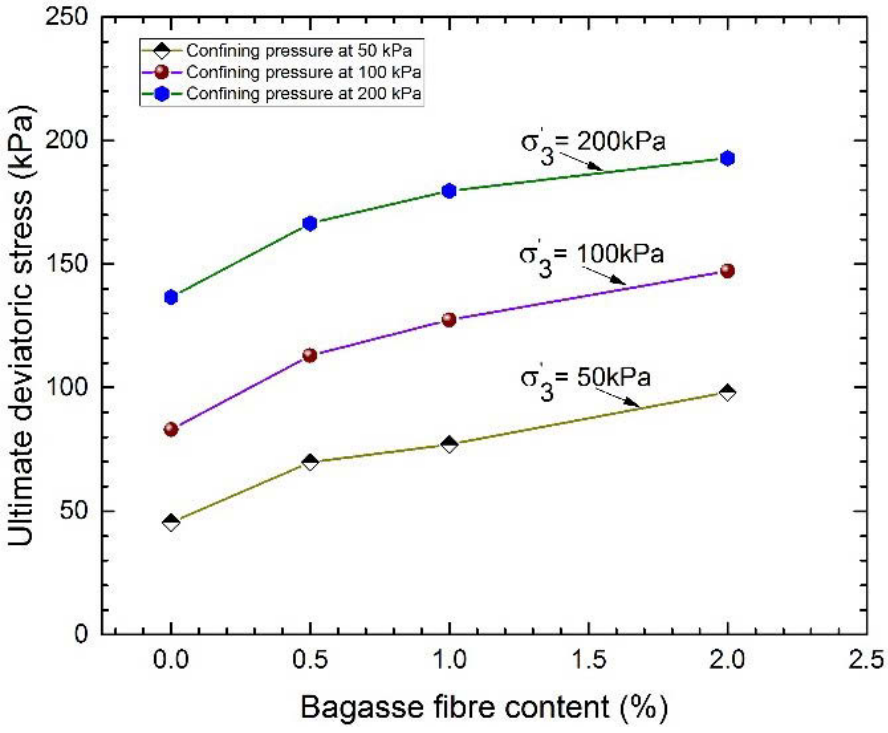

Figure 5.26. Variation of ultimate deviatoric strength of expansive soil reinforced with different bagasse fibre contents at confining pressures of 50, 100 and 200 kPa

5.2.13.4. Effect of bagasse fibre on peak strength envelopes and shear strength parameters

The peak shear strength envelops for both non-reinforced and bagasse fibre reinforced soils are presented in Figure 5.27. Overall, the slopes of the peak shear strength envelopes are steeper in line with the envelope location are higher for bagasse fibre reinforced soils than those of non-reinforced soil. This pattern reveals the effectiveness of bagasse fibre reinforcement in improving the peak shear strength of reinforced soils. From observation of Figure 5.27, the peak shear strength parameters consisting of internal fiction angle and intercept cohesion were derived using linear regression analysis and consequently depicted in Figure 5.28a and 5.28b, respectively.

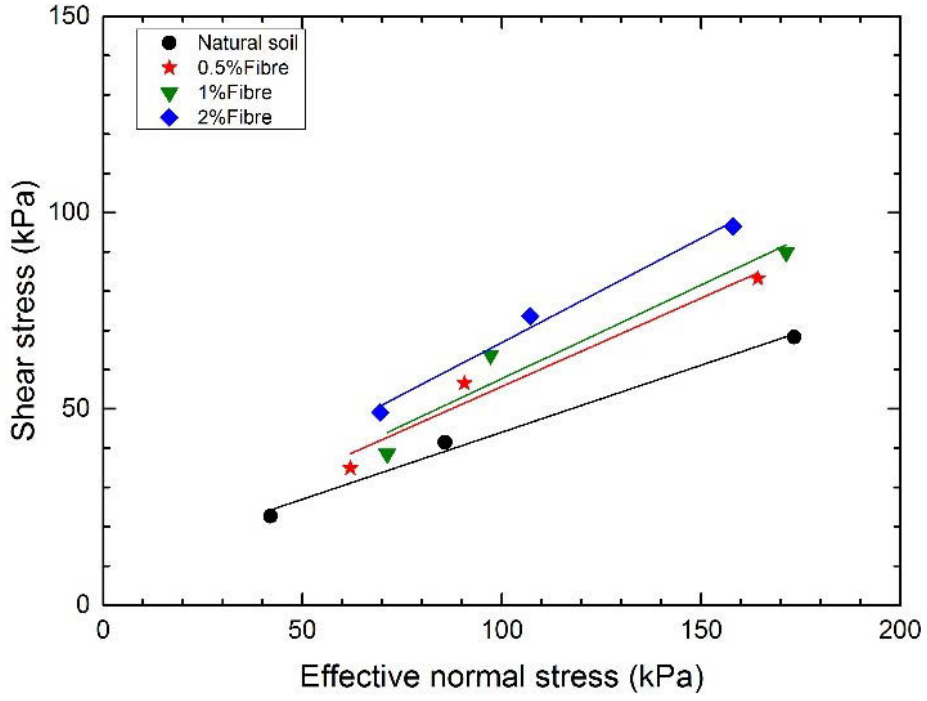

Figure 5.27. Peak strength envelope of expansive soil reinforced with different bagasse fibre contents

General observation of the peak shear strength parameters indicates that both internal friction angle and cohesion parameters increased with bagasse fibre inclusions. As observed in Figure 5.28a, the peak internal friction angle considerably depended on the introduction of different bagasse fibre content. For instance, by increasing bagasse fibre content from 0% for non-reinforced soil to 2% for bagasse fibre reinforced soils, the corresponding peak friction angle significantly increased from approximately 19.5° to 28°, resulting in about 44% increase in the peak friction angle. However, as seen from Figure 5.28b, the bagasse fibre reinforcement seemed to show an insignificant effect on the cohesion improvement of reinforced soils compared to the peak internal fiction improvement of reinforced soils. To illustrate this, when bagasse fibre content increased from 0% to 2%, the cohesion of reinforced soils remained almost unchanged for up to 1% bagasse fibre inclusion and then started to increase significantly as bagasse fibre content exceeded 1%. The author assumes that the improvement in the peak internal friction angle of soils reinforced with bagasse fibre could be contributed from the development of interaction and interlocking mechanism between the fibre surface and the soil matrix formed by compaction energy, as it was visually depicted in Figure 5.29. Meanwhile, the high tensile strength of bagasse fibre might effectively contribute to the improvement in the cohesion of reinforced soils due to enhancing the tension resistance of the fibre-soil matrix during post-peak shearing in progress.

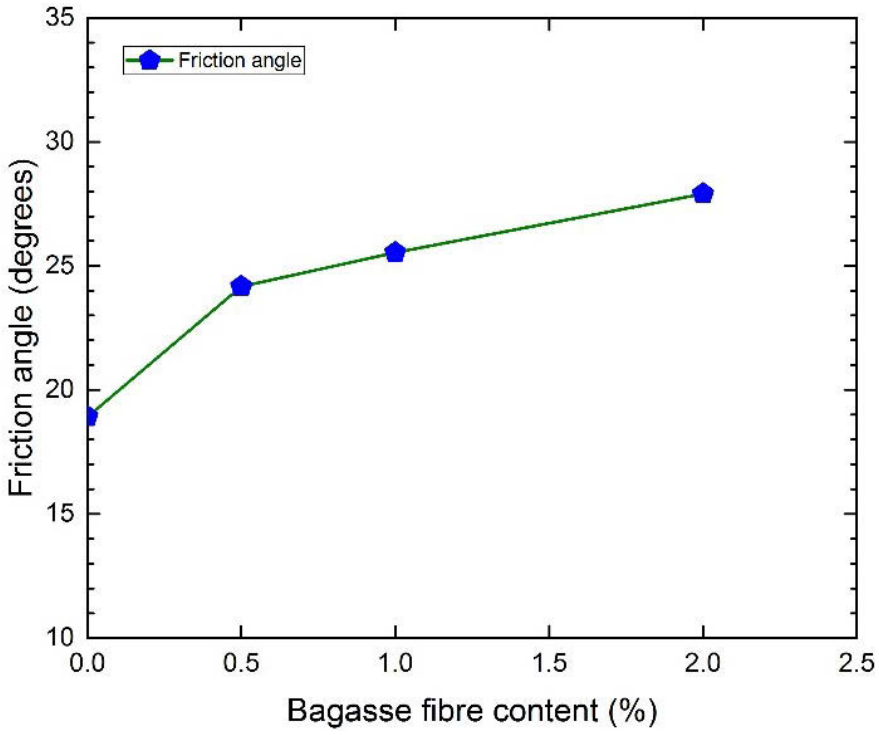

(a)

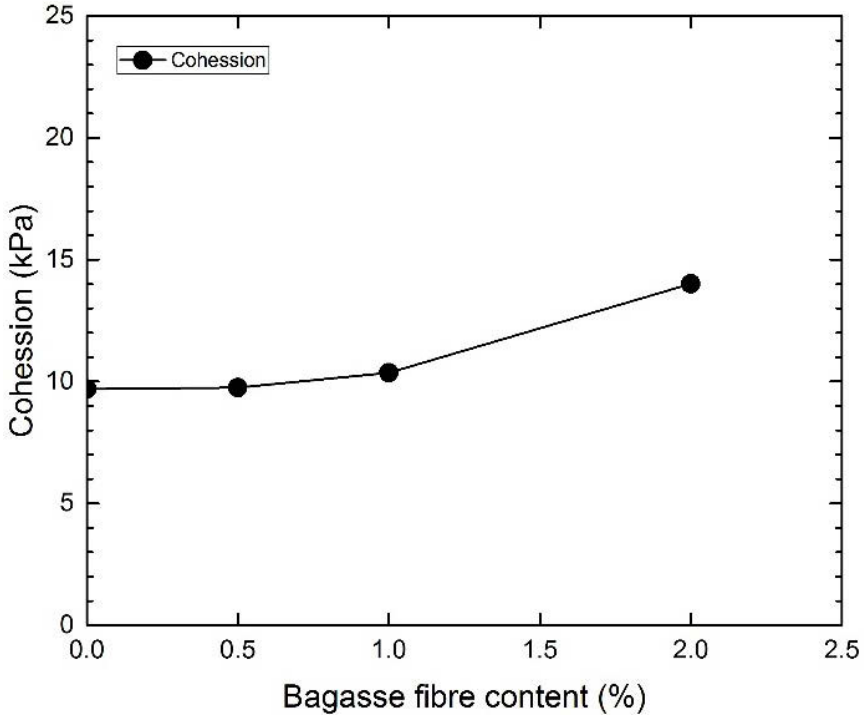

(b)

Figure 5.28. Variation of shear strength parameters with bagasse fibre content, (a) internal friction angle and (b) cohesion

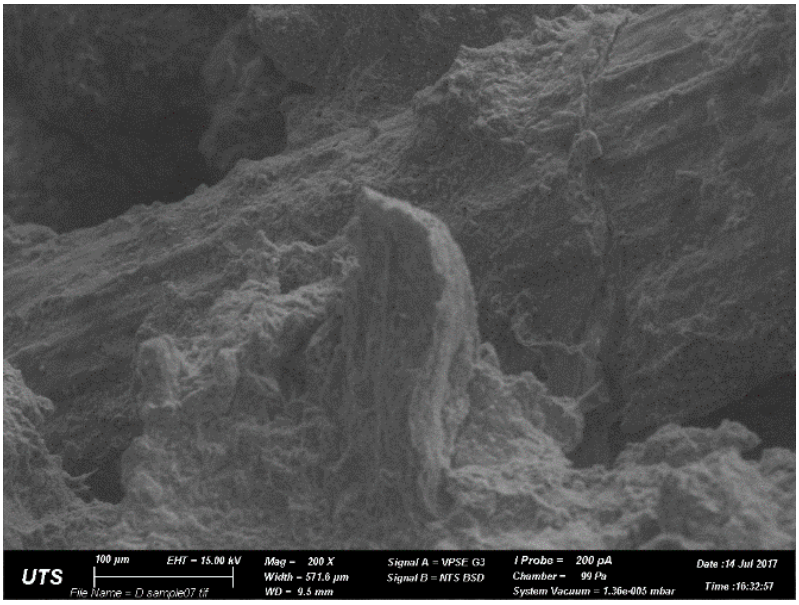

Figure 5.29 SEM image of interaction and interlocking mechanism between bagasse fibre surface and soil matrix

5.2.14. Microstructure Analysis

Figure 5.30a-5.30d present SEM images of natural expansive soil, 6% lime treated soil, and soil treated with 6% lime and bagasse fibre combination after tested for the 28 days UCS, respectively. By inspecting Figure 5.30a, it can be observed that the microstructure of compacted soil without chemical treatment appears to be like wet-state morphology and highly plastic material that represents typical formations of expansive soil. The observation in this study was consistent with the previous finding reported by Aiban (2006). However, when expansive soil was chemically treated with 6% hydrated lime, the wet condition of untreated soil was found to change to be drier and less plastic as evident in Figure 5.30b. As Figure 5.30b shows, formation of cementitious products (e.g. CSH, CAH or CASH) resulted from the time-dependent pozzolanic reactions can clearly be seen in the pore space of lime treated soils. Meanwhile, observation of Figure 5.30c and 5.28d reveals that the cementitious compounds were found to be attached to the

bagasse fibre surface of reinforced soil samples with hydrated lime, causing the better interfacial friction improvement between soil particles and fibre surface. As such, the cementitious products of stabilised soil with bagasse fibre reinforcement became stronger with curing time extended because of crystallization, resulting in the higher interfacial resistance to the applied load. Comparing with the SEM of soil reinforced with only bagasse fibre as shown in Figure 5.29, the interactions of bagasse fibre reinforced soils with lime stabilisation was considerably enhanced as evident in Figure 5.30c and 5.30d. Therefore, it is noteworthy to state that the high tensile strength of bagasse fibre and the stronger mechanical interlock of the contact area between fibre surface, cementitious bonds and clay particles in the lime-fibre-soil matrix were the primary components responsible for the improved soil shear strength and the enhancement of other geotechnical characteristics.

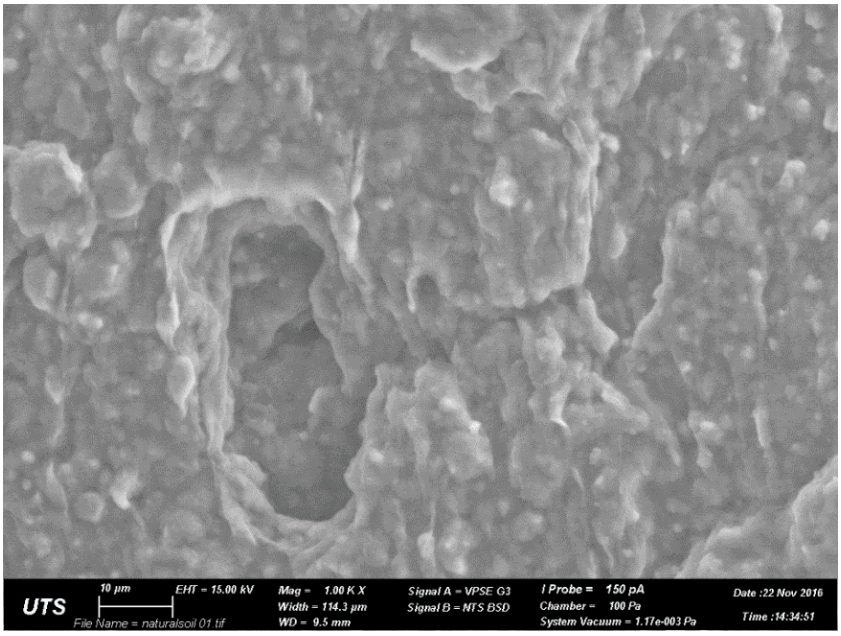
UTS
10 µm
EHT = 15.00 kV
File Name = naturalsoil 01.tif
Mag = 1.00 K X
Width = 114.3 µm
WD = 9.5 mm
Signal A = VPSE G3
Signal B = NTS BSD
I Probe = 150 pA
Chamber = 100 Pa
System Vacuum = 1.17e-003 Pa
Date :22 Nov 2016
Time :14:34:51

(a)

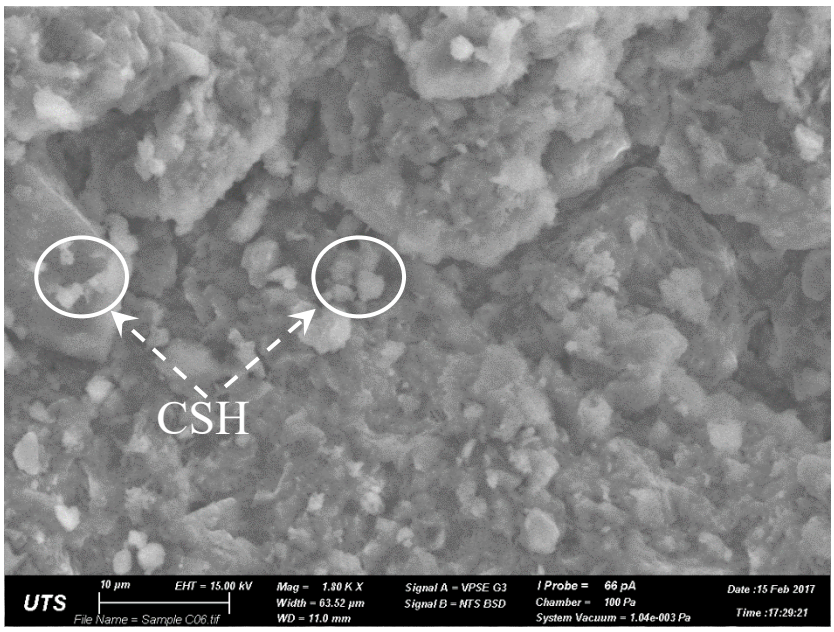
CSH
UTS
10 µm
EHT = 15.00 kV
File Name = Sample C06.tif
Mag = 1.80 K X
Width = 63.52 µm
WD = 11.0 mm
Signal A = VPSE G3
Signal B = NTS BSD
I Probe = 66 pA
Chamber = 100 Pa
System Vacuum = 1.04e-003 Pa
Date :15 Feb 2017
Time :17:29:21

(b)

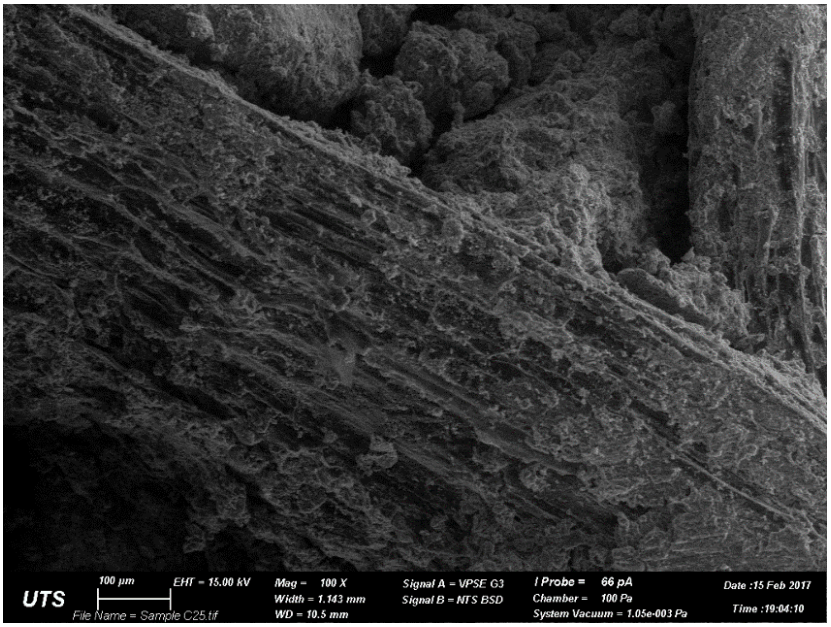

(c)

(d)

Figure 5.30 SEM images of (a) untreated expansive soil, (b) 6% lime treated soil, and (c, d) 6% lime treated soils with 1% bagasse fibre after 28 days of curing

5.3. SUMMARY

This chapter presents the results of the experimental assessment of the effects of bagasse fibre reinforcement on the engineering properties of reinforced soils without or with lime stabilisation. Several series of laboratory investigations were conducted on soil samples stabilised with different percentages of randomly distributed bagasse fibre from 0% to 2% and hydrated lime from 0% to 6% together with various curing times. The test results of this investigation were presented and analysed to examine the compaction properties, the shrinkage potential, the stress-strain behaviour, the unconfined compression strength (UCS), the indirect tensile strength, the California bearing ratio (CBR) of untreated and treated soil. Moreover, other engineering characteristics of untreated and lime treated expansive soil with bagasse fibre reinforcement such as the swell potential and the swelling pressure, the soil-water retention characteristics, the compressibility, and the shear strength properties, were also included and discussed in detail. In addition, the interaction and micromechanical reinforcement between soil particles and fibre surface were examined through scanning electron microscopy (SEM) analysis that was performed on selected soil samples. The key conclusions that were drawn, based on the experimental results, are presented as follows:

- In comparison with the untreated soil, the maximum dry density (MDD) of soils reinforced with only bagasse fibre gradually decreased with increasing the bagasse fibre content from 0% to 2%. With the addition of hydrated lime into the bagasse fibre-soil mixtures, the MDD of combined hydrated lime-bagasse fibre reinforced soils decreased further as the hydrated lime content increased from 0% to 6%. The MDD reduction of stabilised soils with increasing additive content could be attributed

to the lower specific gravity of bagasse fibre together with the larger spaces occupied in the soil matrix due to the flocculation and agglomeration of soil stabilisation with lime. The tiny air gaps trapped into fibre surface could be another influencing factor that also contributes to the MDD decrease of lime-fibre-soil mixtures.

- The linear shrinkage of bagasse fibre reinforced expansive soils without or with lime treatment reduced significantly with increasing additive content and curing time. The improvement was more pronounced for the mixtures of hydrated lime-bagasse fibre combination than only lime or bagasse fibre reinforced expansive soils.

- The UCS of bagasse fibre alone reinforced soils increased with the increase in fibre content along with the extension of curing time. However, it is observed that the UCS improvement with longer 7 days of curing was insignificant. The strength improvement of only bagasse fibres reinforced soil could be attributed to the interaction and interlocking mechanism between clay particles and fibres developed during the specimen preparation process by the compactive effort and with age.

- The compressive strength of the combined hydrated lime-bagasse fibre addition is definitely higher than that of soil reinforced with bagasse fibre alone as well as hydrated lime treated soil without fibre reinforcement. The brittleness index I_B increased with the increase in hydrated lime content from 4% to 6%, but significantly decreased with increasing bagasse fibre content from 0% to 2% when added into lime-soil mixtures. This phenomenon clearly corroborates that the bagasse fibre reinforcement had a notable influence on the ductility of lime treated soils, which transformed the stabilised soil behaviour from brittle to more and more ductile, by

significantly reducing the brittleness index (I_B). As a result of the reduction on the brittleness index, the loss of the post-peak compressive strength of lime treated soil reinforced with bagasse fibre was significantly improved.

- Based on the obtained results of the indirect tensile strength test, the introduction of lime treated soils significantly increased the tensile strength of stabilised soils in comparison with that of untreated soil. The addition of bagasse fibre into the 4% lime-soil mixtures generally enhanced the tensile strength but decreased the stiffness of treated soils. However, adding the higher lime content (i.e. 6% lime) to stabilise expansive soils with bagasse fibre reinforcement improved the tensile strength but the stiffness of stabilised soils remained almost unchanged compared to that of lime alone treated soil. Hence, the brittle behaviour tended to be the dominant mechanism for 6% lime stabilised soil with bagasse fibre.

- The tensile strength improvement of lime treated soils could be attributable to the formation of cementitious bonds between clay particles as a result of cation exchange and pozzolanic reactions. The addition of bagasse fibre into lime-soil mixtures resulted in the additional improvement in the tensile strength of stabilised soils due to the interaction between soil aggregates and fibre surface as well as contribution of high tensile strength from bagasse fibre. The stiffness decrease and the transformation of the stabilised soil behaviour from a brittle material to more ductile one for a certain amount of lime-fibre-soil mixtures may be attributed to bagasse fibre inclusion as a more ductile and deformable material into the lime-soil matrix. However, the addition of high lime content into bagasse fibre reinforced soil produces the high stiffness of stabilised soil matrix mainly contributed by lime stabilisation, and consequently

reduce the effectiveness of fibre reinforcement in improving the ductility of reinforced soils.

- The CBR value of treated expansive soil increased with the increase in content of bagasse fibre and lime-bagasse fibre. The CBR improvement was more noticeable for the combined lime-bagasse fibre reinforced expansive soil than bagasse fibre or hydrated lime alone treated soils. From the outcomes of swell potential and swelling pressure tests, it is noteworthy to state that modifying expansive soil with bagasse fibre in combination of lime has significant effects on minimising the swelling behaviour of expansive soil. The addition of a relatively small content of 2.5% lime plus 0.5% bagasse fibre could result in non-swelling of treated soil. The significant enhancement in the swelling behavior of lime treated expansive soil with bagasse fibre could be attributed due to the facts that, when lime is adopted to treat expansive soil, some physical and chemical changes take place to form agglomeration and flocculation of clay particles. This phenomenon makes the clay particles become coarser, more brittle and less plastic, which promote better resistance to swelling behaviour. More importantly, with the addition of bagasse fibre to lime-soil mixtures, expansive clay partially replaced with non-expansive bagasse fibre and development of interaction and interlocking mechanism between clay particles and fibre could provide the effective resistance to swelling behaviour of lime-bagasse fibre-soil mixtures.

- From the one-dimensional consolidation test results, it is concluded that the compression characteristics of lime-bagasse fibre reinforced expansive soil decreased with increasing lime content from 0% to 4% and then followed by a slight increase in

the compressibility with higher lime inclusion (up to 6%). Likewise, the compressible properties of soils reinforced with lime-bagasse fibre reduced as bagasse fibre content increased from 0% to 1% but then increased with bagasse fibre inclusion greater than 1%. The compressibility improvement of combined lime-bagasse fibre reinforced soils might be attributed to cation exchange reactions between calcium ions in lime and metal ions on surfaces of clay particles as well as contribution of interaction between bagasse fibre surface and lime-soil matrix with curing time. An increase in fibre content increases in the fibre surface area, exposed to soil matrix, which facilitates better resistance to the compression load. Whereas, an excessive fibre content inclusion could increase the compressibility of treated soil to a certain extent due to the relatively high compressibility of natural fibre compared with soil particles.

- From the soil suction tests using contact filter paper technique, the inclusions of lime and bagasse fibre had significant influences on the soil-water characteristic curves (SWCC) of stabilised expansive soil. Overall, the SWCC of stabilised soils tended to increase as the additions of 4% lime combined with increasing percentages of bagasse fibre from 0% to 2%. Analysis of the air entry values (AEV) of lime-fibre reinforced soil indicates that the addition of 4% lime into soil resulted in the AEV increase. However, the combination of 4% lime and different fibre content from 0% to 2.0% caused a slight decrease in the AEV. This behavior means that the presence of bagasse fibre reinforcement showed no notable impacts on the water retention capacity of stabilised soils. The AEV improvement might be mainly due to alteration of a small fraction of clay caused by lime-soil stabilisation.

- The outcomes obtained from the triaxial compression tests reconfirm that bagasse fibre reinforcement of expansive soil enhanced the initial deformation modulus and the peak deviatoric strength, and changed the reinforced soil behaviour from strain softening to strain hardening by minimising the loss of post-peak shear strength. It can be noted that the deviatoric strength of soils reinforced with bagasse fibre reached a peak in a low axial strain level at a low confining pressure of 50 kPa, while the peak deviatoric strength was found in a range of 1% to 3% axial strain with a further increase in the confining pressure exceeded 50 kPa.

- The ultimate deviatoric strength considerably depended on the bagasse fibre content of reinforced soils. The interaction effect between fibre surface and clay particles due to compaction energy plays an important role in improving the ultimate shear strength of reinforced soils. By increasing bagasse fibre content from 0% to 2% to reinforce expansive soils, the peak internal friction angle increased from 19.5° to 28°, meanwhile the corresponding cohesion increased from about 10 kPa to 14 kPa. However, the improvement in the shear strength parameters was visually more noticeable for the peak internal friction angle.

- The microstructure analysis indicated that the improvement in the soil strength, the bearing capacity and the other geotechnical characteristics of lime treated soils with bagasse fibre reinforcement were primarily because of the high tensile strength of bagasse fibre and the stronger interfacial friction and interlocking mechanism between fibre surface, cementitious bonds and clay particles in the lime-fibre-soil matrix.

CHAPTER 6: NUMERICAL ANALYSIS ON THE PERFORMANCE OF FIBRE REINFORCED LOAD TRANSFER PLATFORM AND COLUMNS SUPPORTED EMBANKMENTS

6.1. INTRODUCTION

The fast development of essential infrastructure including roads and rail networks, being constructed in many countries worldwide, is to meet the demand of the dramatic increase in population and economic growth. As a result, many countries are experiencing the lack of readily available stiff grounds in support to such transport infrastructure projects. Thus, many road and highway embankments have to be founded on soft grounds. This practice is highly risky, because soft ground has a low bearing capacity, insufficient shear strength and high compressibility. Therefore, to ensure the stability of embankment during the construction process and its long-term service life, appropriate ground improvement techniques are needed to be adopted in enhancing the engineering properties of soft soil or even for transferring embankment and traffic loads to a deeper and stiffer soil stratum.

A growing number of ground modification approaches have been applied to improve soft soil properties to support embankment construction such as

- Preloading with the vertical drain application (Liu & Rowe 2015; Parsa-Pajouh et al. 2015)

- Excavating the existing soft ground and substituting it with high shear strength and bearing capacity backfill soil
- Reducing embankment load using lightweight fill materials (Dang et al. 2015; Dang & Khabbaz 2018a; Martin et al. 1990)
- Constructing in stages and leaving time for consolidation
- Improving soft ground underneath embankment by chemical treatment (Chai et al. 2015; Dang et al. 2016b; Dang et al. 2016c; Dang & Khabbaz 2018b, 2018c, 2019; Dang et al. 2017b, 2017c; Fatahi & Khabbaz 2013, 2015; Jamsawang et al. 2016)
- Stone columns (Fatahi et al. 2012a)
- Geosynthetic-reinforced and piles supported earth platform (Dang et al. 2016a; Han & Gabr 2002; Liu et al. 2007).

On top of these methods, the ground improvement technique using deep cement mixing (DCM) columns has widely been used in construction practice. Among the main reasons is that it provides an economical and fast ground improvement solution for the construction of road and high way embankments over soft soil (Chai et al. 2015; Venda Oliveira et al. 2011; Yapage et al. 2014; Yapage et al. 2015). To improve the soft soil characteristics such as bearing capacity, shear strength and compressibility, in wet mixing method, slurry cement is mixed with soft ground at a designated water/cement ratio during the DCM columns construction process, while dry cement is mixed with in-situ soils to establish artificial DCM columns in dry mixing method. However, most of road and railway embankments built on end-bearing piles/columns are most likely to be subjected to large differential settlements between the embankment and the adjacent

roads due to the different stiffness levels (Chai et al. 2015; Liu & Rowe 2015). It is known that floating soil columns provide a less stiff ground foundation, but they are more cost-effective and technically feasible than the end bearing columns, when soft foundation soils reach greater depth. Furthermore, one advantage of the floating columns solution is that when a sand layer acting like an aquifer layer directly located below soft ground layers, the soft ground improvement solution using floating DCM columns could be the best choice for not contaminating groundwater during construction and post-construction. The experimental investigation by Chen & Indraratna (2014) also indicated that conventional chemical stabilisers (e.g. lime, cement) for soil stabilisation might cause adverse effects on the environment by changing the pH level of treated soil and its surrounding areas. As a result, the quality of groundwater and the normal growth of vegetation can be affected because of the pH change. As such, Chai et al. (2015) reported that using the floating DCM columns could be the best solution for soft ground improvement because it would leave an intact clay sub-layer below the column tip and immediately above the aquifer. As expected, such soft clay sublayer would serve as a barrier to hindering hazardous chemicals from spreading out of the deep cement mixing soil improvement area into groundwater. Nevertheless, the analysis and design of floating soil columns are complex, involve considering complicated soil-structure interaction, and there are no specific standards and guidelines readily available for the design of embankments supported on floating cement-soil columns.

Numerical modelling based on the finite element method (FEM) has been used as an effective tool in predicting the performance of DCM columns supported embankments founded on soft ground in terms of the total and differential settlements, the horizontal

movement, the rate of settlement, the slope stability and the degree of consolidation over a long period of time. The finite element numerical modelling can reasonably simulate the load transfer mechanism between DCM columns and foundation soil, and the generation and dissipation of excess pore water pressures. Consequently, the numerical modelling assist in predicting the total settlement, the lateral displacement, the bending moment of DCM columns with depth under the embankment using three-dimensional (3D) FEM model or even with an equivalent two-dimensional (2D) plane strain FEM model (Chai et al. 2015; Dang et al. 2016a; Tan et al. 2008; Yapage et al. 2014). Nevertheless, most of the numerical investigations have recently been performed to investigate the behaviour of embankments over DCM columns (Chai et al. 2015; Yapage et al. 2014), the performance of geosynthetic reinforced traditional angular layer as a load transfer platform (LTP) and piles/columns supported embankments over soft soils (Han & Gabr 2002; Liu et al. 2007; Yapage et al. 2015). According to Zhang et al. (2013), the popular applications of the geosynthetic reinforced traditional angular platform over columns supported embankments built on top of soft soils have come up with many geotechnical difficulties, namely intolerable total and differential settlements, larger lateral earth pressure and displacement, local or global instability, and potential failures due to over-bearing or bending capacity of DCM columns. Therefore, a novel ground modification technique utilising eco-friendly, low cost and recycled materials such as lime-soil-fibre reinforced load transfer platform (FRLTP) to be used as a replacement of geosynthetic reinforced traditional angular platform layer combined with DCM columns supported embankments constructed on top of multilayers of soft soils is required to overcome those aforementioned geotechnical difficulties.

Previous studies conducted by Consoli et al. (2009b) show that fibre reinforcement of cement treated soils in engineering practices has been proven very effective in improving the peak and post-peak shear strengths and the bearing capacity of soil foundations, while reducing the initial stiffness and transforming the brittle behaviour of cemented soils to become more ductile material. Furthermore, Consoli et al. (2009a) conducted another experimental program on the effect of relative density on the plate loading test on fibre reinforced sand, and reported that the load-settlement behaviour was significantly affected by the relative density and the fibre inclusion. Specifically, the inclusion of fibres increased the overall strength, stiffness and bearing capacity of sandy soils by a mechanism called the partial suppression of dilation and interaction among sand grains and fibres. Meanwhile, an increase in the relative density significantly reduced the settlement of reinforced soils, when compared to non-reinforced soils. From the experimental results, they also observed and reported that the fibre reinforced sand could be useful for embankments over soft soils because it had high potential to maintain its strength when undergoing large total and differential settlements, and changing to be a very ductile material.

Tang et al. (2007) investigated the strength and mechanical behaviour of short fibre reinforced cemented soils and also confirmed that the improvement of the compressive and shear strength, the axial strain at failure. They found the ductility of clayed soils reinforced with fibre inclusion was greater for a higher soil density. A review of soil reinforcement using randomly distributed fibres by Wang et al. (2017) indicated that adding such type of fibre reinforcement of soils effectively increases the engineering characteristics of reinforced soils. They include an increase in the shear and compressive strengths, California bearing capacity, wetting and drying cycles, freezing-thawing

behaviour, shrinkage and swelling behaviour, ductility (or brittleness reduction), resistance to liquefaction and desiccation cracking. In addition, Wang et al. (2017) reported that as compared to traditional geosynthetic reinforcement, which is normally placed in soils by different layers with a predetermined orientation, the addition of randomly distributed fibres into soils is more effective in maintaining the isotropic soil strength without presenting the potential of weak planes, which tend to develop along with the interfaces between soil and the geosynthetic layer. Therefore, employing fibre reinforcement of soils has increasingly become an extensive research interest in recent years in order to examine its application in various construction practices such as load transfer platform supported embankments.

In recent years, Okyay & Dias (2010) investigated the mechanical characteristics of lime/cement stabilised soils used as an LTP using numerical analysis of a unit cell model, considering the influences of pile spacing, shear strength, stiffness and the height of stabilised soil platform. The results of their numerical analysis revealed that the efficacy of the stabilised soil platform was significantly affected by the shear strength parameters; meanwhile the effect of LTP stiffness reduced with increasing the embankment loading. It is worth mentioning that the numerical investigation of Okyay & Dias (2010) was mainly based on a 2D axisymmetric unit cell model. Hence, it was unable to fully capture the effects of stabilised soils as an LTP on the actual stress transfer mechanism between columns in a group and surrounding soil, the differential settlements and the lateral movement in comparison with the full geometry model of embankment (Yapage & Liyanapathirana 2014). Based on a numerical modelling reported by Okyay & Dias (2010), Anggraini et al. (2015b) studied the performance of a lime-fibre reinforced soil platform and rigid piles supported embankment over soft soil by both physical and

numerical modelling using a 2D axisymmetric unit cell model. From the numerical results, they reported that the application of the lime-fibre reinforced soil platform was very effective in reducing the differential settlement, while relatively enhancing the efficacy and the bending performance of the reinforced soil platform. They also explained that thickness, the tensile stiffness, the shear strength properties of the reinforced soils platform had significant influences on the differential settlement and the efficacy of the embankment. Nonetheless, as a 2D unit cell model scaled down was adopted in their study, the influences of the lime-fibre reinforced LTP and the group effect of rigid pile interactions on the lateral deformation, the soil arching effect, the variations of excess pore water pressure were crucial but not taken into account in the physical and numerical modeling. Due to the above mentioned limitations, the efficacy of the lime-fibre reinforced LTP and piles supported embankment system investigated by Anggraini et al. (2015b) was relatively small (approx. 30%) as compared to the reported efficacy of the lime/cement stabilised LTP supported embankment with piles numerically analysed by Okyay & Dias (2010). Nguyen et al. (2016) conducted 2D numerical investigations on the failure pattern of columns supported embankment with cement stabilised slab as an LTP by taking the effect of the cement stabilised slab on the failure pattern of DCM columns into consideration. The results of finite element analysis revealed that the stabilised LTP thickness and compressive strength exhibited a notable influence on the embankment horizontal displacement. Nguyen et al. (2016) reported that the influences of the stabilised LTP on the embankment lateral displacement and the yield stress of columns subjected to the embankment load were greater for the higher compressive strength regardless of the LTP thickness. Dang et al. (2016a) conducted a 2D numerical assessment of FRLTP as a likely replacement of geosynthetics reinforced traditional

angular LTP in combination with piles supported highway embankments founded on soft grounds. By comparing the predicted results of numerical simulations with both the measured and predicted results, well reported in the literature, they concluded that the combined use of FRLTP and piles supported embankments experienced similar engineering characteristics compared to the geosynthetics reinforced traditional angular LTP supported embankment with piles. However, none of those investigations fully considered the influence of the lime/cement-fibre reinforced LTP (stabilised slab or mat) engineering properties on the performance of columns/piles supported embankments using a full geometry embankment model. As such, investigating the mechanical behaviour (e.g. the stress concentration ratio between columns within a group and surrounding soil with the embankment loading, the differential settlements, and the lateral displacement with depth) of columns supported embankment with a lime-fibre stabilised slab is crucial to be comprehensively considered based on the full geometry embankment model.

In this chapter, a novel ground modification technique utilising FRLTP (fibre reinforced load transfer platform) and DCM columns supported embankment constructed on top of multilayers of soft soils is proposed and investigated based on the finite element method incorporated in PLAXIS. Numerical simulations of three case studies using an equivalent 2D FEM model with proper modified parameters of structure and soil models have been adopted to examine the behaviour of floating DCM columns/piles supported embankment without or with FRLTP built over soft soils. First, a series of numerical analyses was carried out on the full geometry of DCM columns supported (CS) embankment reinforced without or with an FRLTP for various improvement depths of soft soils in a 2D plane strain condition to investigate the effectiveness of adding FRLTP into the CS

embankment system. Several embankment design parameters such as maximum and differential settlements, lateral displacement, load transfer mechanism between columns and foundation soils were analysed and examined. Subsequently, another extensive parametric study on the influential factors such as the FRLTP thickness, the elastic deformation modulus (Young's modulus), the shear strength parameters and the tensile strength of the FRLTP, has been conducted to comprehend the performance of the floating DCM columns combined with FRLTP supported embankment. Based on the numerical findings, comparisons and comprehensive discussion on the variations of the total and differential settlements, the stress transfer mechanism between DCM columns and foundation soils with the embankment height, and the lateral displacement with depth, were undertaken to have a further understanding of the embankment behaviour with FRLTP inclusion. The most influential factors of the FRLTP properties on the performance of the floating DCM columns embankment system are also highlighted and discussed in detail, which aim to enhance the design code for the floating DCM columns and FRLTP supported embankment found on multilayered soft soils.

6.2. CASE STUDY 1

A hypothetical construction of lime-fibre-reinforced earth platform to be used as FRLTP and DCM columns supported highway embankment over soft clay is considered for this numerical simulation. The embankment geometry is shown in Figure 6.1 representing the only right half of the domain of the embankment since the embankment is symmetrical along its centreline. As can be seen in the figure, the embankment is 20 m wide and 4 m high with a 1V:2H side slope. The embankment is made of sandy soil with a cohesion of 1 kPa, a friction angle of 30°, and an average unit weight (γ) of 20 kN/m^3. It is constructed

on a 3 m thick fill material overlaying an 11 m thick deposit of soft clay. This deposit soft clay overlies a 9 m thick medium stiff clay stratum followed by a 5 m thick stiff clay layer. The ground-water table is located at a depth of 1.5 m below the ground surface. A coir fibre-lime-soil layer having an effective cohesion and friction angle of 75 kPa and 42°, respectively, an average unit weight of 12.5 kN/m^3, a Poisson's ratio of 0.32, a Young's modulus of 125.8 MPa, and tensile strength of 240 kPa as adopted by Anggraini et al. (2015b) is employed to reinforce load transfer platform of 0.5 m that is placed on the top of DCM columns. Details of these soil layers are summarised in Table 6.1.

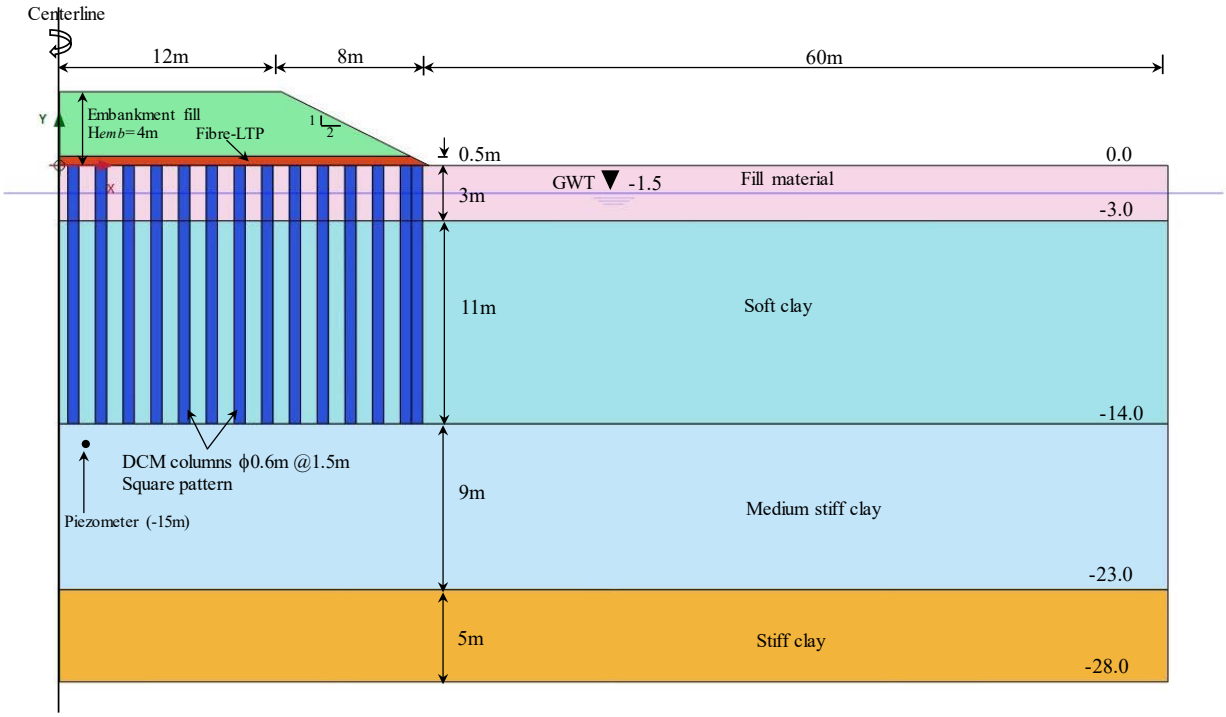

Figure 6.1 Cross section of the fibre reinforced load transfer platform and DCM columns supported embankment (Case study 1)

Table 6.1 Material properties of the embankment and subgrade soil layers

Parameters	Fill material	Soft clay	Medium stiff clay	Stiff clay	Fibre-lime-soil	Embankment fill	DCM columns
Depth (m)	0-3	3-14	14-23	23-28	-	-	-
Material model	MC*	SS*	SS	HS*	MC	MC	MC
γ (kN/m^3)	20	14	16	20	12.5	20	15
E (MPa)	30	-	-	-	125.8	20	80
ν	0.33	0.35	0.15	0.2	0.32	0.33	0.33
c' (kPa)	1	1	10	18	75	1	c_u=450
φ' (°)	32	23	25	25	42	30	0
λ	-	0.18	0.12	-	-	-	-
κ	-	0.04	0.06	-	-	-	-
E_{50}^{ref} (MPa)	-	-	-	50	-	-	-
E_{oed}^{ref} (MPa)	-	-	-	50	-	-	-
E_{ur}^{ref} (MPa)	-	-	-	150	-	-	-
m	-	-	-	1	-	-	-
OCR	-	1.5	2	2.5	-	-	-
k (m/day)	-	$5x10^{-4}$	$2.5x10^{-4}$	$2.5x10^{-4}$	-	-	$5x10^{-4}$
Material behaviour	drained	undrained	undrained	undrained	undrained	drained	undrained type B

*MC: Mohr-Coulomb; SS: Soft Soil; HS: Hardening Soil; OCR: over consolidation ratio

Deep cement mixing columns of 0.6 m diameter and 14 m length are assumed to extend to the medium stiff clay, which is stronger than the upper soft clay stratum. In this case, the DCM columns are considered as fixed type or end bearing columns supported embankment. The DCM columns are arranged in a square grid pattern with a 1.5 m centre-to-centre spacing, which results in an area replacement ratio of approximately 12.5% corresponding to these aforementioned geometric properties. An additional tangential DCM column is added at the embankment toe to increase the rigidity, while facilitating

the better resistance to lateral movement of soft foundation soil. It is assumed that the DCM columns are modeled as a linear elastic-perfectly plastic material using Mohr-Coulomb (MC) model with an average unit weight of 15 kN/m^3, a Poisson's ratio of 0.33, a Young's modulus of 80 MPa, an undrained shear strength of $s_u = c_u$ =450 kPa, and tensile strength of 130 kPa.

Table 6.2. Construction stages adopted in the FEM simulation procedure

Stage	Description	Thickness (m)	Duration (days)
1	Generation on the initial stresses (K_o-condition)	-	-
2	Installation of the DCM columns	-	-
3	Construction of a 0.5m high embankment	0.5	10
3	Construction of a 1.0m high embankment	0.5	45
4	Construction of a 1.5m high embankment	0.5	50
5	Construction of a 2.0m high embankment	0.5	30
6	Consolidation period of 30 days	-	30
7	Construction of a 2.5m high embankment	0.5	30
8	Consolidation period of 30 days	-	30
9	Construction of a 3.0m high embankment	0.5	30
10	Consolidation period of 30 days	-	30
11	Construction of a 3.5m high embankment	0.5	30
12	Consolidation period of 30 days	-	30
13	Construction of a 4.0m high embankment	0.5	30
14	Consolidation period of 2 years	-	730

The construction sequence of the embankment is assumed to be conducted in 8 lifts of 0.5 m increment including the placement of FRLTP. Each lift of embankment height increments is assumed to be completed in 30 days and followed by another 30 days

waiting period of consolidation to dissipate the excess pore water pressure induced as a result of the increase in embankment height. At the completion of embankment construction, the consolidation is left for 2 years. Table 6.2 exhibits the simulated construction sequence of the highway embankment adopted in this numerical analysis.

6.2.1. NUMERICAL MODELING

6.2.1.1. Finite element models and parameters

A two-dimensional plane strain model was built using commercial finite element software PLAXIS 2D version 2015 adopting the equivalent 2D numerical analysis method proposed by previous researchers (Chai et al. 2015; Tan et al. 2008; Yapage et al. 2014) to simulate the performance of the FRLTP and DCM columns supported highway embankment. The equivalent 2D model was selected because of less consuming analysis time, while generating results with reasonable accuracy. The DCM columns were simulated by continuous plane strain walls of 0.19 m thickness for the entire columns length of 14 m to maintain the same area of replacement ratio, taking into account the equivalent normal stiffness (EA) and bending rigidity (EI). Meanwhile, the centre-to-centre spacing between two adjacent walls in this numerical simulation was remained the same as the 1.5 m centre-to centre-spacing between two adjacent DCM columns.

With regard to the constitutive modeling, the DCM columns, as mentioned previously, were modeled using MC model (Huang & Han 2010; Liu & Rowe 2015; Jamsawang et al. 2016). Similarly, the FRLTP, embankment and fill material were simulated using a linear elastic-perfectly plastic model with MC failure criterion. The MC material model requires Young's modulus (E), Poisson's ratio (ν), the effective cohesion (c'), the angle of internal friction (φ'), and the dilation angle (ψ). Subsequently, the soft

soil and medium soft soil strata were represented by the soft soil (SS) model. The required parameters for the SS model include the compression index (λ), the swelling index (κ), the permeability coefficient (k), Young's modulus (E), Poisson's ratio (ν), and the shear strength properties (c', φ', ψ). It is assumed that the permeability coefficient of DCM columns was the same as surrounding soil in accordance with the experimental data reported by Horpibulsuk et al. (2007). Finally, the hardening soil (HS) was adopted to model the stiff clay layer, which requires the input parameters consisting of secant stiffness (E_{50}^{ref}) and unloading and reloading stiffness (E_{ur}^{ref}) derived from triaxial shear tests, tangential stiffness (E_{oed}^{ref}) obtained from primary loading of one-dimensional consolidation tests, power for stress-level dependency of stiffness (m), permeability coefficient (k), and shear strength properties (c', φ', ψ). Assuming all subgrade foundation soils is isotropic, so the horizontal and vertical permeability of the subgrade soils are equal. A summary of the constitutive model parameters is presented in Table 6.1.

Referring to Figure 6.2, the only right half of the embankment is modeled in this numerical simulation. The foundation soil was taken to 28 m depth from the ground surface overlying a stiff clay stratum. The horizontal length of the FEM model was taken to be 80 m, which was almost three times the half width of the embankment base to minimise the boundary effect. All these boundaries were considered to be impermeable, and pore fluid flow was permitted only from the surface.

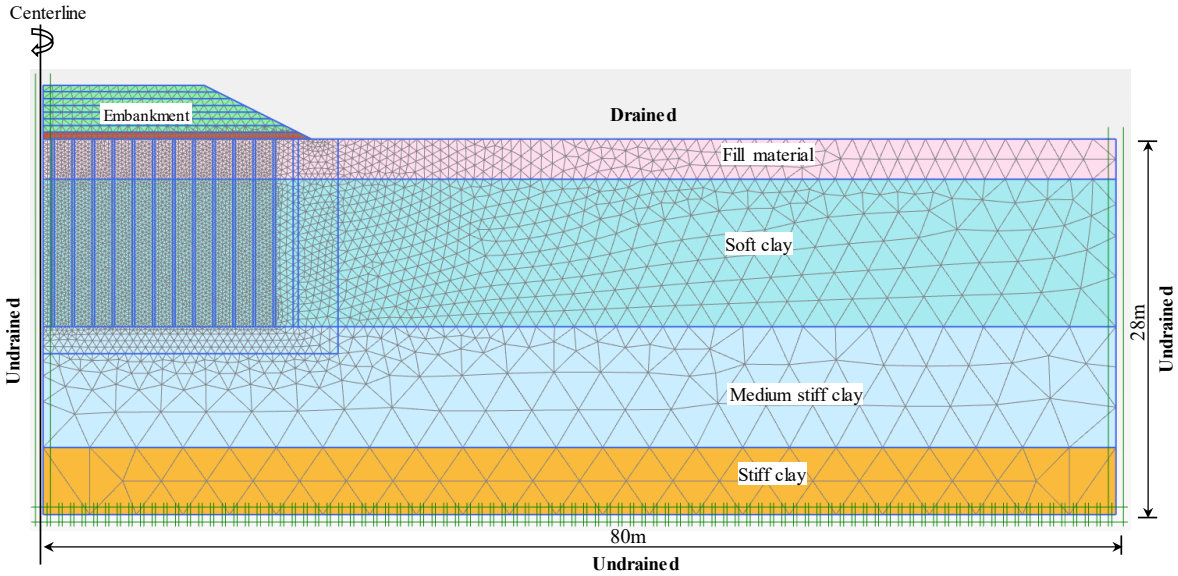

Figure 6.2 Mesh and boundary conditions for a 2D FEM analysis of embankment

In this analysis, for the 2D plane strain FEM model, the horizontal displacement at the left and right boundaries was not permitted but the vertical movement was allowed, whereas both the vertical and horizontal displacements were prevented at the bottom boundary. On one hand, due to the relatively high permeability, the embankment and fill material were assumed to behave in a drained condition. On the other hand, FRLTP, DCM columns, and other four foundation soils were assumed to act as undrained material. In this numerical analysis, fifteen-node triangular elements with excess pore water pressure degrees of freedom at all nodes were adopted to simulate the foundation soils, DCM columns and FRLTP, while fifteen nodes triangular elements without excess pore water pressure degrees of freedom at all nodes were applied to model the embankment and fill material.

6.2.1.2. Model validation

A case study of DCM columns supported highway embankment reported by Jamsawang et al. (2016) was used to validate the proposed modelling approach employed in this numerical investigation. Jamsawang et al. (2016) reported the field measurement of settlement and excess pore water pressure as well as the predicted 3D modelling results for the investigated highway embankment. The detailed simulation procedures for the embankment analysis can be found in Jamsawang et al. (2016). In this numerical simulation, a comparison was undertaken between these current prediction results and those measured and predicted results of Jamsawang et al. (2016) on the base of the settlement at the centreline of the embankment base and the excess pore water pressure with time at a depth of 15 m from the embankment base, which was very closed to the DCM column tips. Figure 6.3(a) indicates that the variation of settlement with time calculated from this equivalent 2D finite element modelling is compared with the measured and predicted settlements reported by Jamsawang et al. (2016). It can be observed that the results of this proposed modelling agree fairly well with those predicted and measured settlements of Jamsawang et al. (2016). Moreover, the variations of the excess pore water pressure with elapsed time obtained from this prediction as presented in Figure 6.3(b) exhibits a good agreement with the 3D modelling results of pore water pressure predicted by Jamsawang et al. (2016). Overall, the predicted results of this numerical analysis indicate that the equivalent 2D FEM model proposed in this study is suitable for simulating the DCM columns supported highway embankment over soft clay.

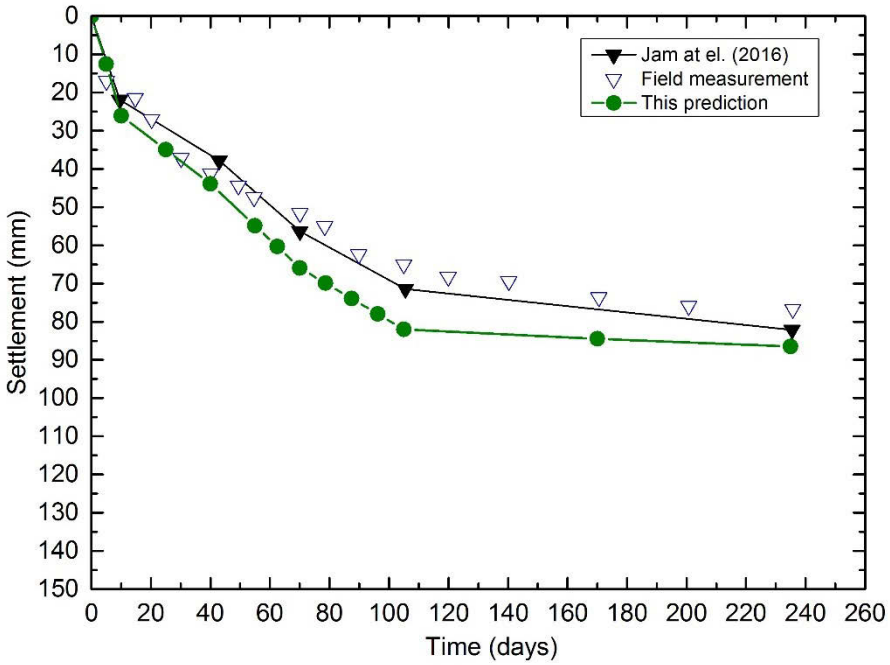

(a)

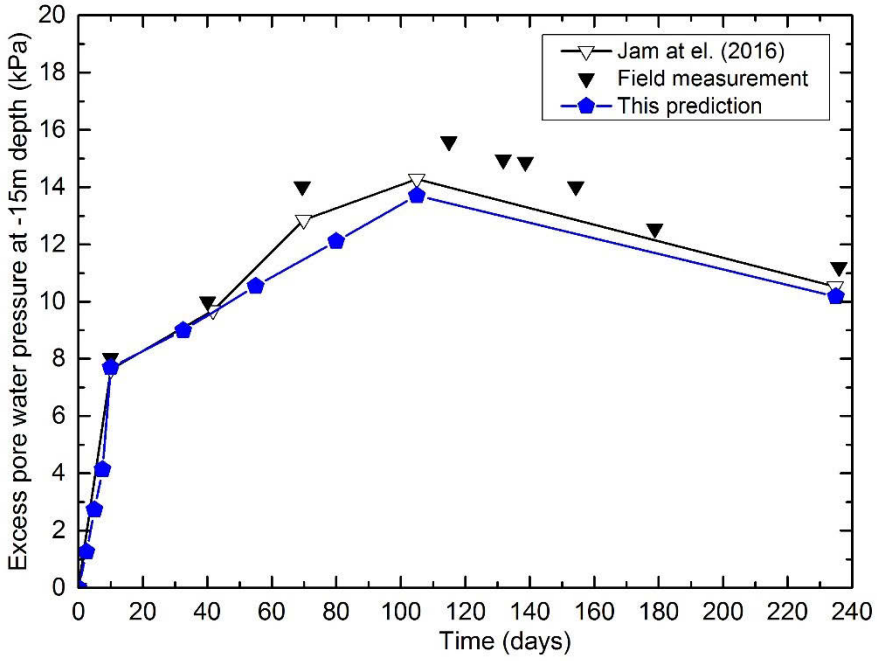

(b)

Figure 6.3 Comparison between field measurement and 2D numerical prediction: (a) settlement with time; (b) excess pore water pressure with time

6.2.2. ANALYSIS OF RESULTS AND DISCUSSION

6.2.2.1. Variation of settlement and excess pore water pressure with time

Figure 6.4a and 6.4b display the development of the surface settlement between two adjacent DCM columns and the variation of excess pore water pressure at a depth of 15 m below the embankment base between two adjacent DCM columns supported embankment without and with FRLTP, respectively. It can be seen in Figure 6.4a that the surface settlement of the highway embankment with time increased significantly during the first period of 375 days due to the increase of embankment height. This was followed by a gradual increase in the surface settlement up to two years after the completion (2 years post-construction) of the embankments owing to the evolution of consolidation with elapsed time. However, the surface settlement of the embankment with FRLTP was smaller than that of the embankment without FRLTP, which can clearly be observed throughout the investigated duration. The maximum post-construction settlement was about 420 mm for the embankments with FRLTP, which was relatively smaller as compared with the 450 mm corresponding settlement of the embankment without FRLTP. In addition, when compared with the embankment without FRLTP, the lower amount of excess pore water pressure generated by the embankment load versus time as presented in Figure 6.4b strongly accounted for the smaller settlement of the embankment with FRLTP. The reduced settlement and excess pore water pressure of the FRLTP and DCM columns supported embankment could be attributed to the inclusion of FRLTP facilitating the effective improvement of load transfer mechanism between DCM columns and foundation soft soil as well as improving the soil arching effect associated with the increases in embankment height.

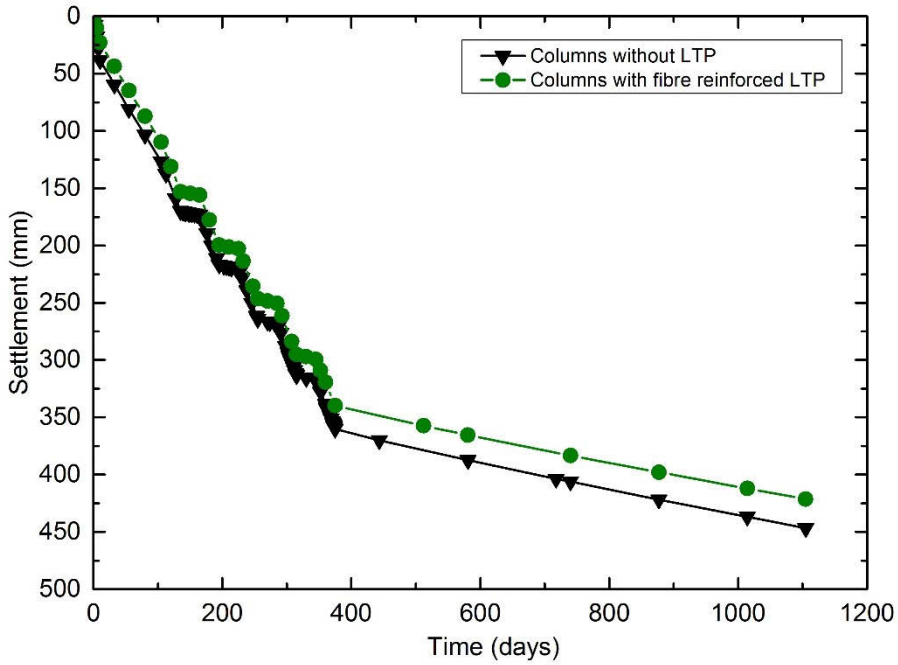

(a)

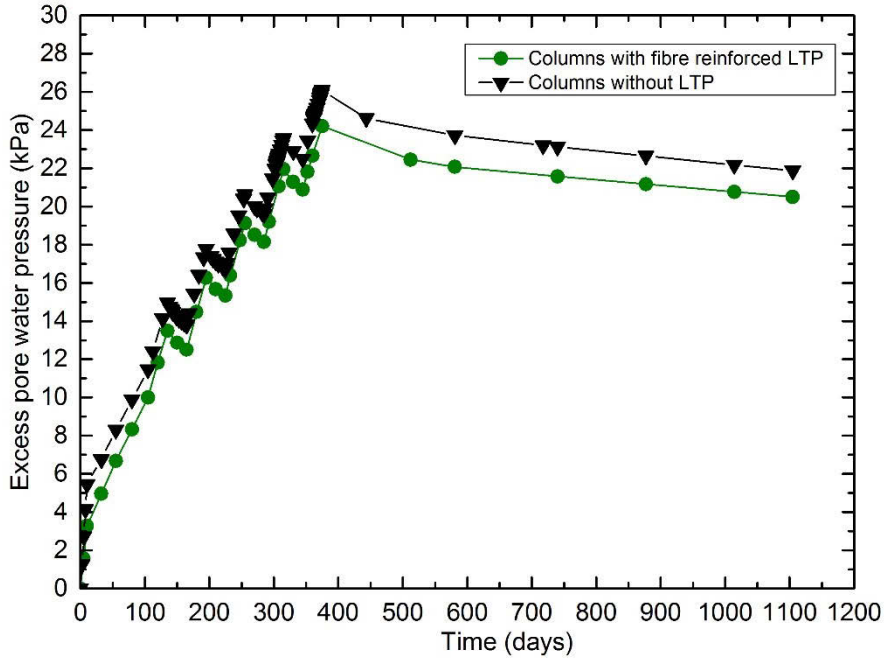

(b)

Figure 6.4 Development of settlement and excess pore water pressure with time: (a) settlement; (b) excess pore water pressure

6.2.2.2. Load transfer mechanism between columns and foundation soil

Figure 6.5a and 6.5b show the development of vertical effective stress on the DCM column head at the centre of the highway embankment and stress concentration ratio (SCR) with time in association with increasing embankment load, respectively. It can be noted that the SCR is defined as the ratio of vertical effective stress on the DCM columns head to vertical effective stress applied on foundation soil between two adjacent DCM columns. By referring to SCR, the quantity of embankment load transfer to the DCM columns can be estimated. As Figure 6.5a shows, the introduction of FRLTP into DCM columns supported embankment resulted in the remarkable increase in the vertical effective stress on the DCM column head induced by the embankment loading when compared with the embankment without FRLTP. In addition, the increase in the vertical effective stress on the DCM column head of the embankment with FRLTP was more noticeable with the higher increase in the embankment height. But then it remained almost constant during the two-year consolidation period after the completion of the embankment construction. The increased amount of vertical effective stress on columns head under the embankment with FRLTP was approximately 25% greater than that of the embankment without FRLTP. The similar trend can be observed in Figure 6.5b for the evolution of SCR versus elapsed time. To be more specific, the embankment with FRLTP yielded a considerably greater SCR value as compared with the embankment without FRLTP. For example, the SCR value of the embankment with FRLTP was roughly 3.7 at the end of embankment construction compared to the SCR of 2.45 for the embankment without FRLTP. The SCR improvement of the embankment with FRLTP was considered as a direct consequence of the reduction of embankment load transfer to the subgrade foundation soft clay.

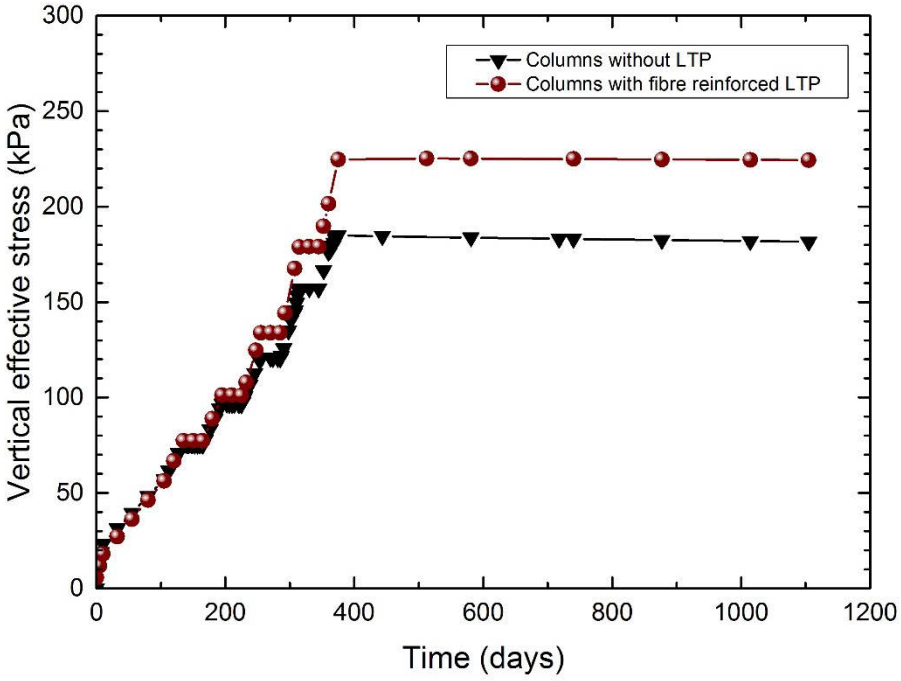

(a)

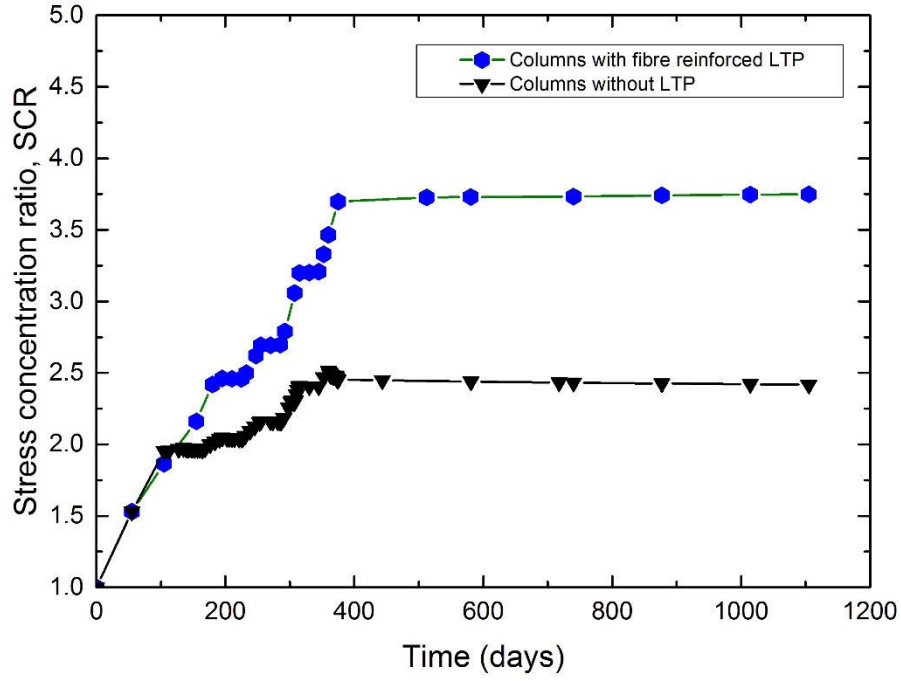

(b)

Figure 6.5 Development of (a) vertical effective stress on the top of DCM columns and (b) stress concentration ratio with time

6.2.2.3. Foundation surface settlement distance from centreline

The effect of the FRLTP on the total settlement of foundation surface obtained at a depth of 0.05 m with regard to horizontal distance from the centreline of the DCM columns supported embankment at the 2 years post-construction is illustrated in Figure 6.6 for further comparisons. It can obviously be seen that the larger settlement was observed for the embankment without FRLTP in the range of embankment width. This behaviour demonstrates that the FRLTP and DCM columns system can alleviate the total settlement of foundation surface effectively. However, the total surface settlement of the DCM column-embankment without or with FRLTP was almost the same beyond the embankment base. Moreover, the upward displacement (heave) was observed away from the embankment width. The maximum heave was obtained at approximately 26 m distance from the centreline of the embankment because of the uneven stress distribution of subgrade foundation soils.

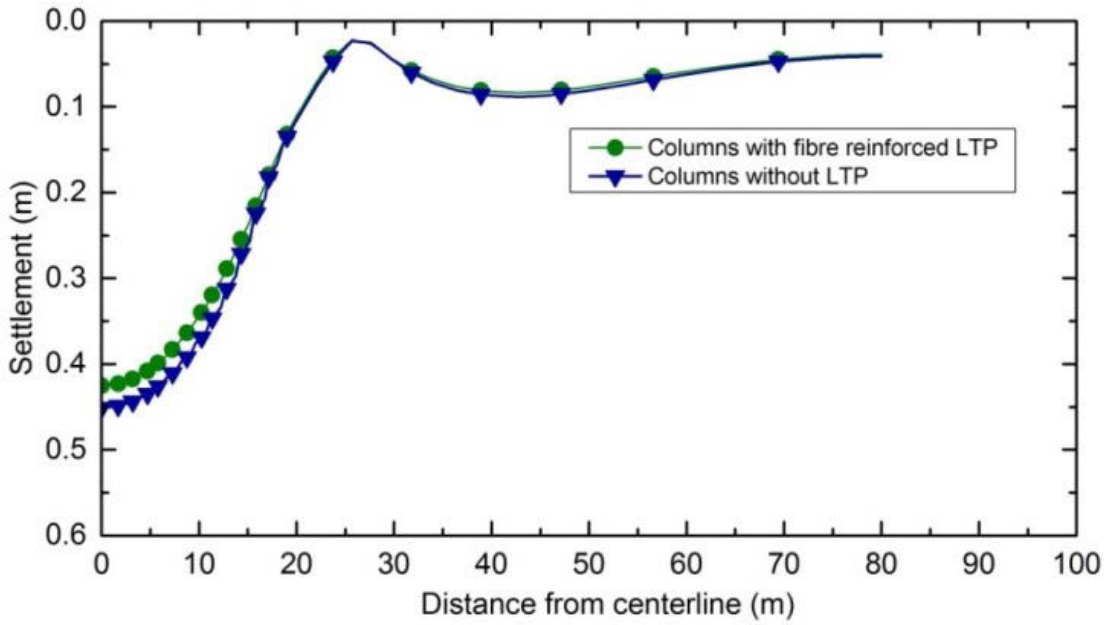

Figure 6.6 Variation of surface settlement versus horizontal distance from centerline

6.2.2.4. Development of settlement versus depth

Figure 6.7 exhibits the fluctuation of the total foundation settlement with different depth and different embankment heights under the centreline of the investigated embankment at the two years post-construction. Generally, the total settlement of foundation soil surface increased in between 200 mm and 450 mm with the increase in embankment height ranging from 2 m to 4 m. Meanwhile, the total settlement linearly decreased with depth downward to a certain level of 23 m and then followed by the significant drop of the total settlement to almost zero ranging from 23 m to 28 m depth. However, the total settlement of foundation soil with depth was more pronounced and larger for the DCM columns supported embankment without FRLTP, which can visibly be observed in any given embankment heights. This indicates the effectiveness of combined FRLTP with DCM columns supported embankment in improving the total settlement of foundation soil underneath the investigated embankment. The better improvement in the vertical deformation of the foundation soils could be due to the inclusion of FRLTP into the DCM column-embankment system, which enhanced the stiffness and arching effect of the entire embankment that facilitated more of the embankment load to be transferred to columns to the stronger and stiffer clay below.

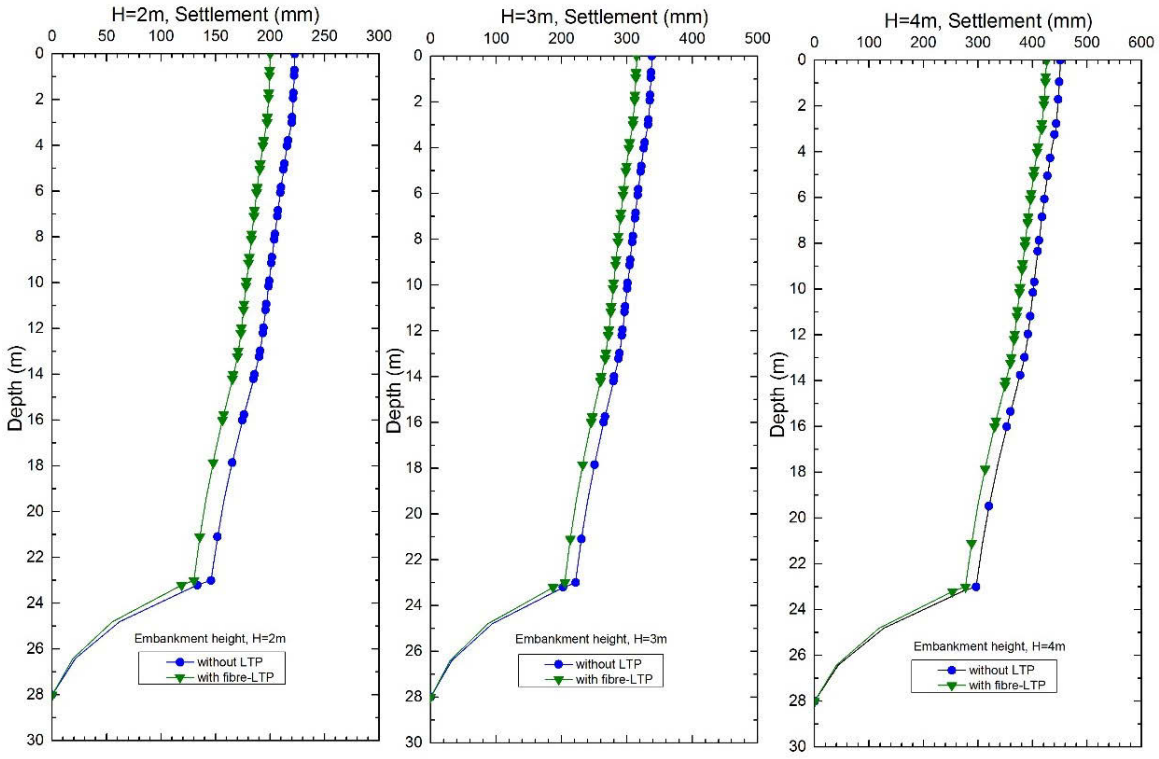

Figure 6.7 Development of settlement with depth for different embankment heights of H=2, 3 & 4m

6.3. CASE STUDY 2

Another hypothetical construction of FRLTP and DCM columns supported highway embankment over soft clay layers is considered in this numerical investigation. The embankment geometry is shown in Figure 6.8 representing the only right half of the domain of the embankment since the embankment is symmetrical along its centreline. As can be seen in Figure 6.8, the embankment is 20.8 m wide and 6 m high with a 1V:1.8H side slope. The embankment is made of good quality soil with a cohesion of 20 kPa, a friction angle of 35° and an average unit weight of 19 kN/m^3. It is constructed on a 1 m thick fill material as a surface layer overlaying an 11 m thick deposit of soft clay. This deposit of soft clay overlies a 3 m thick stiff clay stratum followed by a 15 m thick sand

layer. It should be noted that the stiff clay and sand layers were selected in this case study, as an attempt to simulate typical subsoil conditions in the field below embankments reported by many researchers (Chai et al. 2015; Chai et al. 2017). The ground-water table is located at a depth of 1 m below the ground surface. Details of these soil layers are summarised in Table 6.3 and 6.4. A fibre-lime-soil layer of 0.5 m is adopted in this numerical modelling and serves as an FRLTP, placed on the top of DCM columns improved soft soils.

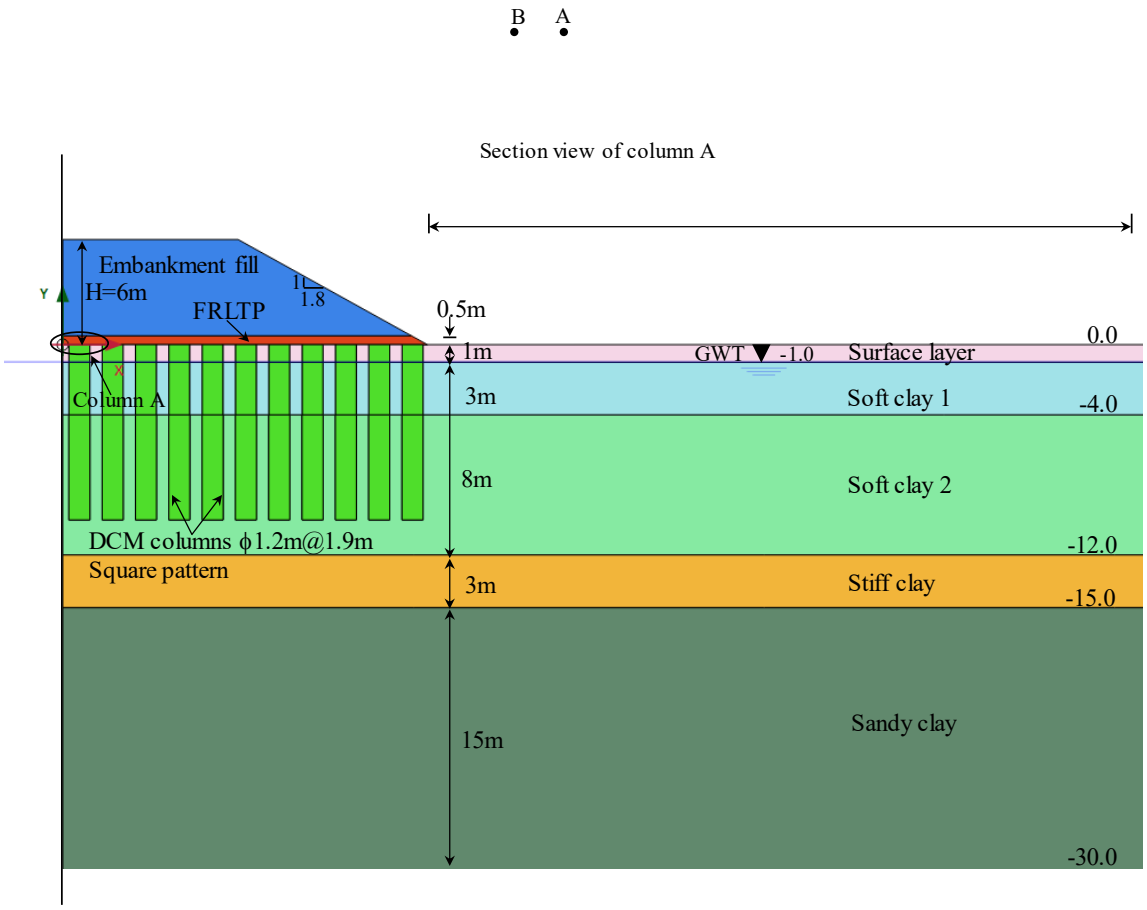

Figure 6.8 Cross-section of the FRLTP and DCM columns supported embankment (Case study 2)

To improve the engineering properties such as bearing capacity, shear strength, and compressibility of the thick soft soil strata of 12 m, deep cement mixing columns with 1.2 m diameter and 10 m length are used, which yield an improvement depth ratio (β) of roughly 83%. It can be noted that the improvement depth ratio (β) is defined as the depth of the DCM columns to the depth of soft soils from the embankment base to the top of a stiffer soil layer, which is the stiff clay in this numerical analysis. β=0 implies that soft soils are not improved with DCM columns, whereas β=1 means that soft soils are fully improved with DCM columns. With the improvement depth ratio of β=0.83 chosen in this case, the DCM columns are considered as floating columns supported embankment. In addition, the DCM columns are arranged in a square grid pattern with a centre-to-centre spacing of 1.9 m, which results in an area replacement ratio (α) of approximately 31% corresponding to those aforementioned geometric properties. It is noted that for a hypothetical embankment modelling, the DCM column parameters were selected to represent the typical soil-cement column properties from published data available in the literature. Therefore, the unconfined compressive strength ($q_{u)}$ was assumed to be 1000 kPa (Chai et al. 2015) and the 100 MPa young modulus (E) of DCM columns was determined using the correlation $E=100q_u$ (Yapage et al. 2014). The 150 kPa tensile strength of the DCM columns was considered to $0.15q_u$ (CDIT 2002; Jamsawang et al. 2016) and the undrained shear strength of 500 kPa of DCM columns was assumed to be $s_u= c_u =1/2q_u$ (Filz & Navin 2006). The average unit weight of 15 kN/m^3 was considered to be in a range of 3%-15% higher than that of soft soils (CDIT 2002) and a Poisson's ratio of 0.15 (Chai et al. 2015) was selected as of the typical properties of DCM columns.

Table 6.3. Material properties of subgrade soil layers used in Modified Cam Clay model

Parameters	Surface layer	Soft clay 1	Soft clay 2	Stiff clay
Depth (m)	0-1	1-4	4-12	12-15
Material model	MCC*	MCC	MCC	MCC
Unit weight, γ (kN/m^3)	16	13.4	14.3	18
Poisson's ratio, ν	0.15	0.15	0.15	0.15
Compression index, λ	0.25	0.87	0.43	0.12
Swelling index, κ	0.025	0.087	0.043	0.012
Over consolidation ratio, OCR	1.5	2.5	1.2	1.0
Slope of the critical state line, M	1.2	1.2	1.2	1.4
Initial void ratio, e_0	1.5	3.1	2.49	0.8
Vertical permeability coefficient, k_v (m/day)	6×10^{-4}	4.4×10^{-4}	4.6×10^{-4}	2.5×10^{-3}
Horizontal permeability coefficient, k_h (m/day)	9.1×10^{-4}	6.6×10^{-4}	6.9×10^{-4}	2.5×10^{-3}
Material behaviour	Undrained	Undrained	Undrained	Undrained

*MCC: Modified Cam Clay

Table 6.4. Material properties of the embankment, FRLTP, DCM columns and sandy clay strata adopted in Mohr-Coulomb model

Parameters	Sandy clay	Fibre-lime-soil	Embankment fill	DCM columns
Depth (m)	15-30	-	-	-
Material model	MC*	MC	MC	MC
Unit weight γ (kN/m^3)	19	12.5	19	15
Young's modulus, E (MPa)	20	125.8	1	100
Poisson's ratio, ν	0.10	0.32	0.40	0.15
Effective cohesion, c′ (kPa)	20	75	20	c_u=500
Effective friction angle, φ' (°)	35	42	35	0
Initial void ratio, e_0	0.7	-	-	-
Vertical permeability coefficient, k_v (m/day)	2.5×10^{-2}	-	-	4.6×10^{-4}
Horizontal permeability coefficient, k_h (m/day)	2.5×10^{-2}	-	-	4.6×10^{-4}
Material behaviour	Drained	Undrained	Drained	Undrained type B

*MC: Mohr-Coulomb model

The construction sequence of the embankment is assumed to be in 0.5-1 m lifts at an average filling rate of 0.06 m/day to a total height of 6 m including the FRLTP with a height of 0.5 m. Following the completion of embankment construction, the consolidation period is left for 2 years. Table 6.5 shows the simulated construction sequence of the highway embankment used in this numerical modelling.

Table 6.5. Construction stages in the FEM simulation of embankment construction procedure

Stage	Description	Thickness (m)	Duration (days)
1	Generation on the initial stresses (Ko-condition)	-	-
2	Installation of the DCM columns	-	-
3	Construction of a 0.5 m high embankment	0.5	8
4	Construction of a 1 m high embankment	0.5	8
5	Construction of a 2 m high embankment	1.0	16
6	Construction of a 3 m high embankment	1.0	16
7	Construction of a 4 m high embankment	1.0	16
8	Construction of a 5 m high embankment	1.0	16
9	Construction of a 6 m high embankment	1.0	20
10	Consolidation period of 2 years	-	730

6.3.1. NUMERICAL MODELING

6.3.1.1. Finite element models and parameters

A two-dimensional plane strain model was built using commercial finite element software PLAXIS 2D, adopting the equivalent 2D numerical analysis method proposed by previous researchers (Chai et al. 2015; Dang et al. 2016a; Dang et al. 2017a; Okyay &

Dias 2010; Tan et al. 2008) to simulate the performance of FRLTP and DCM columns supported highway embankment. The equivalent 2D model was selected because of less analysis time consumed, while generating results with reasonable accuracy. For instance, it was reported that the settlement results predicted by 2D modelling were up to 9% (Tan et al. 2008), around 10% (Chai et al. 2015), and roughly 15% (Ariyarathne et al. 2013), different with the corresponding predictions using 3D modelling. The DCM columns were simulated by continuous plane strain walls of 0.60 m thickness for the entire columns length of 10 m to maintain the same area of replacement ratio of approximately 31%, taking into account the equivalent normal stiffness (EA) as implemented and recommended for numerical simulations of columns supported embankments by many researchers (Chai et al. 2015; Dang et al. 2018; Yapage et al. 2015). Meanwhile, the centre to centre spacing between two adjacent walls in this numerical simulation was remained the same as the 1.9 m centre to centre spacing between two adjacent DCM columns.

Regarding the constitutive modelling, the DCM columns were modeled as a linear elastic-perfectly plastic material using Mohr-Coulomb (MC) model (Huang & Han 2010; Liu & Rowe 2015). Similarly, the FRLTP, embankment and fill material were simulated using a linear elastic-perfectly plastic model with MC failure criterion. The MC material model requires Young's modulus (E), Poisson's ratio (ν), the effective cohesion (c'), the angle of internal friction (φ'), the dilation angle (ψ) and the tensile strength. Subsequently, the soft soil layers were represented by Modified Cam Clay (MCC) model. The required parameters for the MCC model are slope of the virgin consolidation line (λ), the slope of swelling line (κ), the initial void ratio (e_0), the slope of the critical state line (M), and Poisson's ratio (ν). It is assumed that the values of horizontal permeability (k_h) are about

1.5 times the corresponding values of vertical permeability (k_v) of the subgrade soils, whereas the horizontal and vertical permeability of sand and DCM columns are equal. A summary of the constitutive model parameters is presented in Table 6.3 and 6.4. During consolidation process due to an increase in embankment load, the hydraulic permeability was changed attributable to the relationship between the void ratio change and the corresponding embankment load; therefore, the permeable change index $C_k = 0.5e_0$ was adopted in this investigation.

Referring to Figure 6.9, the only right half of the embankment is represented in this numerical simulation, since the embankment is symmetrical along its centreline. The foundation soil was taken to 30 m depth from the ground surface overlying a stiff clay stratum. The horizontal length of the FEM model was taken to be 80 m, which was almost three times the half width of the embankment base, in order to minimise the boundary effect. Both the left and right boundaries were considered to be impermeable, meanwhile pore fluid flow was permitted from both the ground surface and the bottom boundaries. The other boundary displacement was set similar to the case study 1.

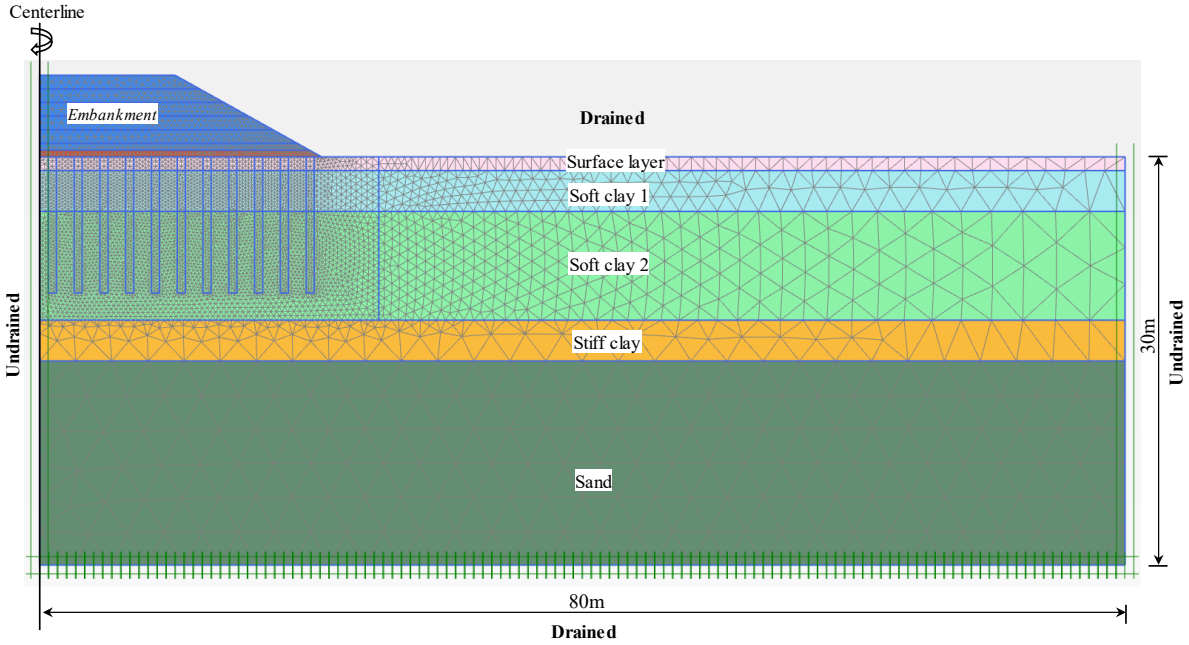

Figure 6.9 Mesh and boundary conditions for a 2D FEM analysis of embankment

6.3.1.2. Model validation

Prior to this numerical modelling, a case study of DCM columns supported highway embankment without reinforcement of load transfer platform reported by Chai et al. (2015) was used to validate the proposed modelling approach of a CS embankment investigated in this numerical simulation working reasonably. Through the field measurements and numerical predictions, Chai et al. (2015) reported the results of settlements with time at column head and foundation soil between two DCM columns under the centre of the CS highway embankment base. The detailed simulation procedure for the embankment analysis can be found in Chai et al. (2015). In this simulation, settlements between these predicted results and those measured and predicted outcomes by Chai et al. (2015) related to the ground surface settlement and the column settlement on top at the centreline of the embankment base during embankment construction and consolidation periods up to 559 days are presented in Figure 6.10 and then a related

thorough comparison was made. Observation of the predicted and measured settlements illustrated in Figure 6.10 notes that the development of the predicted settlements with time derived from this equivalent 2D finite element modelling of a CS embankment shows a good agreement with those measured settlements reported by Chai et al. (2015). Meanwhile, the 3D prediction by Chai et al. (2015) underestimated the settlements at both the column top and the ground surface between two adjacent columns as shown in Figure 6.10a and 6.10b. According to Chai et al. (2015), the influences of 3D simulation could produce the faster load reduction with depth as compared to 2D simulation and the higher order displacement shape function used for elements in the 2D analysis as compared to 3D analysis by PLAXIS could be possible reasons for the underestimated settlements by the 3D prediction. In general, the predicted results reveal that the equivalent 2D FEM model proposed in this numerical analysis is suitable for simulating the behaviour of DCM columns supported embankment built on multilayers of soft soils.

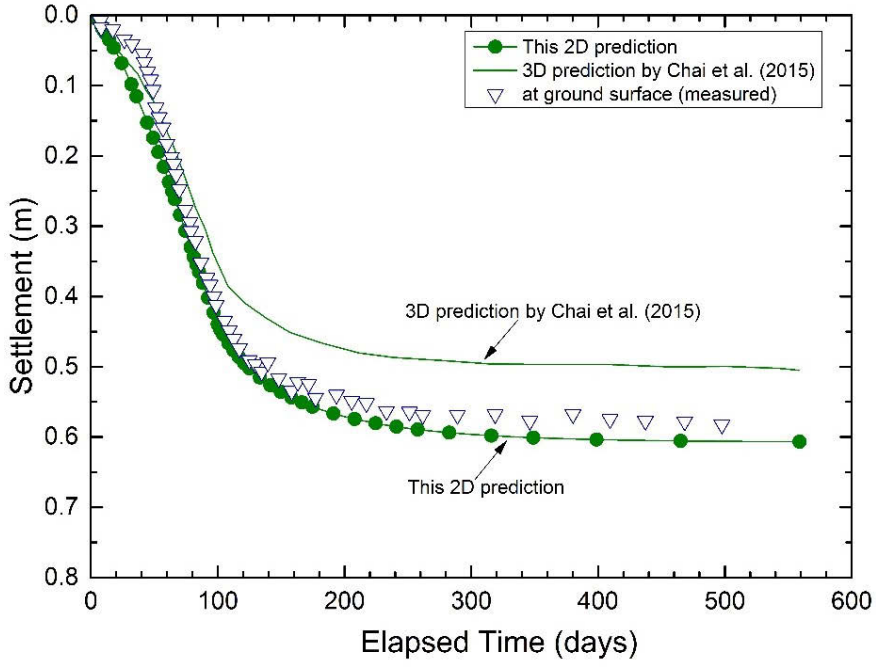

(a)

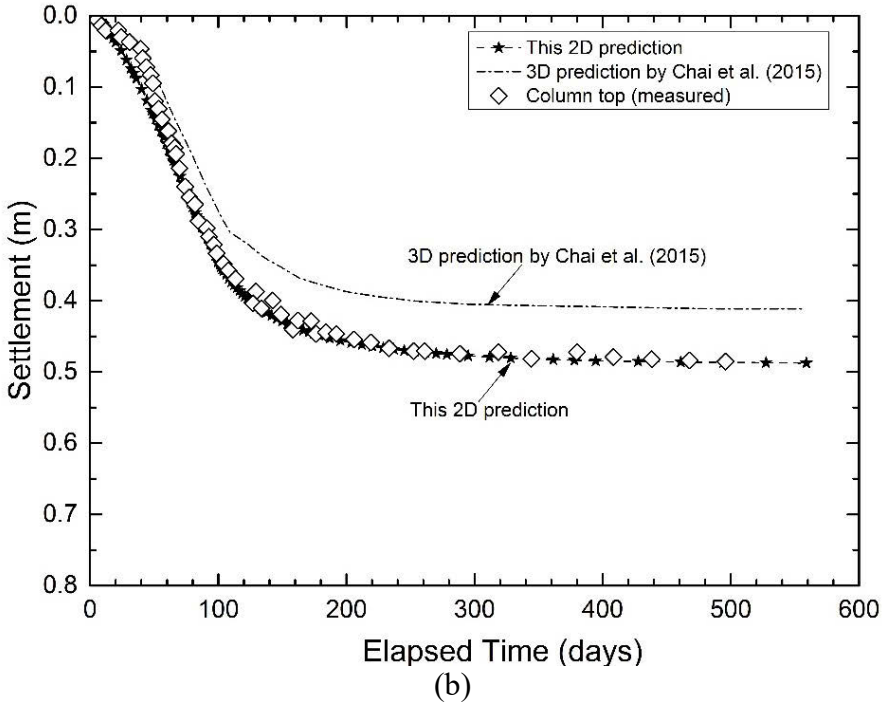

(b)

Figure 6.10 Comparison between field measurements, 2D and 3D numerical predictions of the embankment settlement at (a) ground surface and (b) column top with time

6.3.2. ANALYSIS OF RESULTS AND DISCUSSION

6.3.2.1. Effect of the different improvement depths on the embankment behaviour

6.3.2.1.1. Variation of total and differential settlements for different improvement depths

Figure 6.11a displays the development of the ground surface settlement versus elapsed time between two adjacent DCM columns under the centre of the embankment without or with FRLTP for different improvement depth ratios (β). It can be noted that the improvement depth ratio (β) is defined as the ratio of DCM column length to soft soil thickness. To investigate the effect of floating DCM columns on the total and differential settlements of embankment, the columns length was varied from β=0.5 to β=1. As plotted in Figure 6.11a, the time-dependent surface settlement increased significantly during the first period of 100 days due to the increase in embankment load. This phenomenon was

followed by a gradual increase in the surface settlement up to two years after the completion of the embankment construction owing to the evolution of consolidation with time. Moreover, the significant reduction of surface settlement with increasing the improvement depth ratio from β=0.5 to β=1 was clearly observed in Figure 6.11a. To be more specific, the significant surface settlement of approximately 1.47 m as numerically predicted for the improvement depth ratio of β=0.5 decreased to a relatively small value of 0.35 m with the increase of β value up to 1 (for the end-bearing columns). The predicted settlement results also reveal that the increase in DCM columns length not only decreased the final surface settlement but also resulted in the improvement of consolidation process of soft soil strata. For example, the surface settlement in case of the end-bearing columns (β=1) reached its final settlement after approximately 200 days of elapsed time, whereas the final surface settlement in case of the floating DCM columns (β=0.5) was not reached after the 830 days of investigation period, displaying a trend of continuous settlement.

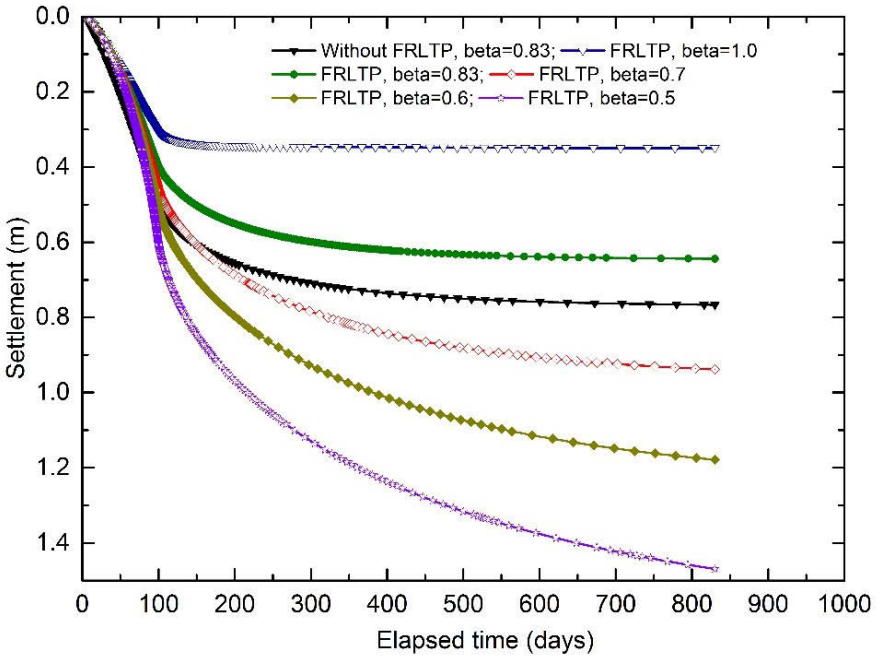

(a)

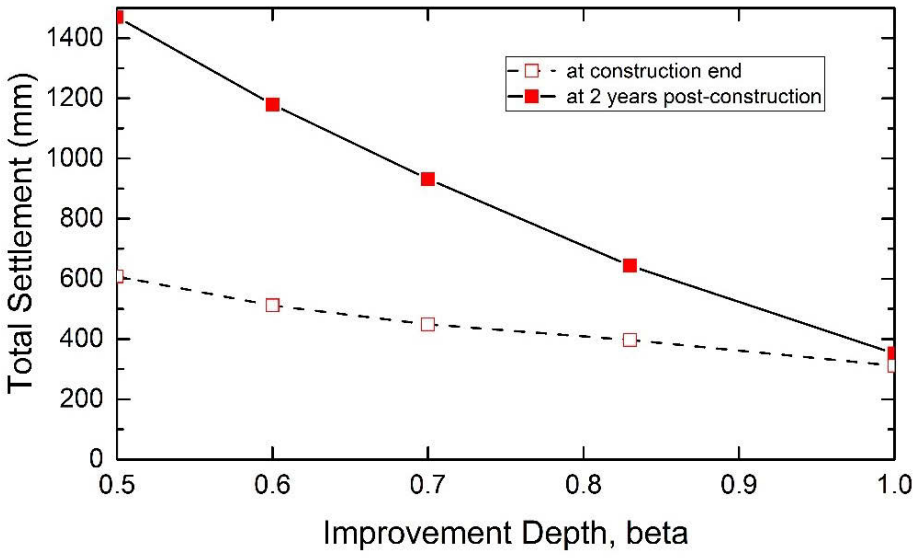

(b)

Figure 6.11 Development of (a) total settlement with time and (b) total settlement at embankment construction completion and 2 years post-construction for different improvement depth ratios (β)

It is also important to note that the surface settlement in the case of floating DCM columns (β=0.83) supported embankment without or with FRLTP was visually depicted in Figure 6.11a for evaluation of the effect of FRLTP inclusion on the total settlement of the entirely DCM columns-embankment system. It can apparently be seen from this figure that the surface settlement of the embankment without FRLTP was definitely larger than that of the embankment with FRLTP, which can clearly be observed throughout the 830 days of investigation period. The maximum settlement of the embankments with FRLTP at the end of the 2 years consolidation period was about 0.64 m, which was relatively smaller than the 0.77 m settlement of the embankment without FRLTP. This numerical finding indicates that the effectiveness of FRLTP inclusion in minimising the final surface settlement of the entire DCM columns-embankment system.

The effect of different improvement depth ratios (β) on the total settlement at the embankment base centre is shown in Figure 6.11b. It is observed that the total settlement significantly and linearly decreased by approximately 76% for the post-construction of embankment case as the improvement depth ratio increased. Figure 6.11b also shows that the consolidation time has a great influence on the changes in the maximum total settlement of the embankment with FRLTP when the improvement depth ratio (β) increases from 0.5 to 1. Approximately 60% difference in the maximum total settlement between the construction completion and the 2 years post-construction can be observed in Figure 6.11b when the column length is short (β=0.5), but it becomes smaller and approaches a comparable value when the column length increases to 12 m (β=1). The improvement in the time-dependent total settlement when the improvement depth ratio increased could be due to an increase in the columns length approaching to a stiffer layer. As expected, in this condition, most of the embankment load transfer to the stiffer clay soil. Therefore, the effects of the time-dependent settlement of the underlying soft soils due to the embankment load become negligible.

The variation of differential settlement under the centre of the embankment base without or with FRLTP inclusion along with embankment height for different improvement depth ratios (β) can be observed in Figure 6.12. Similar to the trend of surface settlement of the embankment with FRLTP, the differential settlement on the ground surface, defined as the settlement difference between the top of DCM columns (see point A in Figure 6.8) and the ground surface between two adjacent DCM columns (see point B in Figure 6.8), increased with an increase in the embankment height, whereas decreased with increasing the improvement depth ratio (β) from 0.5 to 1. By comparing

with the embankment with FRLTP for the same improvement depth ratio (β=0.83), the increase in differential settlement with the embankment height was more noticeable for the embankment without FRLTP as presented in Figure 6.12.

On one hand, the differential settlement of the embankment without FRLTP linearly increased with embankment height from 0.5 m to 6 m, which resulted in the accumulated differential settlement of approximately 125 mm at the end of embankment construction. On the other hand, as evident in Figure 6.12, the differential settlement of the embankment with FRLTP showed a nonlinear increase with increasing the embankment height and it seemly started to appear when embankment height increased from only 3 m to 6 m. The accumulated differential settlement of the embankment with FRLTP was about 33 mm at the end of embankment construction, which led to about 73% reduction of the differential settlement compared with that of the embankment without FRLTP. Furthermore, in the cases of the embankment with FRLTP for different improvement depths, a significant reduction of the maximum differential settlement was observed in a wide range between 52% and 80% in comparison with that of the embankment without FRLTP when the β value increased from 0.5 to 1. It can be concluded that the FRLTP inclusion showed a significant improvement in reducing the differential settlement of the DCM columns–embankment system. The improvement in the differential settlement could be attributed to the enhancement of soil arching effect above the top of DCM columns facilitated by the FRLTP inclusion as visibly illustrated in Figure 6.13.

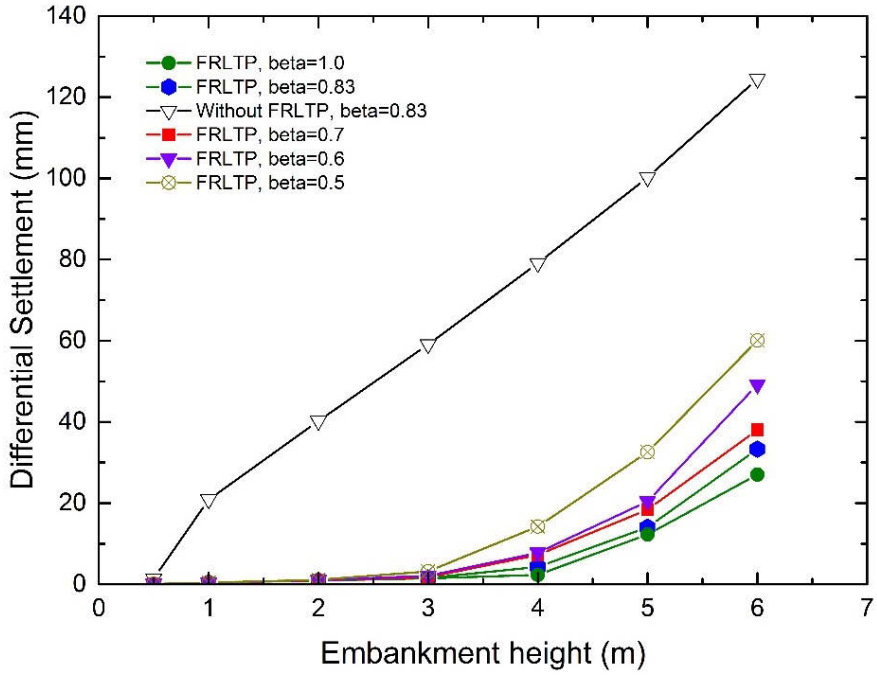

Figure 6.12 Variation of differential settlement versus embankment height for different improvement depth ratios (β)

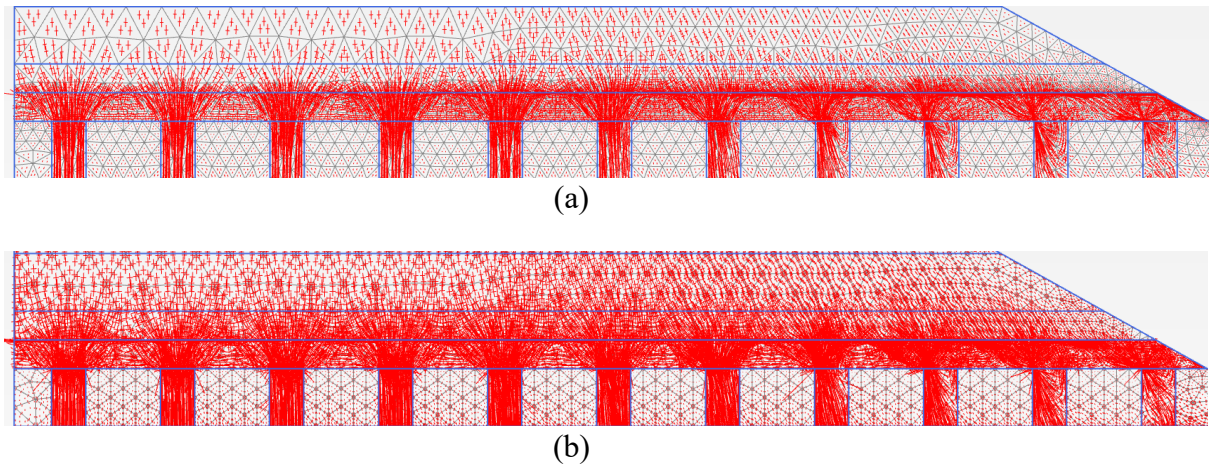

Figure 6.13 Effective principle stresses of the embankment with FRLTP at the construction end for the improvement depth ratios of (a) β=0.5 and (b) β=0.83

6.3.2.1.2. Load transfer mechanism between columns and foundation soil for different improvement depths

Han & Gabr (2002) used the load transfer mechanism proposed by Terzaghi (1943) to examine the proportion of the embankment load transfer between columns and surrounding foundation soil, taking into consideration of the soil arching effect. According to Terzaghi (1943), with an increase in embankment fill causing embankment load increase, the embankment fill between columns tends to move downward due to the presence of soft foundation soil. The fill movement is partially resisted by its shear strength above the columns. Such shear strength resistance reduces the load from embankment to be transferred to soft foundation soil but increases the embankment load imposed on columns by way of the soil arching effect. The ratio of soil arching effect in embankment fill is defined in Equation (1) proposed by Terzaghi (1943) as follows.

$$\rho = \frac{P_b}{\gamma H + q} \tag{6.1}$$

where ρ is the soil arching ratio; $\rho=0$ implies the complete soil arching, whereas $\rho=1$ means no soil arching; P_b represents the amount of earth pressure on the surface of foundation soil between columns; γ represents the unit weight of embankment fill; H is the height of embankment; and q represents the uniform surcharge on the embankment if applicable.

According to Liu et al. (2007), the soil arching effect in embankment results in more of the embankment load transfer to columns from soft foundation soil. The load transfer between columns and surrounding soil can be estimated by a stress concentration ratio (SCR) defined in Equation (2) as the ratio of vertical effective stress on the DCM

columns head (σ_c) to vertical effective stress applied to foundation soil (σ_s) between two adjacent DCM columns.

$$\text{SCR} = \frac{\sigma_c}{\sigma_s} \tag{6.2}$$

Figure 6.14 depicts the fluctuation of the stress concentration ratio on the DCM column head at the embankment centre in association with an increase in the embankment height for different improvement depth ratios (β). As illustrated in Figure 6.14, the SCR generally increased as the embankment height increased to a certain high value and then it decreased with higher increase in the embankment height in the cases of the embankment with FRLTP for different β values. Except for the embankment without FRLTP, that showed a minor increase in the SCR with further increase in the embankment height up to 6 m. For example, the SCR value of the embankment without FRLTP significantly increased from approximately 2.5 to 12.5 with a relatively small increase in the embankment height from 0.5 m to 2 m. This was followed by a slight increase from 12.5 to a certain value of 14.7 with a further increase in the embankment height up to 6 m. However, for the embankment reinforced with an FRLTP as plotted in Figure 6.14, the increase in embankment height from 0.5 m to 4 m resulted in the substantial increase in the SCR value ranging from approximately 5 to reach a peak between 57 and 100 for the improvement depth ratio (β) between 0.5 and 1, respectively. As observed in Figure 6.14, the additional increase in the embankment height up to 6 m gave rise to the corresponding decrease in the SCR value to a certainly high level between 20 and 58.

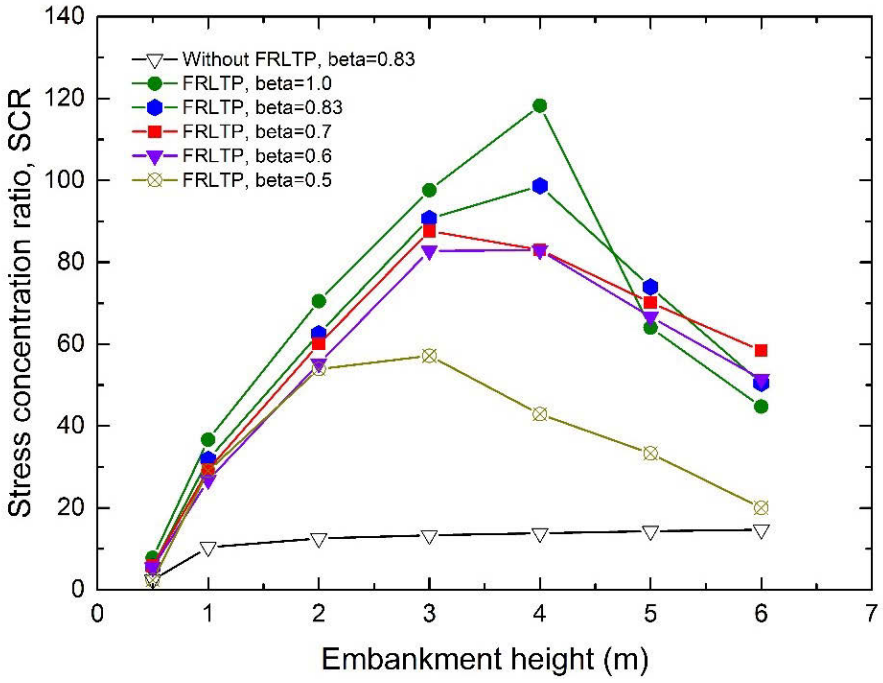

Figure 6.14 Variation of SCR with embankment height for different improvement depth ratios (β)

In comparison with the embankment without FRLTP, the peak SCR value of the embankment with FRLTP was about 3.9-7.2 times greater as the β value increased between 0.5 and 1. A significant improvement in SCR (or the increase in the soil arching effect) of the embankment with FRLTP to a certain height of the embankment, regardless of the improvement depth ratios (β), was considered as a direct consequence of reduction of the embankment load transfer to the foundation soil facilitated by the FRLTP inclusion. The high shear strength of lime-fibre reinforced load transfer platform contributed to the effective improvement in the SCR as recently reported by researchers (Dang et al. 2016a; Okyay & Dias 2010). However, a further increase in the embankment height resulted in a decrease in the SCR value after reaching a peak, which might be due to the over-bearing capacity of the DCM columns. In that circumstance, the additional increase in the

embankment height would decrease the arching effect of the embankment, resulting in more load transferred to the foundation soil between columns. Thus, a decrease in the SCR value seems to signal the start of an increase in the differential settlement of the DCM columns supported embankment, as supporting evidence can be found in Figure 6.12 and 6.14.

6.3.2.1.3. Variation of lateral displacement with depth for different improvement depths

Figure 6.15a and 6.15b display the lateral displacement with depth of the DCM column under the embankment toe. It can obviously be seen from these figures that the lateral displacement decreased with an increase in the improvement depth ratio (β) from 0.5 to 1 regardless of the construction end or the 2 years post-construction. However, as observed in Figure 6.15a and 6.15b, the lateral displacement of DCM column tip increased significantly during the 2 year consolidation period, except for the case of the high improvement depth ratio between β=0.83 and β=1 for the end-bearing columns showing that the lateral displacement at 2 years post-construction remained almost constant. The increase in the lateral displacement is primarily resulted from an increase in the height of the embankment fill that induces lateral spreading forces and lateral earth pressures acting on the DCM columns. An excessive increase in the lateral deformation can cause sliding, bending and tensile failure of the embankment. Thus, it is essential to prevent the excessive lateral deformation causing such aforementioned types of failure of the CS embankment by properly determining an optimum improvement depth ratio. In this investigation, the short floating DCM columns with β=0.5-0.7 revealed the remarkable lateral displacement at both ends of the DCM column, especially in the column tip. Hence, it could be unacceptable for the CS embankment design in terms of

stability. However, as illustrated in Figure 6.16, with increasing the improvement depth ratio to β=0.7 or beyond, the lateral displacement decreased significantly and could be accepted. This is consistent with the early research (Jamsawang et al. 2016) reporting that the improvement depth ratio of β=0.7 might be an optimal value, required for the stability of a floating DCM columns-supported embankment over soft soils. The improvement of the lateral deformation along with the increase in the columns length could be attributed to approaching the fixity condition of the DCM columns into the stiffer layer below. In other words, the longer columns facilitate the better-restrained condition in support of the embankment loading and consequently minimise the lateral displacement.

In addition, the lateral movement of the DCM column under the toe of the embankment without or with FRLTP was depicted in Figure 6.15a and 6.15b for the completion of the embankment construction and the 2 years post-construction cases, respectively, for comparison purposes. As observed in Figure 6.15a and 6.15b, the introduction of the FRLTP into the CS embankment system reduced significantly the lateral movement of the column head compared to that of the embankment without FRLTP for the same improvement depth ratio of β=0.83. This improvement reconfirms that the FRLTP inclusion is highly effective in alleviating the lateral movement of the embankment, resulting in the enhancement of the embankment stability. The improvement in the lateral displacement of the embankment with FRLTP could be due to the high shear strength and tensile strength contributed from the lime-fibre reinforced platform.

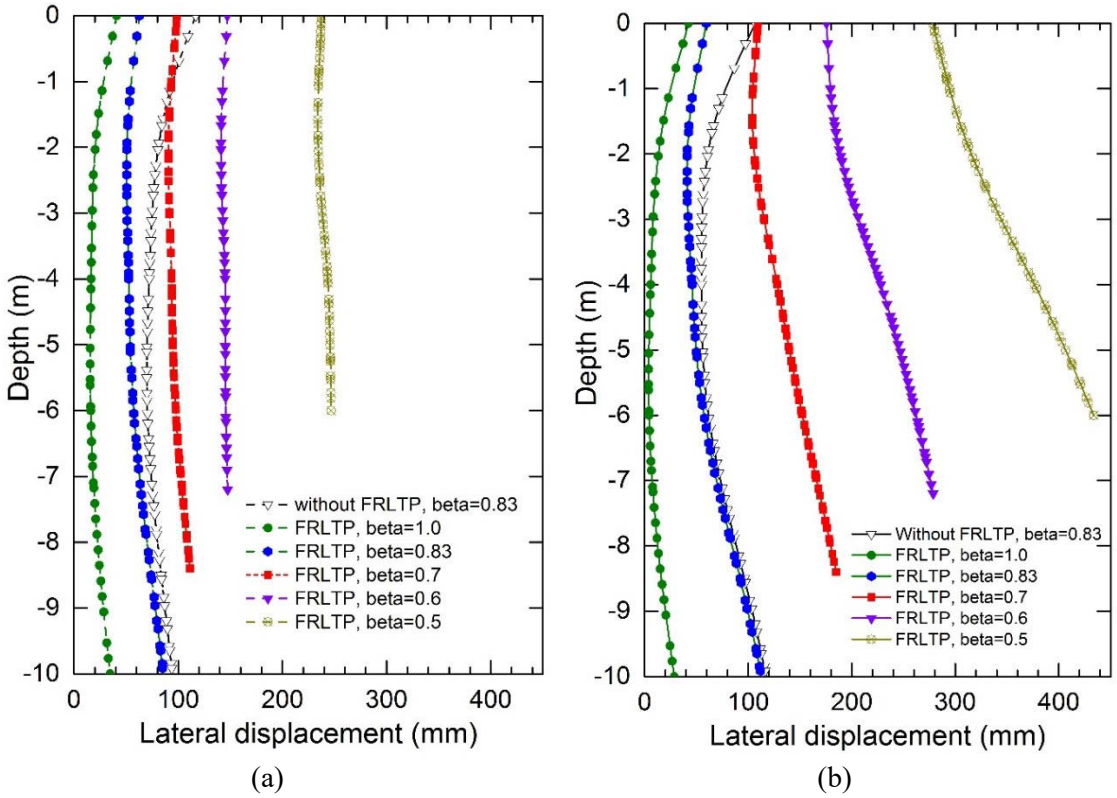

Figure 6.15 Variation of lateral displacement with depth for different improvement depth ratios (β) at (a) completion of embankment construction and (b) 2 years post-construction

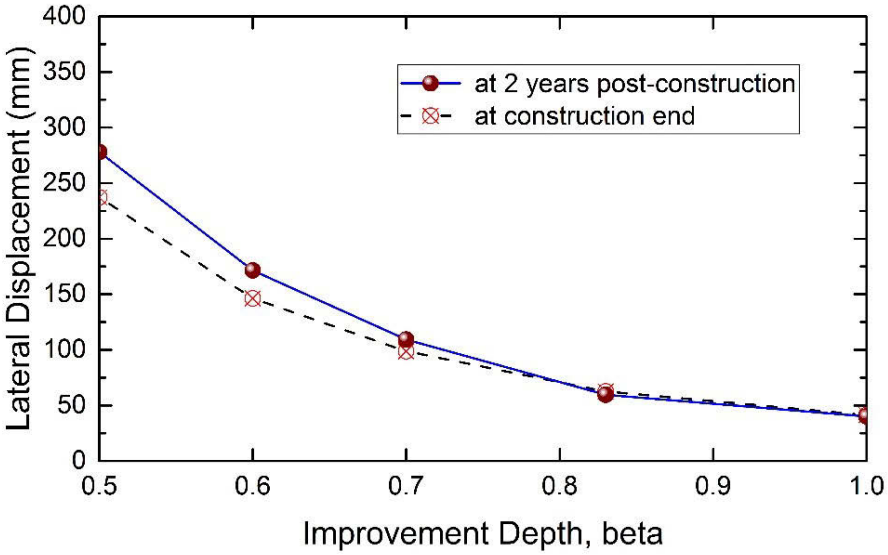

Figure 6.16 Variation of lateral displacement of the embankment toe for different improvement depth ratio at embankment construction completion and 2 years post-construction

6.3.2.2. Effect of the FRLTP thickness (H) on the embankment behaviour

6.3.2.2.1. Variation of the total and differential settlements for various FRLTP thickness

The thickness of the FRLTP plays an essential role in facilitating the embankment load to be transferred effectively from soft foundation soil to the DCM columns and reducing the possibility of the FRLTP punching failure induced by column heads. The FRLTP thickness (H) was changed from 0 m for the embankment without FRLTP to 3 m for the embankment reinforced with an FRLPT to investigate the effect of various FRLTP thickness on the total and differential settlements of the floating DCM columns supported embankment. As Figure 6.17 shows, the ground surface settlement at the middle of two adjacent DCM columns under the embankment centre evolved with elapsed time, for various FRLTP thicknesses (H). As visually illustrated in Figure 6.17, the time-dependent ground surface settlement was found to increase significantly during the first period of 100 days because of the embankment loading. That behaviour was followed by a gradual increase in the surface settlement up to two years after the completion of the embankment construction due to the evolution of consolidation with elapsed time. However, it is observed in Figure 6.17 that there was a significant reduction in the ground surface settlement when the FRLTP thickness increased from H=0 m to H=3 m. For example, the surface settlements of approximately 0.52 m were numerically calculated for the embankment with an FRLTP thickness of H=3 m at the end of the 2 years post-construction period, resulting in the considerable reduction of approximately 32% when compared with the total settlement of the embankment without FRLTP (the FRLTP thickness of H=0 m). This phenomenon reveals the benefits of the FRLTP inclusion in minimising the final surface settlement of the entire CS embankment system. In addition, the calculated settlement results exhibit that the embankment with FRLTP not only

reduced the final surface settlement but also accelerated the consolidation process of soft soil layers. For instance, as depicted in Figure 6.17, the maximum total settlement at the ground surface of the embankment with a 0.5 m FRLTP thickness reached 95% of its total settlement after 335 days. Meanwhile, the corresponding total settlement of the embankment without FRLTP was numerically calculated after approximately 385 days. This reconfirms the FRLTP inclusion into the embankment was certainly effective in accelerating the consolidation process of underlying soft soils subjected to the embankment loading. However, the improvement in the consolidation process of soft soils with further increase in the FRLTP thickness up to H=3 m was found to be insignificant.

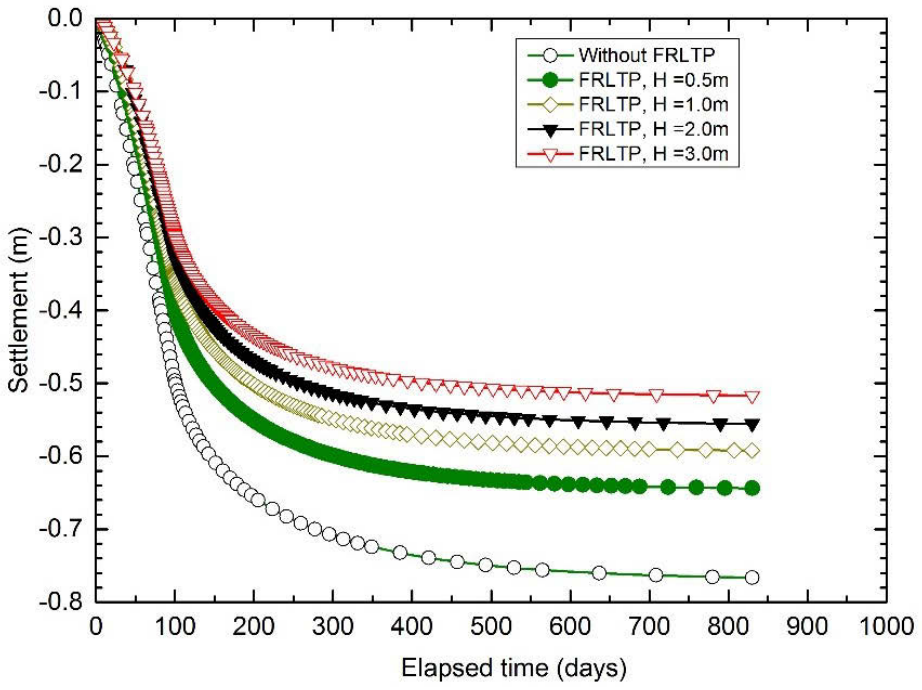

Figure 6.17 Variation of total settlement with time for different FRLTP thickness

Figure 6.18 illustrates the changes of the differential settlement at the ground surface under the embankment base centre with respect to the embankment height for different FRLTP thickness (H). It is noted that the differential settlement is defined as the maximum settlement difference between the top of DCM columns and surrounding soils at the embankment base centre. As Figure 6.18 shows, the differential settlement at the ground surface during the embankment construction increased as the height of the embankment fill increased, but it was found to decrease greatly as the thickness of FRLTP increased from H=0 m (the embankment without FRLTP) to H=3 m. For example, the differential settlement of the embankment without FRLTP was observed to linearly increase with a rapid rate corresponding to the increase in the embankment height ranging from 0.5 m to 6 m as shown in Figure 6.18. However, when the embankment was reinforced with an FRLTP thickness of H=0.5 m, increasing the embankment height up to 3 m corresponded to insignificant (almost zero) development of the differential settlement. An additional increase in the embankment height greater than 3 m was found to increase the differential settlement with a rapid rate to a certain value of 33 mm. This means that approximately 73% reduction of the differential settlement at the construction end was calculated for the embankment with an FRLTP thickness of 0.5 m compared with the embankment without FLRP (H=0 m). The reduced differential settlement confirms the highly positive effect of the FRLTP inclusion on the embankment behaviour. Moreover, inspection of Figure 6.18 reveals that as a further increase in the FRLTP thickness ranging between H=1 m and H=3 m, the maximum differential settlement during the embankment construction was noted to be negligible (almost null) in the investigated range of the embankment height. Therefore, it is worth mentioning that the FRLTP thickness was found to have a significant effect on the differential settlement. The

effective contribution from the high shear strength and the high stiffness of the FRLTP inclusion could be responsible for the differential settlement under the embankment base greatly improved by a thicker FRLTP. Therefore, as the FRLTP becomes thicker, the greater shear strength and stiffness of the FRLTP would be, it effectively enables more of the embankment load to be transferred from soft foundation soil to DCM columns. Consequently, the thicker FRLTP results in less differential settlement and even can completely control the zero differential settlement during the embankment construction by using an FRLLP with a thickness of 1 m or beyond.

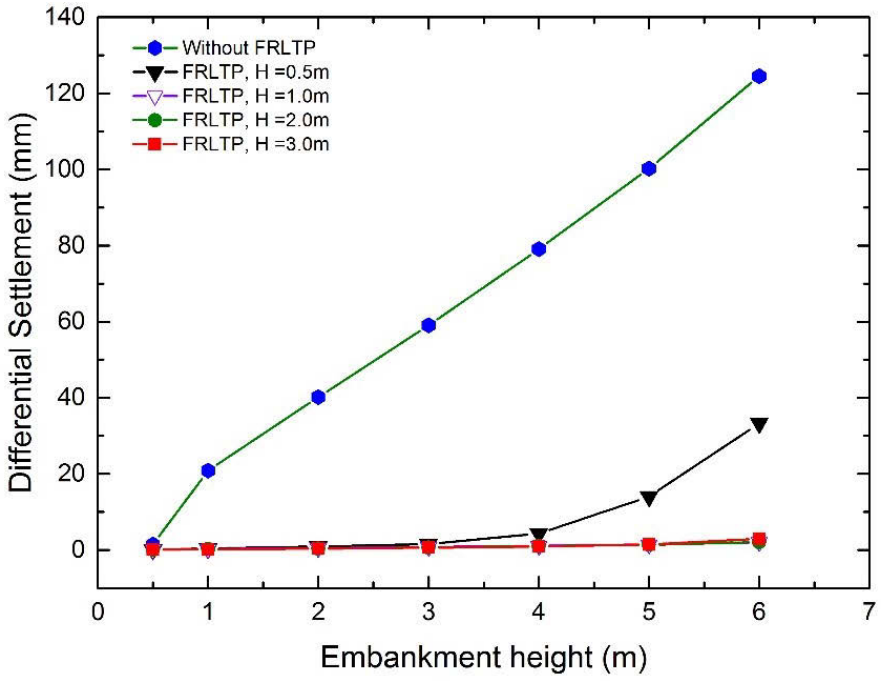

Figure 6.18 Variation of differential settlement with embankment height for various FRLTP thickness

6.3.2.2.2. Load transfer mechanism between columns and foundation soil for various FRLTP thickness

Figure 6.19 displays variation of stress concentration ratio (SCR) with an increase in the embankment height for various FRLTP thickness. As observed in Figure 6.19, the SCR generally increased with increasing the embankment height to H=4 m. That was followed by either a marginal increase in SCR value for the embankment without FRLTP or a linear increase in the SCR value for the embankment with FRLTP thickness beyond 0.5 m as further increase in the embankment height up to 6m. Except for the embankment with FRLTP thickness of 0.5 m, it showed a gradual drop in the SCR to a certain high value after reaching a peak. Referring to Figure 6.19, for example, the SCR value of the embankment without FRLTP gradually increased from approximately 2.5 to 13.8 with an initial increase in the embankment height from 0.5 m to 4 m and afterward observed a marginal increase in SCR value to 14.7 with further increase in the embankment height up to 6 m. However, for the embankment with FRLTP thickness of 0.5 m, when the increase in embankment height from 0.5 m to 4 m resulted in the initial increase in the SCR value from about 5 to a great value of 98 followed by a gradual drop in the SCR to a certain high value of 50 with additional increase in the embankment height up to 6 m. Meanwhile, the SCR of the embankment with the FRLTP thickness ranging between 1 m and 3 m observed a linear increase in the SCR value to a great value between 120 and 140 as the embankment height further increased from 4 m to 6 m.

According to Han & Gabr (2002), the higher SCR value, the more embankment load is transferred to DCM columns, thereby decreasing the total and differential settlement as illustrated in Figure 6.17 and 6.18. As shown in Figure 6.19, although the SCR linearly increased and paralleled with the increase in the embankment height from 4 m to 6 m, the

SCR value tended to be greater for the embankment with the thinner FRLTP (H = 1 m) than those of the embankment with the thicker FRLTP (H > 1 m). The lower SCR value found for the thicker FRLTP could be due the embankment fill replaced with the lighter weight material (lime-fibre-soil) served as an FRLTP. Such lightweight material platform resulted in the relative decrease in the embankment load transferred to DCM columns but did not diminish the beneficial effect of the thicker FRLTP in enhancing the platform stiffness and rigidity. In addition, it did not reduce the effectiveness of a thicker FRLPT in enhancing the stress transfer mechanism between DCM columns and soft foundation soil, whereas minimising the total and differential settlement as evident in Figure 6.17 and 6.18. Therefore, increasing the FRLTP thickness has a significant effect on the embankment behaviour by increasing the stress concentration ratio.

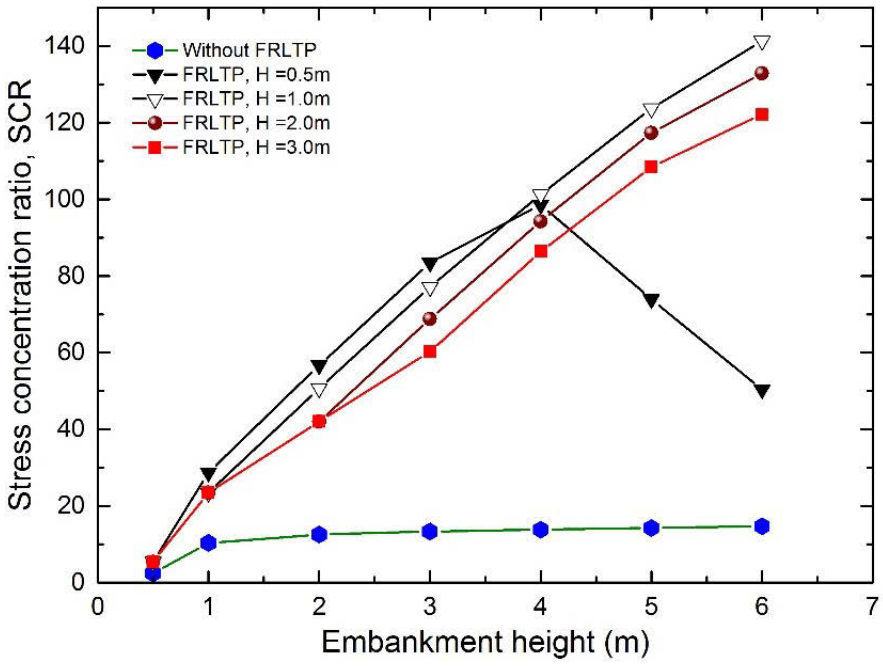

Figure 6.19 Variation of SCR with embankment height for various FRLTP thickness

6.3.2.2.3. Variation of lateral displacement with depth for various FRLTP thickness

As shown in Figure 6.20, the lateral displacement of the columns head under the embankment toe at the two years post-construction significantly decreased with an initial increase in the FRLTP thickness from 0 m to 1 m. That behaviour was followed by a slight increase in the lateral displacement of the columns head but a gradual decrease in the lateral displacement at the columns tip as a further increase in the FRLTP thickness up to 3 m. As expected, the lateral displacement of the embankment without FRLTP (i.e. FRLTP thickness of H = 0 m) was larger than those of the embankment reinforced with an FRLPT (H = 0.5~3 m), which confirms the FRLTP inclusion was effective in controlling the lateral deformation and consequently increasing the stability of the embankment.

Referring to Figure 6.20, it should be noted that at the shallow depth, the effect of the FRLTP was significant in improving the lateral resistance to the embankment deformation. For example, the difference in the lateral displacement was visually observed to a depth of 4 m to 5 m from the ground surface. The lateral displacement reduced by almost 6 times as the FRLTP thickness from H=0 m to H=1 m (equivalent to about 83% reduction in the lateral displacement). However, it can be seen in Figure 6.20 that the lateral displacement linearly increased with greater depth (i.e. from 5 m to 10 m) but decreased with the increase in the FRLTP thickness from 0 m to 3 m. The difference in the lateral displacement was insignificant for the greater depth between 5 m and 10 m compared to those of the shallow depth of less than 5 m. The decrease in the lateral movement observed at the greater depth as the FRLTP thickness increased up to 3 m could be mainly due to the replacement of the embankment fill by the lighter weight material of lime-fibre-soil as discussed earlier. That resulted in the reduction of the lateral

earth pressure applied on the DCM columns with the greater depth where the lateral resistance effect of the FRLTP inclusion was insignificant. As evident in Figure 6.20, the FRLTP thickness has a notable influence on the final (post-construction) lateral displacement of the embankment.

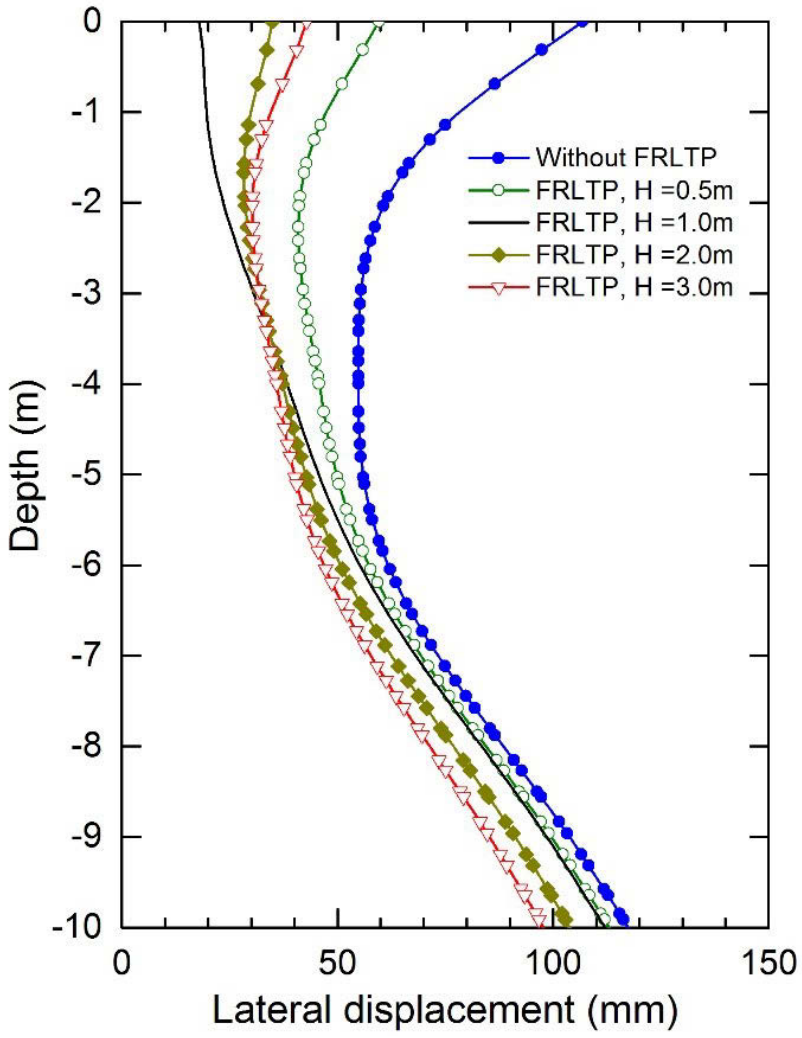

Figure 6.20 Variation of lateral displacement with depth for various FRLTP thickness at 2 years post-construction

6.3.2.3. Effect of the FRLTP elastic deformation modulus (Young's modulus, E) on the embankment behaviour

6.3.2.3.1. Effect of the FRLTP elastic deformation modulus on stress concentration ratio

To investigate the effect of the elastic deformation modulus (stiffness) of FRLTP on the performance of the embankment with the same platform thickness (H = 0.5 m), a series of extensive parametric study has been undertaken using in the same FEM simulation procedures and mesh as shown in Table 6.5 and Figure 6.9, respectively. The parametric study was performed by changing only the deformation modulus of the FRLTP ranging between 10 MPa and 250 MPa, while the improvement depth ratio of β=0.83 and the other properties of the FRLTP were remained unchanged. Figure 6.21 presents the variation of the SCR with an increase in the embankment height for various elastic deformation modulus of the FRLTP. As expected, an increase in the height of the embankment fill caused the initial increase in the SCR value subjected to the given embankment loading. This was followed by a gradual reduction of the SCR to a certain high value as the embankment height continuously increased to reach its final height of 6 m as illustrated in Figure 6.21. However, it is observed that the SCR value of the embankment reinforced with an FRLTP was certainly larger than that of the embankment without FRLTP. For example, during the embankment construction, when the height of the embankment fill increased from 0.5 m to 4 m, the SCR increased by approximately 50% as the deformation modulus of FRLTP increased from 10 MPa to 50 MPa. However, a further increase in the deformation modulus showed the negligible increase in the SCR for that given embankment height. Even though a decreasing trend of the SCR was observed in Figure 6.21 as the embankment height further increased to obtain its final height of 6 m, the SCR was higher for the FRLTP with higher deformation modulus. As

Figure 6.21 shows, the effect of the FRLTP stiffness on the arching effect of the embankment was significant for the higher elastic deformation modulus of FRLTP (i.e. up to E=50 MPa), whereas the effect of the FRLTP Young's modulus greater than 50 MPa was negligible.

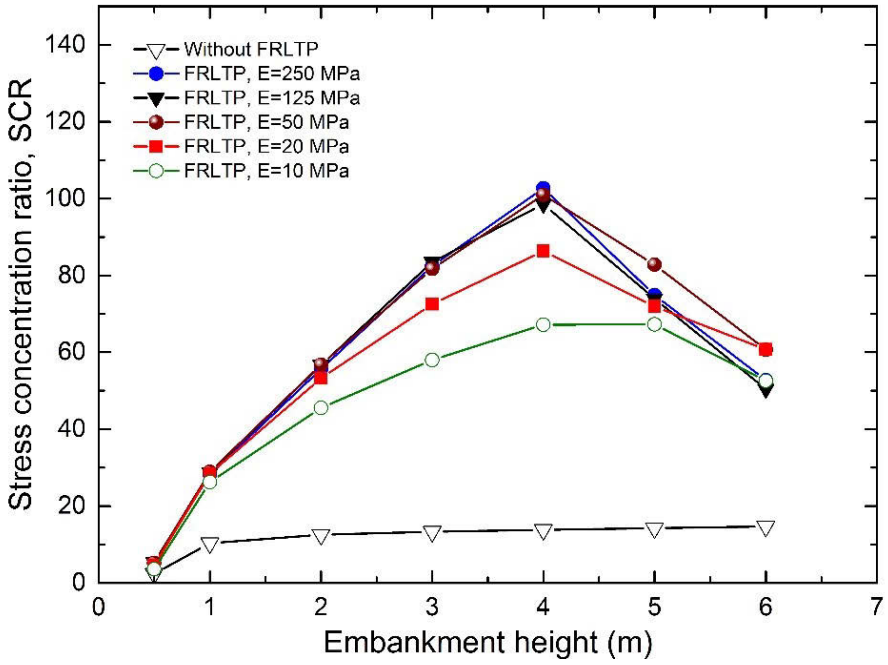

Figure 6.21 Effect of FRLTP Young's modulus variation on stress concentration ratio

6.3.2.3.2. Effect of the FRLTP elastic deformation modulus on differential settlement

The effect of the FRLTP stiffness on the change of the differential settlement under the centre of the embankment is shown in Figure 6.22. It is found that for the FRLTP inclusion with a low deformation modulus of 10 MPa, the differential settlement at the completion at the embankment construction decreased by approximately 68% (from 125 mm to 40.5 mm) compared with that of the embankment without FRLTP. As the deformation modulus of the FRLTP increased to E=50 MPa, the corresponding differential settlement additionally reduced to 76%. However, a further increase in the

FRLTP stiffness exceeded E=50 MPa led to a marginal improvement in the differential settlement. In other words, the effect of the FRLTP deformation modulus exceeded a certain value of E=50 MPa on the differential settlement was insignificant. Thus, an elastic deformation modulus of E=50 MPa is required to consider for the FRLTP design to support the given embankment height found on soft soils. Based on the numerical results presented in Figure 6.22, it can be concluded that the stiffness of the FRLTP showed a notable effect of the embankment differential settlement.

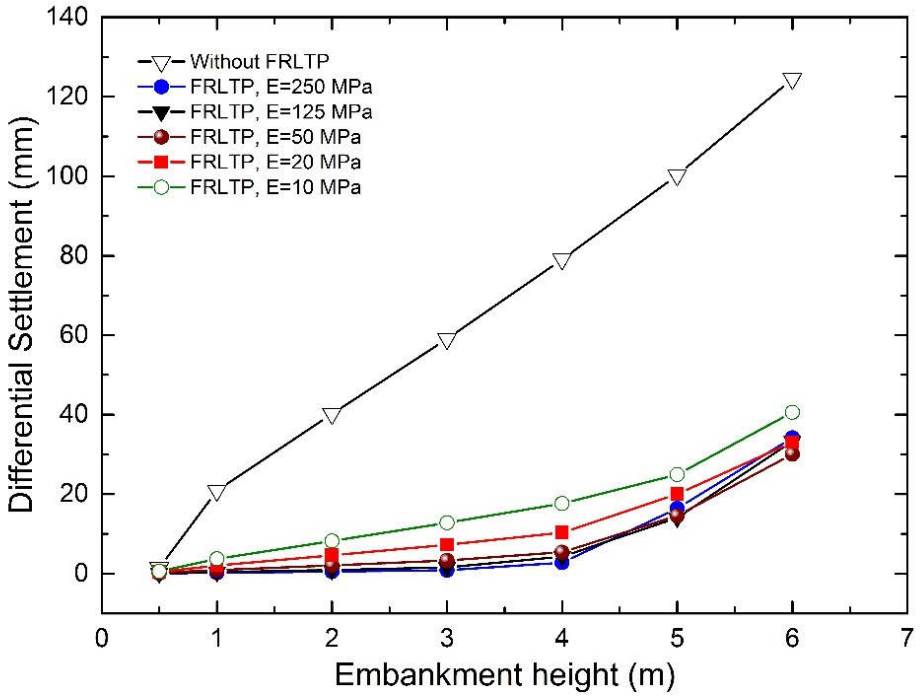

Figure 6.22 Effect of FRLTP Young's modulus on differential settlement

6.3.2.3.3. Effect of the FRLTP Young's modulus on the lateral displacement with depth

Figure 6.23 illustrates the change in the lateral displacement of a DCM column under the embankment toe along with depth at 2 years post-construction for the different FRLTP stiffness. The lateral displacement of the embankment without FRLTP is also illustrated

in Figure 6.23 for reference. It is observed that the lateral displacement of the embankment with FRLTP decreased gradually to a depth of around 2 m from the ground surface and then remained almost unchanged to a certain depth of 5 m. This was followed by a gradual increase again in the lateral deformation to the greater depth of 10 m (column tip) as shown in Figure 6.23. The larger lateral displacement was visually observed in Figure 6.23 for the embankment without FRLTP to the depth of around 5 m, and subsequently the difference in the lateral displacement between the embankment without and with FRLTP was negligible as the depth increased beyond 5 m. This phenomenon reconfirms the effectiveness of the FRLTP inclusion in controlling the lateral deformation of the embankment at a shallow depth. A similar trend of the lateral displacement with depth was numerically predicted and reported by Zhang et al. (2013) for a geosynthetic reinforced and piles supported embankment. However, the numerical prediction results presented in Figure 6.23 indicate that the lateral displacement slightly increased with an increase in the elastic deformation modulus of the FRLTP from 10 MPa to 250 MPa although the increase in the lateral displacement appeared to be nominal. Referring to Figure 6.23, it is concluded that the stiffer FRLTP tended to show an adverse effect on the lateral resistance to the embankment deformation, but the adverse effect was insignificant.

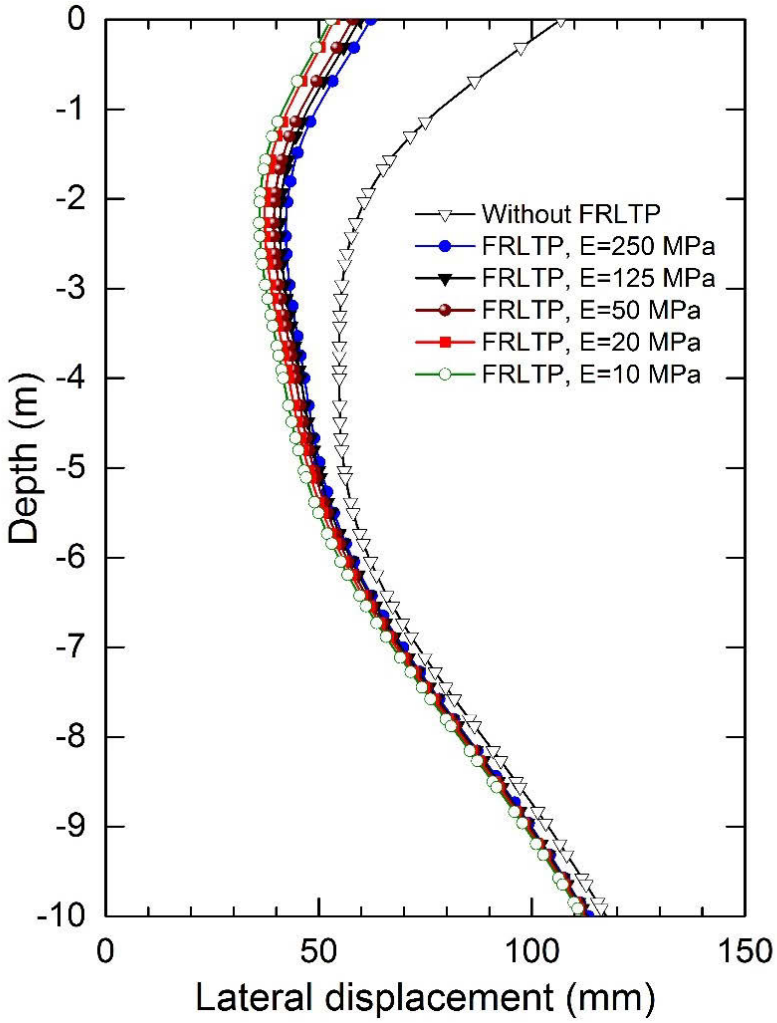

Figure 6.23 Variation of the lateral displacement with depth for various elastic deformation modulus of FRLTP at 2 years post-construction

6.3.2.4. Effect of the FRLTP shear strength properties on the embankment behaviour

6.3.2.4.1. Effect of the FRLTP cohesion

To study the effect of the shear strength characteristics of FRLTP on the behaviour of the CS embankment with the same improvement depth ratio (β=0.83), a series of extensive parametric study was conducted by changing merely cohesion value of the FRLTP ranging between 10 kPa and 300 kPa, while the other properties of the FRLTP were remained unchanged. The predicted results of the parametric study were plotted in Figure

6.24-6.26 showing the variations of the SCR, the differential settlement of the ground surface against the embankment height, and the lateral displacement with depth, respectively. Figure 6.24 reveals that the SCR increased with an increase in cohesion of the FRLTP and embankment height to a great extent. It is observed that increasing the FRLTP cohesion value from 10 kPa to 75 kPa led to a remarkable increase in the SCR value from roughly 5 to between 20 and 98 when the embankment height increased from 0.5 m to 4 m. This behaviour was followed by a decrease in the SCR value to a certainly high value (e.g. an SCR of 50 for the FRLTP cohesion of 75 kPa) with the increase in embankment height greater than 4 m, as depicted in Figure 6.24. A drop in the SCR value showed an indication of the increase in differential settlement of the ground surface due to the over-bearing capacity of the DCM columns induced by increasing the embankment height. However, the further increase in the FRLTP cohesion value up to 150 kPa and 300 kPa, respectively, exhibited a linearly significant increase in the SCR to a great value of around 150 without presenting a decreased in the SCR value as the embankment height increased from 0.5 m to its final height of 6 m. The higher SCR value is most likely to promote the better embankment load transfer from foundation soil to DCM columns due to the enhancement of arching effect and consequently prevent the development of the differential settlement of the ground surface as the following discussion. However, the FRLTP cohesion value of 300 kPa did not produce the greater SCR value compared with the 150 kPa cohesion of the FRLTP irrespective of any of the embankment height. This implies that the lime-fibre-soil having a high cohesion of 150 kPa reached an optimum value to be adopted as an FRLTP, further increase in the FRLTP cohesion would not generate a significant effect on the SCR of the embankment.

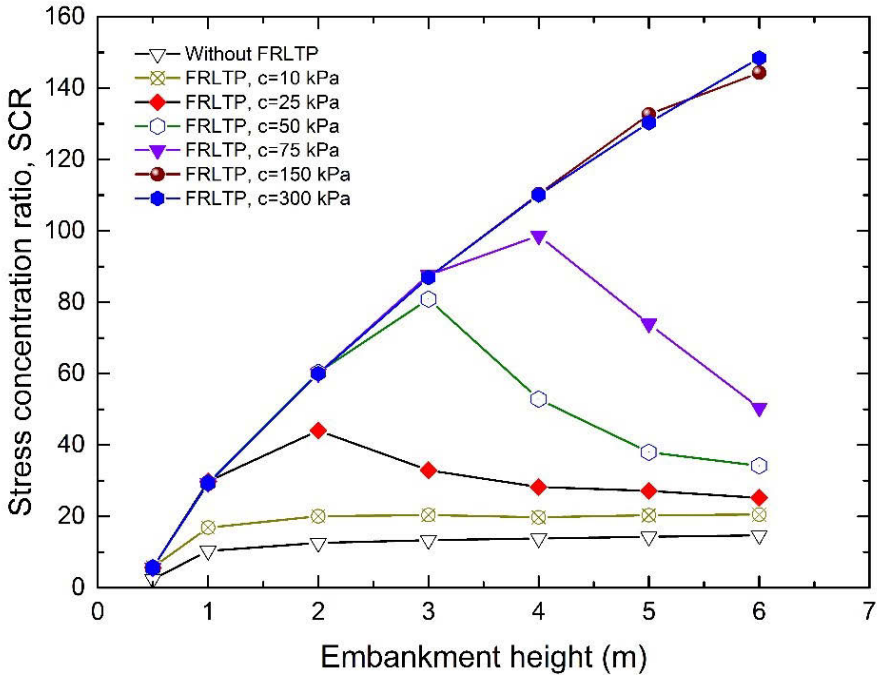

Figure 6.24 Effect of the FRLTP cohesion on stress concentration ratio

In addition, the effect of the FRLTP cohesion of the differential settlement of the ground surface can be seen in Figure 6.25. Similar to the trend of SCR, an increase in cohesion of the FRLTP resulted in the improvement in the differential settlement of the ground surface caused by the increase in the embankment height. For example, the increase in cohesion from 10 kPa to 150 kPa resulted in the significant reduction in the maximum differential settlement ranging from roughly 80 mm to 6 mm, which yielded approximately 92% reduction of the differential settlement. However, the higher increase in the FRLPT cohesion up to 300 kPa produced the insignificant decrease in the maximum differential settlement to a certainly low level of around 4 mm as the embankment height increased up to 6 m. Thus, it can be concluded that the FRLTP cohesion is highly effective in controlling the differential ground surface settlement. The FRLTP cohesion of 150 kPa or greater could minimise almost the entire differential settlement induced by a certain embankment height.

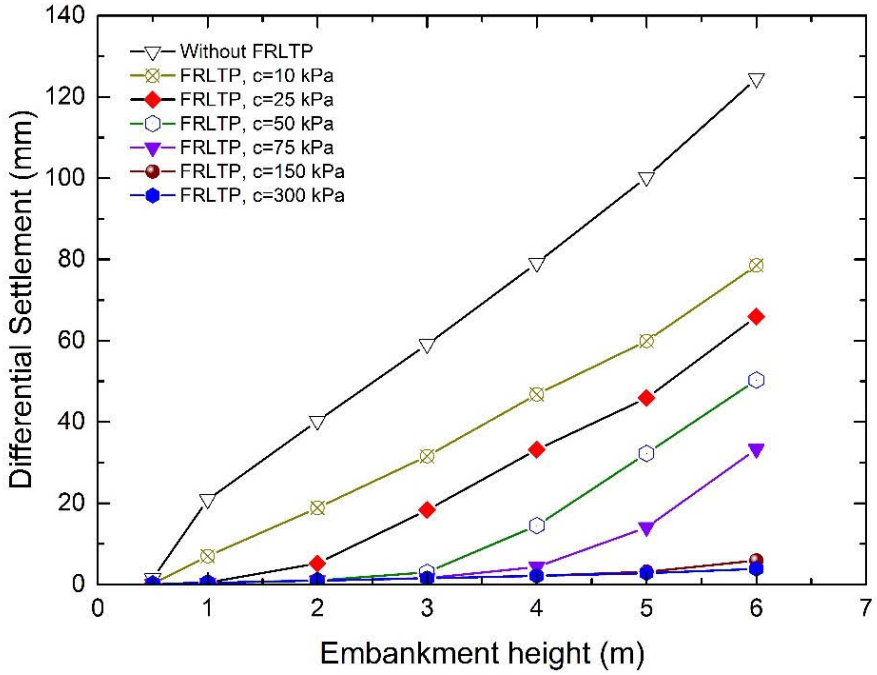

Figure 6.25 Effect of FRLTP cohesion on differential settlement

Figure 4.26 shows the effect on the FRLTP cohesion on the lateral displacement with depth of the DCM column under the embankment toe at 2 years post-construction. As illustrated in Figure 4.26, the lateral displacement of the embankment with FRLTP significantly reduced to a small value (around 5 mm at the column head) when the FRLTP cohesion increased from 10 kPa to 300 kPa, which means the higher cohesion of the FRLTP can control zero lateral deformation of the embankment toe. Moreover, the increase of the FRLTP cohesion reveals a notable influence on the lateral displacement of the CS embankment to a certain depth of around 5 m from the ground surface and then it exhibits an insignificant impact on the lateral deformation to a greater depth. As Figure 4.26 shows, the embankment without FRLTP obviously illustrated the larger lateral displacement in comparison with the embankment with FRLTP. This numerical

prediction indicates that the FRLTP cohesion has a significant effect on the lateral resistance to the embankment deformation.

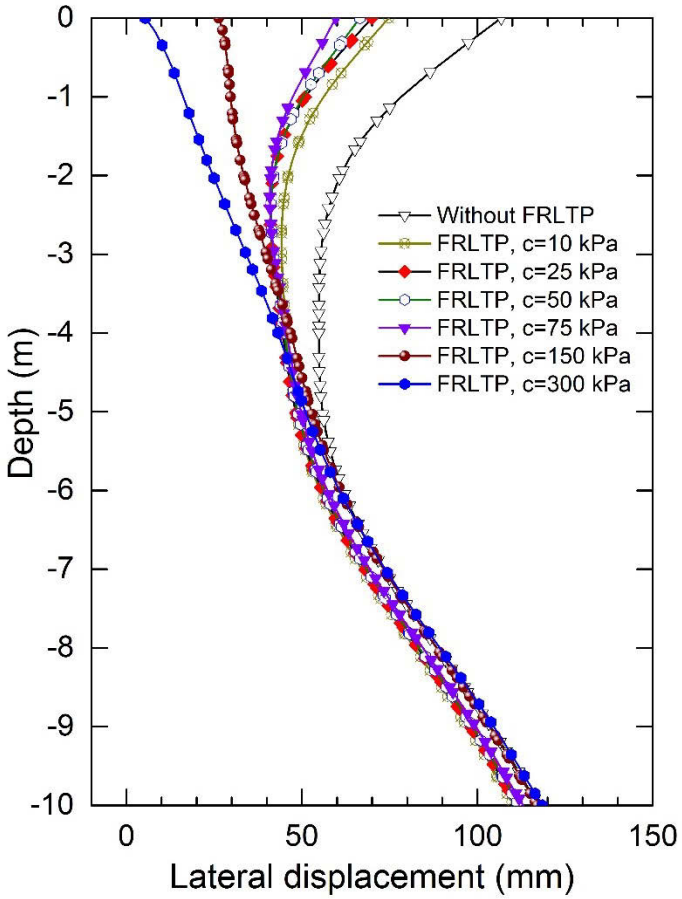

Figure 6.26 Variation of the lateral displacement with depth for various cohesion values of FRLTP at 2 years post-construction

6.3.2.4.2. Influence of the FRLTP friction angle

Another series of the parametric study was undertaken by only varying the internal friction angle of the FRLTP ranging between 1° and 42° together with an increase in the embankment height. Meanwhile, the cohesion value of 75 kPa, the improvement depth ratio (β=0.83), and other properties of the FRLTP were kept constant as shown in Figure 6.8. The fluctuations of the SCR, the differential settlement and the lateral deformation

against the embankment height for different friction angles of the FRLTP were presented in Figure 6.27-6.29, respectively. Overall, the SCR value as shown in Figure 6.27 increased to a great value as the embankment height increased. This was followed by a drop in the SCR value to a certainly high level, which can clearly be observed in any cases of the FRLTP friction angle. Dissimilar to the trend of SCR caused by the increase in the FRLTP cohesion, the increase in the FRLTP fiction angle produced almost the same SCR values as the embankment height increased from 0.5 m to 3 m. Following, when the embankment height increased higher than 3 m, the SCR tended to decrease after approaching a peak around 4 m of the embankment height. Although the SCR decrease was observed for the embankment height exceeded 4 m, a greater SCR value was clearly observed for the higher friction angle of the FRLTP. However, Figure 6.27 reveals that the increase in the FRLTP friction angle higher than 30° resulted in an insignificant improvement in the SCR value.

Furthermore, the effect of the FRLTP friction angle on the differential settlement of the ground surface can be observed in Figure 6.28. Generally, observation of the predicted results in Figure 6.28 indicates that an increase in the embankment height from 0.5 m to 3 m caused a minimal increase in the differential settlement of the ground surface. Moreover, the increase in the FRLTP friction angle from 1° to 42° showed no notable effect on the improvement in the differential settlement in that range of the embankment height. Nonetheless, when the embankment height increased further from 3 m to 6 m, an increase in the FRLTP friction angle from 1° to 30° led to a decrease in the differential settlement of the ground surface from 60 mm to approximately 30 mm. The additional increase in the FRLTP friction angle exceeded 30° revealed the insignificant

improvement or even resulted in a slight increase in the differential settlement as presented in Figure 6.28. It can be concluded that the increase in friction angle of the FRLTP effectively promoted the improvement in the SCR and the differential settlement on the ground surface. However, when comparing with the FRLTP cohesion, the improvement in the SCR and the differential settlement of the investigated embankment is more dominant for the increase in the FRLTP cohesion than those subjected to the increase in the FRLTP friction angle.

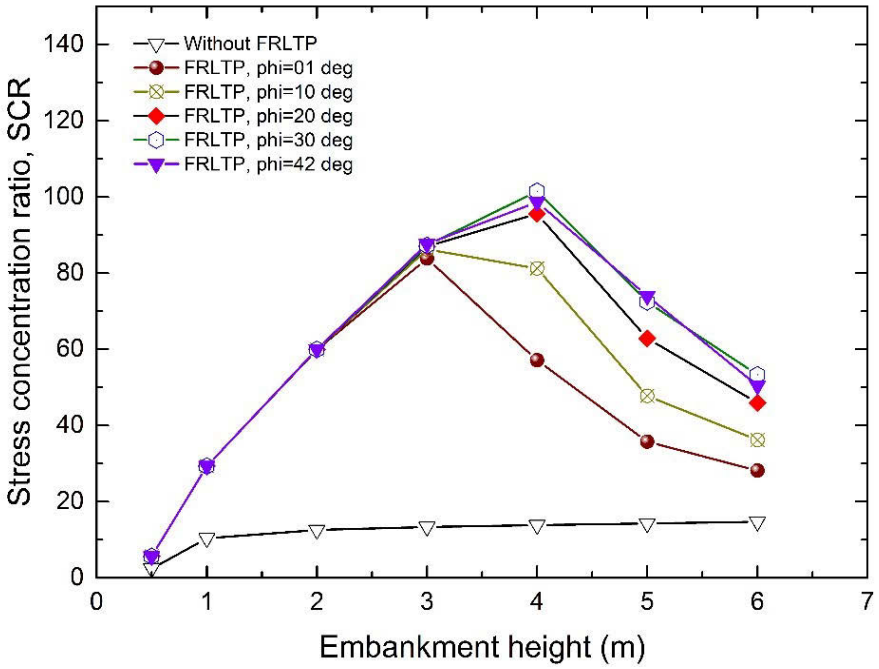

Figure 6.27 Effect of FRLTP friction angle on stress concentration ratio

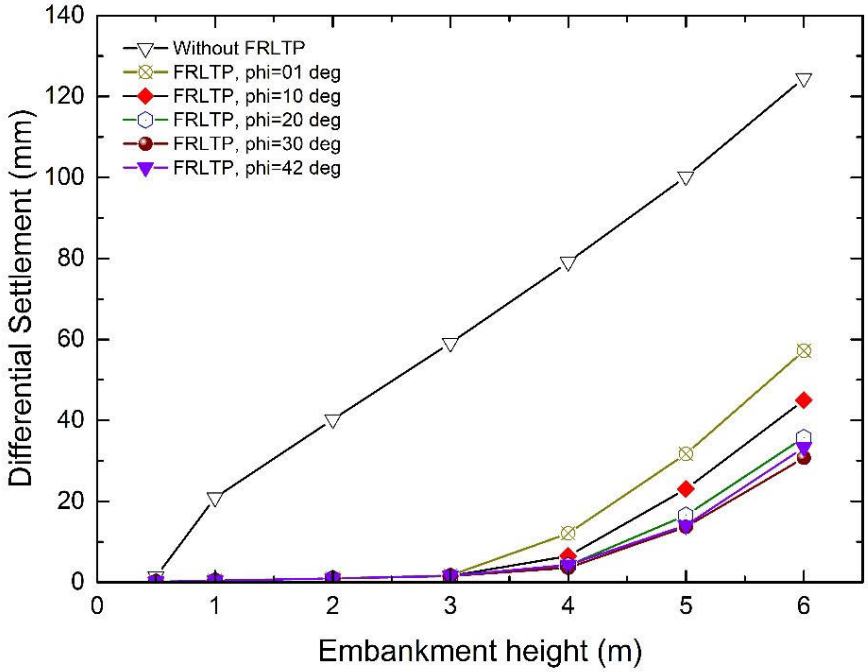

Figure 6.28 Effect of FRLTP friction angle on differential settlement

The influence on the FRLTP friction angle on the 2 years post-construction lateral displacement with depth of the DCM column under the embankment toe is shown in Figure 6.29. It can be seen that when the FRLTP friction angle increased from 1° to 42°, the lateral displacement of the embankment with FRLTP decreased considerably and nonlinearly with depth. For example, the corresponding reduction of the lateral displacement of column head was from approximately 100 mm for the FRLTP friction angle of 1° to about 60 mm for the FRLTP friction angle of 42°, resulting in the significant improvement of around 40% in the lateral deformation at the embankment toe. However, the additional increase in the FRLTP friction angle beyond 42° yielded a negligible improvement in the embankment lateral displacement. Similar to the trend of the lateral displacement of the CS embankment associated with the fluctuations of FRLTP cohesion,

the influence of the FRLTP friction angle changes on the lateral deformation was found to take place to a shallow depth of around 5 m from the ground surface. Afterwards, its influence on the lateral deformation was negligible as the depth increased further to the DCM columns tip. It is also noted that the predicted lateral displacement of the embankment without FRLTP was visibly larger compared to the embankment reinforced with an FRLTP. Referring to Figure 6.29, it can be concluded that the effect of the FRLTP friction angle on the 2 years post-construction lateral displacement of the CS embankment was significant.

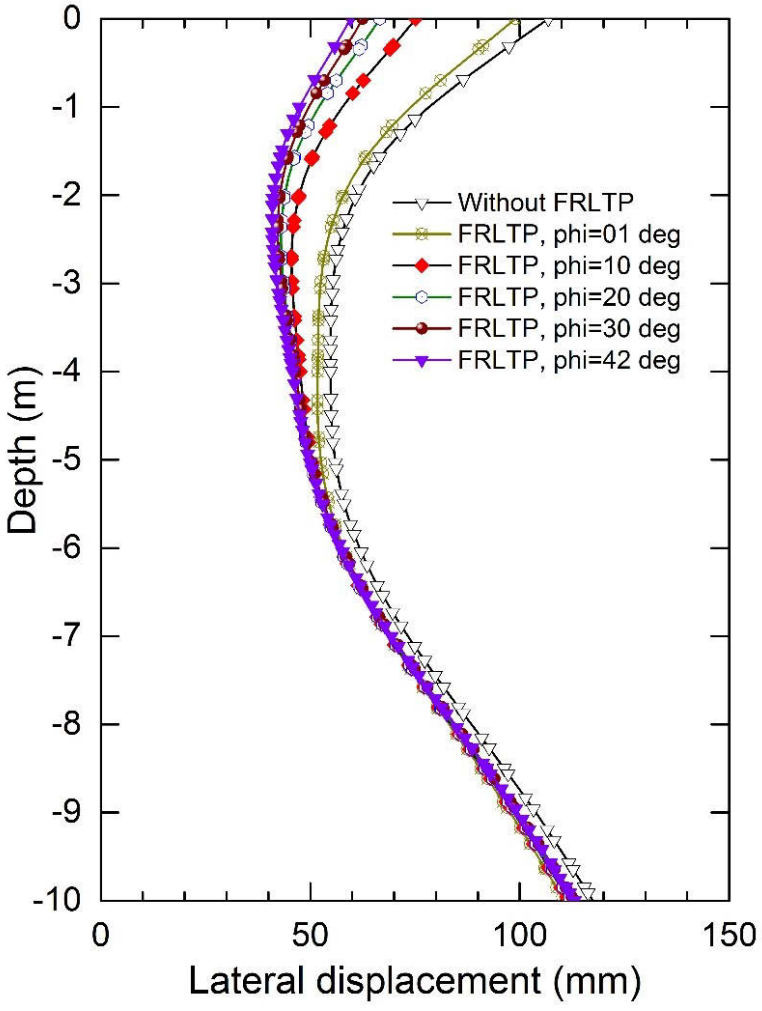

Figure 6.29 Variation of the lateral displacement with depth for various friction angles of FRLTP at 2 years of post-construction

6.3.2.5. Effect of the FRLTP tensile strength on the embankment behaviour

The effect of the tensile strength characteristics of FRLTP on the embankment behaviour with the same improvement depth ratio (β=0.83) was numerically investigated by varying the only tensile strength value of the FRLTP ranging between 10 kPa and 240 kPa, while the other properties of the FRLTP were kept constant. As observed in Figure 6.30, the SCR increased with the embankment height but decreased with increasing the FRLTP tensile strength. The SCR difference associated with the increase in the FRLTP tensile strength from 10 kPa and 240 kPa can visibly be observed when the embankment height increased from 4 m to 6 m during the construction process. As Figure 6.30 illustrates, the reduction of the SCR indicated the decrease in the arching effect of the embankment as the FRLTP tensile strength increased. Consequently, this resulted in the corresponding increase in the embankment (differential) settlement as shown in Figure 6.31 since the more embankment load transferred to foundation soils. Although the embankment SCR was greater and the differential settlement was smaller for the embankment with the higher FRLTP tensile strength when comparing the embankment without FRLTP as presented in Figure 6.30 and 6.31, the predicted results of this parametric study revealed that the influence of the FRLRP tensile strength increase became negative.

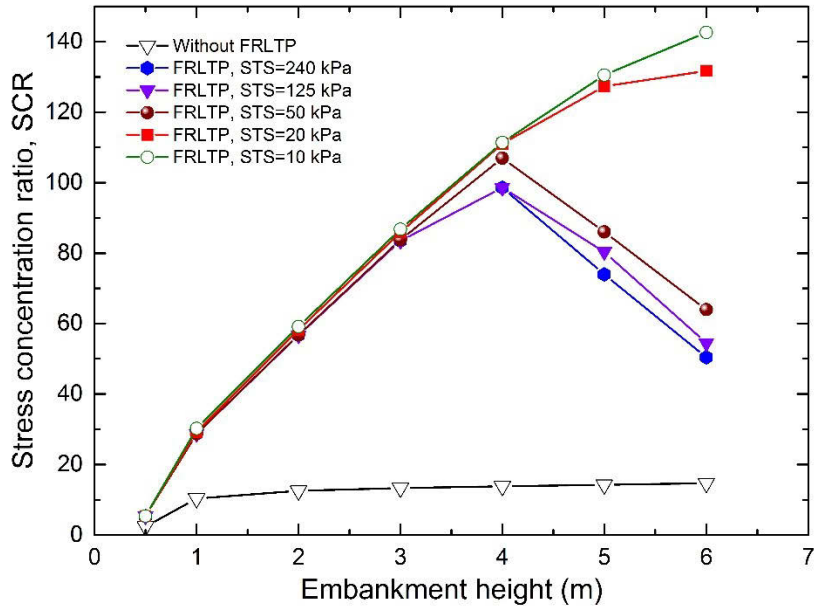

Figure 6.30 Effect of the FRLTP tensile strength (STS) on stress concentration ratio

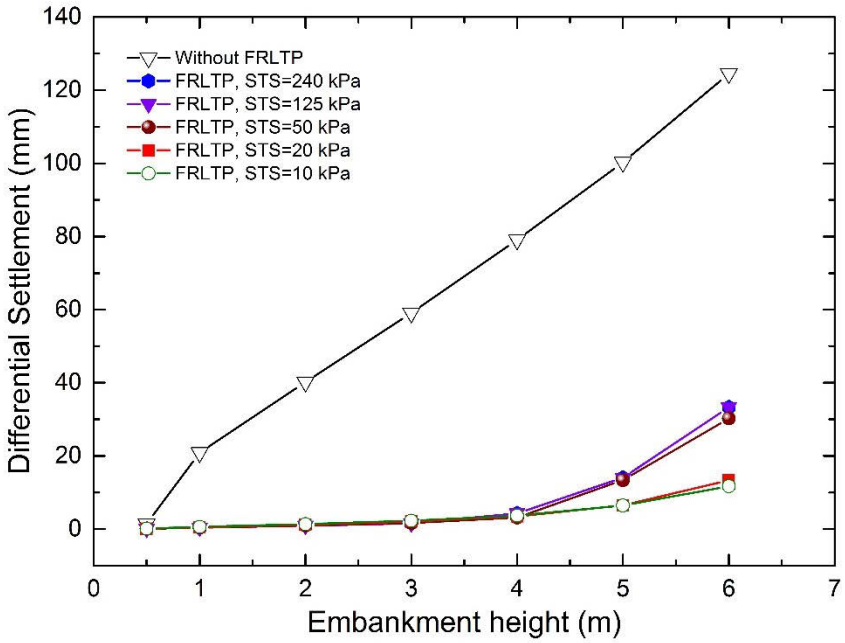

Figure 6.31 Effect of the FRLTP tensile strength (STS) on differential settlement

Figure 6.32 shows that the increase in the FRLTP tensile strength becomes very effective in improving the lateral displacement of the embankment with depth. As illustrated in Figure 6.32, the post-construction lateral deformation of the embankment toe decreased by approximately 52% as the FRLTP tensile strength increased from 10 kPa to 125 kPa. Meanwhile, a further increase in the FRLTP tensile strength up to 240 kPa yielded an insignificant effect on the improvement in the lateral deformation. Therefore, a tensile strength of 125 kPa is required to consider for the FRLTP design in support of the 6 m embankment height built columns improved soft soils. The improvement of the lateral displacement could be attributed to the higher tensile strength of FRLTP that facilities the better resistance to the lateral spreading forces caused by an increase in the height of the embankment fill and consequently reduces the lateral earth pressure acting on the DCM columns with depth.

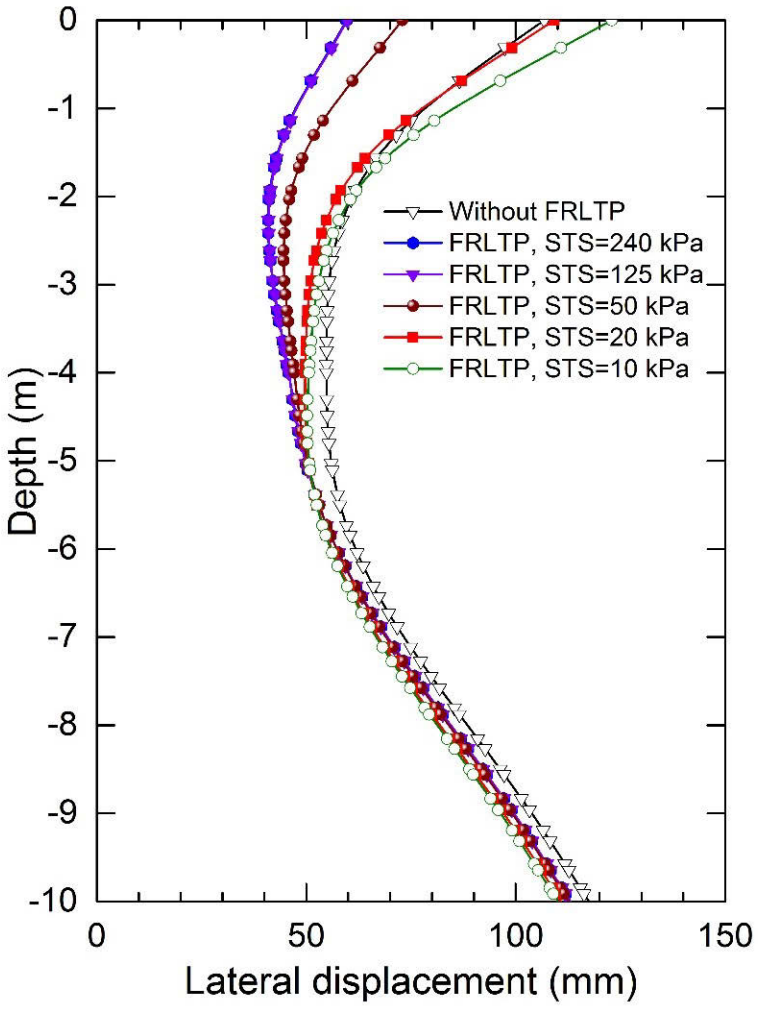

Figure 6.32 Variation of lateral displacement with depth for various FRLTP tensile strength (STS) at 2 years of post-construction

6.4. CASE STUDY 3

Figure 6.33 displays a schematic diagram of the embankment supported on piles, considered in this investigation. While the entire embankment cross section is shown in Figure 6.33, only half of the embankment around its centre, presented in Figure 6.34, is adopted to model in this numerical analysis due to the embankment's symmetry. As can be seen in Figure 6.33, the embankment has 5.6 m height and 120 m length with a crest width of 35 m, and its side slopes are 1V:1.5H. The embankment is made of fill material with a cohesion of 10 kPa, a friction angle of 30°, and an average unit weight of 18.5 kN/m^3. It is constructed on a 1.5 m thick coarse-grained fill overlaying a 2.3 m thick deposit of silty clay. This deposit of silty clay overlies a 10.2 m thick soft silty clay stratum. Underneath the soft silty clay layer, there is a 2 m thick medium silty clay layer followed by a 9 m thick sandy silt layer. The ground-water table is located at a depth of 1.5 m below the ground surface. A fibre-lime reinforced earth platform of 0.5m, known as FRLTP, is placed on the top of piles. Details of these soil layers are summarised in Table 6.6 and 6.7.

Referring to Figure 6.33, annulus concrete piles of 1 m diameter and 16 m length used to support embankment are cast in place with a 120 mm wall thickness. The 0.5 m top pile head is cast as solid cylindrical piles. The annulus piles are arranged in a square grid pattern with a 3 m centre-to-centre spacing, giving an area replacement ratio of approximately 8.7%. The construction of embankment is performed in 0.5 m increment to a height of 5.6 m over a period of 55 days followed by 125 days of a waiting period for consolidation after the end of embankment construction.

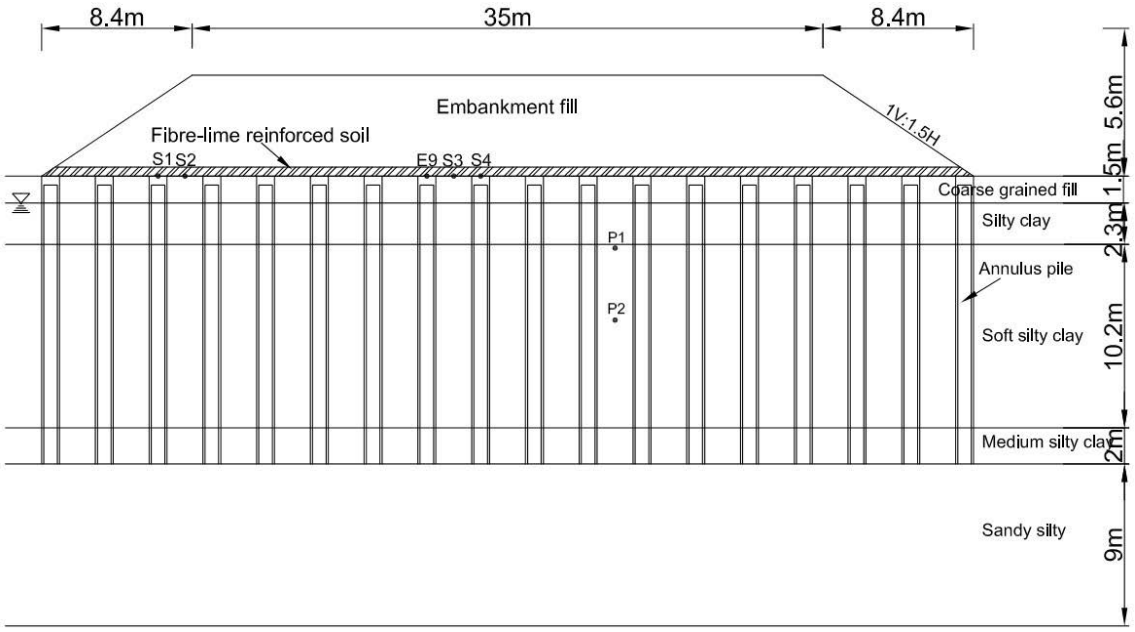

Figure 6.33 Cross-section of the FRLTP and piles supported embankment (case study 3)

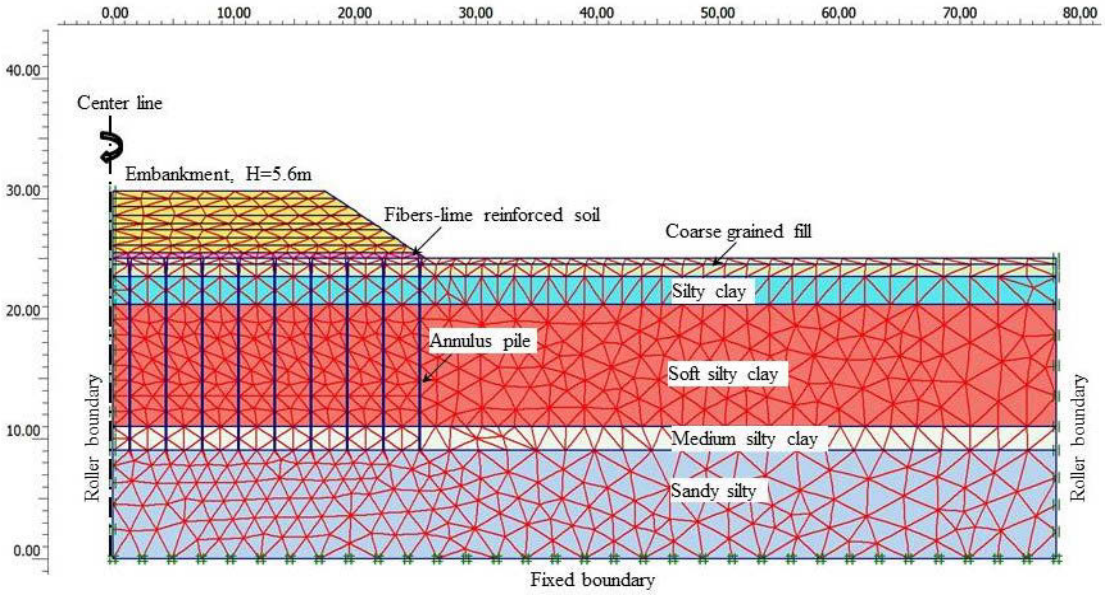

Figure 6.34 2D Model adopted for analysis of embankment

6.4.1. NUMERICAL MODELING

6.4.1.1. 2D Finite Element Model

A 2D plane strain model was built using commercial finite element software PLAXIS, adopting the equivalent 2D numerical method proposed by Tan et al. (2008). The annulus concrete piles were simulated by continuous plane strain walls of 0.26 m thickness for the top 0.5 m of piles and 0.11 m for the rest of the pile length, considering equivalent axial rigidity (EA) and bending rigidity (EI). With regard to the constitutive modelling, the annulus piles were modelled as an isotropic linear elastic material with Young's modulus of 20 GPa, and a Poisson's ratio of 0.2. The FRLTP, embankment fill, coarse-grain fill were simulated using a linear elastic-perfectly plastic model with MC failure criterion. The four foundation soils shown in Figure 6.33 and 6.34 were represented by MCC (Modified Cam Clay) material model. A summary of the constitutive model parameters is given in Table 6.6 and Table 6.7.

Table 6.6 Material properties for Mohr-Coulomb Model used in the FEM simulation (after Liu et al. 2007; Anggraini et al. 2015)

Material	γ (kN/m^3)	E_s (MPa)	c' (kPa)	φ' (deg)	ψ (deg)	k (m/day)	ν
Embankment Fill	18.5	20	10	30	0	-	0.3
Natural fibre-lime-soil	12.5	51	75	42	0	-	0.32
Coarse grained fill	20	7	15	28	0	-	0.3
Pile	25	20000	-	-	-	-	0.2

Table 6.7 Material properties for Modified Cam Clay model used in the FEM simulation (after Liu et al. 2007)

Material	γ (kN/m^3)	λ	κ	M	e_1	k (m/day)	ν
Silty clay	20	0.06	0.012	1.2	0.87	$8.64\text{x}10^{-4}$	0.35
Soft silty clay	17	0.15	0.03	0.95	1.79	$4.32\text{x}10^{-4}$	0.4
Medium silty clay	20.5	0.05	0.01	1.1	0.88	$4.32\text{x}10^{-4}$	0.35
Sandy silt	20	0.03	0.005	0.28	0.97	$4.32\text{x}10^{-3}$	0.35

As mentioned earlier, only half of the embankment is represented in this numerical simulation since the embankment is symmetrical along its centerline. The foundation soil is taken to 25 m depth from the ground surface overlying a stiff impermeable stratum. The horizontal length of the FEM model is taken to be 78 m, which is almost three times the half width of the embankment base, aimed to minimise the boundary effects. All these boundaries are considered to be impermeable, and pore fluid flow is only permitted from the ground surface.

In this analysis, for the 2D plane strain FEM modelling, the horizontal displacement at the left and right boundaries was not permitted but the vertical movement was allowed, whereas both the vertical and horizontal displacements were prevented at the bottom boundary. On one hand, due to the relatively high permeability, the embankment fill, coarse-grained fill were assumed to behave in a drained condition. On the other hand, FRLTP, annulus piles, and other four foundation soils were assumed to act as undrained materials. In this analysis, fifteen-node triangular elements with excess pore water pressure degrees of freedom at all nodes were adopted to simulate the foundation soils, while fifteen nodes triangular elements without excess pore water

pressure degrees of freedom at all nodes were applied to model the embankment fill and annulus concrete piles.

The embankment is constructed in nine lifts including the 0.5 m thick FRLTP. During the first step of analysis, all the elements corresponding to fill materials were inactivated and the foundation soil and piles were activated. Then, elements associating with each layer were added one by one in each step until the 5.6 m embankment height was reached over a period of 55 days. In the final step, the fully constructed embankment was left for 125 days for consolidation.

6.4.1.2. Validation of 2D Finite Element Model

A full-scale load test and a 3D numerical model of geogrid-reinforced and piles supported highway embankment with an area replacement ratio of 8.7% reported by Liu et al. (2007) were used to validate the modelling approach adopted in this study. The simulation procedures in detail for an embankment analysis conducted by Liu et al. (2007) in step by step was followed in this research when FRLTP was adopted to substitute the geogrid reinforced load transfer platform in the simulation by Liu et al. (2007). The measured and computed embankment load between piles and foundation soil surface, the variation of pore water pressure presented by Liu et al. (2007) were compared in Figure 6.35-6.37. The outcomes of this numerical analysis indicate that the equivalent 2D FEM model proposed in this study is suitable for simulating piles supported embankment over soft soil.

6.4.2. ANALYSIS OF RESULTS AND DISCUSSION

6.4.2.1. Load Transfer to the Piles and Soft Soil

Figure 6.35 and 6.36 show the variation of computed vertical effective pressure acting on foundation soil and pile heads in this numerical prediction, respectively, when FRLTP was used to support embankment over piles in comparison with the field measurement pressure of geogrid reinforced LTP (load transfer platform) previously reported by Liu et al. (2007). In general, an increase in the embankment height caused additional vertical pressure, known as embankment load increasing with time. It can be observed in these figures that when the embankment height increased to 5.6 m over a period of 55 days, an increase in the corresponding embankment load was 104 kPa, while the vertical pressure acting on foundation soil between piles was constantly less than that of embankment load. For example, the maximum computed pressure transferred to foundation soil plotted in Figure 6.35 from this numerical analysis was about 45 kPa at the end of embankment construction, which is roughly 43% of the embankment load and 79% of the measured pressure in the case of geogrid-reinforced embankment. However, the computed pressure transferred to pile heads significantly increased with the embankment load as presented in Figure 6.36. For example, the maximum computed pressure acting on pile head in this numerical prediction at the completion of embankment construction was about 625 kPa, which is approximately 14 times greater than the pressure transferred to foundation soil and 6 times larger than the embankment load. This has a good agreement with the field measurement data previously presented by Liu et al. (2007) for the case of geogrid reinforced LTP. It can be noted that with the use of FRLTP and piles-supported embankment, the piles carried the major load of embankment due to soil arching effect contributing from the higher internal friction angle and cohesion of lime-fibre-reinforced

earth platform. Thus, a relatively small embankment load was transferred to the foundation soil between piles.

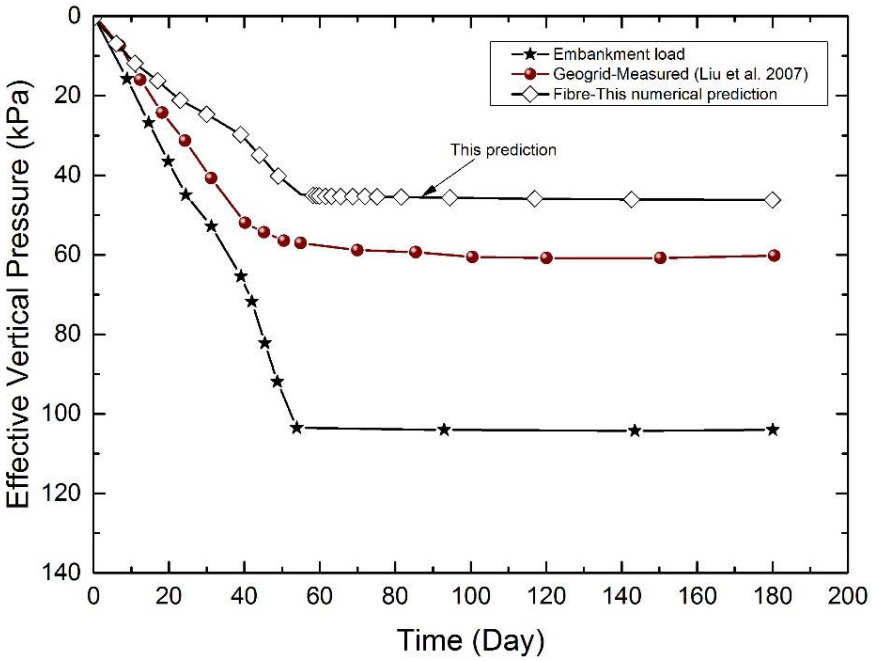

Figure 6.35 Earth pressure acting on soil surface between piles

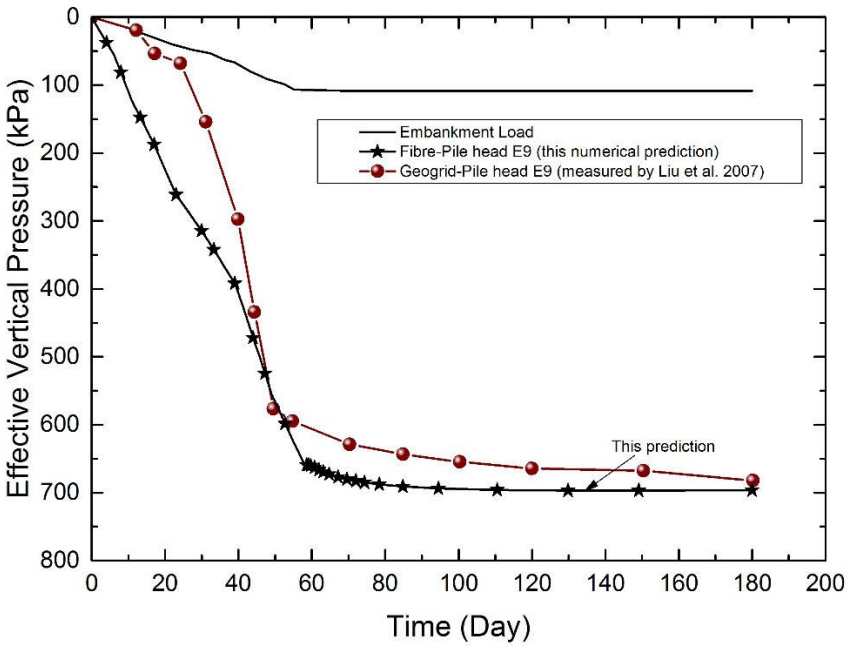

Figure 6.36 Earth pressure acting on the top of reinforced concrete

6.4.2.2. Variation of excess pore water pressure

Figure 6.37 shows the variations of simulated excess pore water pressure (EPWP) with time in the soft silty clay stratum at 8.0 m depth (P2) under the embankment base centre for the case of FRLTP in comparison with both the computed and measured EPWP data previously reported by Liu et al. (2007) for the case of geogrid reinforced LTP. As can be observed in the figure, the simulated EPWP in this numerical prediction reached its peak value of approximately 16 kPa at the end of embankment construction and then dissipated almost 84% after 125 days of consolidation. As expected, there was a high increase in the EPWP during the embankment construction process as observed in both the numerical predictions and field measurements, which was associated with the staged construction of the embankment. Nonetheless, the maximum predicted excess pore water pressure for the case of FRLTP was only about 16 kPa in the middle of soft silty clay since the embankment load was mainly transferred to piles. Moreover, the simulated dissipation in case of FRLTP was very fast compared to the measured EPWP in the case of geogrid-reinforced LTP. This behaviour may be attributed to the decrease in hydraulic conductivity of soft silty clay due to the decrease in void ratio during the consolidation process that was not taken into account in this numerical analysis. Overall, the simulated EPWP generation and dissipation in the case of FRLTP and piles supported embankment agree well with the computed data previously reported by Liu et al. (2007) for the case of geogrid-reinforced embankment. This indicates that fibre-lime treated soil can be successfully adopted as a load transfer platform.

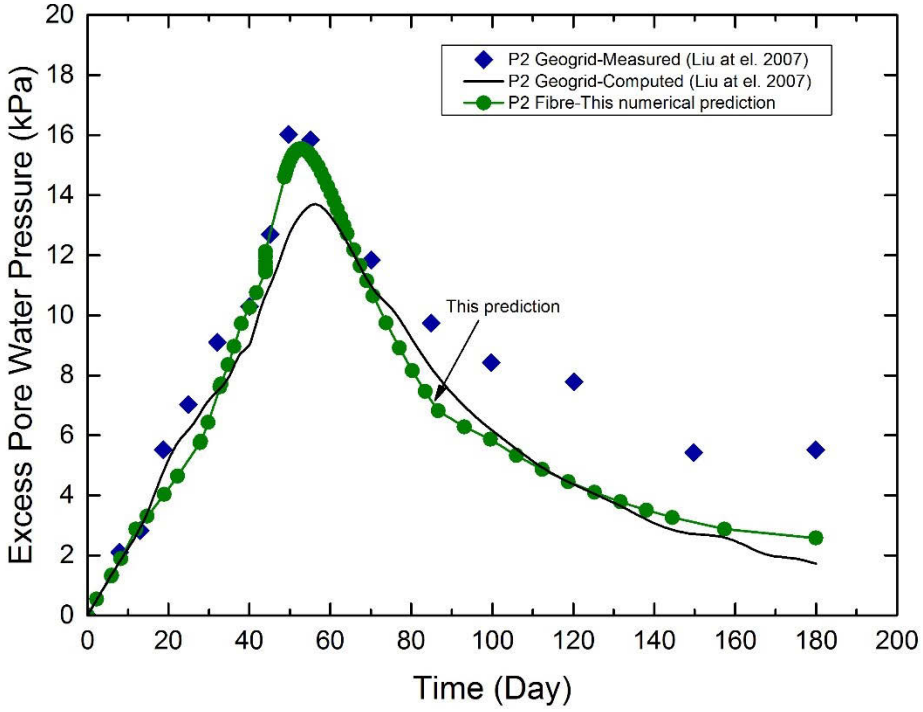

Figure 6.37 Comparison between measured and computed excess pore water pressure

6.5. SUMMARY

This chapter presents numerical investigations of three case studies on the performance of fibre reinforced load transfer platform (FRLTP) and deep cement mixing (DCM) columns or piles supported embankments constructed on soft soils. An equivalent two-dimensional (2D) plane strain finite element method (FEM) model was adopted to evaluate the behaviour of the embankment without or with FRLTP. An extensive parametric study on the full geometry of the DCM columns supported embankment was also numerically carried out to further investigate the influence of the FRLTP parameters such as the platform thickness, the elastic deformation modulus (Young's modulus) and the shear strength properties and the tensile strength, and the soft soil improvement depth on the performance of the embankment during construction and post-construction

periods. The predicted results have been analysed and discussed in detail. Some of the main findings of this numerical study can be summarised as follows:

- Comparing with the DCM columns supported embankment without FRLTP, the numerical results indicated that the application of the FRLTP combined with DCM columns supported embankment can minimise the total settlement significantly, meanwhile effectively alleviate the lateral displacement and consequently increase the stability of the entire embankment system built over multilayers of soft soils. Furthermore, the embankment with FRLTP can not only enhance the stress concentration ratio between DCM columns and surrounding soils to a great extent but also accelerate the consolidation progress subjected to embankment load.

- The findings of the parametric study confirm that the improvement depth ratio and the thickness of the FRLTP has significant effects on the total and differential settlements, the load transfer mechanism between DCM columns and foundation soils by means of the enhancement of the stress concentration ratio, and the lateral displacement of the embankment during the construction and post-construction times. Moreover, the elastic deformation modulus of the FRLTP had considerable effects on the differential settlement, the stress concentration ratio but showed a negligible effect on the lateral deformation of the investigated embankment.

- The numerical results derived from the parametric study on the shear strength properties also indicates that the cohesion and the internal friction angle of the FRLTP have significant effects on improving the lateral deformation, the stress concentration ratio and the differential settlement of the investigated embankment. However, the

improvement in the overall embankment behaviour dependent on the shear strength properties was more pronounced for the cohesion of the FRLTP.

- The predicted results of this numerical modelling reveal that the tensile strength of the FRLTP has considerable effects on the lateral displacement of the investigated embankment, but shows negative impacts on the SCR and the differential settlement.

- This numerical modelling also confirms that the application of eco-friendly and recycled fibre-lime reinforced soil can effectively be used as an alternative green load transfer platform combined with DCM columns supported embankments built on top of multilayered soft soils due to the significant improvement in the SCR, the total and differential settlements, and the lateral displacement of the examined embankment. It should be noted that this finding was primarily derived from the comparison between the columns supported embankments without and with FRLTP.

- Finally but most importantly, this numerical investigation has explored an interesting potential for making use of agricultural waste by-products such as coconut coir fibre, jute fibre and bagasse fibre as construction fill materials for sustainable civil infrastructure development.

CHAPTER 7: CONCLUSIONS AND RECOMMENDATIONS

7.1. SUMMARY

Expansive soils are originated from decomposed rocks mainly containing fine-grained particles that exhibit massive volume change against fluctuations of moisture content. Evaporation, rainwater, dewatering, waste and supply water pipe leak phenomena, just to name a few, are primarily responsible for changes in the moisture content. Shrinkage and expansion of soil can commonly take place near the ground surface, where it is instantaneously subjected to seasonal and environmental variations. The expansive soils are usually at unsaturated state and consist of montmorillonite clay minerals. Such clay minerals normally account for the main portion of the expansive soil, which highly yield the change in volume against the alteration of the moisture content. The severity of the damage induced by the expansive soil depends on the amount of monovalent cations absorbed in the clay minerals. Civil engineering structures such as highways, bridges, seaports and airports as well as residential buildings constructed on expansive soils are highly risky as this type of soil is susceptible to seasonal drying and wetting cycles, causing significant deformations. Frequent soil movements can generate cracks and the damage superstructures, roads, freeways, and other civil construction directly placed on this type of problematic soil. The average annual cost of damage to structures due to shrinkage and swelling is estimated about £400 million in the UK, $15 billion in the USA,

and many billions of dollars worldwide (Gourley et al. 1993; Jones & Jefferson 2012; Nelson & Miller 1997).

Lime stabilisation is the most commonly used method for controlling the shrink-swell behaviour of expansive soil due to seasonal variations. Lime reacts with expansive clay in the presence of water and changes the physicochemical properties of expansive soil, which in turn alters the engineering properties of treated soil. Moreover, soil improvement and reinforcement using lime combined with agricultural and industrial waste by-products such as fly ash, bagasse ash, rice husk ash, coconut coir fibre, recycled carpet fibre and bagasse fibre, just to name a few, can extend the effectiveness of lime stabilised expansive soil in terms of compressive strength, shear strength and ductility, bearing capacity and compressibility. Furthermore, the application of lime and waste by-products combination for expansive soil stabilisation can minimise the construction costs by curtailing lime usage, meanwhile facilitates effectively minimisation of the potential impacts on the environment for sustainable development and economic growth. This gains special attention from many researchers around the world in recent years in carrying out research for utilisation of the waste by-products in the area of infrastructure foundations.

Sugar-cane bagasse is obtained in abundant quantities from sugar-refining industry. After crushing of sugar-cane in sugar mills and extraction of juice from processed sugar-cane by milling, the discarded fibrous matter is called bagasse fibre (bagasse). Bagasse fibre has been used for many purposes as a combustible material for energy supply in sugar-cane factories, a pulp raw material in paper industries, and building materials like bagasse-cement composites, treated bagasse fibre reinforced

biodegradable composites. One of the popular applications of bagasse fibre is used as fuel in the cogeneration boiler to generate steam for the production of sugar as well as electricity. Bagasse is burnt at high temperature around 700°C to 900°C in a controlled process to use its maximum fuel value, while producing bagasse ash with high amorphous silica, low carbon content and high specific surface area. Generally, bagasse ash is disposed of in a landfill and now is becoming an environmental burden. However, it is well-documented in the literature that sugar-cane bagasse ash is classified as a pozzolanic material because it is rich in amorphous silica, which is effectively used together with hydrated lime as a replacement for cement or lime in improving the engineering properties of concrete or clayey soils, respectively. Meanwhile, bagasse fibre is an eco-friendly and low-cost material that has physical and mechanical properties similar to other natural fibres such as jute, sisal, pineapple and coir fibres. Hence, bagasse fibre has a high potential to be applied in the field of construction as building materials and reinforcing components for soil reinforcement in support of subgrade beneath pavements and roads.

In this experimental investigation, an attempt was made to investigate the possibility of utilising agricultural waste by-products such as bagasse ash and fibre without or with hydrated lime combination in improving the shrink-swell behaviour and other engineering characteristics of expansive soil. Meanwhile, other two main objectives consist of curtailing the agricultural and industrial waste by-products (i.e., bagasse ash and fibre) together with diminishing hydrated lime dosage to stabilise expansive soils for sustainable development. Several series of laboratory experiments have been performed consisting of compaction, linear shrinkage, swell potential, swelling pressure, unconfined compressive strength (UCS), indirect tensile strength, California bearing ratio (CBR),

consolidation, soil suction, and triaxial shear tests on untreated and treated expansive soil samples with different additive contents in line with various curing times of 3, 7, 28, and 56 days. Another extensive study, carried out on the microstructure development of untreated and treated expansive soils, have been using scanning electron microscopy (SEM), pH measurements, and Fourier transform infrared (FTIR) techniques. The outcomes of these experimental investigations were analysed and discussed to obtain a better understanding of the effects of the hydrated lime, bagasse ash, and bagasse fibre, and their combination on the shrink-swell behaviour, the compressive strength and stiffness, the bearing capacity, the brittleness, the ductility, and the compressibility characteristics of the untreated and treated expansive soil. It is worthy to note that the utilisation of hydrated lime combined with bagasse ash or bagasse fibre for expansive soil stabilised can be highly effective not only in improving the geotechnical properties of expansive soil, but also assist in hindering the influence of industrial waste by-products on the environment. This investigation has explored the potential use of eco-friendly waste materials, bagasse ash and fibre, for sustainable infrastructure development by means of reducing the consumption of conventional stabilisers, such as lime or cement, commonly adopted in expansive soil treatment.

Furthermore, numerical investigations were conducted to evaluate a possible practical application of eco-friendly, inexpensive, and recycled fibre-lime reinforced soil as a replacement of geosynthetic reinforced traditional angular load transfer platform layer combined with columns or piles supported embankments found on soft soils. The application of lime-fibre reinforced soils to be used as fibre reinforced load transfer platform (FRLTP) is feasible a novel ground modification technique in combination with

deep cement mixing (DCM) columns supported embankments placed over soft soils. Due to facts, the popular applications of the geosynthetic reinforced traditional angular platform over columns supported embankments built on top of soft soils have come up with many geotechnical difficulties, namely intolerable total and differential settlements, larger lateral earth pressure and displacement, local or global instability, and potential failures due to over bearing or bending capacity of DCM columns. Therefore, a novel ground modification technique utilising eco-friendly, low-cost and recycled materials as an FRLTP to be used a replacement of geosynthetic reinforced traditional angular platform layer and DCM columns supported embankments is required to overcome those aforementioned geotechnical difficulties.

Numerical investigations based on the finite element method (FEM) incorporated in PLAXIS were proposed and conducted. An equivalent 2D FEM model with proper modified parameters of structure and soil models has been adopted to investigate the performance of floating DCM columns or piles supported embankments (through three case studies) without or with FRLTP built on top of soft soils. First, a series of numerical analysis was performed on the full geometry of DCM columns supported (CS) embankment reinforced without or with an FRLTP in a 2D plane strain condition to examine the effectiveness of the FRLTP inclusion into the CS embankment system. Several essential parameters required from the design of a CS embankment such as maximum settlement and lateral displacement, generation and dissipation of excess pore water pressure or load transfer mechanism between columns and foundation soils, were investigated and discussed. Subsequently, several series of extensive parametric studies on the influence of FRLTP properties (e.g., the FRLTP thickness, the elastic deformation

modulus and the shear strength parameters), the improvement depth of soft soils, were carried out to assess the behaviour of the CS embankment with FRLTP. Results of the numerical investigations reveal that the introduction of FRLTP and DCM columns supported embankments can assist the higher embankment load transfer to DCM columns, while minimising the embankment load transfer to foundation soil between two adjacent DCM columns, and consequently mitigates the generation of excess pore water pressure in the soft soil stratum. As a result, the utilisation of FRLTP and DCM columns supported embankment prevents the total and differential settlements effectively, minimise the lateral displacement, whilst enhancing the rigidity and stability of the embankment in comparison with those of the CS embankment system without FRLTP. Therefore, this numerical investigation has explored an interesting potential for making use of agricultural waste by-products such as coconut coir fibre, bagasse fibre and jute fibre as components to reinforce load transfer platform combined with columns supported embankment for sustainable development in the area of infrastructure foundations.

7.2. CONCLUSIONS

7.2.1. Application of Bagasse Ash and Hydrated Lime Treated Expansive Soil

The main conclusions of this experimental investigation are summarised as follows:

- The findings of the experimental study indicated that the addition of bagasse ash and hydrated lime had significant influences on the geotechnical properties of stabilised expansive soils. Based on the results of pH measurements, it was found that about 5% hydrated lime was the optimum lime content to stabilise expansive soil, which required for cation exchanges between soil particles and lime to take place, meanwhile

18% hydrated lime-bagasse ash combination were experimentally determined as the optimum additive combination for expansive soil stabilisation. The standard compaction results showed that compared with untreated soil, the maximum dry density (MDD) of soils stabilised with bagasse ash (BA), hydrated lime (L), and the BA+L combination decreased as the additive content increased.

- The unconfined compressive strength (UCS) of treated soils greatly increased when additive content and curing time increased. The strength development of soils treated with BA+L was certainly higher than that of bagasse ash, hydrated lime alone treated soils. Moreover, soils treated with BA+L combination exhibited more ductile behaviour than hydrated lime alone treated soils. Inspection of the UCS results of treated soils with curing time revealed that the strength increased significantly during the first 7 days of curing followed by a gradual increase in strength with further curing time up to 28 days. It is important to note that after 28 days of curing, the compressive strength remained almost constant for soils treated with hydrated lime alone, meanwhile the strength of BA+L treated soils continued to develop up to 56 days of curing. The low quantity of employed stabilisers had a little effect on the strength gain of stabilised soil with time. The low compressive strength gain with time might be due to inadequate free lime available in bagasse ash or BA+L admixtures necessarily to accelerate the activity of pozzolan to form cementitious compounds that play a key role in binding clay aggregates together as well as improving the strength of stabilised soils with time.

- Adding hydrated lime into soil mixtures resulted in the significant improvement in the obtained secant modulus (stiffness) during the first 7 days of curing, the increment

of the secant modulus with the further increase in curing time up to 28 days was less noticeable than that of the first 7 days of curing. However, the secant modulus of only BA or BA+L stabilised soils increased steadily during the 28 days of curing period.

- The results of the CBR tests indicated that the CBR value of stabilised soil increased significantly as the additive content and curing time increased. The addition of bagasse ash into lime-soil mixtures would not produce an adverse effect on the strength and bearing capacity of the lime stabilised soil. In general, the 6% BA+L stabilised soil could easily satisfy the minimum 15% CBR requirements adopted by most of the selected subgrade design guidelines. Meanwhile, the higher contents of BA+L in stabilised soil could easily meet the CBR requirement for subbase course materials.

- The linear shrinkage, swelling strain, free swell potential, and swelling pressure of BA+L stabilised soils were significantly improved in comparison with that of soils stabilised bagasse ash or hydrated lime alone. The improvement in the shrink-swell behaviour of stabilised soils could be due to flocculation and aggregation of modified clay particles in the short term together with the new cementitious products attached to the bagasse ash and clay particles because of pozzolanic reactions. Such modification and pozzolanic reactions changed the soil particles to be coarser and stronger, decreased the plasticity of the specific surface of soil particles, and eventually enhanced the strength of the treated soil. In other words, the finer clay particles were substituted by relatively stronger and coarser particles that could be the key factors resulting in the considerable decrease in shrinkage and expansion of the treated soil samples with time.

- The addition of hydrated lime stabilised expansive soil combined with bagasse ash resulted in the remarkable influence on the compression curve and compression index of stabilised soil. When BA+L content increased, the compressibility characteristics of treated soils significantly reduced. The lowest slope of the compression curve was visually observed for 25% BA+L treated soil, while the highest reduction in compression index (C_c) was achieved for the 18% BA+L stabilised soils within the high pressure applied ranging between 400 kPa and 600 kPa.

- Based on the results of The FTIR analysis, the obtained FTIR spectra of untreated soil and hydrated lime or BA+L treated with soil samples confirmed the appearance of a broad band of Si-O-Si in the range between 600 and 1500 cm^{-1}. The prominent difference in the transmittance percentages at around 1000 cm^{-1} of the untreated soil, hydrated lime, and BA+L treated soil samples revealed the change in microstructure or the formation of new cementitious compounds of Calcium-Silicate-Hydrate (C-S-H). Furthermore, the SEM results indicated the formation of cementitious products (i.e., CSH, CAH or CASH) as a result of the time-dependent pozzolanic reactions between clay or bagasse ash particles together with hydrated lime could be primarily responsible for the strength development and the stiffness improvement as well as the enhanced other geotechnical properties of treated soils.

7.2.2. Application of Hydrated Lime and Bagasse Fibre Reinforced Expansive Soil

The key conclusions that were drawn, based on the experimental results, are as follows:

- The standard compaction results revealed that the MDD of soil samples treated with bagasse fibre gradually decreased as the bagasse fibre content increased from 0% to

2%. The MDD of bagasse fibre reinforced soils combined with hydrated lime decreased further as the hydrated lime content increased from 0% to 6%. The lower specific gravity of bagasse fibre together with the larger spaces occupied in the soil matrix because of the flocculation and agglomeration of soil stabilisation with lime could be the main reasons resulting in the MDD reduction of stabilised soils as additive content increased. The tiny air gaps trapped into fibre surface could cause the MDD decrease of lime-fibre-soil mixtures.

- Based on the obtained results of the linear shrinkage tests, with the introduction of bagasse fibre reinforced expansive soils without or with lime treatment, it was observed that the reduction of linear shrinkage was significant with increasing additive contents and curing time. The remarkable improvement was more noticeable for the combined hydrated lime-bagasse fibre reinforced soils than only bagasse fibre or hydrated lime treated expansive soils.

- From the UCS test results conducted on soil samples reinforced with only bagasse fibre, the initial stiffness and the peak strength of reinforced soils improved with the inclusion of bagasse fibre, meanwhile changed the reinforced soil behaviour from strain softening to strain hardening by reducing the loss of the post-peak strength. The UCS value of soils reinforced with bagasse fibre alone increased as the fibre content and curing time increased. However, the UCS improvement of bagasse fibre reinforced soil was insignificant as curing time exceeded 7 days. The strength improvement of only bagasse fibres reinforcement of soil could be attributed to the interaction and interlocking mechanism between fibre surface and soil particles

developed during specimen preparation process by the compactive effort and with age.

- The compressive strength development was certainly higher for lime treated soils reinforced with bagasse fibre than the strength of soils reinforced with bagasse fibre or hydrated lime alone treated soil without fibre reinforcement. An increase in hydrated lime content from 4% to 6% caused the marked increased in the brittleness index I_B of stabilised soil, but I_B significantly decreased with the inclusion of bagasse fibre content into lime-soil mixtures increased from 0% to 2%. This behaviour obviously confirmed that the bagasse fibre reinforcement had a notable influence on the ductility of lime treated soils, which changed the stabilised soil behaviour from brittle to more and more ductile one, by diminishing the brittleness index (I_B) significantly. The loss of the post-peak compressive strength was significantly improved as a result of the brittleness index decrease of lime treated soil with bagasse fibre reinforcement.

- The obtained results of the indirect tensile strength tests showed that when comparing with untreated soil, the tensile strength of stabilised soils significantly increased with the addition of lime into soils. Moreover, adding bagasse fibre into the 4% lime-soil mixtures increased the tensile strength but decreased the stiffness of treated soils. However, adding a higher lime content (i.e., 6% lime) to stabilise soil, the inclusion of bagasse fibre into the limed soils enhanced the tensile strength, but the stabilised soil stiffness remained almost unchanged when compared with that of 6% lime treated soil without fibre reinforcement. It is concluded that the brittle behaviour seemed to

be the dominant mechanism for 6% lime stabilised soil with bagasse fibre reinforcement.

- From the result analysis of the CBR tests, it was found that the CBR of lime treated soil increased steadily when the addition of bagasse fibre content increased from 0% to 2%. For soil samples reinforced with only bagasse fibre, the CBR value increased slightly as bagasse fibre content increased up to 2%. However, it observed that the CBR increase was certainly more remarkable for soil samples treated with lime-bagasse fibre combination than for samples reinforced with bagasse fibre or hydrated lime alone.

- Observation of the measured results of free swell potential and swelling pressure tests noted that a combination of bagasse fibre and lime for expansive soil stabilisation resulted in the significant improvement in the swelling behaviour of expansive soil. The addition of a relatively small content of 2.5% lime-0.5% bagasse fibre could result in non-swelling of treated soil. The swelling behaviour of expansive soil treated with bagasse fibre and lime combined was considerably improved because expansive soil stabilization with lime changed the physical and chemical properties of clay particles, as a consequence of cation exchange between lime and clay particles. This phenomenon transformed the clay particles to coarser and stronger, more brittle and less plastic, which promoted the better swelling resistance. Furthermore, when bagasse fibre was added to lime-soil mixtures, expansive clay was substituted with non-expansive bagasse fibre and the development of interaction and interlocking mechanism between clay particles and fibre surface could improve the effectiveness of the swelling resistance of lime treated soil with bagasse fibre reinforcement.

- From the obtained results of the 1D consolidation tests, it was noted that the compressible properties of expansive soil reinforced with bagasse fibre reduced as lime content increased from 0% to 4% followed by the slight compressibility increase with further inclusion of lime content up to 6%. Meanwhile, the compressibility properties of soils treated with lime decreased as bagasse fibre content increased from 0% to 1% but then it increased with further increase in bagasse fibre inclusion greater than 1%.

- Analysis of the soil suction tests using contact filter paper technique found that the inclusions of lime and bagasse fibre had a significant influence on the soil-water characteristic curves (SWCC) of stabilised expansive soil. By comparing with untreated soils, the SWCC appeared to improve as the additions of 4% lime combined with bagasse fibre inclusion increased from 0% to 2%. Analysing the air entry values (AEV) of soils treated with combined lime-bagasse fibre showed that the addition of 4% lime into soil resulted in the AEV increase. Whereas, the addition of 4% lime combined with an increase in fibre content from 0% to 2.0% slightly decreased the AEV. This behaviour implies that the presence of bagasse fibre reinforcement had a negative impact on the water retention capacity of stabilised soils, but the negative impact was insignificant. The AEV improvement of stabilised soils could be mainly contributed from the alteration of a small fraction of clay as well as the enhancement of pore size distribution of the soil caused by lime stabilisation.

- From the triaxial compression tests, it was found that bagasse fibre reinforcement of expansive soil enhanced the initial deformation modulus and the peak deviatoric strength, and changed the reinforced soil behaviour from strain softening to strain

hardening by minimising the loss of post-peak shear strength. It can also be noted that at a low confining pressure of 50 kPa, the deviatoric strength of soils reinforced with bagasse fibre reached a peak in a low deviatoric strain level between 0.5% and 1%. Meanwhile, the peak deviatoric strength was found in a range of 1% to 3% axial strain with a further increase in the confining pressure up to 200 kPa. With increasing bagasse fibre content from 0% to 2% to reinforce expansive soil, the peak internal friction angle increased from 19.5° to 28°, meanwhile the corresponding cohesion increased from about 10 kPa to 14 kPa. However, the shear strength development was certainly more remarkable for the peak internal friction angle.

- The SEM analysis showed that compared lime treated soils, the improvement in the soil strength, the bearing capacity and the other geotechnical characteristics of lime treated soils with bagasse fibre reinforcement were mainly because of the high tensile strength of bagasse fibre and the stronger interfacial friction and interlocking mechanism between fibre surface, cementitious bonds and clay particles in the lime-fibre-soil matrix.

- Based on the findings of this experimental investigation, it can be concluded that the utilisation of hydrated lime-bagasse fibre combination in expansive soil stabilisation could not only improve the engineering properties of expansive soil but also minimise the environmental impacts of agricultural waste by-product such as bagasse fibre and the construction costs because of reduction of lime usage. This experimental study provides a detailed insight into promoting the applications of agricultural waste by-products such as bagasse fibre as a reinforcing component in construction fill materials for sustainable development in the area of infrastructure foundations.

7.2.3. Numerical Simulations on the Behaviour of FRLTP and Columns Supported Embankments

The predicted results of the numerical simulations of three case studies of the CS embankment without or with FRLTP were analysed and comprehensively discussed. The main findings of this numerical modelling are summarised as follows:

- The numerical results indicate that the application of the FRLTP combined with DCM columns supported embankment can minimise the total settlement and the lateral displacement significantly, and hence increase the stability of the entire embankment system built over multilayers of soft soils, compared with the CS embankment without FRLTP. In addition, the embankment with FRLTP can not only enhance the load transfer mechanism between DCM columns and surrounding soils effectively but also accelerate the consolidation progress of soft soil strata subjected to embankment load.

- Analysing the predicted results of the parametric study corroborates that the FRLTP thickness has significant effects on the total and differential settlements, the lateral deformation as well as the load transfer mechanism between DCM columns and foundation soils of a CS embankment. In addition, Young's modulus of the FRLTP has considerable effects on the differential settlement, the stress concentration ratio, but shows a negligible effect on the lateral deformation of the investigated embankment.

- From the extensive parametric study, it is found that the improvement depth has substantial impacts on the final settlement and the lateral deformation on the embankment during the embankment construction and post-construction time.

However, the influence on the stress concentration ratio and the differential settlement of a CS embankment with FRLTP is likely to be insignificant when compared with the final settlement and the lateral deformation as the improvement depth ratio (β) increases from 0.5 to 1.

- The predicted results of the parametric study also reveal that the FRLTP shear strength parameters (i.e. the internal friction angle and cohesion) show significant influences on the stress concentration ratio, the differential settlement, and the lateral displacement of the embankment. Nonetheless, the enhancement in the overall performance of a CS embankment with FRLTP is more noticeable for the cohesion than the internal friction angle of the FRLTP.

- The numerical modelling shows that a replacement of geosynthetic reinforced traditional angular LTP layer with FRLTP combined with DCM columns supported embankments constructed on multilayers of soft soils can be a possible practical application because of the significant enhancement in the investigated embankment performance. It is important to note that this numerical investigation has explored an interesting potential for making use of agricultural waste by-products consisting of eco-friendly, inexpensive, and recycled fibres (e.g. bagasse fibre, coconut coir fibre or jute fibre) as construction fill materials for sustainable development of the civil infrastructure foundations.

7.3. RECOMMENDATIONS FOR FUTURE INVESTIGATIONS

From analysing the results of the experimental and numerical investigations, several recommendations are highlighted below for future investigations

- Another series of comprehensive microstructure investigations can be conducted to examine and quantify the physiochemical development (i.e. pore size distribution, particle size distribution, specific surface area, formation of new cementitious products, chemical composition) and the mineralogical changes of lime treated soil without or with bagasse ash or bagasse fibre.

- Since bagasse fibre is a type of natural fibres that can be degradable with time, so the effects of fibre degradation, the durability improvement of bagasse fibre using chemical treatment, (i.e. sodium hydroxide, sodium silica, sodium sulphite) and/or coating (asphalt emulsion, rosin-alcohol, acrylic, polystyrene, and silane) to prevent water absorption, and the enhancement in the interaction between bagasse fibre and limed soil matrix are required further investigations. Similarly, the degradable effects on the performance of combined bagasse ash-hydrated lime treated soils need to be investigated further.

- Further experimental investigations, subjected to cyclic and dynamic loading conditions and variations of curing temperatures, should be performed to investigate the behaviour of lime treated soils with randomly distributed bagasse fibre or bagasse ash.

- The combined effects of bagasse ash-hydrated lime treated soils together with bagasse fibre reinforcement on the engineering properties of treated soils can be investigated to compare with the measured test results in this investigation. This will enable to gain a better understanding as well as provide a possible option for utilising waste by-products for expansive soil stabilisation with lime.

- Further numerical investigations are required to assess the efficiency and the interaction between DCM columns, FRLTP and soft foundation soils varied with the other properties of the columns stiffness, the stiffness and permeability of soft soil layers, and the columns distance ratio, during embankment construction and serviceability.

- Numerical modelling of FRLTP with different advanced constitutive models such as the hardening soil model, modified Cam-clay model or a user-defined soil model implemented in PLAXIS to simulate the behaviour of fibre and lime treated soils when taking into account the degradation of cementitious products and the failure mechanism of fibre reinforcement of clayey soils, can be conducted. The numerical modelling of the FRLTP using the advanced constitutive soil models may enable to simulate the more realistic behaviour of lime-fibre reinforced soils to be used as an FRLTP when comparing with the Mohr-Coulomb model adopted in this numerical study. Consequently, it may impart a deeper understanding, and a more precise prediction of the behaviour of the DCM columns supported embankment with FRLTP.

- A full-scale model test in the construction field or a small-scale, physical model of the CS embankment with FRLTP in the laboratory should be carried out to examine the reliable prediction of the proposed model for numerical simulations.

REFERENCES

Abduljauwad, S.N. 1993, 'Treatment of calcareous expansive clays', *FLY ASH FOR SOIL IMPROVEMENT*, ed. K.D. Sharp, vol. Geotechnical Special Publication 36, ASCE, New York, USA, pp. 100-15.

Ahmed, A., Ugai, K. & Kamei, T. 2011, 'Investigation of recycled gypsum in conjunction with waste plastic trays for ground improvement', *Construction and Building Materials*, vol. 25, no. 1, pp. 208-17.

Aiban, S.A. 2006, 'Compressibility and swelling characteristics of Al-Khobar Palygorskite, eastern Saudi Arabia', *Engineering Geology*, vol. 87, no. 3–4, pp. 205-19.

Al-Mukhtar, M., Khattab, S. & Alcover, J.F. 2012, 'Microstructure and geotechnical properties of lime-treated expansive clayey soil', *Engineering Geology*, vol. 139–140, pp. 17-27.

Al-Rawas, A.A., Hago, A.W. & Al-Sarmi, H. 2005, 'Effect of lime, cement and Sarooj (artificial pozzolan) on the swelling potential of an expansive soil from Oman', *Building and Environment*, vol. 40, no. 5, pp. 681-7.

Alavéz-Ramírez, R., Montes-García, P., Martínez-Reyes, J., Altamirano-Juárez, D.C. & Gochi-Ponce, Y. 2012, 'The use of sugarcane bagasse ash and lime to improve the durability and mechanical properties of compacted soil blocks', *Construction and Building Materials*, vol. 34, no. 0, pp. 296-305.

Aldaood, A., Bouasker, M. & Al-Mukhtar, M. 2014a, 'Free swell potential of lime-treated gypseous soil', *Applied Clay Science*, vol. 102, no. 0, pp. 93-103.

Aldaood, A., Bouasker, M. & Al-Mukhtar, M. 2014b, 'Impact of wetting–drying cycles on the microstructure and mechanical properties of lime-stabilized gypseous soils', *Engineering Geology*, vol. 174, no. 0, pp. 11-21.

Alsafi, S., Farzadnia, N., Asadi, A. & Huat, B.K. 2017, 'Collapsibility potential of gypseous soil stabilized with fly ash geopolymer; characterization and assessment', *Construction and Building Materials*, vol. 137, pp. 390-409.

Anggraini, V., Asadi, A., Farzadnia, N., Jahangirian, H. & Huat, B. 2016, 'Reinforcement Benefits of Nanomodified Coir Fiber in Lime-Treated Marine Clay', *Journal of Materials in Civil Engineering*, vol. 0, no. 0, p. 06016005.

Anggraini, V., Asadi, A., Farzadnia, N., Jahangirian, H. & Huat, B.B.K. 2015a, 'Effects of coir fibres modified with $Ca(OH)_2$ and $Mg(OH)_2$ nanoparticles on mechanical properties of lime-treated marine clay', *Geosynthetics International*, vol. 0, no. 0, pp. 1-13.

Anggraini, V., Asadi, A., Huat, B.B.K. & Nahazanan, H. 2015b, 'Performance of Chemically Treated Natural Fibres and Lime in Soft Soil for the Utilisation as Pile-Supported Earth Platform', *International Journal of Geosynthetics and Ground Engineering*, vol. 1, no. 3, pp. 1-14.

Anupam, A.K., Kumar, P. & Ransinchung, G.D. 2013, 'Use of Various Agricultural and Industrial Waste Materials in Road Construction', *Procedia - Social and Behavioral Sciences*, vol. 104, pp. 264-73.

Ariyarathne, P., Liyanapathirana, D. & Leo, C. 2013, 'Comparison of Different Two-Dimensional Idealizations for a Geosynthetic-Reinforced Pile-Supported Embankment', *International Journal of Geomechanics*, vol. 13, no. 6, pp. 754-68.

AS 1993, *Geotechnical Site Investigations*, AS 1726-1993, Standards Australia, Sydney, Australia.

AS 1998, *Determination of the one-dimensional consolidation properties of a soil - Standard method*, AS 1289.6.6.1-1998, Standards Australia, Sydney, Australia.

AS 2000, *Methods of testing concrete - Determination of indirect tensile strength of concrete cylinders (Brasil or splitting test)*,

AS 1012.10-2000 (R2014), Standards Australia, Sydney, Australia.

AS 2001, *Methods of testing soils for engineering purposes - Sampling and preparation of soils - Preparation of disturbed soil samples for testing* AS 1289.1.1, Standards Australia, Sydney, Australia.

AS 2008a, *Methods for preparation and testing of stabilized materials - Unconfined compressive strength of compacted materials* AS 5101.4-2008 Standards Australia, Sydney, Australia.

AS 2008b, *Soil classification test-Determination of the linear shrinkage of a soil-Standard method* AS 1289.3.4.1-2008, Standards Australia, Sydney, Australia.

AS 2014, *Determination of the California Bearing Ratio of a soil - Standard laboratory method for a remoulded specimen*, AS 1289.6.1.1-2014, Standards Australia, Sydney, Australia.

AS 2017, *Determination of the dry density/moisture content relation of a soil using standard compactive effort*, AS 1289.5.1.1:2017, Standards Australia, Sydney, Australia.

ASTM 2015, *Standard Specification for Coal Fly Ash and Raw or Calcined Natural Pozzolan for Use in Concrete*, ASTM C618-15, ASTM International standard, West Conshohocken, PA.

ASTM 2016, *Standard Test Method for Measurement of Soil Potential (Suction) Using Filter Paper*, ASTM D5298-16, ASTM International, West Conshohocken, PA.

Ayeldeen, M. & Kitazume, M. 2017, 'Using fiber and liquid polymer to improve the behaviour of cement-stabilized soft clay', *Geotextiles and Geomembranes*, vol. 45, no. 6, pp. 592-602.

Bahar, R., Benazzoug, M. & Kenai, S. 2004, 'Performance of compacted cement-stabilised soil', *Cement and Concrete Composites*, vol. 26, no. 7, pp. 811-20.

Bahmani, S.H., Farzadnia, N., Asadi, A. & Huat, B.B.K. 2016, 'The effect of size and replacement content of nanosilica on strength development of cement treated residual soil', *Construction and Building Materials*, vol. 118, pp. 294-306.

Bahmani, S.H., Huat, B.B.K., Asadi, A. & Farzadnia, N. 2014, 'Stabilization of residual soil using SiO2 nanoparticles and cement', *Construction and Building Materials*, vol. 64, pp. 350-9.

Bahurudeen, A., Marckson, A.V., Kishore, A. & Santhanam, M. 2014, 'Development of sugarcane bagasse ash based Portland pozzolana cement and evaluation of compatibility with superplasticizers', *Construction and Building Materials*, vol. 68, no. 0, pp. 465-75.

Bahurudeen, A. & Santhanam, M. 2014, 'Performance Evaluation of Sugarcane Bagasse Ash-Based Cement for Durable Concrete', *Proceedings of 4th International Conference on the Durability of Concrete Structures*, pp. 275-81.

Bahurudeen, A., Wani, K., Basit, M.A. & Santhanam, M. 2016, 'Assesment of Pozzolanic Performance of Sugarcane Bagasse Ash', *Journal of Materials in Civil Engineering*, vol. 28, no. 2, p. 04015095.

Basha, E.A., Hashim, R., Mahmud, H.B. & Muntohar, A.S. 2005, 'Stabilization of residual soil with rice husk ash and cement', *Construction and Building Materials*, vol. 19, no. 6, pp. 448-53.

Bell, F.G. 1996, 'Lime stabilization of clay minerals and soils', *Engineering Geology*, vol. 42, no. 4, pp. 223-37.

Bergado, D., Anderson, L., Miura, N. & Balasubramaniam, A. 1996, 'Soft ground improvement in lowland and other environments', ASCE.

Bhadriraju, V., Puppala, A.J., Enayatpour, S. & Pathivada, S. 2005, 'Digital Imaging Technique to Evaluate Shrinkage Strain Potentials of Fiber Reinforced Expansive Soils', *Site Characterization and Modeling*, vol. GSP 138.

Bilba, K. & Arsene, M.A. 2008, 'Silane treatment of bagasse fiber for reinforcement of cementitious composites', *Composites Part A: Applied Science and Manufacturing*, vol. 39, no. 9, pp. 1488-95.

Bilba, K., Arsene, M.A. & Ouensanga, A. 2003, 'Sugar cane bagasse fibre reinforced cement composites. Part I. Influence of the botanical components of bagasse on the setting of bagasse/cement composite', *Cement and Concrete Composites*, vol. 25, no. 1, pp. 91-6.

Bishop, A.W. 1959, 'The principle of effective stress', *Tecknish Ukeblad*, vol. 106, no. 39, pp. 859–63.

Boardman, D.I., Glendinning, S. & Rogers, C.D.F. 2001, 'Development of stabilisation and solidification in lime–clay mixes', *Géotechnique*, vol. 51, pp. 533-43.

Boone, S.J. 2010, 'A critical reappraisal of “preconsolidation pressure” interpretations using the oedometer test', *Canadian Geotechnical Journal*, vol. 47, no. 3, pp. 281-96.

Brooks, R., Udoeyo, F. & Takkalapelli, K. 2011, 'Geotechnical Properties of Problem Soils Stabilized with Fly Ash and Limestone Dust in Philadelphia', *Journal of Materials in Civil Engineering*, vol. 23, no. 5, pp. 711-6.

Bulut, R. & Leong, E.C. 2008, 'Indirect measurement of suction', *Geotechnical and Geological Engineering*, vol. 26, no. 6, pp. 633-44.

Bulut, R., Lytton, R.L. & Wray, W.K. 2001, 'Soil suction measurements by filter paper', *Expansive Clay Soils and Vegetative Influence on Shallow Foundations*, ASCE, pp. 243-61.

Cai, Y., Shi, B., Ng, C.W.W. & Tang, C.-s. 2006, 'Effect of polypropylene fibre and lime admixture on engineering properties of clayey soil', *Engineering Geology*, vol. 87, no. 3-4, pp. 230-40.

Cao, Y., Shibata, S. & Fukumoto, I. 2006, 'Mechanical properties of biodegradable composites reinforced with bagasse fibre before and after alkali treatments', *Composites Part A: Applied Science and Manufacturing*, vol. 37, no. 3, pp. 423-9.

Cardoso, R. & Maranha das Neves, E. 2012, 'Hydro-mechanical characterization of lime-treated and untreated marls used in a motorway embankment', *Engineering Geology*, vol. 133–134, pp. 76-84.

CDIT 2002, *The Deep Mixing Method: Principle, Design and Construction*, CRC Press/Balkema The Netherlands.

Celik, E. & Nalbantoglu, Z. 2013, 'Effects of ground granulated blastfurnace slag (GGBS) on the swelling properties of lime-stabilized sulfate-bearing soils', *Engineering Geology*, vol. 163, pp. 20-5.

Chai, J.-C., Shrestha, S., Hino, T., Ding, W.-Q., Kamo, Y. & Carter, J. 2015, '2D and 3D analyses of an embankment on clay improved by soil–cement columns', *Computers and Geotechnics*, vol. 68, pp. 28-37.

Chai, J.-c., Shrestha, S., Hino, T. & Uchikoshi, T. 2017, 'Predicting bending failure of CDM columns under embankment loading', *Computers and Geotechnics*, vol. 91, pp. 169-78.

Chen, F.H. 1988, *Foundations on expansive soils*, Amsterdam: Elsevier.

Chen, L. & Lin, D.-F. 2009, 'Stabilization treatment of soft subgrade soil by sewage sludge ash and cement', *Journal of Hazardous Materials*, vol. 162, no. 1, pp. 321-7.

Chen, Q. & Indraratna, B. 2014, 'Shear behaviour of sandy silt treated with lignosulfonate', *Canadian Geotechnical Journal*, vol. 52, no. 8, pp. 1180-5.

Chew, S., Kamruzzaman, A. & Lee, F. 2004, 'Physicochemical and Engineering Behavior of Cement Treated Clays', *Journal of Geotechnical and Geoenvironmental Engineering*, vol. 130, no. 7, pp. 696-706.

Chusilp, N., Jaturapitakkul, C. & Kiattikomol, K. 2009a, 'Utilization of bagasse ash as a pozzolanic material in concrete', *Construction and Building Materials*, vol. 23, no. 11, pp. 3352-8.

Chusilp, N., Likhitsripaiboon, N. & Jaturapitakkul, C. 2009b, 'Development of bagasse ash as a pozzolanic material in concrete ', *Asian Journal on Energy and Environment*, vol. 10, no. 02, pp. 149-59.

Çokça, E. 2001, 'Use of Class C Fly Ashes for the Stabilization of an Expansive Soil', *Journal of Geotechnical and Geoenvironmental Engineering*, vol. 127, no. 7, pp. 568-73.

Cong, M., Longzhu, C. & Bing, C. 2014, 'Analysis of strength development in soft clay stabilized with cement-based stabilizer', *Construction and Building Materials*, vol. 71, pp. 354-62.

Considine, M.L. 1984, 'Soils shrink, trees drink, and houses crack', *Ecos: CSIRO Environmental Research*, vol. 41, pp. 13-5.

Consoli, N., Festugato, L., Consoli, B. & da Silva Lopes, L., Jr. 2015, 'Assessing Failure Envelopes of Soil–Fly Ash–Lime Blends', *Journal of Materials in Civil Engineering*, vol. 27, no. 5, p. 04014174.

Consoli, N.C., Casagrande, M.D.T., Thomé, A., Rosa, F.D. & Fahey, M. 2009a, 'Effect of relative density on plate loading tests on fibre-reinforced sand', *Géotechnique*, vol. 59, no. 5, pp. 471-6.

Consoli, N.C., Vendruscolo, M.A., Fonini, A. & Rosa, F.D. 2009b, 'Fiber reinforcement effects on sand considering a wide cementation range', *Geotextiles and Geomembranes*, vol. 27, no. 3, pp. 196-203.

Cordeiro, G.C., Toledo Filho, R.D., Tavares, L.M. & Fairbairn, E.d.M.R. 2009, 'Ultrafine grinding of sugar cane bagasse ash for application as pozzolanic admixture in concrete', *Cement and Concrete Research*, vol. 39, no. 2, pp. 110-5.

Cordeiro, G.C., Toledo Filho, R.D., Tavares, L.M. & Fairbairn, E.M.R. 2008, 'Pozzolanic activity and filler effect of sugar cane bagasse ash in Portland cement and lime mortars', *Cement and Concrete Composites*, vol. 30, no. 5, pp. 410-8.

Correia, A.A.S., Oliveira, P.J.V. & Custódio, D.G. 2015, 'Effect of polypropylene fibres on the compressive and tensile strength of a soft soil, artificially stabilised with binders', *Geotextiles and Geomembranes*, vol. 43, no. 2, pp. 97-106.

Dang, L.C., Dang, C., Fatahi, B. & Khabbaz, H. 2016a, 'Numerical Assessment of Fibre Inclusion in a Load Transfer Platform for Pile-Supported Embankments over Soft Soil', *Geo-China 2016*, eds D. Chen, J. Lee & W.J. Steyn, vol. GSP 266, ASCE, pp. 148-55.

Dang, L.C., Dang, C.C. & Khabbaz, H. 2017a, 'Behaviour of Columns and Fibre Reinforced Load Transfer Platform Supported Embankments Built on Soft Soil', *the 15th International Conference of the International Association for Computer Methods and Advances in Geomechanics*, Wuhan, China.

Dang, L.C., Dang, C.C. & Khabbaz, H. 2018, 'Numerical Analysis on the Performance of Fibre Reinforced Load Transfer Platform and Deep Mixing Columns Supported Embankments', in M. Bouassida & M.A. Meguid (eds), *Ground Improvement and Earth Structures*, Springer, Cham, pp. 157-69.

Dang, L.C., Fatahi, B. & Khabbaz, H. 2016b, 'Behaviour of Expansive Soils Stabilized with Hydrated Lime and Bagasse Fibres', *Procedia Engineering*, vol. 143, pp. 658-65.

Dang, L.C., Hasan, H., Fatahi, B., Jones, R. & Khabbaz, H. 2016c, 'Enhancing the Engineering Properties of Expansive Soil Using Bagasse Ash and Hydrated Lime', *International Journal of GEOMATE*, vol. 11, no. 25, pp. 2447-54.

Dang, L.C., Hasan, H., Fatahi, B. & Khabbaz, H. 2015, 'Influence of Bagasse Ash and Hydrated Lime on Strength and Mechanical Behaviour of Stabilised Expansive Soil', *the 68th Canadian Geotechnical Conference and the 7th Canadian Permafrost Conference, (GEOQuébec 2015)*, Canadian Geotechnical Society, Québec City, Canada.

Dang, L.C. & Khabbaz, H. 2018a, 'Assessment of the Geotechnical and Microstructural Characteristics of Lime Stabilised Expansive Soil with Bagasse Ash', *the 71st*

Canadian Geotechnical Conference and the 13th Joint CGS/IAH-CNC Groundwater Conference (GeoEdmonton 2018), Canadian Geotechnical Society, Alberta, Canada.

Dang, L.C. & Khabbaz, H. 2018b, 'Enhancing the Strength Characteristics of Expansive Soil Using Bagasse Fibre', in W. Wu & H.-S. Yu (eds), *Proceedings of China-Europe Conference on Geotechnical Engineering. Springer Series in Geomechanics and Geoengineering*, Springer, Cham, pp. 792-6.

Dang, L.C. & Khabbaz, H. 2018c, 'Shear Strength Behaviour of Bagasse Fibre Reinforced Expansive Soil', *IACGE2018*, vol. Geotechnical Special Publications, ASCE, Chongqing, China.

Dang, L.C. & Khabbaz, H. 2019, 'Experimental Investigation on the Compaction and Compressible Properties of Expansive Soil Reinforced with Bagasse Fibre and Lime', in J.S. McCartney & L.R. Hoyos (eds), *Recent Advancements on Expansive Soils*, Springer, Cham, pp. 64-78.

Dang, L.C., Khabbaz, H. & Fatahi, B. 2017b, 'Evaluation of Swelling Behaviour and Soil Water Characteristic Curve of Bagasse Fibre and Lime Stabilised Expansive Soil', *PanAm-UNSAT 2017*, vol. GSP 303, ASCE, Texas, USA, pp. 58-70.

Dang, L.C., Khabbaz, H. & Fatahi, B. 2017c, 'An Experimental Study on Engineering Behaviour of Lime and Bagasse Fibre Reinforced Expansive Soils', *19th International Conference on Soil Mechanics and Geotechnical Engineering (19th ICSMGE)*, ISSMGE, Seoul, Republic of Korea, pp. 2497-500.

Dash, S. & Hussain, M. 2012, 'Lime Stabilization of Soils: Reappraisal', *Journal of Materials in Civil Engineering*, vol. 24, no. 6, pp. 707-14.

Eades, J.L. & Grim, R.E. 1966, 'A quick test to determine lime requirements for lime stabilization', *Highway Research Record*, no. 139.

Elkady, T., Al-Mahbashi, A. & Al-Refeai, T. 2015, 'Stress-Dependent Soil-Water Characteristic Curves of Lime-Treated Expansive Clay', *Journal of Materials in Civil Engineering*, vol. 27, no. 3, p. 04014127.

Ene, E. & Okagbue, C. 2009, 'Some basic geotechnical properties of expansive soil modified using pyroclastic dust', *Engineering Geology*, vol. 107, no. 1–2, pp. 61-5.

Estabragh, A.R., Rafatjo, H. & Javadi, A.A. 2014, 'Treatment of an expansive soil by mechanical and chemical techniques', *Geosynthetics International*, vol. 21, no. 3, pp. 233-43.

Fang, Z. 2006, 'Physical and numerical modelling of the soft soil ground improved by deep cement mixing method', The Hong Kong Polytechnic University.

Faria, K.C.P., Gurgel, R.F. & Holanda, J.N.F. 2012, 'Recycling of sugarcane bagasse ash waste in the production of clay bricks', *Journal of Environmental Management*, vol. 101, no. 0, pp. 7-12.

Fasihnikoutalab, M.H., Asadi, A., Unluer, C., Huat, B.K., Ball, R.J. & Pourakbar, S. 2017, 'Utilization of Alkali-Activated Olivine in Soil Stabilization and the Effect of Carbonation on Unconfined Compressive Strength and Microstructure', *Journal of Materials in Civil Engineering*, vol. 0, no. 0.

Fatahi, B., Basack, S., Premananda, S. & Khabbaz, H. 2012a, 'Settlement prediction and back analysis of Young's modulus and dilation angle of stone columns', *Australian Journal of Civil Engineering*, vol. 10, no. 1, p. 67.

Fatahi, B. & Khabbaz, H. 2013, 'Influence of fly ash and quicklime addition on behaviour of municipal solid wastes', *Journal of Soils and Sediments*, vol. 13, no. 7, pp. 1201-12.

Fatahi, B. & Khabbaz, H. 2014, 'Influence of Chemical Stabilisation on Permeability of Municipal Solid Wastes', *Geotechnical and Geological Engineering*, pp. 1-12.

Fatahi, B. & Khabbaz, H. 2015, 'Influence of Chemical Stabilisation on Permeability of Municipal Solid Wastes', *Geotechnical and Geological Engineering*, vol. 33, no. 3, pp. 455–66.

Fatahi, B., Khabbaz, H. & Fatahi, B. 2012b, 'Mechanical characteristics of soft clay treated with fibre and cement', *Geosynthetics International*, vol. 19, pp. 252-62.

Filz, G.M. & Navin, M.P. 2006, *Stability of column-supported embankments*, Virginia Transportation Research Council, Charlottesville, VA., Report No. VTRC 06-CR13.

Fredlund, D.G. & Xing, A. 1994, 'Equations for the soil-water characteristic curve', *Canadian Geotechnical Journal*, vol. 31, no. 4, pp. 521-32.

Frías, M., Villar, E. & Savastano, H. 2011, 'Brazilian sugar cane bagasse ashes from the cogeneration industry as active pozzolans for cement manufacture', *Cement and Concrete Composites*, vol. 33, no. 4, pp. 490-6.

Ganesan, K., Rajagopal, K. & Thangavel, K. 2007, 'Evaluation of bagasse ash as supplementary cementitious material', *Cement and Concrete Composites*, vol. 29, no. 6, pp. 515-24.

Ghosh, A. & Dey, U. 2009, 'Bearing ratio of reinforced fly ash overlying soft soil and deformation modulus of fly ash', *Geotextiles and Geomembranes*, vol. 27, no. 4, pp. 313-20.

Gourley, C.S., Newill, D. & Schreiner, H.D. 1993, 'Expansive soils: TRL's research strategy', *1st international symposium on engineering characteristics of arid soils*, London, UK, pp. 247-60.

Goyal, A., Anwar, A.M., Kunio, H. & Hidehiko, O. 2007, 'Properties of sugarcane bagasse ash and its potential as cement - Pozzolana binder', *Twelfth International Colloquium on Structural and Geotechnical Engineering*, Cairo, Egypt.

Güllü, H. 2014, 'Factorial experimental approach for effective dosage rate of stabilizer: Application for fine-grained soil treated with bottom ash', *Soils and Foundations*, vol. 54, no. 3, pp. 462-77.

Han, J. & Gabr, M. 2002, 'Numerical Analysis of Geosynthetic-Reinforced and Pile-Supported Earth Platforms over Soft Soil', *Journal of Geotechnical and Geoenvironmental Engineering*, vol. 128, no. 1, pp. 44-53.

Horpibulsuk, S., Shibuya, S., Fuenkajorn, K. & Katkan, W. 2007, 'Assessment of engineering properties of Bangkok clay', *Canadian Geotechnical Journal*, vol. 44, no. 2, pp. 173-87.

Hou, P., Wang, K., Qian, J., Kawashima, S., Kong, D. & Shah, S.P. 2012, 'Effects of colloidal nanoSiO2 on fly ash hydration', *Cement and Concrete Composites*, vol. 34, no. 10, pp. 1095-103.

Huang, J. & Han, J. 2010, 'Two-dimensional parametric study of geosynthetic-reinforced column-supported embankments by coupled hydraulic and mechanical modeling', *Computers and Geotechnics*, vol. 37, no. 5, pp. 638-48.

Jamsawang, P., Poorahong, H., Yoobanpot, N., Songpiriyakij, S. & Jongpradist, P. 2017, 'Improvement of soft clay with cement and bagasse ash waste', *Construction and Building Materials*, vol. 154, pp. 61-71.

Jamsawang, P., Yoobanpot, N., Thanasisathit, N., Voottipruex, P. & Jongpradist, P. 2016, 'Three-dimensional numerical analysis of a DCM column-supported highway embankment', *Computers and Geotechnics*, vol. 72, pp. 42-56.

Jayasree, P., Balan, K., Peter, L. & Nisha, K. 2015, 'Volume Change Behavior of Expansive Soil Stabilized with Coir Waste', *Journal of Materials in Civil Engineering*, vol. 27, no. 6, p. 04014195.

Jha, A.K. & Sivapullaiah, P.V. 2015, 'Mechanism of improvement in the strength and volume change behavior of lime stabilized soil', *Engineering Geology*, vol. 198, pp. 53-64.

Jiang, N.-J., Du, Y.-J., Liu, S.-Y., Wei, M.-L., Horpibulsuk, S. & Arulrajah, A. 2015, 'Multi-scale laboratory evaluation of the physical, mechanical, and microstructural properties of soft highway subgrade soil stabilized with calcium carbide residue', *Canadian Geotechnical Journal*, vol. 53, no. 3, pp. 373-83.

Jo, B.-W., Kim, C.-H., Tae, G.-h. & Park, J.-B. 2007, 'Characteristics of cement mortar with nano-SiO2 particles', *Construction and Building Materials*, vol. 21, no. 6, pp. 1351-5.

Jones, D.E. & Holtz, W.G. 1973, 'Expansive soils — the hidden disaster', *Civil Engineering*, vol. 43, pp. 49-51.

Jones, L.D. & Jefferson, I. 2012, 'Expansive soils', *ICE manual of geotechnical engineering*, ICE Publishing, London, pp. 413-41.

Kalkan, E. 2013, 'Preparation of scrap tire rubber fiber–silica fume mixtures for modification of clayey soils', *Applied Clay Science*, vol. 80–81, pp. 117-25.

Kamei, T., Ahmed, A. & Shibi, T. 2013, 'The use of recycled bassanite and coal ash to enhance the strength of very soft clay in dry and wet environmental conditions', *Construction and Building Materials*, vol. 38, pp. 224-35.

Kampala, A. & Horpibulsuk, S. 2013, 'Engineering Properties of Silty Clay Stabilized with Calcium Carbide Residue', *Journal of Materials in Civil Engineering*, vol. 25, no. 5, pp. 632-44.

Kehew, A.E. 2006, *Geology for engineers and environmental scientists*, 3rd, illustrated edn, Prentice Hall.

Khalili, N. & Khabbaz, M.H. 1998, 'A unique relationship for χ for the determination of the shear strength of unsaturated soils', *Géotechnique*, vol. 48, no. 5, pp. 681-7.

Kim, B., Prezzi, M. & Salgado, R. 2005, 'Geotechnical Properties of Fly and Bottom Ash Mixtures for Use in Highway Embankments', *Journal of Geotechnical and Geoenvironmental Engineering*, vol. 131, no. 7, pp. 914-24.

Kim, Y.T., Kim, H.J. & Lee, G.H. 2008, 'Mechanical behavior of lightweight soil reinforced with waste fishing net', *Geotextiles and Geomembranes*, vol. 26, no. 6, pp. 512-8.

Kinuthia, J.M., Wild, S. & Jones, G.I. 1999, 'Effects of monovalent and divalent metal sulphates on consistency and compaction of lime-stabilised kaolinite', *Applied Clay Science*, vol. 14, no. 1, pp. 27-45.

Kota, P., Hazlett, D. & Perrin, L. 1996, 'Sulfate-bearing soils: Problems with calcium-based stabilizers', *Transportation Research Board*, vol. Geotechnical Engineering Research, no. 1546, pp. 62-9.

Kumar, A. & Gupta, D. 2016, 'Behavior of cement-stabilized fiber-reinforced pond ash, rice husk ash–soil mixtures', *Geotextiles and Geomembranes*, vol. 44, no. 3, pp. 466-74.

Kumar, A., Walia, B. & Bajaj, A. 2007, 'Influence of Fly Ash, Lime, and Polyester Fibers on Compaction and Strength Properties of Expansive Soil', *Journal of Materials in Civil Engineering*, vol. 19, no. 3, pp. 242-8.

Lea, F.M. 1956, *The chemistry of cement and concrete*, Edward Arnold, London

Lima, S.A., Varum, H., Sales, A. & Neto, V.F. 2012, 'Analysis of the mechanical properties of compressed earth block masonry using the sugarcane bagasse ash', *Construction and Building Materials*, vol. 35, no. 0, pp. 829-37.

Liu, H., Ng, C. & Fei, K. 2007, 'Performance of a Geogrid-Reinforced and Pile-Supported Highway Embankment over Soft Clay: Case Study', *Journal of Geotechnical and Geoenvironmental Engineering*, vol. 133, no. 12, pp. 1483-93.

Liu, K.W. & Rowe, R.K. 2015, 'Numerical modelling of prefabricated vertical drains and surcharge on reinforced floating column-supported embankment behaviour', *Geotextiles and Geomembranes*, vol. 43, no. 6, pp. 493-505.

Lo, S.R. & Wardani, S.P. 2002, 'Strength and dilatancy of a silt stabilized by a cement and fly ash mixture', *Canadian Geotechnical Journal*, vol. 39, no. 1, pp. 77-89.

López-López, E., Vega-Zamanillo, Á., Calzada-Pérez, M.Á. & Taborga-Sedano, M.A. 2016, 'Use of bottom ash from thermal power plant and lime as filler in bituminous mixtures', *Materiales de Construcción*, vol. 65, no. 318.

Lorenzo, G. & Bergado, D. 2006, 'Fundamental Characteristics of Cement-Admixed Clay in Deep Mixing', *Journal of Materials in Civil Engineering*, vol. 18, no. 2, pp. 161-74.

Malekzadeh, M. & Bilsel, H. 2014, 'Hydro-mechanical behavior of polypropylene fiber reinforced expansive soils', *KSCE Journal of Civil Engineering*, vol. 18, no. 7, pp. 2028-33.

Manikandan, A. & Moganraj, M. 2014, 'Consolidation and Rebound Characteristics of Expansive Soil by Using Lime and Bagasse Ash', *International Journal of Research in Engineering and Technology*, vol. 03, no. 04, pp. 403-11.

Martin, J., Collins, R., Browning, J. & Biehl, F. 1990, 'Properties and Use of Fly Ashes for Embankments', *Journal of Energy Engineering*, vol. 116, no. 2, pp. 71-86.

Millogo, Y., Morel, J.-C., Traoré, K. & Ouedraogo, R. 2012, 'Microstructure, geotechnical and mechanical characteristics of quicklime-lateritic gravels mixtures used in road construction', *Construction and Building Materials*, vol. 26, no. 1, pp. 663-9.

Mitchell, J.K. 1993, *Fundamentals of soil behavior*, 2nd edn, Wiley, New York.

Mitchell, J.K. & Hooper, D.R. 1961, 'Influence of time between mixing and compaction on properties of a lime-stabilized expansive clay', *Highway Research Board Bulletin*, no. 304, pp. 14-31.

Mohamed, A.E.M.K. 2013, 'Improvement of swelling clay properties using hay fibers', *Construction and Building Materials*, vol. 38, pp. 242-7.

Mohammadi, I., Khabbaz, H. & Vessalas, K. 2014, 'In-depth assessment of Crumb Rubber Concrete (CRC) prepared by water-soaking treatment method for rigid pavements', *Construction and Building Materials*, vol. 71, no. 0, pp. 456-71.

Mokhtari, M. & Dehghani, M. 2012, 'Swell-shrink behavior of expansive soils, damage and control', *Electronic Journal of Geotechnical Engineering*, vol. 17, pp. 2673-82.

Mozgawa, W. & Deja, J. 2009, 'Spectroscopic studies of alkaline activated slag geopolymers', *Journal of Molecular Structure*, vol. 924, pp. 434-41.

Muntohar, A., Widianti, A., Hartono, E. & Diana, W. 2013, 'Engineering Properties of Silty Soil Stabilized with Lime and Rice Husk Ash and Reinforced with Waste Plastic Fiber', *Journal of Materials in Civil Engineering*, vol. 25, no. 9, pp. 1260-70.

Nalbantoglu, Z. & Tuncer, E.R. 2001, 'Compressibility and hydraulic conductivity of a chemically treated expansive clay', *Canadian geotechnical journal*, vol. 38, no. 1, pp. 154-60.

Nataraj, M.S. & McManis, K.L. 1997, 'Strength and Deformation Properties of Soils Reinforced With Fibrillated Fibers', *Geosynthetics International*, vol. 4, no. 1, pp. 65-79.

Nelson, J.D. & Miller, D.J. 1997, *Expansive soils: problems and practice in foundation and pavement engineering*, Wiley-Interscience, New York.

Nguyen, B.T.T., Takeyama, T. & Kitazume, M. 2016, 'Numerical analyses on the failure of deep mixing columns reinforced by a shallow mixing layer', *Japanese Geotechnical Society Special Publication*, vol. 2, no. 63, pp. 2144-8.

NLA 2004, *Lime-treated soil construction manual*, NLA, Arlington (Online).

Okyay, U.S. & Dias, D. 2010, 'Use of lime and cement treated soils as pile supported load transfer platform', *Engineering Geology*, vol. 114, no. 1–2, pp. 34-44.

Olgun, M. 2013, 'Effects of polypropylene fiber inclusion on the strength and volume change characteristics of cement-fly ash stabilized clay soil', *Geosynthetics International*, vol. 20, no. 4, pp. 263-75.

Oliveira De Paula, M., Ferreira Tinôco, I.D.F., De Souza Rodrigues, C. & Osorio Saraz, J.A. 2010, 'Sugarcane Bagasse Ash as a Partial-Portland-Cement-Replacement Material', *DYNA*, vol. 77, pp. 47-54.

Oliveira, P., Correia, A., Teles, J. & Custódio, D. 2016, 'Effect of fibre type on the compressive and tensile strength of a soft soil chemically stabilised', *Geosynthetics International*, vol. 23, no. 3, pp. 171-82.

Onésippe, C., Passe-Coutrin, N., Toro, F., Delvasto, S., Bilba, K. & Arsène, M.-A. 2010, 'Sugar cane bagasse fibres reinforced cement composites: Thermal considerations', *Composites Part A: Applied Science and Manufacturing*, vol. 41, no. 4, pp. 549-56.

Osinubi, K.J., Bafyau, V. & Eberemu, A.O. 2009a, 'Bagasse Ash Stabilization of Lateritic Soil', *Appropriate Technologies for Environmental Protection in the Developing World*, pp. 271-80.

Osinubi, K.J., Ijimdiya, T.S. & Nmadu, I. 2009b, 'Lime Stabilization of Black Cotton Soil Using Bagasse Ash as Admixture', *Advanced Materials Research*, vol. 62-64, pp. 3-10.

Panias, D., Giannopoulou, I.P. & Perraki, T. 2007, 'Effect of synthesis parameters on the mechanical properties of fly ash-based geopolymers', *Colloids and Surfaces A: Physicochemical and Engineering Aspects*, vol. 301, no. 1, pp. 246-54.

Parsa-Pajouh, A., Fatahi, B. & Khabbaz, H. 2015, 'Experimental and Numerical Investigations to Evaluate Two-Dimensional Modeling of Vertical Drain–Assisted Preloading', *International Journal of Geomechanics*, vol. 16, no. 1, p. B4015003.

Part 4: Pavement Materials 2007, Austroads, Sydney, Australia.

Part 4A: Granular Base and Subbase Materials 2009, Austroads, Sydney, Australia.

Pasha, A.Y., Khoshghalb, A. & Khalili, N. 2016, 'Pitfalls in Interpretation of Gravimetric Water Content–Based Soil-Water Characteristic Curve for Deformable Porous Media', *International Journal of Geomechanics*.

Phanikumar, B.R. 1997, 'A Study of Swelling Characteristics and Granular Pile-Anchor Foundation (GPAF) System in Expansive Soils', Doctoral Thesis thesis, JN Technological University, Hyderabad, India.

Phanikumar, B.R. 2009, 'Effect of lime and fly ash on swell, consolidation and shear strength characteristics of expansive clays_a comparative study', *Geomechanics and Geoengineering: An International Journal*, vol. 4, no. 2, pp. 175-81.

Phanikumar, B.R., Sreedharana, R. & Aniruddh, C. 2014, 'Swell-compressibility characteristics of lime-blended and cement-blended expansive clays – A comparative study', *Geomechanics and Geoengineering: An International Journal*.

Porbaha, A., Shibuya, S. & Kishida, T. 2000a, 'State of the art in deep mixing technology. Part III: Geomaterial characterization', *Proceedings of the ICE-Ground Improvement*, vol. 4, no. 3, pp. 91-110.

Porbaha, A., Shibuya, S. & Kishida, T. 2000b, 'State of the art in deep mixing technology. Part III:geomaterial characterization', *Proceedings of the Institution of Civil Engineers - Ground Improvement*, vol. 4, no. 3, pp. 91-110.

Pourakbar, S., Asadi, A., Huat, B.B.K., Cristelo, N. & Fasihnikoutalab, M.H. 2016, 'Application of Alkali-Activated Agro-Waste Reinforced with Wollastonite Fibers in Soil Stabilization', *Journal of Materials in Civil Engineering*, vol. 0, no. 0, p. 04016206.

Prusinski, J. & Bhattacharja, S. 1999, 'Effectiveness of Portland cement and lime in stabilizing clay soils', *Transportation Research Record*, no. 1652, pp. 215-27.

Punthutaecha, K. 2002, 'Volume change behavior of expansive soils modified with recycled materials', Ph.D. thesis, University of Texas at Arlington.

Punthutaecha, K., Puppala, A., Vanapalli, S. & Inyang, H. 2006, 'Volume Change Behaviors of Expansive Soils Stabilized with Recycled Ashes and Fibers', *Journal of Materials in Civil Engineering*, vol. 18, no. 2, pp. 295-306.

Puppala, A., Punthutaecha, K. & Vanapalli, S. 2006, 'Soil-Water Characteristic Curves of Stabilized Expansive Soils', *Journal of Geotechnical and Geoenvironmental Engineering*, vol. 132, no. 6, pp. 736-51.

Rahman, M.D.A. 1986, 'The potentials of some stabilizers for the use of lateritic soil in construction', *Building and Environment*, vol. 21, no. 1, pp. 57-61.

Rezende, L.R.d., Curado, T.d.S., Silva, M.V. & Mascarenha, M.M.d.A. 2017, 'Laboratory Study of Phosphogypsum, Stabilizers, and Tropical Soil Mixtures', *Journal of Materials in Civil Engineering*, vol. 29, no. 1.

Richards, B.G., Peter, P. & Emerson, W.W. 1983, 'The effects of vegetation on the swelling and shrinking of soils in Australia', *Géotechnique*, vol. 33, pp. 127-39.

Salih, M.A., Abang Ali, A.A. & Farzadnia, N. 2014, 'Characterization of mechanical and microstructural properties of palm oil fuel ash geopolymer cement paste', *Construction and Building Materials*, vol. 65, pp. 592-603.

Salih, M.A., Farzadnia, N., Abang Ali, A.A. & Demirboga, R. 2015a, 'Development of high strength alkali activated binder using palm oil fuel ash and GGBS at ambient temperature', *Construction and Building Materials*, vol. 93, pp. 289-300.

Salih, M.A., Farzadnia, N., Abang Ali, A.A. & Demirboga, R. 2015b, 'Effect of different curing temperatures on alkali activated palm oil fuel ash paste', *Construction and Building Materials*, vol. 94, pp. 116-25.

Satyanarayana, B. 1966, 'Swelling pressure and related mechanical properties of block cotton soil', PhD thesis, Indian Institute of Science, Bangalore.

Section4-Flexible Pavement Construction 2010, Transport Canberra and City Services, Canberra, Australia.

Sharma, R., Phanikumar, B. & Rao, B. 2008, 'Engineering Behavior of a Remolded Expansive Clay Blended with Lime, Calcium Chloride, and Rice-Husk Ash', *Journal of Materials in Civil Engineering*, vol. 20, no. 8, pp. 509-15.

Sharma, V., Vinayak, H.K. & Marwaha, B.M. 2005, 'Enhancing compressive strength of soil using natural fibers', *Construction and Building Materials*, vol. 93, no. 0, pp. 943-9.

Sherwood, P.T. 1993, 'Soil Stabilization With Cement and Lime', *Transport Research Laboratory*, HMSO, London p. 153.

Sivakumar Babu, G.L., Vasudevan, A.K. & Sayida, M.K. 2008, 'Use of Coir Fibers for Improving the Engineering Properties of Expansive Soils', *Journal of Natural Fibers*, vol. 5, no. 1, pp. 61-75.

Solanki, P., Khoury, N. & Zaman, M. 2009, 'Engineering Properties and Moisture Susceptibility of Silty Clay Stabilized with Lime, Class C Fly Ash, and Cement Kiln Dust', *Journal of Materials in Civil Engineering*, vol. 21, no. 12, pp. 749-57.

Sujjavanidi, S. & Duangchan, A. 2004, 'Pozzolanic reactivity and water requirement of bagasse ash', *Proc. In the 2nd Concrete National Conference*, Chiengmai, Thailand.

Tafreshi, S.N.M. & Norouzi, A.H. 2015, 'Application of waste rubber to reduce the settlement of road embankment', *Geomechanics and Engineering*, vol. 9, no. 2, pp. 219-41.

Tan, S., Tjahyono, S. & Oo, K. 2008, 'Simplified Plane-Strain Modeling of Stone-Column Reinforced Ground', *Journal of Geotechnical and Geoenvironmental Engineering*, vol. 134, no. 2, pp. 185-94.

Tan, T., Goh, T. & Yong, K. 2002, 'Properties of Singapore Marine Clays Improved by Cement Mixing', *Geotechnical Testing Journal*, vol. 25, no. 4, pp. 1-12.

Tang, C., Shi, B., Gao, W., Chen, F. & Cai, Y. 2007, 'Strength and mechanical behavior of short polypropylene fiber reinforced and cement stabilized clayey soil', *Geotextiles and Geomembranes*, vol. 25, no. 3, pp. 194-202.

Terzaghi, K. 1943, *Theoretical soil mechanics*, vol. 18, Wiley New York.

Tian, H. & Zhang, Y.X. 2016, 'The influence of bagasse fibre and fly ash on the long-term properties of green cementitious composites', *Construction and Building Materials*, vol. 111, pp. 237-50.

Tian, H., Zhang, Y.X., Ye, L. & Yang, C. 2015, 'Mechanical behaviours of green hybrid fibre-reinforced cementitious composites', *Construction and Building Materials*, vol. 95, pp. 152-63.

Usman, A.M., Raji, A., Waziri, N.H. & Hassan, M.A. 2014, 'A Study on Silica and Alumina Potential of the Savannah Bagasse Ash', *IOSR Journal of Mechanical and Civil Engineering*, vol. 11, no. 3, pp. 48-52.

van Genuchten, M.T. 1980, 'A closed-form equation for predicting the hydraulic conductivity of unsaturated soils', *Soil Science Society of America Journal*, vol. 44, no. 5, pp. 892-8.

Venda Oliveira, P.J., Pinheiro, J.L.P. & Correia, A.A.S. 2011, 'Numerical analysis of an embankment built on soft soil reinforced with deep mixing columns: Parametric study', *Computers and Geotechnics*, vol. 38, no. 4, pp. 566-76.

Viswanadham, B.V.S., Phanikumar, B.R. & Mukherjeeb, R.V. 2009, 'Swelling behaviour of a geofiber-reinforced expansive soil', *Geotextiles and Geomembranes*.

Wang, Y.-X., Guo, P.-P., Ren, W.-X., Yuan, B.-X., Yuan, H.-P., Zhao, Y.-L., Shan, S.-B. & Cao, P. 2017, 'Laboratory Investigation on Strength Characteristics of Expansive Soil Treated with Jute Fiber Reinforcement', *International Journal of Geomechanics*, vol. 17, no. 11, p. 04017101.

Wang, Y., Cui, Y.J., Tang, A.M., Tang, C.S. & Benahmed, N. 2016, 'Changes in thermal conductivity, suction and microstructure of a compacted lime-treated silty soil during curing', *Engineering Geology*, vol. 202, pp. 114-21.

Wild, S., Kinuthia, J.M., Jones, G.I. & Higgins, D.D. 1999, 'Suppression of swelling associated with ettringite formation in lime stabilized sulphate bearing clay soils by partial substitution of lime with ground granulated blastfurnace slag (GGBS)', *Engineering Geology*, vol. 51, no. 4, pp. 257-77.

Wong, L.S., Hashim, R. & Ali, F. 2013, 'Utilization of sodium bentonite to maximize the filler and pozzolanic effects of stabilized peat', *Engineering Geology*, vol. 152, no. 1, pp. 56-66.

Wu, H., Huang, B., Shu, X. & Yin, J. 2016, 'Utilization of solid wastes/byproducts from paper mills in Controlled Low Strength Material (CLSM)', *Construction and Building Materials*, vol. 118, pp. 155-63.

Yapage, N., Liyanapathirana, D., Kelly, R., Poulos, H. & Leo, C. 2014, 'Numerical Modeling of an Embankment over Soft Ground Improved with Deep Cement Mixed Columns: Case History', *Journal of Geotechnical and Geoenvironmental Engineering*, vol. 140, no. 11, p. 04014062.

Yapage, N., Liyanapathirana, D., Poulos, H., Kelly, R. & Leo, C. 2015, 'Numerical Modeling of Geotextile-Reinforced Embankments over Deep Cement Mixed Columns Incorporating Strain-Softening Behavior of Columns', *International Journal of Geomechanics*, vol. 15, no. 2, p. 04014047.

Yapage, N.N.S. & Liyanapathirana, D.S. 2014, 'A parametric study of geosynthetic-reinforced column-supported embankments', *Geosynthetics International*, vol. 21, no. 3, pp. 213-32.

Yi, Y., Li, C. & Liu, S. 2015, 'Alkali-Activated Ground-Granulated Blast Furnace Slag for Stabilization of Marine Soft Clay', *Journal of Materials in Civil Engineering*, vol. 27, no. 4, p. 04014146.

Yilmaz, Y. 2015, 'Compaction and strength characteristics of fly ash and fiber amended clayey soil', *Engineering Geology*, vol. 188, no. 0, pp. 168-77.

Yu, Y., Yin, J. & Zhong, Z. 2006, 'Shape effects in the Braziliantensile strength test and a 3D FEM correction', *International Journal of Rock Mechanics and Mining Sciences*, vol. 43, no. 4, pp. 623–7.

Yunsheng, Z., Wei, S., Qianli, C. & Lin, C. 2007, 'Synthesis and heavy metal immobilization behaviors of slag based geopolymer', *Journal of Hazardous Materials*, vol. 143, no. 1, pp. 206-13.

Zha, F., Liu, S., Du, Y. & Cui, K. 2008, 'Behavior of expansive soils stabilized with fly ash', *Natural Hazards*, vol. 47, no. 3, pp. 509-23.

Zhang, J., Zheng, J.-J., Chen, B.-G. & Yin, J.-H. 2013, 'Coupled mechanical and hydraulic modeling of a geosynthetic-reinforced and pile-supported embankment', *Computers and Geotechnics*, vol. 52, pp. 28-37.

Zhang, T., Yue, X., Deng, Y.F., Zhang, D.W. & Liu, S. 2014, 'Mechanical behaviour and micro-structure of cement-stabilised marine clay with a metakaolin agent', *Construction and Building Materials*, vol. 73, pp. 51-7.

Zhang, X., Mavroulidou, M. & Gunn, M.J. 2015, 'Mechanical properties and behaviour of a partially saturated lime-treated, high plasticity clay', *Engineering Geology*, vol. 193, pp. 320-36.